HYDROGEN STORAGE APPLICATIONS OF 1,2-AZABORINES

by

PATRICK GRANGER CAMPBELL

A DISSERTATION

Presented to the Department of Chemistry
and the Graduate School of the University of Oregon
in partial fulfillment of the requirements
for the degree of
Doctor of Philosophy

September 2012

DISSERTATION APPROVAL PAGE

Student: Patrick Granger Campbell

Title: Hydrogen Storage Applications of 1,2-Azaborines

This dissertation has been accepted and approved in partial fulfillment of the requirements for the Doctor of Philosophy degree in the Department of Chemistry by:

Professor David R. Tyler	Chairperson
Professor Shih-Yuan Liu	Advisor
Professor Victoria J. DeRose	Member
Professor Kenneth M. Doxsee	Member
Professor Benjamin J. McMorran	Outside Member

and

Kimberly Andrews Espy	Vice President for Research & Innovation and Dean of the Graduate School

Original approval signatures are on file with the University of Oregon Graduate School.

Degree awarded September 2012

DISSERTATION ABSTRACT

Patrick Granger Campbell

Doctor of Philosophy

Department of Chemistry

September 2012

Title: Hydrogen Storage Applications of 1,2-Azaborines

The development of safe and efficient hydrogen storage materials will aid in the transition away from fossil fuels toward a renewable, hydrogen-based energy infrastructure. Boron-nitrogen (BN) containing materials have attracted much attention due to their high hydrogen storage capacity and fast kinetics of hydrogen release. Furthermore, computational studies predict that hydrogen storage materials based on the BN-heterocycle 1,2-azaborine may enable reversible H_2 uptake and release, with little additional energy input. This thesis develops the basic science needed for a hydrogen storage platform based on BN-heterocycles such as 1,2-azaborine. Chapter I is a review of recent developments in azaborine chemistry. Chapter II describes a regeneration scheme from a "spent" 1,2-azaborine hydrogen storage material to "fully charged" fuel using molecular H_2 and H^-/H^+ equivalents. Chapter III describes the experimental determination of the resonance stabilization energy of 1,2-azaborines using reaction calorimetry. Chapter IV explores the effect of boron-substitution on the rate and extent of hydrogen release from BN materials. Chapter V describes work on a project unrelated to hydrogen storage, the synthesis and electronic parameter determination of the first 1,2-azaborine-containing phosphine ligand analog.

This dissertation includes previously published and unpublished co-authored material.

CURRICULUM VITAE

NAME OF AUTHOR: Patrick Granger Campbell

GRADUATE AND UNDERGRADUATE SCHOOLS ATTENDED:

University of Oregon, Eugene, OR
Macalester College, St. Paul, MN

DEGREES AWARDED:

Doctor of Philosophy, Chemistry, 2012, University of Oregon
Master of Science, Chemistry, 2008, University of Oregon
Bachelor of Arts, Chemistry, 2005, Macalester College

AREAS OF SPECIAL INTEREST

Synthetic Organic Chemistry
Hydrogen Storage Materials

PROFESSIONAL EXPERIENCE:

Research Assistant, University of Oregon, 2008-2012
Graduate Teaching Fellow, University of Oregon, 2007-2008

GRANTS, AWARDS, AND HONORS:

IME Boron XIV, Contributed Lecture, 2011
UO Technology Entrepreneurship Program Fellow, 2011
National Science Foundation GAANN Fellow, 2010

PUBLICATIONS:

Fristoe, C. R, **Campbell, P. G.**; Zakharov, L. N.; Liu, S.-Y. "Synthesis and Electronic Parameter Determination of a 1,2-Azaborine-Containing Phosphine Ligand" *Manuscript Submitted.*

Campbell, P. G.; Marwitz, A. J. V.; Liu, S.-Y. "Recent Advances in Azaborine Chemistry" *Angew. Chem. Int. Ed.* **2012**, *51*, 6074-6092.

Luo, W.; **Campbell, P. G.;** Zakharov, L. N.; Liu, S.-Y. "A Single-Component Liquid-Phase Hydrogen Storage Material" *J. Am. Chem. Soc.* **2011**, *133*, 19326-19329.

Campbell, P. G; Abbey, E. R.; Neiner, D.; Grant, D. J.; Dixon, D. A.; Liu, S.-Y. "Resonance Stabilization Energy of 1,2-Azaborines: A Quantitative Experimental Study by Reaction Calorimetry" *J. Am. Chem. Soc.* **2010,** *132,* 18048-18050.

Campbell, P. G.; Zakharov, L. N.; Grant, D. J.; Dixon, D. A.; Liu, S.-Y. "Hydrogen Storage by Boron-Nitrogen Heterocycles: A Simple Route for Spent Fuel Regeneration" *J. Am. Chem. Soc.* **2010**, *132*, 3289-3291.

ACKNOWLEDGMENTS

I would like to thank my research advisor Professor Shih-Yuan Liu for his guidance, critical eye, honest evaluations, and for the opportunities he has given me to develop as a scientist. I thank my committee chairman, Professor David Tyler, for his help navigating the intricacies of advancement and annual reviews, and for many pleasant chats in the copy room. Thanks to Professor Victoria DeRose for her service on my committee and for valuable career advice and introductions. Thanks to my committee members Professor Kenneth Doxsee, Professor Nathan Tublitz and the last-minute addition, Professor Benjamin McMorran, for spending their valuable time serving on my committee and for their helpful input into my projects. Special thanks are due to Dr. Mike Strain for his vigilance in maintaining the NMR facilities and to Dr. Lev Zakharov for his heroic efforts to get crystal structures from the most unlikely samples. I would also like to thank Dr. Donald Upson for the opportunity to participate in the UO Technology Entrepreneurship Program, and for helpful advice in my search for a job.

I would like to thank Dr. Eric Abbey, Dr. Adam Glass and Dr. Adam Marwitz for mentoring me in my early days in the Liu Group, and for their friendship over the years. Thanks to Dr. Ashley Lamm for her support and friendship from day one of our graduate studies. Special thanks to Carey Fristoe for his four years of hard work and dedication to our projects together, and his passion for the finer things in life. And thanks to the entire Liu group for making it a pleasure to come into work each morning. I would also like to thank my mother Suzanne Tripp and my sister Charlotte Campbell as well as my entire extended family for all their sympathy and support. Finally, I would like to thank my wonderful fiancé, Danielle Biselli, who has been there for me every step of the way.

TABLE OF CONTENTS

LIST OF FIGURES

LIST OF TABLES

LIST OF SCHEMES

Scheme Page

Scheme Page

Scheme Page

Scheme Page

CHAPTER I

RECENT ADVANCES IN AZABORINE CHEMISTRY

1.1. General Overview

This chapter is a review of recent advances in azaborine chemistry. It primarily focuses on reports published since the last comprehensive review on the subject by Piers and coworkers,[28] but includes a brief discussion of important early work to provide context for the new developments. This chapter contains published material: Campbell, P. G.; Marwitz, A. J. V.; Liu, S.-Y. *Angew. Chem. Int. Ed.* **2012**, *51*, 6074–6092. Professor Shih-Yuan Liu provided editorial assistance and scientific guidance in this chapter.

1.2. Introduction

Boron has been playing a crucial role in the field of chemistry. William Lipscomb (1976),[1] Herbert C. Brown (1979),[2] and more recently, Akira Suzuki (2010)[3] have each been recognized with the Nobel Prize for their contributions in boron chemistry. Today, boron-containing compounds represent a powerful tool for synthetic chemists.[4–7] In most targeted synthetic applications, however, the element boron typically is not part of the final functional structure. Because of boron's unique electronic structure and its ability to form covalent bonds with carbon, the inclusion of boron in organic structures has recently received significant attention in biomedical research[8] and in optoelectronic materials applications.[9]

An emerging strategy of incorporation of boron in organic structures is the substitution of a CC bond with an isoelectronic and isosteric BN unit (BN/CC isosterism). The isoelectronic nature between the BN and CC bonding arises from the fact that boron has three valence electrons and nitrogen has five valence electrons, and consequently, a BN unit has the same valence electron count (that is, 8 valence electrons) as a corresponding CC unit in which each carbon contributes 4 valence electrons (Figure 1.1).

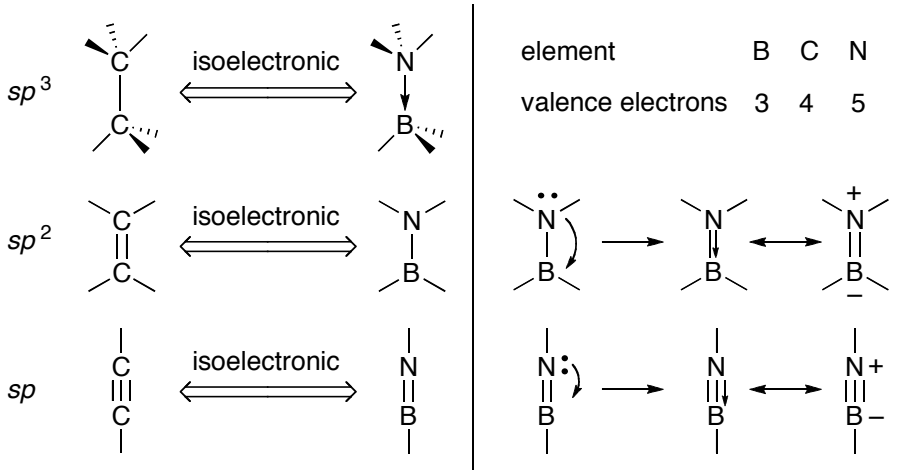

Figure 1.1. Isoelectronic relationship between CC and BN. The notation illustrated on the left column is used throughout this review.

Despite the same total valence electron count, differences in molecular properties can be expected when replacing an organic CC unit with the corresponding BN unit. The comparison between ethane vs. ammonia borane (AB) and ethene vs. aminoborane nicely illustrates this point (Figure 1.2). Ethane is a volatile gas under standard conditions (bp: −89 °C); it has no effective dipole moment;[10] the CC bond dissociation energy (BDE) is 90.1 kcal/mol.[11] In contrast, ammonia borane is a solid under standard conditions (mp: 104 °C); it has a strong dipole moment of 5.2 D;[12] its bond dissociation energy (27.2

kcal/mol) is significantly smaller than that of ethane.[13] Similar to ethane, the unsaturated ethene is an isolable volatile gas under standard conditions (bp: –104 °C); due to symmetry of the molecule, its dipole moment is also zero;[10] the BDE is 174.1 kcal/mol of which 109.1 kcal/mol is due to σ bond contribution and 65 kcal/mol is due to π contribution.[11,14] On the other hand, the BN analogue of ethene, aminoborane, is a reactive molecule with a strong tendency to polymerize/oligomerize under standard conditions. The parent aminoborane monomer has been characterized in the gas phase by microwave spectroscopy, which indicated an ethene-like planar structure.[15] The BN BDE in aminoborane is 139.7 kcal/mol of which 109.8 kcal/mol is attributed to the σ bond and only 29.9 kcal/mol to the π contribution.[13] Aminoborane has a dipole moment of 1.84 D,[15] which is significantly less than that of ammonia borane.

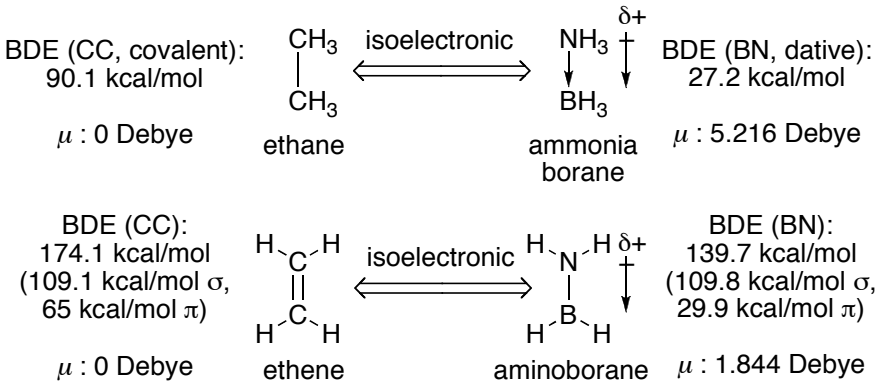

Figure 1.2. Molecular consequences of BN/CC isosterism.

It has been postulated that the reduced dipolemoment in aminoborane (vs. AB) is a result of opposing forces present in the two resonance structures representing aminoborane.[16] Figure 1.3 illustrates that the dipole that is due to nitrogen's higher electronegativity (vs. boron) in the left resonance structure opposes the dipole that is due to the formal charges in the right resonance structure as a result of π-bonding.

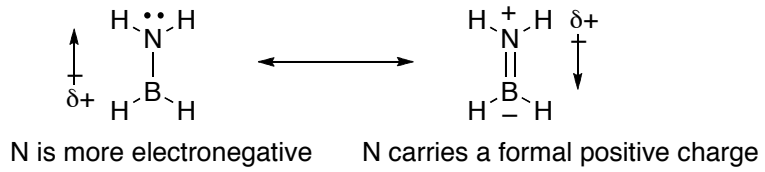

Figure 1.3. An intuitive explanation for reduced dipolemoment in aminoborane vs. AB.

Among the three possible variants to replace a CC with a BN (Figure 1.1), the sp^2-type BN/CC isosterism associated with conjugated aromatic systems has received the most attention. This is because of the ubiquity and wide utility of arene-containing compounds and the increased stability of the corresponding BN-containing isosteres compared to sp^3-type BN isosteres. The potential to dramatically increase the diversity of aromatic structures and tune their electronic properties through BN/CC isosterism have led to a burgeoning interest in this area. The first example of BN/CC isosterism of an arene was reported by Alfred Stock in 1926[17] with the synthesis of borazine (*c*-$B_3N_3H_6$), the inorganic counterpart to the quintessential aromatic compound benzene (*c*-C_6H_6). Similar to benzene, borazine continues to receive significant attention in pure and applied chemistry.[18–23] Although commonly referred to as the "inorganic benzene", borazine's aromatic character remains controversial to date.[24–27]

Since the pioneering contribution by Stock, the isoelectronic relationship between B–N and C=C has led to the development of aromatic systems *partially* substituted with boron and nitrogen (carbon-boron-nitrogen (CBN) heterocycles). Though somewhat limited in scope, the first major achievements in the synthesis of CBN heterocycles took place in the 1960s. After several decades of diminished activity in the field, modern

synthetic protocols have prompted a resurgence in the study of CBN heterocycles since the turn of the millennium.

This review is a summary of the advances made since the last comprehensive review on the subject by Piers and coworkers in early 2009,[28] and is not an exhaustive history of CBN heterocycle chemistry. For the sake of brevity, and in recognition of the 50th Anniversary of Dewar's first synthesis of a monocyclic 1,2-dihydro-1,2-azaborine, we will focus on aromatic 6-membered heterocycles that are isoelectronic with benzene and which contain only one BN substitution. This particular substitution pattern results in three possible isomers, referred to throughout this text as 1,2-azaborine **A**, 1,3-azaborine **B** and 1,4-azaboine **C** (Figure 1.4). Examples of each isomer have now been synthesized and will be discussed here, along with polycyclic compounds containing either the 1,2- or 1,4-azaborine core (1,3-azaborine-containing polycyclic compounds are as yet unknown). Important early work that has been covered in prior reviews will be discussed briefly to provide context for recent developments. The chemistry of boron dipyrrole (BODIPY)[29] and phthalocyanine dyes[30] as well as substitution with BN units in cluster compounds and graphitic materials,[28] are beyond the scope of this work. This review is organized by research group and will explore how the targeted applications of the products, along with the unique methodologies employed in their synthesis, have contributed to the present wealth and diversity of BN-containing compounds.

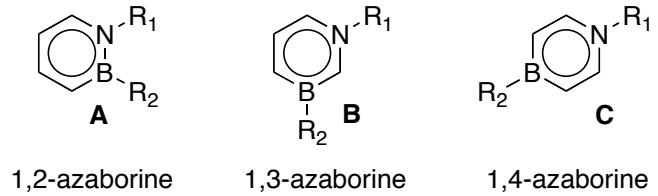

Figure 1.4. Isomeric forms of singly substituted aromatic CBN heterocycles

1.3. Pioneering Work

In 1958 Dewar reported the synthesis of the first singly B-N substituted aromatic compounds, 9,10-azaboraphenanthrenes.[31] The reaction of 2-phenylaniline with BCl_3 and $AlCl_3$ gave 9,10-azaboraphenanthrene **2** (Scheme 1.1), presumably through the Friedel-Crafts cyclization of intermediate **1**. The substitution of various nucleophiles at the reactive B–Cl unit of **2** allowed for the synthesis of several BN-phenanthrene derivatives **3**−**6**. The isoelectronic relationship between BN-phenanthrene **6** and its carbon analog was explored by UV/Vis spectroscopy. The spectrum of **6** resembles very closely that of phenanthrene in the position of the main absorption bands. However, an increase in the intensity of the α band was observed, an effect that was attributed to removing the molecular orbital degeneracy in the BN-substituted heterocycle. The reactivity of BN-phenanthrene was explored in depth. It was found to undergo electrophilic aromatic substitution regioselectively at the 6 and 8 positions, depending on the electrophile.[32–35] Deprotonation/substitution was possible at the nitrogen position, and tuning the electronics of the nitrogen substituent was found to have an effect on the electronics of the heterocycle as a whole. For example, the N-acyl substituted compound **8** rapidly oxidized when exposed to air, in sharp contrast to other derivatives that were quite air-stable (Scheme 1.2).[36]

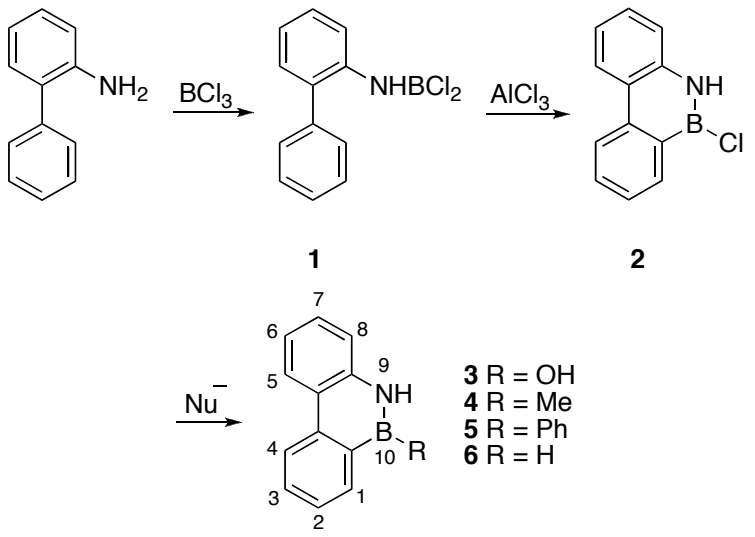

Scheme 1.1. Preparation of boron-substituted 9,10-azaboraphenanthrene derivatives.

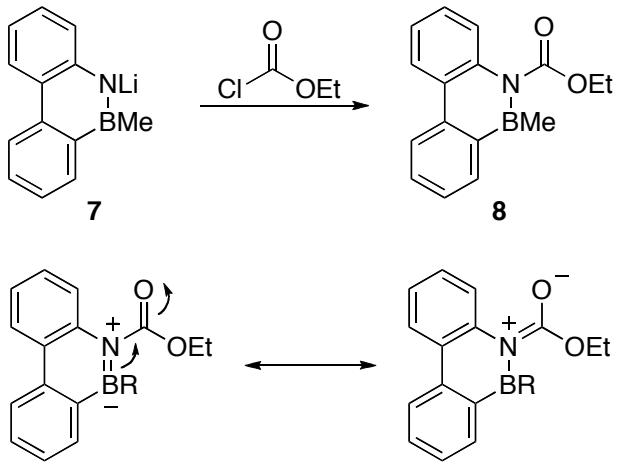

Scheme 1.2. Installation of a p-accepting group at the nitrogen of BN-phenanthrene.

The first BN-naphthalene was synthesized by Dewar and coworkers in 1959.[37] The reaction of 2-aminostyrene with phenylboron dichloride led to the direct formation of 2-phenyl-1,2-azaboranaphthalene **9** (Scheme 1.3). BN-naphthalenes **9, 11−13** were reported to be unreactive toward strong base and $KMnO_4$, signifying a high degree of resonance stabilization.[38] Further evidence of resonance stabilization in BN-naphthalene

was provided via the comparative reactivity of partially reduced heterocycle **14**, which reacted immediately with acid or base to give ring-opened **15** (Scheme 1.4).[39] In contrast, BN-naphthalene **11** was completely stable to hydrolysis, even upon heating.

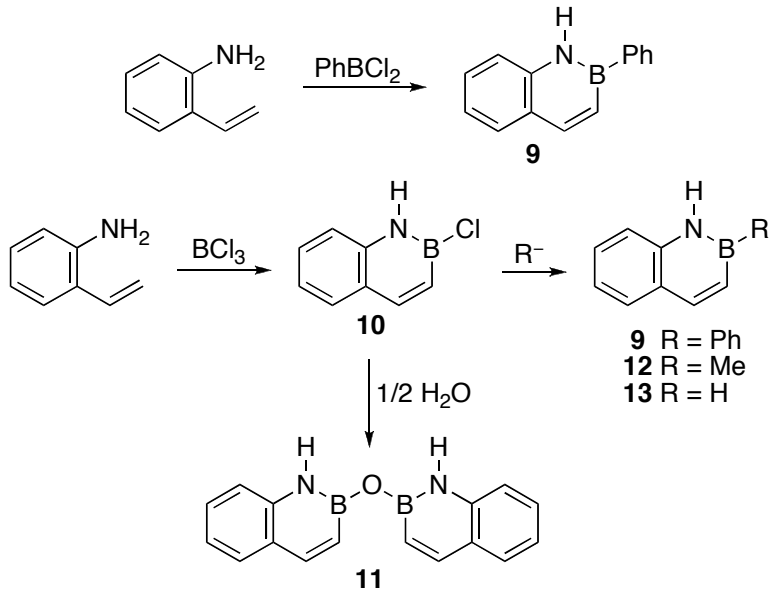

Scheme 1.3. Synthesis of B-substituted 1,2-azaboranaphthalenes.

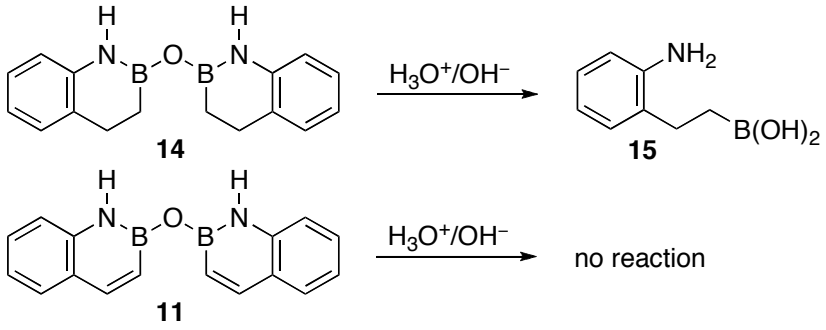

Scheme 1.4. Comparison of hydrolytic stability of BN-naphthalene **11** versus reduced anhydride **14**.

Dewar and coworkers also reported the first electrophilic aromatic substitution reactions of BN-naphthalene (Scheme 1.5).[40] The halogenation of 1,2-

azaboranaphthalene **12** with Cl_2 and Br_2 produced a mixture of C3-substituted products **16** and **17** and ring-opened side-products **18** and **19.** The structural assignments of **16** and **17** were confirmed by an independent synthesis of these compounds.

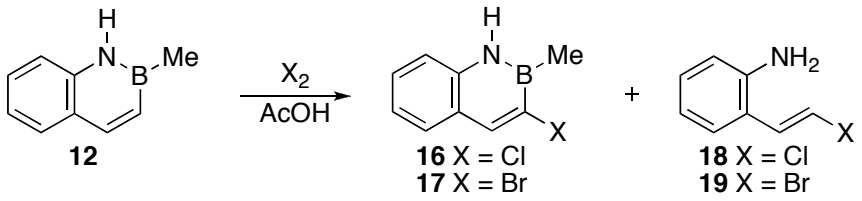

Scheme 1.5. EAS reactivity of BN-naphthalene **12**.

The aqueous stability of 1,2-azaboranaphthalenes made them attractive targets for the biological incorporation of boron (for example, cancer treatment using boron neutron capture therapy).[41] However, 1,2-azaboranaphthalene was found to be water-insoluble, limiting its use in biological systems. Dewar and coworkers were able to improve the solubility of 1,2-azaboranaphthalenes by functionalizing **12** at the nitrogen position (Scheme 1.6).[41]

Dewar and coworkers also synthesized the 9,10 isomer of BN-naphthalene (Scheme 1.7).[42] Treatment of di-3-butenylamine with trimethylamine borane formed bicycle **28**. Subsequent oxidation with Pd/C at high temperature afforded **29**, which was characterized by ^{1}H and ^{11}B NMR spectroscopy as well as mass spectrometry. Notably, the bridgehead-substituted BN-naphthalene **29** was found to have the same odor as naphthalene, which is a qualitative yet astounding testament to the chemical similarity between BN heterocycles and their all-carbon analogs.

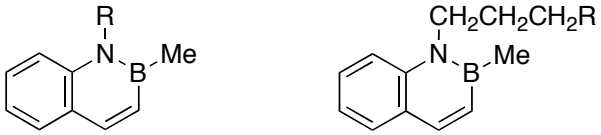

12 R = H
20 R = Li
21 R = $CH_2CH_2CH_2Cl$
27 R = CO_2Et

22 R = NMe_2
23 R = NEt_2
24 R = piperidino
25 R = morpholino
26 R = CN

Scheme 1.6. Synthesis of water-soluble BN-naphthalenes.

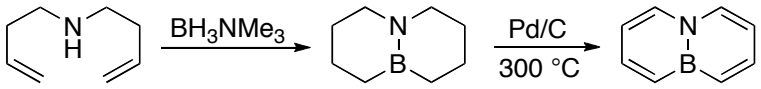

28 **29**

Scheme 1.7. Synthesis of bridgehead BN-naphthalene **29**.

The EAS reactivity of **29** was demonstrated, by H/D exchange, to occur at the carbons α to boron.[37] Dewar and coworkers therefore sought to synthesize the 10,11-azaboraphenalenium cation **30** by substitution at the alpha carbons of **29**.[43] The reaction of **29** with malonaldehyde bis-diethylacetal and CF_3CO_2H led to the formation of an intense purple solution attributed to the formation of **30** (characterized by ^1H NMR spectroscopy and mass spectrometry) that was stable at −78 °C but decomposed at higher temperatures (Scheme 1.8). The 1H NMR spectrum of the BN-phenalenium cation was similar to that of its carbon analog.

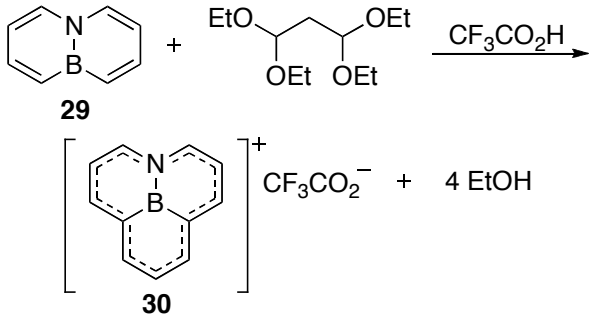

Scheme 1.8. Formation of BN-phenalenium cation **30** from BN-naphthalene **29**.

Dewar and White pioneered the first syntheses of monocyclic 1,2-azaborine derivatives independently in the early 1960s. In 1962, Dewar and coworkers used a desulfurization strategy from BN-benzothiophene **31** to generate highly-substituted 1,2-azaborine **32** (Scheme 1.9).[44] Compound **32** was resistant to degradation under prolonged exposure to both acid and base in ethanol. Acid/base stability and the inertness of the 1,2-azaborine double bonds toward Raney nickel are indications of the aromatic stability of the 1,2-azaborine core. In 1963, White reported the synthesis of 1-H-2-phenyl-1,2-azaborine **34** via Pd-catalyzed dehydrogenation from saturated heterocycle **33** (Scheme 1.10).[45]

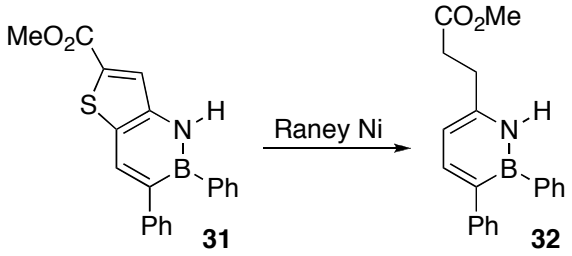

Scheme 1.9. Synthesis of 1,2-azaborine derivative **32** via desulfurization with Raney nickel (Dewar, 1962).

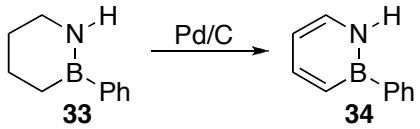

33 **34**

Scheme 1.10. Dehydrogenation route to 1,2-azaborine **34** (White, 1963).

In 1967, Dewar and coworkers attempted the first synthesis of the parent 1,2-Dihydro-1,2-azaborine using a hydroboration-oxidation protocol, but were unsuccessful (Scheme 1.11).[46] They concluded that, "Borazarene [1,2-Dihydro-1,2-azaborine] therefore seems to be a very reactive and chemically unstable system, prone to polymerization and other reactions…" In fact, multiple attempts to isolate the parent 1,2-Dihydro-1,2-azaborine from BN-triphenylene **36** were unsuccessful.

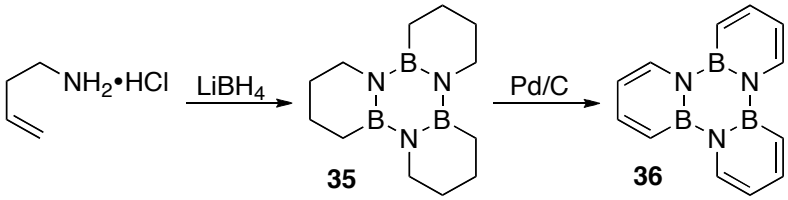

35 **36**

Scheme 1.11. Hydroboration-oxidation protocol leading to undesired trimerization to BN-triphenylene **36**.

Other pioneers of BN-heterocycle chemistry include Polivka and coworkers who followed a similar route to Dewar's BN-naphthalene synthesis to generate 1,2-azaboracyclohexane **37** from dimethylaminobut-3-ene (Scheme 1.12), however no attempts were made to aromatize this compound.[47,48]

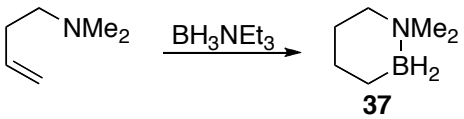

37

Scheme 1.12. Hydroboration to stable 1,2-azaboracyclohexane **37**.

Goubeau and coworkers used a secondary butenyl amine (as in White's earlier work) to form the cyclohexene analog **38** via hydroboration (Scheme 1.13).[49] Dehydrogenation with Pd/Al_2O_3 provided the first B−H substituted 1,2-azaborine **39**, which was characterized by mass spectrometry.[50]

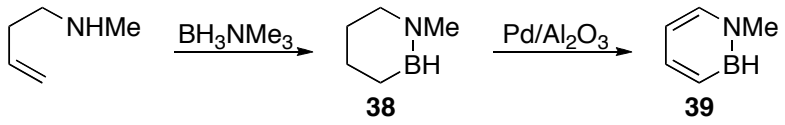

Scheme 1.13. Hydroboration-oxidation to generate 1,2-azaborine **39** containing a B–H group.

Gronowitz and coworkers synthesized a series of BN-benzothiophenes, which upon desulfurization yielded the first examples of monocyclic 1,2-azaborines substituted at C4 and/or C5 (Scheme 1.14).[51–53]

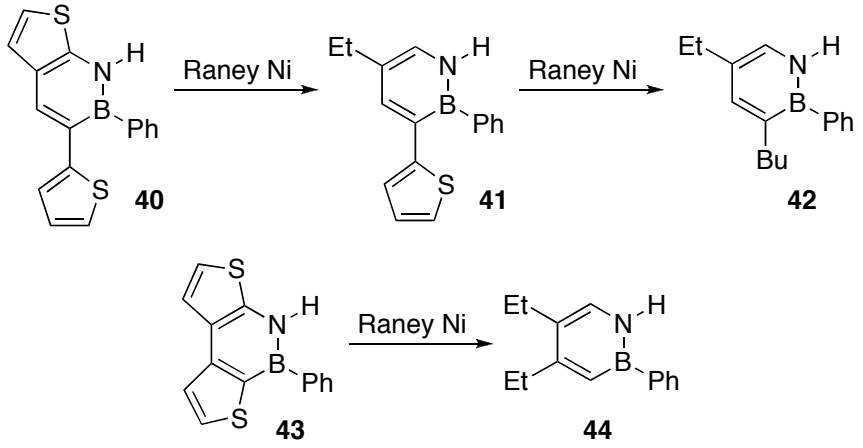

Scheme 1.14. Desulfurization of BN-benzothiophenes with Raney nickel to generate 4- and 5-substituted 1,2-azaborines.

The pioneering efforts of these groups hinted at the potential of azaborine-containing compounds as arene mimics in a diverse variety of structural motifs. However, early development was hampered by the limited material characterization capabilities of

the times and harsh synthetic conditions incompatible with many functional groups. Modern synthetic protocols and instrumentation have enabled a new generation of chemists to pick up where Dewar, White and others left off, and take azaborine chemistry into uncharted and exciting territory.

1.4. The Ashe Group – University of Michigan

The Ashe group achieved a breakthrough in the mild synthesis of monocyclic 1,2-azaborines in 2000 and sparked renewed interest in the field of aromatic BN-heterocycles. Previous syntheses relied on desulfurization or dehydrogenation at extreme temperatures as discussed above, but Ashe and coworkers developed a ring-closing metathesis/oxidation protocol that enabled mild and efficient formation of 1,2-azaborines (Scheme 1.15).[54] Transmetallation of allyltributyltin with BCl_3 generated allylboron dichloride **45** *in situ*. Condensation with allylethylamine produced bisallyl aminoborane **46**. The addition of PhLi led to the displacement of chloride from the labile B−Cl bond to give B−Ph aminoborane **47** in good yield. Ring-closing metathesis with Grubbs' first generation catalyst formed 1,2-azaborine precursor **48** featuring an olefin at the 4-position. The oxidation to 1,2-azaborine **49** was accomplished in good yield using 2,3-dichloro-5,6-dicyano-1,4-benzoquinone (DDQ) at 35 °C.

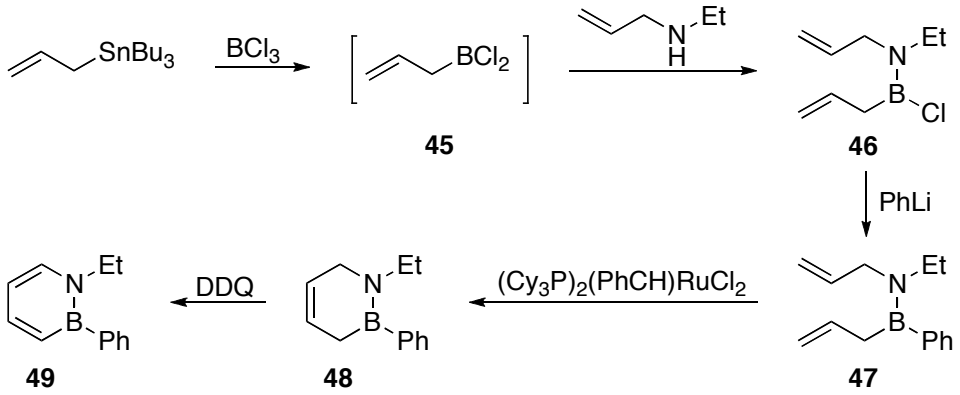

Scheme 1.15. Mild synthesis of 1,2-azaborine **49** by ring-closing metathesis.

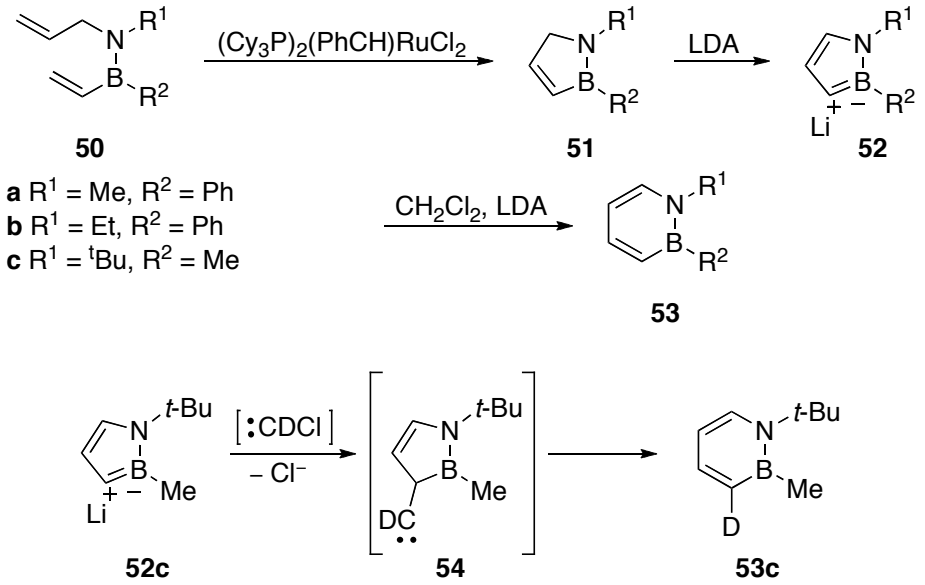

Scheme 1.16. Ring-expansion route to 1,2-azaborines **53a–c** and deuterium labeling.

A year later, Ashe and coworkers explored a ring-expansion route to 1,2-azaborines from the 1,2-azaborolide heterocycle, which is formally isoelectronic with the ubiquitous cyclopentadienide (Cp) anion (Scheme 1.16).[55] Ring-closing metathesis from B−vinyl aminoboranes **50** provided heterocycles **51**, which were deprotonated to give 1,2-azaborolides **52**. The reaction of **52** with CH_2Cl_2 and lithium diisopropylamide

(LDA) (the Katz reaction) gave 1,2-azaborines **53a**−**c**. A deuterium labeling study suggested that the initial attack of chlorocarbene occurs at the C3 position of **52c**. Carbene insertion into the B−C bond leads to a 3-deuterio isomer of **53c** via carbene **54**. Deuterium incorporation at this position rules out initial substitution at C5.

In one report, Ashe and coworkers investigated the haptotropic migration of B−phenyl 1,2-azaboranaphthalene **9** in $Cr(CO)_3$ piano-stool complexes (Scheme 1.17).[60] The complexation of **9** with $Cr(CO)_3$ was envisioned to occur at the benzenoid, 1,2-azaborine, or even the boron-substituted phenyl ring. In fact, η^6 binding of the benzenoid ring was observed under mild heating to form complex **55**. At higher temperatures, however, a shift of chromium complexation to the boron-substituted phenyl ring occurred forming complex **56**, with no evidence for the formation of complex **57**. In fact, even when **56** was deprotonated with LiTMP to generate complex **58**, no haptotropic migration to **59** was observed; instead complex **58** was prone to thermal degradation. These data indicate that the heterocyclic ring of BN-naphthalene is a poor ligand for transition metals relative to monocyclic 1,2-azaborines.

Ashe and coworkers strategized that removal of the competitive B-phenyl binding site would allow for the binding of transition metals to the heterocyclic fragment of BN-naphthalene. To that end, B-methyl 1,2-azaboranaphthalene **12** was treated with $(MeCN)_3Cr(CO)_3$ to give complex **60** (Scheme 1.18). Though no complexation to the heterocyclic fragment was observed, deprotonation of **60** with potassium hexamethyldisilazide provided **61**, which increased the electron-richness of the 1,2-azaborine heterocycle. Upon heating, complex **61** underwent a haptotropic migration to afford the desired anionic complex **62** in which chromium is η^6-bound to the heterocyclic

ring. Methylation of **62** presumably led to complex **63**, however the coordination of the neutral heterocyclic fragment was so tenuous that decomplexation to free BN-naphthalene **64** occurred at room temperature.

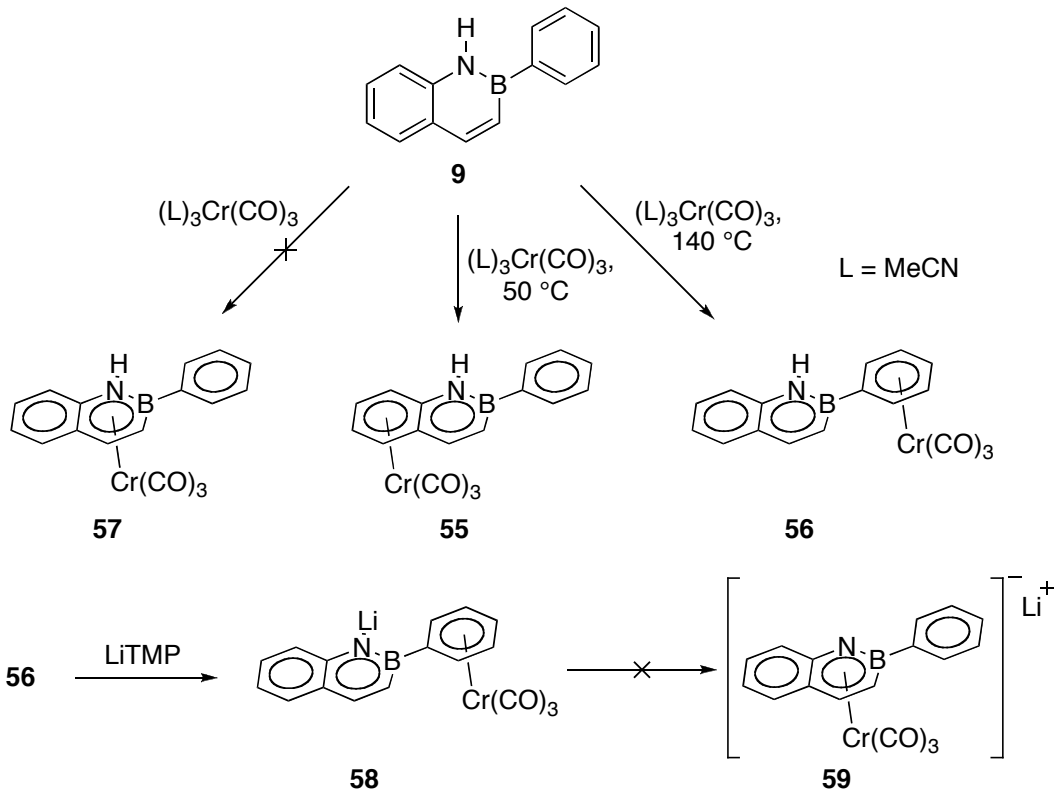

Scheme 1.17. Haptotropic migration of Cr-complexes of B-phenyl-1,2-azaboranaphthalene **9**.

In their most recent report in this field, the Ashe group explored the ligand properties of deprotonated BN-styrene **65**, which was synthesized via the ring expansion route discussed above (Scheme 1.19).[61] The reaction of **65** with one equivalent of [{Cp*RuCl}$_4$] gave complex **66** in which BN-styrene is η^6-bound to ruthenium. However, when two equivalents of [{Cp*RuCl}$_4$] were added, diruthenium complex **67** was formed in which η^6-binding occurs between one ruthenium atom and the 1,2-azaborine ring,

while the second ruthenium binds η^1 to the 1,2-azaborine nitrogen and η^2 to the B-vinyl group.

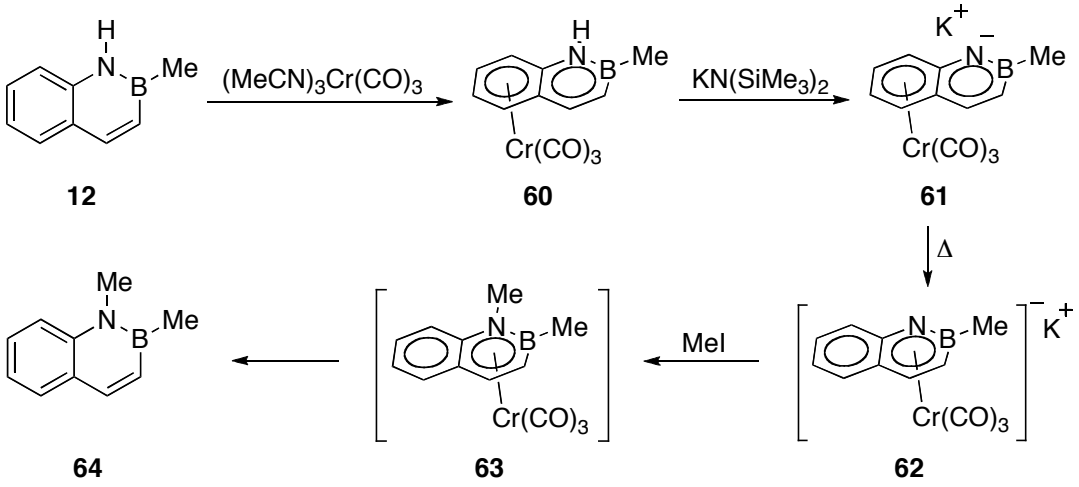

Scheme 1.18. Haptotropic migration of Cr-complexes of B-methyl-1,2-azaboranaphthalene **12**.

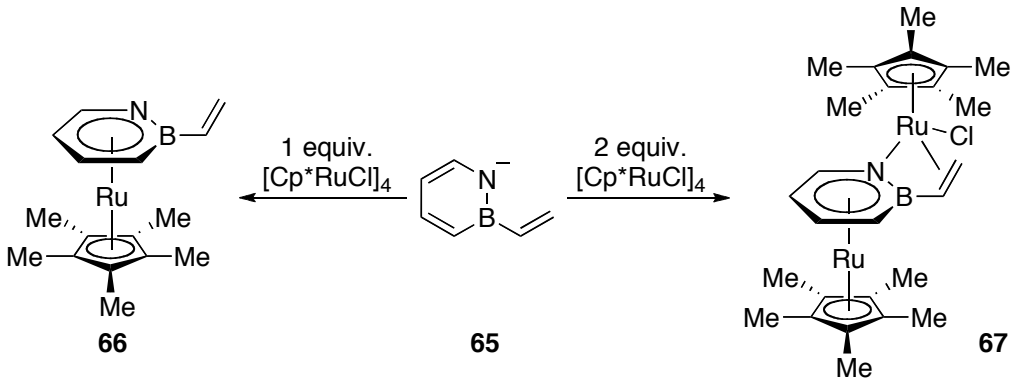

Scheme 1.19. Synthesis of complexes **66** and **67** from BN-styrene **65**.

1.5. The Liu Group – University of Oregon

Liu and coworkers have extended the synthetic methods developed by Ashe to create 1,2-azaborines with various heteroatom substituents at boron. Catalytic ring-closing metathesis in the presence of the reactive B−Cl bond of bisallyl aminoborane **46**

readily furnished cyclized aminoborane **68** (Scheme 1.20).[62] Oxidation conditions were screened and it was determined that Pd black efficiently dehydrogenates **68** to give 1,2-azaborine **69**. Treatment with various carbon-based and heteroatomic nucleophiles provided the known 1,2-azaborine **49** as well as new 1,2-azaborine derivatives **70a–h** in good yield. Several of these derivatives are of particular interest as they relate to their phenyl analogs, including glycolate-substituted **70h**, which is isoelectronic with a known hypolipidemic agent.[63] The stability of 1,2-azaborines to H_2O and O_2 was demonstrated for a series of boron- and C3-substituted derivatives and it was determined using kinetics experiments that substitution at these positions had a substantial effect on compound stability.[64]

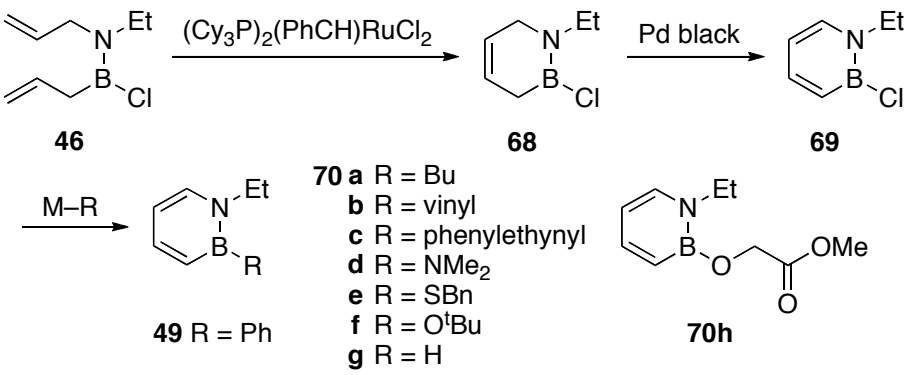

Scheme 1.20. Nucleophilic substitution of **69** to generate B-substituted 1,2-azaborines.

In a subsequent report, Liu and coworkers demonstrated that the 1,2-azaborine analog of benzonitrile **71** was readily available by treating **69** with AgCN (Scheme 1.21).[65] The formation of the B−CN bond rather than the alternative B−NC bond was supported by calculations and was unambiguously confirmed by an isotopic labeling experiment using $Ag^{13}C^{15}N$. Complexation of **71** with chromium(0) led to a surprising

isomerization of the CN group to form complex **72**, which was characterized by X-ray crystallography. Complex **72** was also readily available by the direct reaction of **69** with $Na^{+}[Cr(CO)_5CN]^{-}$.

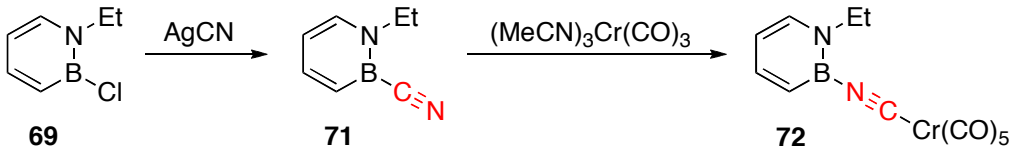

69 **71** **72**

Scheme 1.21. Synthesis of BN-benzonitrile and unexpected isomerization to complex **72**.

While the B–Cl bond in compound **69** is susceptible to nucleophilic aromatic substitution with a variety of anionic nucleophiles, less reactive neutral nucleophiles do not displace chloride from the boron atom. Liu and coworkers found that treatment of **69** with AgOTf smoothly forms species **73**, which contains the much more labile B–OTf bond. Compound **73** was shown to react with both electron-rich and electron-poor *para*-substituted pyridines to generate the first examples of 1,2-azaborine cations, **74a–e** (Scheme 1.22, top).[66] The solid-state fluorescence was measured for **74a–e** and compared to their all-carbon analogs. It was found that 1,2-azaborine substitution causes a red-shift of the emission maxima relative to the all-carbon species, and that the nature of the *para* substituent has a substantial effect on the emissive properties. Protonated pyridinium analogs of **74** (that is, without the 1,2-azaborine group) were not fluorescent under identical conditions, confirming the critical role the 1,2-azaborine moiety plays in the observed emissions. In a later paper, the synthetic protocol was expanded to include substitution of **73** with trimethylphosphine, triphenylphosphine oxide, and pyridine-*N*-oxide to generate the cationic 1,2-azaborines **75–77** (Scheme 1.22, bottom).[67]

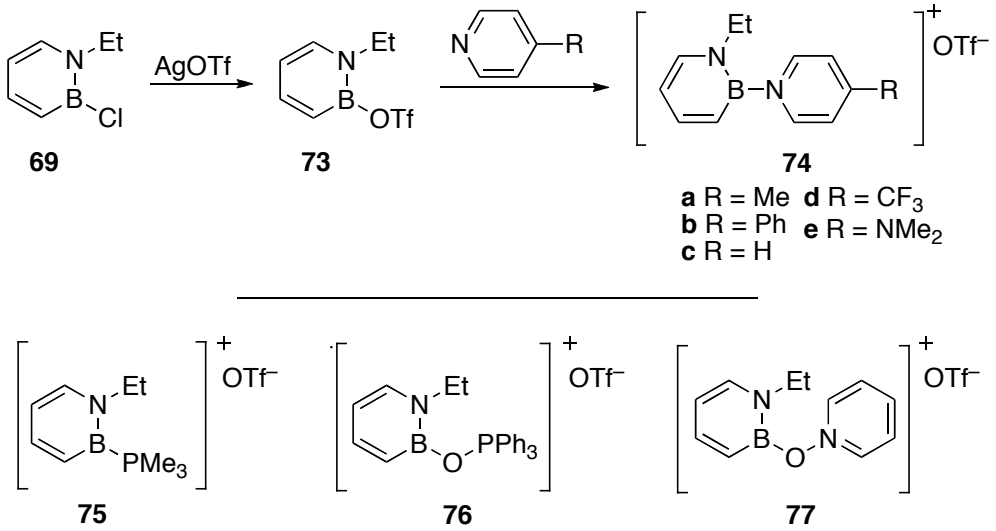

Scheme 1.22. Synthesis of 1,2-azaborine cations **74**–**77**.

The first successful synthesis of the parent 1,2-dihydro-1,2-azaborine **82** was reported by Liu and coworkers in 2009 (Scheme 1.23).[68] The incorporation of the *tert*-butyldimethylsilyl (TBS) nitrogen protecting group permitted the formation of a versatile 1,2-azaborine **78** via the same ring-closing/oxidation protocol presented above. Substitution at boron with superhydride provided *N*−TBS-1,2-azaborine **79** with a B–H bond. Direct deprotection to the parent compound was unsuccessful, however treatment with $[Cr(CO)_3(MeCN)_3]$ to form complex **80** activated the N−TBS group toward cleavage by HF-pyridine and afforded complex **81** in which 1,2-dihydro-1,2-azaborine is η^6-bound to the $Cr(CO)_3$ fragment. X-ray quality crystals of **81** were obtained, which showed that chromium is centered about the planar 1,2-dihydro-1,2-azaborine ring in analogy to the corresponding benzene–$Cr(CO)_3$ complex. Bond lengths, carbonyl-stretching frequencies, along with computationally predicted parameters are presented in Figure 1.5. Decomplexation of the 1,2-dihydro-1,2-azaborine ligand by exchange with PPh_3 provided **82** in good yield by ^{1}H NMR, however the volatility of **82** resulted in a

low yield of isolated product. Compound **82** was characterized by ^{1}H, ^{11}B, and ^{13}C NMR spectroscopy, as well as IR spectroscopy and HRMS, which supported the assigned structure. The UV/Vis spectrum of **82** is consistent with an aromatic heterocycle; the lowest energy absorption at 269 nm (ε = 15632 $Lmol^{-1}cm^{-1}$) is close in energy to the α band of benzene (255 nm, ε = 977 $Lmol^{-1}cm^{-1}$), however this absorption was much stronger in **82**. The corresponding band in borazine is virtually non-existent. The electronic spectra indicate that **82** possesses significant aromatic character and more closely resembles benzene than borazine. 1,2-Dihydro-1,2-azaborine was found to be quite thermally and hydrolytically stable. Deuterium exchange at the N−H position occurred over approximately 24 hours in a CD_3OD solution of **82**, demonstrating the unique reactivity of **82** relative to benzene.

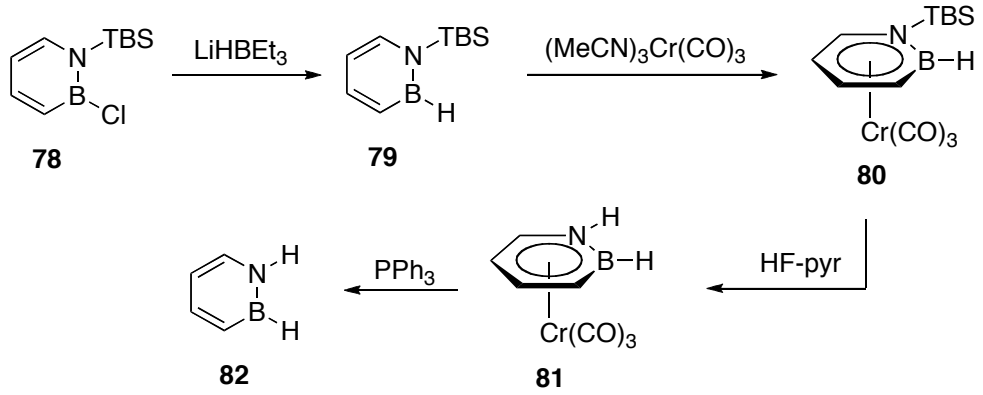

Scheme 1.23. Synthesis of 1,2-dihydro-1,2-azaborine **82**.

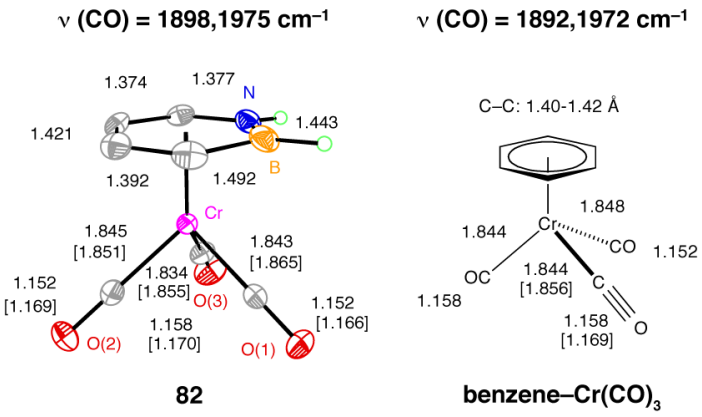

Figure 1.5. Bond lengths (in Å) and carbonyl stretching frequencies for **82** and benzene–$Cr(CO)_3$. Computed values are in parentheses.

The aromaticity of azaborine systems is of considerable interest not only from a fundamental point of view, but also as it relates to potential applications of BN/CC isosterism. Reactivity, structure, energy and magnetic criteria are the four metrics most used to characterize the aromaticity of a compound. Dewar, Ashe and others have demonstrated reactivity consistent with aromatic systems (e.g., electrophilic aromatic substitution, π-complexation), and the reported structures of azaborine compounds have indicated planarity and bond-lengths typical of aromatic systems. In a series of reports, the Liu group has endeavored to systematically characterize the aromaticity of 1,2-azaborine systems with regard to bond-delocalization, resonance stabilization energy, reactivity and magnetic properties. The results are summarized below.

Though the solid-state structural analysis of **82** (mp: −45 °C) has not been reported, microwave spectroscopy has provided a means of elucidating the structural features. Kukolich, Liu, and coworkers recently collected microwave spectroscopic data for several isotopomers of **82**.[69] The results indicate that the 1,2-dihydro-1,2-azaborine ring is planar with a B−N bond length of 1.45(3) Å. The B−C and N−C bond lengths

were found to be 1.51(1) Å and 1.37(3) Å, respectively. These bond lengths are somewhat longer than the values reported for substituted derivatives in the solid state (see Table 1.1).

Liu and coworkers obtained evidence of bond delocalization in 1,2-azaborine via crystallographic analysis.[70] 1,2-azaborine precursor **83** was a versatile intermediate in the formation of a family of aminoboranes in various oxidation states with respect to the intra-ring carbon atoms (**84**−**87** in Scheme 1.24). Transition-metal catalysis was used in all cases to generate the desired heterocycle. The isomerization of **83** to B-vinyl **84** was achieved in good yield using $[Ru(Cl)_2(PPh3)_3]$. Alternatively, $[Ru(H)(Cl)(CO)(PPh_3)_3]$ isomerized the olefin in **83** to N-vinyl **85**. Pd black catalyzed oxidation to 1,2-azaborine **86**. The same catalyst in the presence of H_2 reduced **83** to **87**. Structural data for compounds **83**−**87** were obtained by single-crystal X-ray diffraction and are presented in Table 1.1. Upon oxidation to 1,2-azaborine **86**, the B−N bond lengthens relative to that in the other heterocycles. Similarly, the C=C bonds in **84** and **85** are shorter than the corresponding bonds in **86**. The lengthening of these formal double bonds in the structure of **86** is an indication of bond delocalization. Conversely, the C4−C5 single bond in **86** is shorter than the corresponding bonds in **84** and **85** by over 0.07 Å. A similar shortening of the B−C3 and C6−N bonds in 1,2-azaborine **86** versus all other derivatives is consistent with bond delocalization.

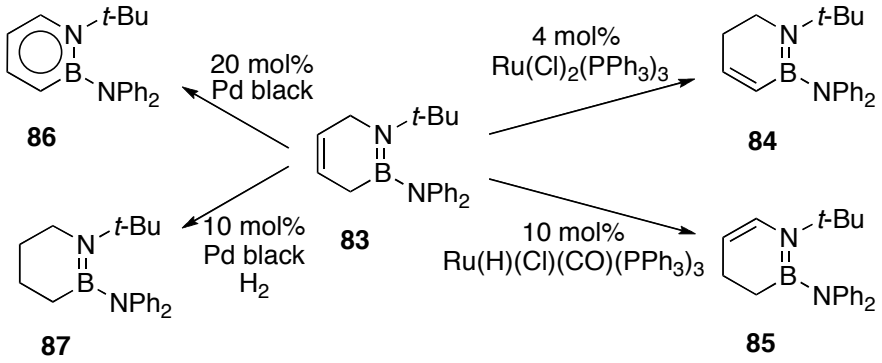

Scheme 1.24. Catalytic formation of 1,2-azaborine isomers **84**–**87** from common intermediate **83**.

Table 1.1. Selected bond distances and deviations from planarity (Å) for heterocycles **83**–**87.**

	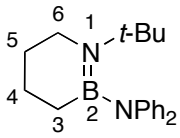	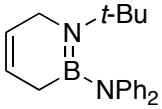	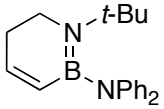	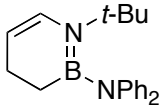	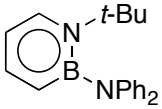
	87	**83**	**84**	**85**	**86**
B–N_{ring}	1.403(2)	1.405(2)	1.407(2)	1.417(3)	1.446(2)
B–C3	1.584(3)	1.590(2)	1.559(2)	1.579(4)	1.518(2)
C3–C4	1.511(3)	1.493(2)	1.338(2)	1.504(4)	1.363(2)
C4–C5	1.511(3)	1.319(2)	1.479(2)	1.494(4)	1.412(2)
C5–C6	1.508(3)	1.493(2)	1.503(2)	1.319(3)	1.356(2)
C6–N_{ring}	1.479(2)	1.477(2)	1.479(2)	1.432(3)	1.383(2)
B–N_{exo}	1.488(2)	1.478(2)	1.483(2)	1.480(3)	1.486(2)
planarity[a]	0.226	0.164	0.199	0.183	0.048

[a] Root mean square deviation of intra-ring atoms from least-squares plane (in Å).

In 2010, Liu and coworkers reported the experimental determination of the resonance stabilization energy (RSE) of 1,2-azaborine, a quantitative measure of aromaticity.[71] By comparing the heat of hydrogenation (measured using reaction calorimetry) of the aromatic compound **89** against the sum of the heats of hydrogenation of the "pre-aromatic" compounds **90** and **91** [that is, RSE = ΔH1 − (ΔH2 + ΔH3)], the

RSE of 1,2-azaborine was found to be 16.6 ± 1.3 kcal mol^{-1}, which is consistent with significant aromatic character (Scheme 1.25). This result is in good agreement with computationally predicted values for 1,2-azaborines, and quite a bit less than the RSE of benzene (32.4 kcal mol^{-1}).

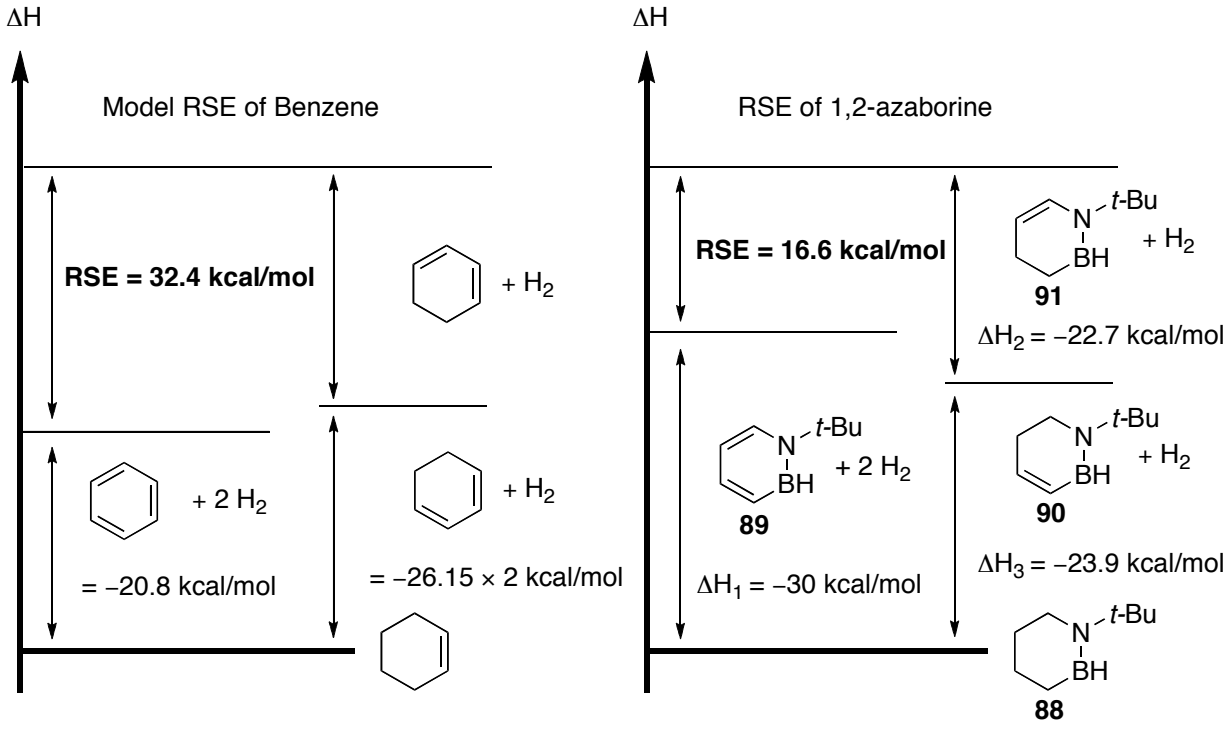

Scheme 1.25. Experimentally determined resonance stabilization energy of 1,2-azaborine.

Protons attached to aromatic systems typically display downfield NMR chemical shifts due to the shielding effects of the ring current. Liu and coworkers have performed ^{1}H NMR experiments that confirm that azaborine protons are indeed shifted downfield as the molecules become aromatic. The NMR chemical shifts of the "pre-aromatic" compounds **90**–**92** along with the aromatic compound **89** are presented in Table 1.2. All

protons were assigned using the 2D HETCOR technique. There is a clear down field shift ranging from $\Delta\delta$ = 0.76 to 1.83 ppm as isolated olifinic protons become aromatic.

Table 1.2. $\delta(^1H)$ values (in ppm) for **89–92** and downfield shifts $\Delta\delta$ (in ppm) of the signals for aromatic 1,2-azaborine **89**.

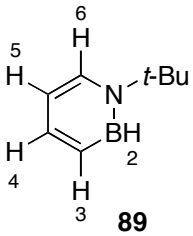

89

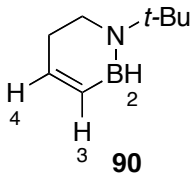

90

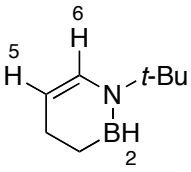

91

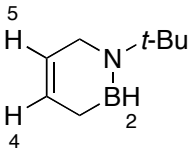

92

	89	**90**	**91**	**92**	**Δδ downfield**
$H_{B(2)}$ δ:	5.23	4.45	4.91	4.75	0.78, 0.32, 0.48
$H_{C(3)}$ δ:	6.84	5.91			0.93
$H_{C(4)}$ δ:	7.54	6.55		5.71	0.99, 1.83
$H_{C(5)}$ δ:	6.38		5.02	5.62	1.36, 0.76
$H_{C(6)}$ δ:	7.63		6.21		1.42

Complementing Ashe's pioneering work on electrophillic aromatic substitution of 1,2-azaborines, Liu and coworkers studied nucleophillic aromatic substitution of the parent 1,2-dihydro-1,2-azaborine **82**.[72] Treatment of **82** with two equivalents of nucleophile led to deprotonation at the nitrogen position and substitution at boron; reactions with only one equivalent of nucleophile had dramatically lower yields. Quenching with an appropriate electrophile (including H^+) led to a diverse array of products, summarized in Table 1.3. Thorough experimental and computational mechanistic analysis revealed that the reaction most likely proceeds via two distinct pathways depending on the nature of the nucleophile.

Table 1.3. Substrate scope of nucleophilic aromatic substitution of **82.**

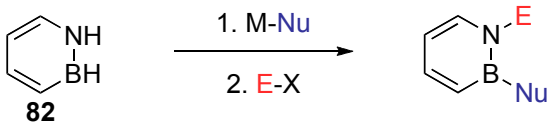

82

Entry	M-Nu	E-X	Yield (%)[a]
1	Na-O*t*-Bu	H-Cl	63
2	K-Oallyl	H-Cl	79
3	Li-*t*-Bu	H-Cl	81
4	Li-*n*-Bu	H-Cl	80
5	Li-Ph	H-Cl	98
6	BrMg-vinyl	H-Cl	59
7	BrMg—≡—Ph	H-Cl	71
8	Li-*n*-Bu	TMS-Cl	89
9	Li-*n*-Bu	Me-I	67
10	Li-*n*-Bu	Bn-Br	60

[a] Isolated yield

Apart from exploring the fundamental properties of 1,2-azaborines, the Liu group is interested in utilizing these compounds in biological and materials science applications. A proof-of-concept demonstration of the biomimetic potential of 1,2-azaborine was reported in 2009 by Matthews, Liu, and coworkers.[73] The L99A mutant of T4 lysozyme is known to possess an internalized hydrophobic pocket that selectively binds aromatic hydrocarbons such as benzene. Using X-ray crystallography, neat 1,2-dihydro-1,2-azaborine **82** and N−ethyl 1,2-azaborine **70g** were found to diffuse into the hydrophobic pocket of crystalline L99A lysozyme in an identical manner to benzene and ethylbenzene, respectively. The selective binding of **82** within this hydrophobic pocket is quite interesting given the potential for the N−H group of **82** to undergo non-specific hydrogen bonding with the protein. Thus, 1,2-dihydro-1,2-azaborine effectively acts as a boron-

containing hydrophobic benzene mimic in this specific pocket, and may provide access to the study of 1,2-azaborine in a biological context.

Indole is a ubiquitious heterocyclic motif in nature. It is found free in cells, as part of the amino acid tryptophan and the indole moiety is present in myriad natural products and biologically active compounds. Externally substituted, phenylenediamine-type BN-indole analogs were reported as early as 1957.[74] In 2010, Liu and coworkers reported the syntheses and reactivity of the first internally substituted ("fused") BN-indole derivatives.[75] The synthesis of N-*t*Bu-protected BN-indole **93** is analogous to the route previously describe for monocyclic 1,2-azaborine derivatives (Scheme 1.26). It begins with the condensation of *N*-*t*Bu-*N'*-allylethylenediamine with allylborondichloride generated in situ to generate bis(allyl) species **94**. Ring-closing metathesis was found to proceed in high yield using Schrock's molybdenum RCM catalyst to give bicycle **95**. Both rings were dehydrogenated using Pd/C to give the desired product **93**. Electrophilic aromatic substitution (EAS) reactivity, which is a crucial reaction in the biochemistry of indoles (and one which has not been shown for externally BN substituted indole analogs), was demonstrated for **93**, and as with natural indole, EAS reactions of **93** were regioselective for the 3-position exclusively. EAS competition experiments between **93** and natural indole using dimethylimminum chloride revealed that **93** is significantly more nucleophilic.

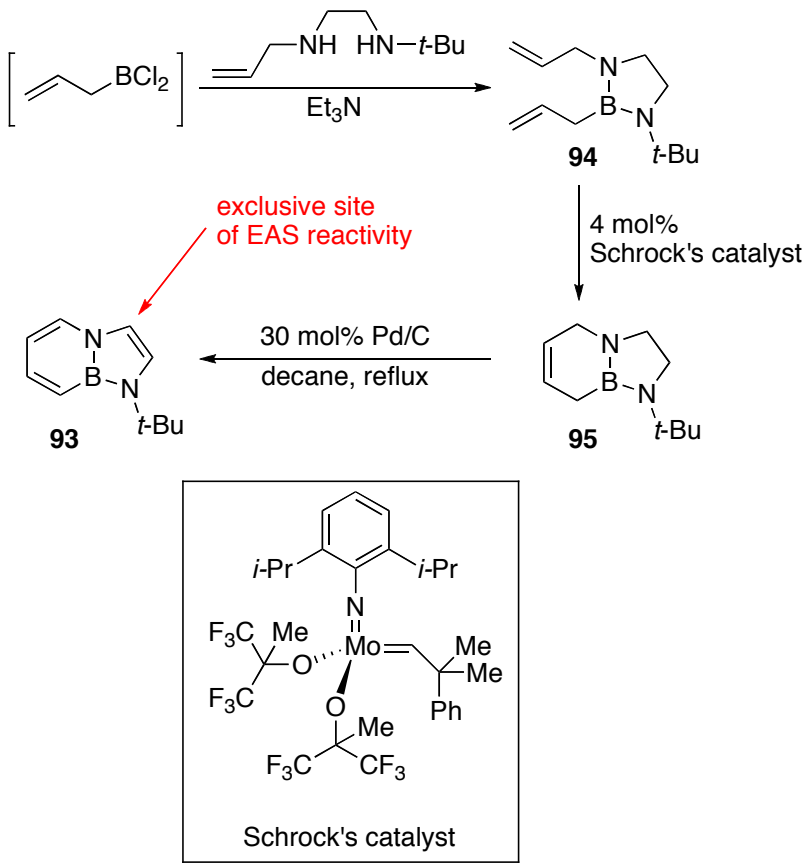

Scheme 1.26. Synthesis of *N*-*t*Bu-BN-indole **93**.

In 2011, Liu and coworkers reported the synthesis of the parent "fused" BN-indole **96**.[76] This molecule contains the free N−H fragment that is an important feature in the biochemistry of indole and its derivatives. Synthesis was similar to the route described above, with a number of key distinctions (Scheme 1.27). First, the use of TBS rather than *t*Bu as a nitrogen protecting group allowed for its facile removal later in the synthesis. Second, the use of Grubbs' first generation catalyst was found to be more effective for the RCM generation of **98** than Schrock's catalyst. Third, the use of perfluorodecalin as the solvent for the oxidation step allowed the aromatic product **99** to be recovered with simple THF extraction rather than distillation. The TBS group could be

removed in the last step using nBu$_4$NF to afford the product **96** in moderate yield. A non-disordered single crystal X-ray structure was obtained by co-crystallization of **96** with ethyl-4-chloro-3,5-nitrobenzoate and revealed **96** to be a planar molecule with bond-lengths consistent with aromatic delocalization. The optical and electronic properties of **96** were probed and compared to natural indole. BN-indole's absorption maximum is red-shifted from that of natural indole (λ = 293 nm vs 268 nm in CH_3CN). The emission maximum is likewise red-shifted for **96** compared to natural indole (λ_{em} = 360 nm vs. 315 nm, in CH_3CN) and displays a greater Stokes shift and lower quantum yield (Φ = 0.08 vs. 0.32 for indole). The red-shifted absorbance and emission maxima are consistent with a smaller HOMO-LUMO gap for **96**. Using ^{1}H NMR bracketing experiments, the pKa of the N–H proton was estimated to be about 30, which is roughly nine orders of magnitude less acidic than natural indole (pKa = 20.95).

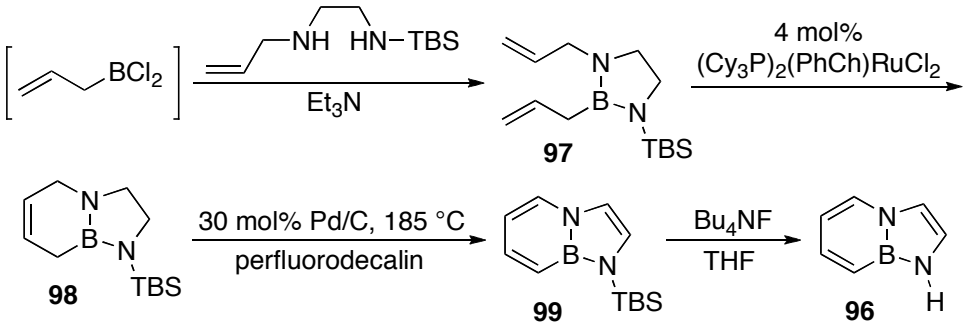

Scheme 1.27. Synthesis of the parent "fused" BN-indole **96**.

Boron-nitrogen containing compounds have received considerable attention as potential hydrogen storage materials owing to their high hydrogen capacity and favorable kinetics of H_2 release. Moreover, calculations suggest that H_2 uptake and release by a

combined CC/BN system should be essentially free-energy-neutral (that is, $\Delta G \approx 0$), potentially allowing efficient H_2 absorption/desorption with minimal energy input. Liu and coworkers have described a system by which 1,2-azaborines can potentially store and release three equivalents of H_2 per molecule (Scheme 1.28). As a proof of concept, they reported the mild regeneration of the "spent fuel" (that is, aromatic, unsaturated) 1,2-azaborine to the "charged fuel" (that is, fully H_2 saturated) amine-borane fuel by the formal addition of three equivalents of H_2.[77]

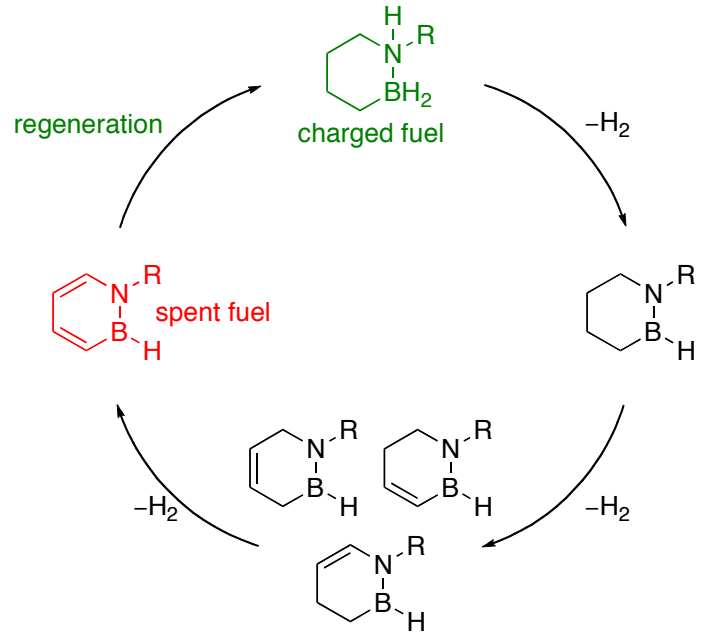

Scheme 1.28. Hydrogen storage by CBN heterocycles.

The first two equivalents of H_2 were added across the formal C=C bonds of **89** using catalytic hydrogenation with Pd/C and H_2 gas to give heterocycle **88** (Scheme 1.29). Under identical conditions, the reduction of benzene was not observed. The third equivalent of "H_2" was added across the B−N bond in a sequential manner. The reaction of KH with **88** installed H^- at the boron atom to give anionic intermediate **100**, which was then treated with HCl to give the fully charged fuel **101**.

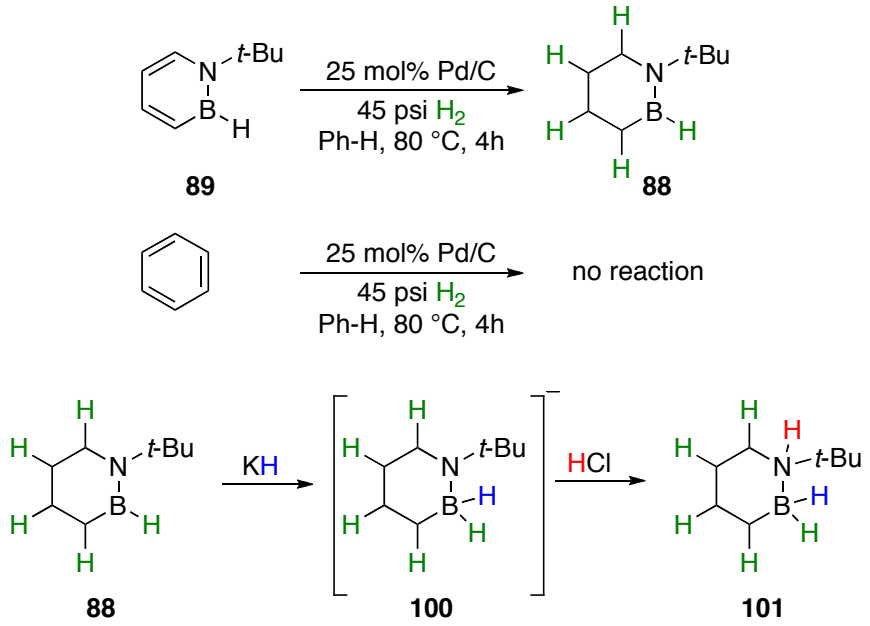

Scheme 1.29. Regeneration of 1,2-azaborine spent fuel **89** by catalytic hydrogenation of C=C bonds and sequential addition of H^-/H^+ across the B−N bond.

As part of their effort to develop a BN-heterocycle based hydrogen storage platform, Liu and coworkers published an alternative route to fully saturated 6-membered BN-heterocycles like **101**, including the parent 1,2-azaboracyclohexane **102** (Scheme 1.30).[78] Treatment of a bistrimethylsilyl-protected homoallylamine with BH_3 THF and subsequent addition of KH gave a monotrimethysilyl-protected BN-cyclohexane potassium salt **103** in moderate yield. Deprotection/protonation with HF pyridine

generated 1,2-azaboracyclohexane **102**. X-ray structural analysis confirmed the assigned structure, which, like cyclohexane, assumes a chair conformation. The free energy of activation for the chair flip was found to be significantly lower for **102** than for the all carbon version (8.8 vs 10.5 kcal mol^{-1}, under identical conditions), attributed to the longer B−N bond length (1.614(1) Å) vs. the C−C bond length in cyclohexane (1.51-1.53(1) Å) and to the shallow potential curve for the B–N stretch. Upon thermal activation (150 °C) **102** underwent a timerization reaction to form **104** with concomitant release of six equivalents of H_2. The conversion was clean and quantitative, in marked contrast to dehydrogenation reactions of ammonia borane ($H_3N{-}BH_3$), which can produce various mixtures of oligomeric products depending on the dehydrogenation conditions used. Clean dehydrogenation to a well-defined single product using mild conditions make **102** a promising material for hydrogen storage. Additionally, the moderate hydrogen capacity of 4.7 wt.% can potentially be increased to 9.4 wt.% if the H_2 release from BN can be coupled with dehydrogenation from the carbon positions as well.

In a further refinement of the intramolecular hydroboration/cyclization medthodolgy described above, Liu and coworkers recently disclosed the synthesis of BN-methycyclopentane material **105** (Scheme 1.31).[79] This material is liquid at room temperature and can release hydrogen using cheap metal halide catalysts (for example, $FeCl_2$) at 80 °C, which are both very desirable properties for potential hydrogen storage materials.

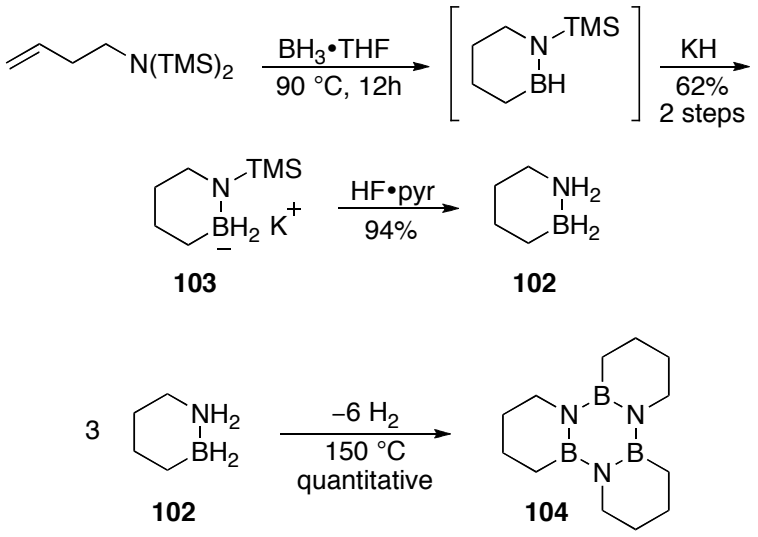

Scheme 1.30. Synthetic route to 1,2-azaboracyclohexane **102** and dehydrogenation/trimerization to form **104**.

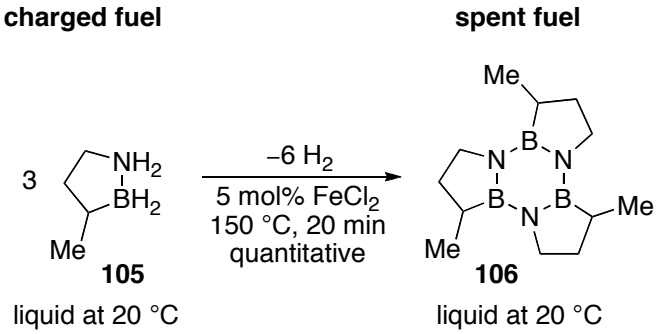

Scheme 1.31. Liquid hydrogen storage material based on BN-methylcyclopentane **105**.

As part of their effort to develop π-conjugated azaborine optical materials, Liu and coworkers reported the synthesis and characterization of the BN analog of diphenylacetylene (tolan; Scheme 1.32).[80] Synthesis of BN-tolan **107** and bis(BN)-tolan **108** was achieved by reaction of the known TBS-protected precursor **78** with either phenylethynylmagnesium bromide or the Grignard reagent **109**. The resulting compounds were deprotected using a Cr-complexation route analogous to that used in the parent 1,2-

dihydro-1,2-azaborine synthesis (see Scheme 1.23). Single crystal X-ray analysis revealed both compounds **107** and **108** to be linear with respect to the B−C≡C−X axis with a coplanar orientation of the aromatic rings, which is indicative of significant π-overlap throughout the bicycle. The other noteworthy feature of the crystal structure was the observation dimers formed through a rarely seen N−H−π(C≡C) hydrogen bonding interaction. UV/Vis absorance maxima for **107** and **108** are centered at 299 nm and are broadened relative to tolan. Emission maxima in THF for **107** and **108** are 350 nm (Φ = 0.012) and 388 nm (Φ = 0.020), respectively, which are significantly red-shifted from tolan (317 nm, Φ = 0.007); the emissions display minimal solvatochromism.

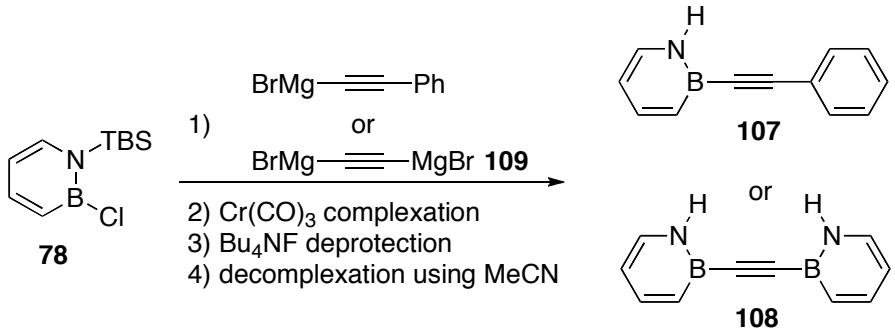

Scheme 1.32. Synthesis of BN-tolan analogs **107** and **108**.

One of the most exciting recent developments to emerge from the Liu group is the disclosure of the first example of a 1,3-azaborine.[81] This significant synthetic achievement was accomplished by harnessing the power of ring-closing metathesis and tin chemistry previously developed in the Liu group, with several substantial modifications (Scheme 1.33). The stannane reagent **110** was produced in two steps from allylmethylamine, formaldehyde and benzotriazole. Direct transmetallation between **110**

and the vinylboron chloride **111** was unsuccessful, however lithium-tin exchange followed by addition of the electrophile **111** afforded the RCM precursor **112** in modest yield. Both Grubbs' first generation and Schrock's catalysts failed to cyclize **112**, presumably due to degradation of the catalyst caused by the relatively nucliophilic amine. This was overcome by first forming the ammonium salt of **112** with triflic acid, closing the ring using Grubbs' first generation catalyst, and finally deprotonating the ring-closed ammonium salt with DBU to furnish **113**.

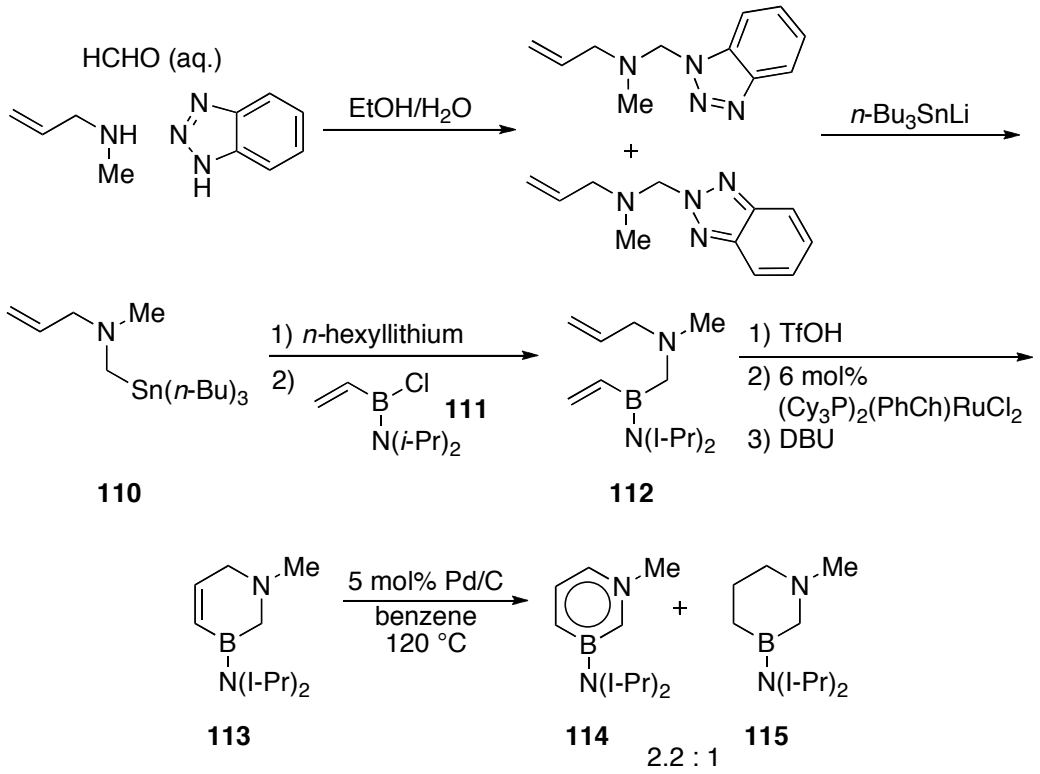

Scheme 1.33. Synthesis of the first 1,3-azaborine **114**.

Dehydrogenation of **113** to generate the aromatic final product also proved to be a challenge, with significant formation of fully reduced species **114** (2.2:1 **114**/**115**) observed even under optimized conditions. The desired product was isolated by

distillation and fully characterized. Single crystal X-ray analysis revealed that the 1,3-azaborine ring is completely planar, with intra-ring bond-lengths consistent with electron delocalization. To further probe the aromatic nature of the 1,3-azaborine ring, **114** was treated with $[Cr(CO)_3(MeCN)_3]$ to generate the piano-stool complex. A close inspection of the crystal structure of the complex showed that it is best characterized as an η^5 π-complex in which the boron atom does not participate, as it lies 0.21 Å above the root-mean-square of the plane containing the other five atoms. Compound **114** was found to be inert to a variety of nucleophiles, but reacts with acetic acid to form a B−OAc adduct. Electrophilic aromatic substitution reactivity was also probed, and **114** was found to undergo EAS regioselectively in the presence of dimethyl(methylene)ammonium chloride.

1.6. The Perepichka Group – McGill University

In 2010 Perepichka and coworkers investigated the incorporation of 1,2-azaborines into oligothiophene organic electronic materials.[82] Structurally related thienoazaborine and dithienoazaborines have been reported, but their optoelectonic properties were not explored in depth. The addition of boron into conjugated systems has been shown to increase luminescence efficiency and improve light-emitting properties of a material.[83] The Lewis acidic boron centers have typically been stabilized through steric screening using bulky aryl substituents, but in the solid state these groups can suppress π-stacking critical to intermolecular charge transfer. In 1,2-azaborines the boron center is stabilized through orbital interactions with a lone pair of electrons from the adjacent nitrogen atom and the resulting planar molecules should not interfere with π-stacking.

Treatment of known diaminothiophene **116** with excess $PhBCl_2$ (a synthetic strategy reminiscent of Dewar's early work) afforded bis(azaborine) **117** (Scheme 1.34). It was anticipated that the strong acidity of the N−H protons could be problematic for the intended applications or further functionalization, so the ethylene-linked species **120** was synthesized by boryation of the ethylenediaminothiophene compound **119**. The ethylene linker does not distort the planarity of the ring system. X-ray crystallographic analysis of **117** and **120** revealed B−N bond lengths of 1.405-1.460 Å, similar to other reported azaborines and consistent with electron delocalization in the azaborine ring. The structures were almost planar with regard to thiophene rings, however the phenyl rings lie out of the plane, limiting their conjugation with the polycyclic moiety. Both compounds formed slipped π-stacks with alternating head-to-tail orientation and interplanar distances between the parallel thiophene ring systems of 3.47−3.83 Å.

Analysis of UV/vis absorption spectra for **117** and **120** revealed that the ethylene bridge does not significantly affect the electronic structure; both compounds display almost identical absorption spectra (λ_{abs} = 395 and 397 for **117** and **120**, respectively). λ_{max} for **117** and **120** is red-shifted compared to non-fused terthiophene (354 nm) and S-bridged pentathienoacene (357 nm). Compounds **117** and **120** exhibit deep-blue photoluminescence at λ_{max} = 407−410 nm, with Φ_{PL} = 25−34%. Redox properties for the two compounds were studied by cyclic voltammetry. Both compounds undergo irreversible electrochemical oxidation with anodic peak potential E_{pa} at 0.48 V vs. $[Cp_2Fe]/[Cp_2Fe]^+$, ca. 0.2 V more positive than diaminoterthiophene and consistent with the electron withdrawing effects of boron.

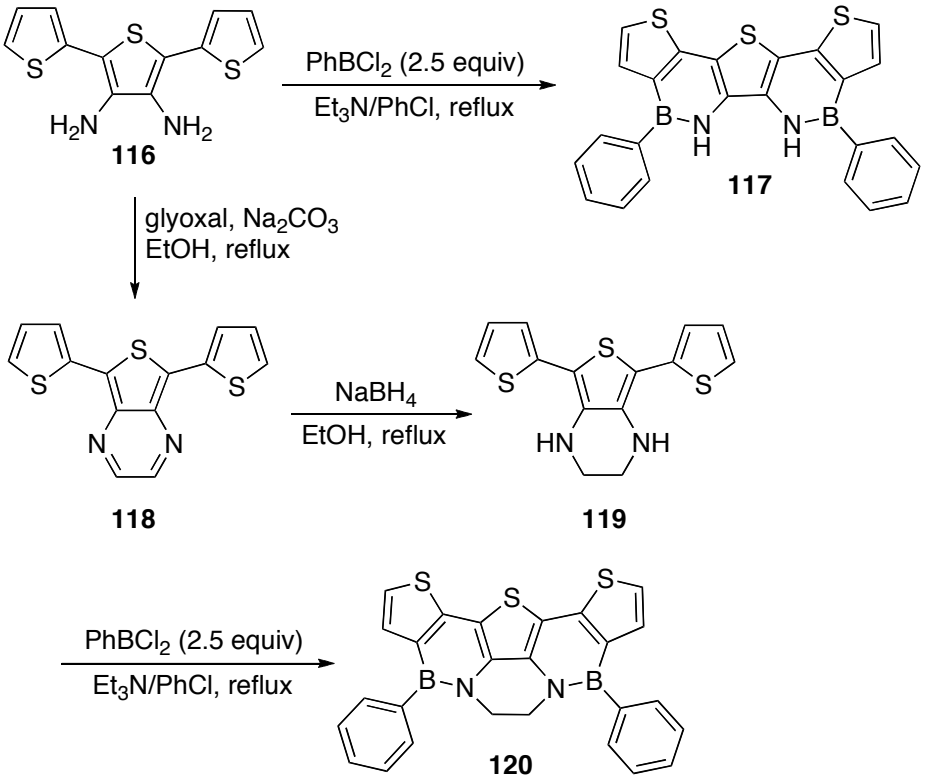

Scheme 1.34. Synthesis of 1,2,-azaborine-fused oligothiophene materials **117** and **120**.

The stabilizing effect of the intramolecular Lewis acid-base interaction between nitrogen and boron was probed by introducing weak to moderate Lewis bases to solutions of **117** and **120**. No complexation was detected with H_2O, THF, amines, Cl^-, Br^-, I^-, OH^-, or OCH_3^-. However, addition of Bu_4NF to solutions of **120** led to the formation of a mono-fluoride adduct, even in the presence of a very larges excess of F^-. The binding constant (log K_a = 3.3 ± 0.1 in CH_2Cl_2) is lower than that of triarylboranes without electronic stabilization of the empty p-orbital (for example, log K_a = 6.3 for dithienylmesitylborane in CH_2Cl_2). The emission band of the fluoride adduct is red-shifted to 540 nm with a corresponding color change from blue to green observable by the naked eye. While fluoride sensing by conjugated boron derivatives is well known,

most systems are characterized by a blue-shift of the absorbance and quenching of the fluorescence. The authors propose that systems based on **120** could be used as an "off-on" sensor for F^-.

In a subsequent report, Perepichka and coworkers subjected the compounds **117** and **120** to higher oxidation potentials and discovered interesting electropolymerization reactivity that ultimately led to the expulsion of boron and the formation of a low band-gap polymer.[84] Through careful isolation of partially deborylated donor-acceptor oligomer intermediates **121** and **122** and comprehensive spectroscopic characterization, they were able to elucidate the composition of the insoluble polymer **123**. The proposed formation of electrochemical products is illustrated in Scheme 1.35.

Controlled potential electrolysis of solutions of **117** was performed at 100 mV more positive than the first oxidation wave. During the first oxidation process, boron elimination and the formation of a new C−C bond between the thiophene and phenyl ring occurs to give species **121**. The first oxidation process of **121** does not lead to boron elimination but instead to a radical coupling process to form the dimer **122** (as in usual thiophene polymerzation). Exposing **122** to high potential (1.07 V vs. $[Cp_2Fe]/[Cp_2Fe]^+$) led to the formation of polymer films analogous to those grown directly from **117**.

The optical properties of **121** and **122** were probed by UV/Vis and fluorescence spectroscopy. **121** displays blue-shifted absorption (λ_{max} = 352 nm, log ε = 4.1) compared to the starting material **117** (λ_{max} = 391 nm), attributed to an out-of-plane shift of the deborylated thiophene ring. **122** has a red-shifted absorption compared to both **117** and **121** (λmax = 420 nm, log ε = 4.0) due to extended π-conjugation. The fluorescence spectra of **121** and **122** exhibit large Stokes shifts of 0.9 and 0.6 eV (6950 and 5013 cm^{-1}),

respectively, which points to large structural rearrangements in the excited state. The emission color shifts from deep-blue for **117** to sky-blue for **121** to bright-green-yellow for the dimer **122**.

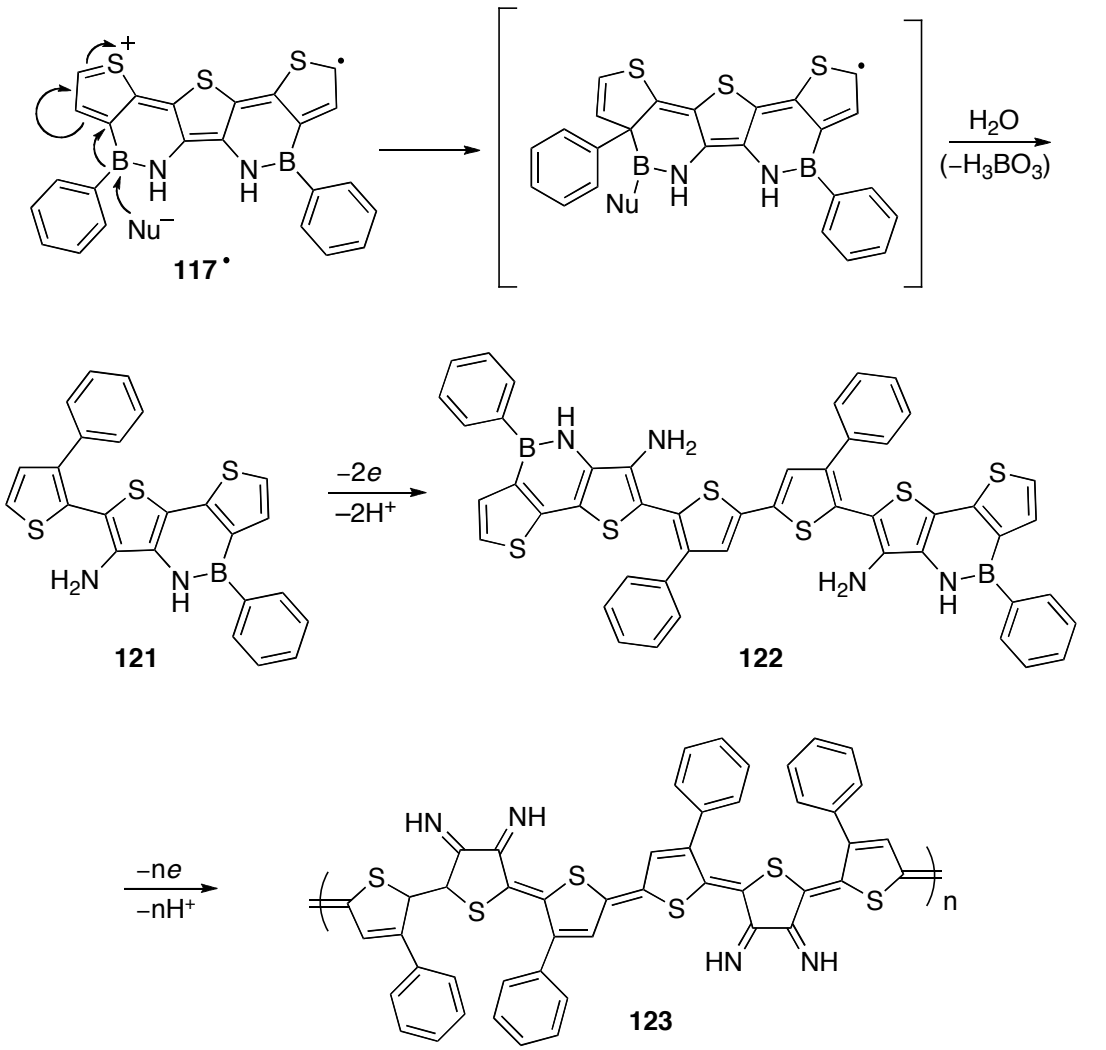

Scheme 1.35. Proposed formation of deborylated polymer **123** from **117** via intermediates **121** and **122**.

1.7. The Yamaguchi Group – Nagoya University

Yamaguchi and coworkers recently reported the synthesis of 1,2-azaborine in an extended π-conjugated system, unexpectedly obtained in the course of their studies of triarylborane-based functional materials.[85] Attempts to remove the Boc protecting group from triarylborane species **124** by treatment with $BF_3 \cdot OEt_2$ in refluxing THF led to a complex mixture of products (Scheme 1.36). Careful separation using preparative gel permeation chromatography enabled the isolation of migratory ring expanded product **125** in 13% yield along with products (totalling 60% yield) resulting from the cleavage of the pyrrole-boron bond. Seizing the opportunity to investigate the potential utility of 1,2-azaborine as a building block in π-conjugated materials, structural, photophysical and electrochemical studies of **125** were undertaken and the results were compared with the all carbon analog **126**.

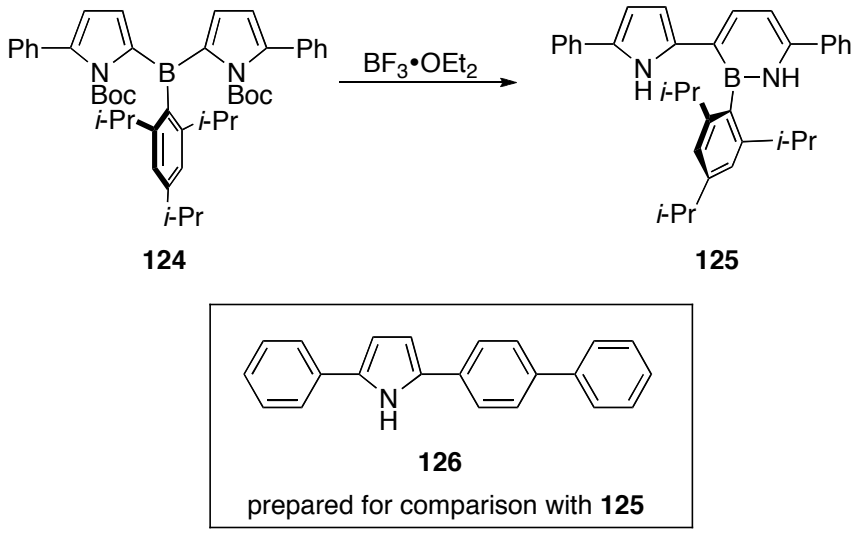

Scheme 1.36. Synthesis of π-congugated 1,2-azaborine material **125**.

Two crystallographically independent molecules of **125** exist in a unit, with reasonably coplanar π-conjugated skeletons. Dihedral angles between the pyrrole and the azaborine and between the azaborine and the phenyl group are in the range of 7-14° and 30-34°, respectively. The bulky 2,4,6-triisopropylphenyl (Tip) group does not impede π-conjugation over the framework, but prevents intermolecular π-π interactions. Analysis of bond lengths in the azaborine portion of **125** revealed that the B−N moiety has less double bond character than an isolated B−N bond due to π-conjugation in the azaborine ring, however the extension of the π-conjugation at the 3- and 6-positions may decrease the aromatic character of the azaborine ring compared to non-π-extended 1,2-azaborines.

In CH_2Cl_2, UV/Vis absorbance and fluorescence maxima for **125** are red-shifted from the all-carbon analog **126** by 57 and 70 nm, respectively. Both compounds show only subtle solvatochromism in both the absorbance and emission spectra. **125** has very high quantum yields, close to unity even in polar solvents like MeOH and significantly higher than **126**.

Cyclic voltametry experiments performed on **125** and **126** indicate a higher HOMO level and a narrower HOMO–LUMO gap for **125**, consistent with the red-shifted absorption maximum. The authors reasoned that the differences in the redox potential and photophysical properties between **125** and **126** are due to the nonaromatic character of the azaborine ring. In this context, the azaborine ring can be considered a cyclic butadiene analog and, in fact, DFT calculations at the B3LYP/6-31G(d) level revealed that the frontier orbital energy levels of **125** are more similar to a cyclohexa-1,3-diene model than the benzene-containing **126**. NICS(0) calculations performed on the 1,2-

azaborine ring in **125** were slightly more positive (δ = −4.73 ppm) than the parent 1,2-azaborine (δ = −5.10 ppm), which is indicative of decreased aromaticity.

1.8. The Kawashima Group – University of Tokyo

Kawashima and coworkers have explored the incorporation of the 1,4-azaborine motif into anthracene and ladder-type pentacene and heptacene analogs, with the goal of utilizing these compounds in OLED devices.[86] The synthesis of BN-pentacene **128** was achieved by treatment of the para-diamino arene **127** with $MesB(OMe)_2$ (Scheme 1.37). Similar transformations from meta-diamino arene **129** and triaminoarene **131** generated **130** and **132**, respectively. All three compounds were air- and moisture-stable, which was ascribed in part to the sterically demanding mesityl substituents at boron.

The X-ray crystal structure of **128** revealed that the BN-pentacene framework is virtually co-planar, indicating an extended π-conjugated system. No evidence of intermolecular π-stacking was observed due to the bulky mesityl groups, which interfere with close packing. The absorption and emission properties of **128**, **130** and **132** were examined and are summarized in Table 1.4. The absorption and emission maxima observed for **128** and **132** are red-shifted relative to BN-anthracene, which is consistent with extended conjugation. On the other hand, BN-pentacene **130**, in which the 1,4-azaborine rings are oriented parallel to each other, displayed optoelectronic properties which were very similar to BN-anthracene.

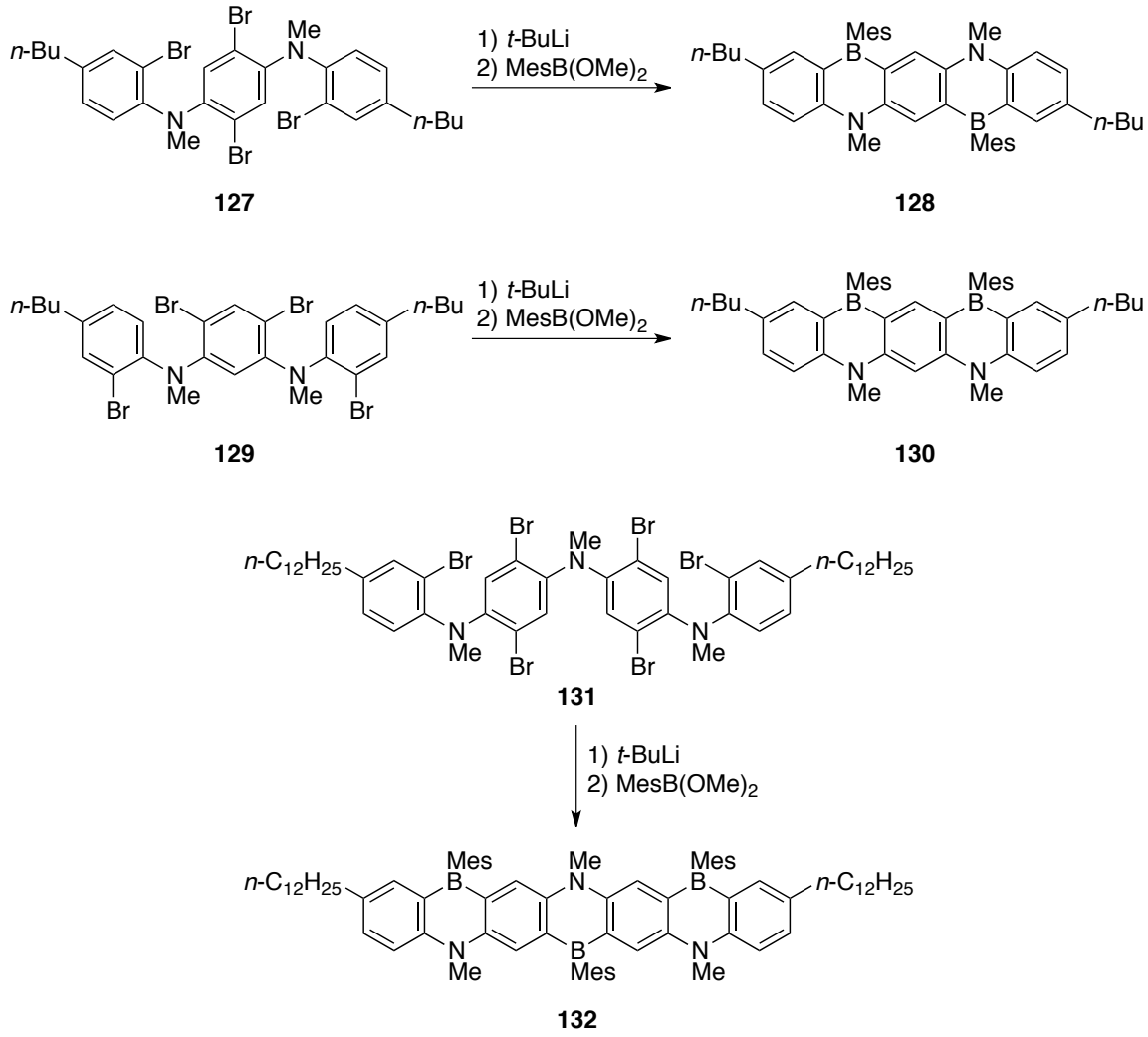

Scheme 1.37. Synthesis of BN-pentacene isomers **123** and **125** and BN-heptacene **127**.

Table 1.4. Photophysical properties of BN-acenes.

compound	λ_{max} (nm) / log (ε)	λ_{em} (nm)	Φ
127	523 / 4.23	534	0.69
130	415 / 3.94	428	0.21
132	608 / 4.28	625	0.55

After their initial report on BN-pentacene and heptacene analogs, Kawashima and coworkers developed a more general route to substituted 1,4-azaborine containing anthracene as well as previously described anti-parallel pentacene derivatives (Scheme 1.38).[87] An *ortho*-selective dilithiation of **133** and subsequent treatment with arylbroronic esters generated dibromo-substituted products **134**, which could be further elaborated via Buchwald-Hartwig amination, Sonogashira cross-coupling or lithium-halogen exchange/electrophile addition (MeI) to give products **135**−**137**. The same protocol could be expanded to the synthesis of ladder-type azaborines via tetralitiation of **138**. The bromonated product of this reaction, compound **139**, could not be isolated due to poor solubility; however solublizing groups could be added to the crude mixture and the substituted BN-pentacene compounds **140a**−**c** could be isolated in moderate yield.

UV/Vis spectra for compounds bearing electron-donating amino groups (that is, HexNH in **135a** and Ph_2N in **135b**) showed red-shifted absorptions relative to the reference compound, Me-substituted **137a**, due to elevation of the HOMO level. The carbazolyl-substituted BN-anthracene **135c** had an absorption wavelength close to the reference compound and had a fluorescence quantum yield of unity, attributed to molecular rigidity. The ladder-type azaborines **140a**−**c** displayed similar absorbance properties, with red-shifted absorption maxima corresponding to increasing electron donating ability of the pendant amine groups. The carbazolyl substituted derivative **140c** also showed the highest fluorescence quantum yield.

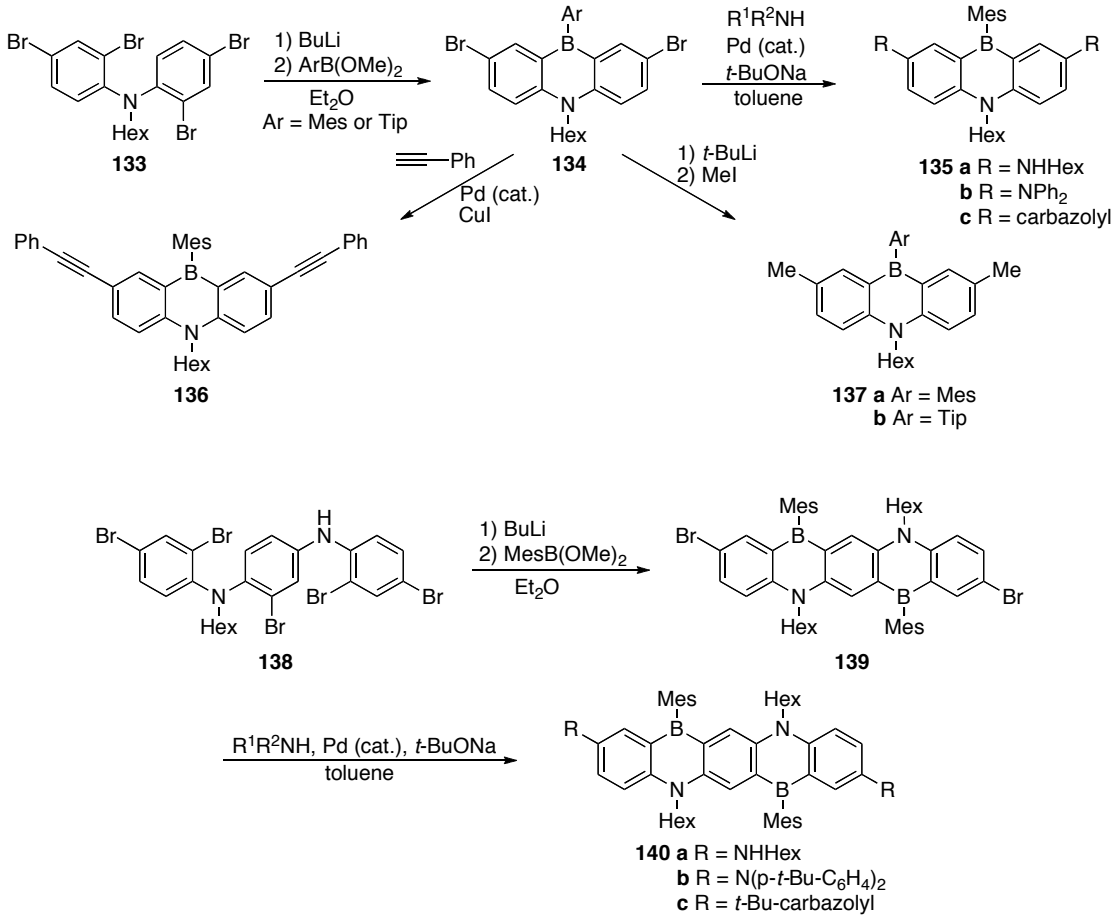

133

134

135 a R = NHHex
b R = NPh_2
c R = carbazolyl

136

137 a Ar = Mes
b Ar = Tip

138

139

140 a R = NHHex
b R = N(p-*t*-Bu-C_6H_4)$_2$
c R = *t*-Bu-carbazolyl

Scheme 1.38. General route to BN-anthracenes **135**–**137** and BN-pentacenes **140a**–**c**.

In a subsequent report, Kawashima and coworkers utilized the same general reaction sequence to develop dicationic ammonium and phosphonium functionalized BN-acenes **141** and **142**, capable of acting as fluorescent sensors for biologically relevant anions such as fluoride and cyanide (Scheme 1.39).[88] These compounds retain the optical properties of the azaborine motif and do not aggregate in aqueous media. The complexation ability of ammonium functionalized species **141** with all anions screened was too weak to observe by UV/Vis or fluorescence spectroscopy; however the phosphonium species **142** displayed a very high affinity for the cyanide ion and was

almost inactive against other environmentally common anions under the testing conditions. Titration experiments were used to find the complex formation constant between **142** and the cyanide ion (1.2(4) × 10^5 M^{-1} in DMSO/H_2O (4:6 v/v) and 5.2(5) × 10^4 M^{-1} in 100% H_2O). Fluorescence quenching experiments with various anions revealed that only CN^- quenched the emission of **142** to a degree that was clearly observable with the naked eye.

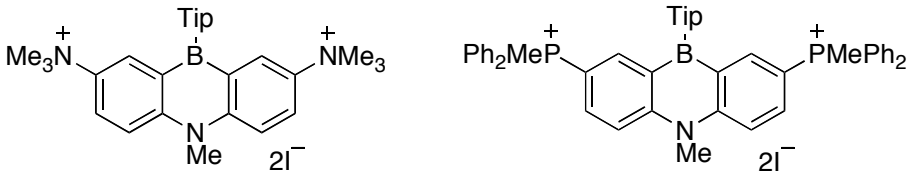

141 **142**

Scheme 1.39. Dicationic BN-anthracenes **141** and **142**.

Around the same time, Kawashima and coworkers reported the synthesis and fluoride sensing ability of a bis(dimesitylboryl)azaborine **143**, again taking advantage of the general synthetic methodology they had previously developed (Scheme 1.40, series **a**).[89] Their rational for the introduction of strong π-acceptors (that is, Mes_2B) into the 1,4-azaborine framework was two-fold: First, the Mes2B group decreases the LUMO energy level, thus increasing the Lewis acidity of the azaborine unit. Second, coordination of multiple Lewis bases to the peripheral boron atoms (in addition to the azaborine boron center) can alter the donor–acceptor interactions within the molecule and thus vary the absorption and emission color based on the amount of guest ion. The introduction of dimesitylboryl groups resulted in a hypsochromic shift in the absorbance maximum (377 nm vs. 405 nm for the N−Me derivative of **137a)** and an about tenfold increase in the

extinction coefficient. To investigate the Lewis base detection ability, **143** was treated with excess nBu$_4$NF and monitored by FAB mass spectrometry and ^{11}B NMR. Signals consistent with the formation of **144a** and **145a**, rather than **146a** were observed (that is, shifting of the peak corresponding to Mes$_2$B groups but not the azaborine peak). This conclusion was supported by molecular orbital calculations, which show that the LUMO is distributed over the two Mes$_2$B groups, kinetically favoring Lewis base coordination at those sites. UV/Vis titration of **143** with nBu$_4$NF showed the stepwise formation of **144a** and **145a** and the values of K_1 and K_2 were determined to be $>10^8$ M^{-1} and 7×10^5 M^{-1}, respectively. Fluorescence spectrometry could also be used to monitor complex formation and it was possible to detect the fluoride ion at sub-micromolar concentrations. However, because of the much smaller value of K_2 than K_1, the blue-shifted emission band corresponding to species **145a** was only visible upon addition of a large excess of fluoride ion.

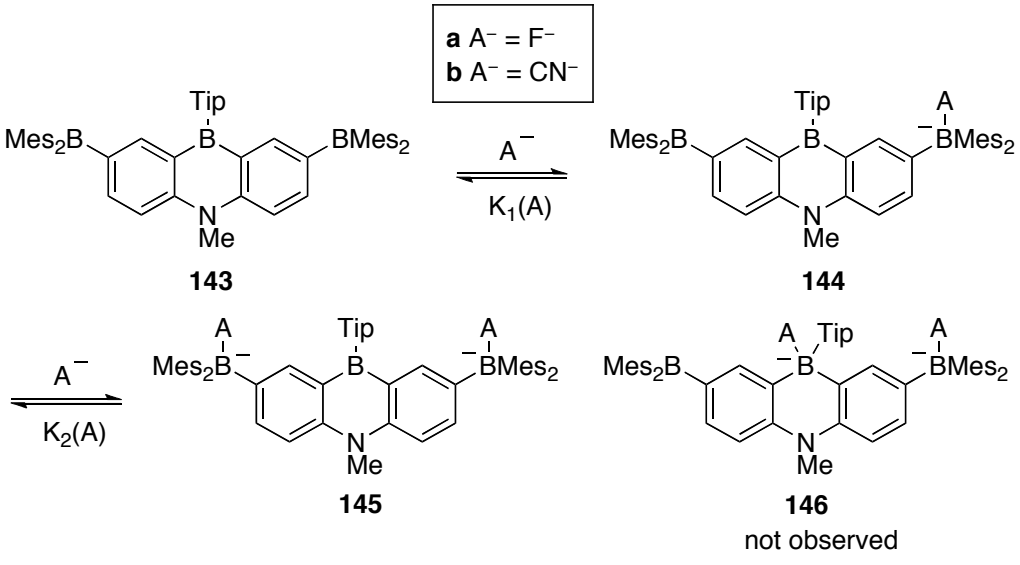

Scheme 1.40. Multistep F$^-$ and CN$^-$ anion sensing with bis(dimesitylboryl)azaborine **143**.

In another report published in 2009, Kawashima and coworkers used the bis(dimesitylboryl)azaborine **143** for multistep detection of the cyanide ion (Scheme 1.40, series **b**).[90] In the case of CN^-, the values of both K_1 and K_2 exceed the limit of precise estimation ($>10^8$ M^{-1} in THF), thus the cyanide ion seems to form a much stronger complex with **143** than the fluoride ion does, despite boron's affinity for fluoride. The fluorescent color shift from violet (λ = 420 nm) corresponding to the monocyanoborate species **144b** to blue (λ = 433 nm) corresponding to dicyanoborate **145b** was visible with the naked eye upon addition of just 2.6 equiv of CN^-.

The Kawashima group has also reported the construction of π-conjugated dendrimeric structures based on a 1,4-BN-anthracene branching unit that features additional pendant BN-acene groups (Scheme 1.41).[91] Conjugated dendrimers bearing both electron donors and acceptors are expected to show n-type or ambipolar charge transfer ability, both of which are important in organic field-effect transistors. Both the branching and terminal BN-acene moieties were synthesized in a similar manner to the compounds described above, and the dendron arms were synthesized by Pd-catalyzed coupling reactions between branching and terminal units. The optical properties of the dendrons are similar to those of the parent azaborines, indicating that the azaborine units are aligned perpendicularly to each other. Dendrimers **147**−**149** were constructed from TMS-protected dendrons using standard Sonogashira conditions. Emission from the dendrimers stems from an intramolecular charge transfer (ICT) between the dendrons and the core. DFT calculations suggest that electron transfer from the dendrons to the core is

thermodynamically favorable process, but experimental results indicate that the fate of the ICT excited states strongly depends on the generation of the dendron.

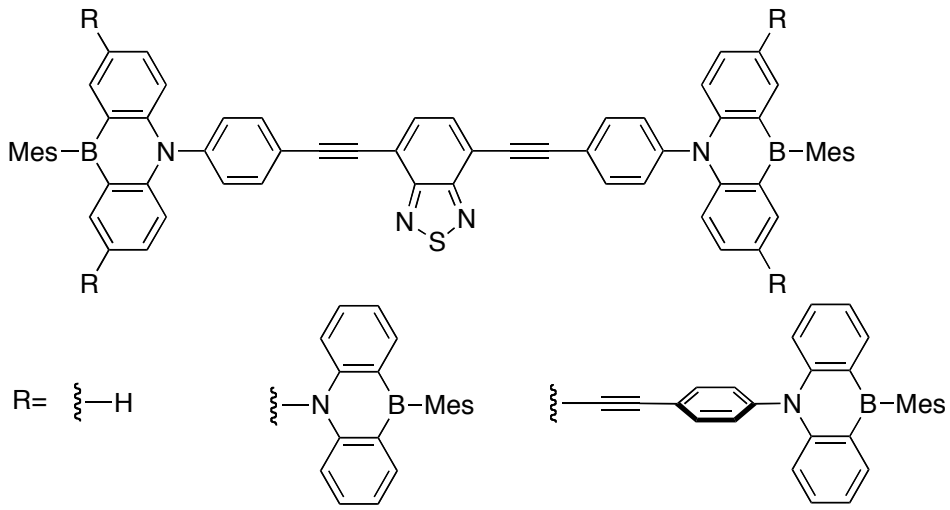

Scheme 1.41. π-Conjugated dendrimers based on BN-anthracene.

In 2010 Kawashima and coworkers reported the synthesis of a dinaphthoazaborine based on a modification of their general synthetic methodology (Scheme 1.42).[92] Dilithiation of the dibromoamino species **150** with subsequent addition $MesB(OMe)_2$ at −78 °C afforded dinaphthoazaborine **151**. Analysis of the single crystal X-ray structure of **151** showed that the dinaphthoazaborine skeleton is butterfly-like and the angle between the two naphthalene rings is 15°, compared to the 9° (average) bent angle between the two benzene rings of the N–Me derivative of **137a**. In contrast to **137a**, there are clear intermolecular π–π and CH–π interactions between molecules of **151** in the solid state, which affect its solid-state fluorescence properties. In hexanes, the UV/Vis absorbance maximum for **151** (λ = 519 nm) is red-shifted by 114 nm from that of **137a**,

indicating elongation of the π-system and a decreased HOMO–LUMO energy gap. Emission maximum of **151** is red-shifted by 103 nm, however the quantum yield is lower than that of **137a**. Also, unlike **137a**, **151** does not show detectable solid-state fluorescence. Electrochemical analyses revealed that 151 forms a stable radical anion at relatively low potential (−2.1 V vs. $[Cp_2Fe]/[Cp_2Fe]^+$), which could lead to possible applications as an electron-acceptor and anion sensor.

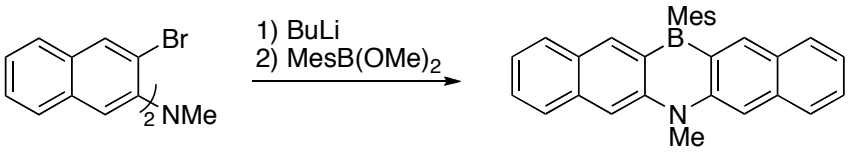

150 **151**

Scheme 1.42. Synthesis of dinaphthoazaborine **151**.

1.9. The Nakamura Group – Kyoto Univeristy

Hatakeyama, Nakamura and coworkers very recently reported an efficient route to BN-fused analogs of polycyclic aromatic hydrocarbons (PAHs), based on a tandem intramolecular electrophilic arene borylation protocol (Scheme 1.43).[93] Facile access to this structural motif allowed them to characterize these materials with an eye toward potential applications in organic electronic functional materials. The arene borylation precursor, dichloroboraneamine **153** was generated in situ from bis(biphenyl-2-yl)amine **152**). After screening a variety of Lewis acids and Brønsted bases, it was found that treatment of **153** with 4 equivalents of $AlCl_3$ and 1.5 equivalents of 2,2,6,6-tetramethylpiperidene (TMP) afforded the BN-PAH **154** in 67% yield. It was also determined that the $AlCl_3$/TMP stoichiometry is critical to achieving a high yield. The

same optimized conditions could be used to generate the bis(BN)-fused PAH **156** from starting amine **155**.

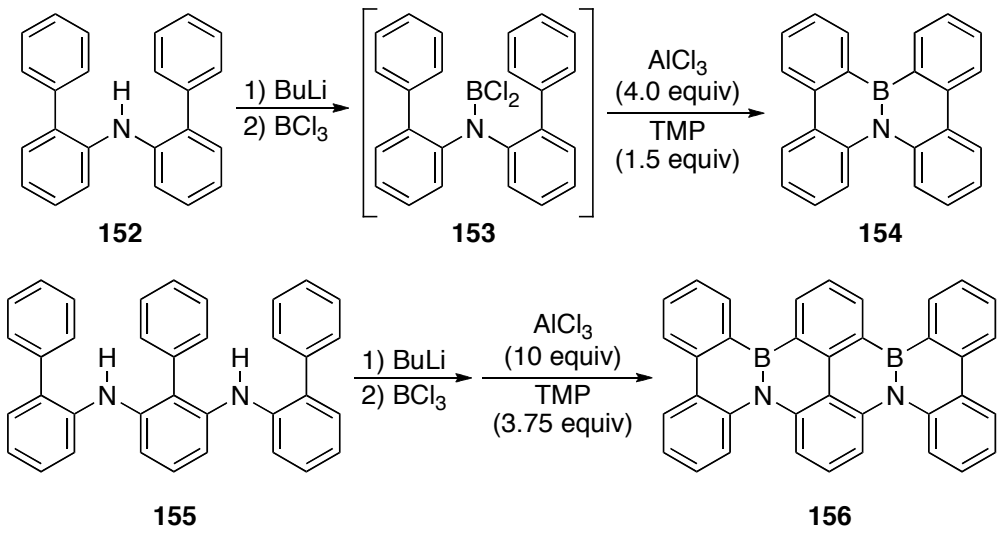

Scheme 1.43. Synthesis of BN-fused polyaromatics **154** and **156**.

The X-ray crystal structure of **154** revealed that the B–N bond-length (1.426(3) Å) is shorter than typical BN-aromatics (1.45–1.47 Å) and more consistent with a B=N double bond. B–C and N–C bond-lengths are consistent with single bond character. The low apparent aromaticity of the azaborine ring is in agreement with the calculated NICS(1) value of –2.9. In the solid state, **154** adopts a twisted configuration at the heteroatom bridge and an alternating enantiomeric (that is, left- or right-handed) helical packing structure. The all-carbon analog of **154**, dibenzo[*g,p*]chrysene, was also analyzed by X-ray crystallography and displayed remarkably similar solid state parameters (for example, twisted structure with significant double bond character of bridging C−C bond) and similar physical properties, including melting point (229 °C vs. 227 °C for **154**). However, the solubility of **154** was much higher than dibenzo[*g,p*]chrysene in common

organic solvents, presumably due to its dipole moment. Surprisingly, despite its extended polycyclic aromatic structure, **156** was found to be moderately soluble in organic solvents such as chloro- and 1,2-dichlorobenzene.

Using time-resolved microwave conductivity measurements, **154** was found to have high intrinsic hole mobility (0.07 $cm^2\ V^{-1}s^{-1}$), ten times higher than dibenzo[*g,p*]chrysene, and rivalling rubrene (0.05 $cm^2\ V^{-1}s^{-1}$), one of the most popular organic semiconductors. The superior hole mobility of **154** was attributed to partial localization of the frontier orbitals induced by BN-substitution, which strengthens the electronic coupling between neighboring atoms in the solid state. The favorable electronic properties, straightforward synthesis and surprising solubility make **154** and **156** suitable for use in organic electronics.

1.10. Emerging Applications and Future Directions

From the breadth of synthetic approaches and novel reactivity presented herein it is clear that the ubiquity of the arene motif coupled with the unique properties stemming from BN/CC isosterism present no shortage of potential applications for this chemistry. BN incorporation into aromatic scaffolds can lend favorable properties to organic optoelectronic materials and create highly selective molecular ion sensing platforms. The dual hydridic/protic nature of B−H/N−H bonds can be harnessed for chemical hydrogen storage. BN/CC isosterism can also be used as a way to "disguise" boron for potential biological applications. The study of BN-aromatic compounds can also enrich our fundamental understanding of aromaticity itself. Emerging synthetic techniques

stemming from this research may further expand the toolkit available to curious chemists in other fields as well.

CHAPTER II

HYDROGEN STORAGE BY BORON–NITROGEN HETEROCYCLES: A SIMPLE ROUTE FOR SPENT FUEL REGENERATION

2.1. General Overview

This chapter describes a potentially reversible hydrogen storage system based on 1,2-azaborine. A model spent fuel compound is synthesized and "regenerated" by catalytic hydrogenation of the carbon-carbon bonds followed by sequential hydride/proton addition to the boron-nitrogen bond. This chapter contains previously published material: Campbell, P. G.; Zakharov, L. N.; Grant, D. J.; Dixon, D. A.; Liu, S.-Y. *J. Am. Chem. Soc.* **2010**, *132*, 3289–3291. I preformed all the lab work, Daniel J. Grant and David A. Dixon provided computational data, Lev N. Zakharov provided single-crystal X-ray analysis, and Shih-Yuan Liu provided editorial assistance and scientific guidance.

2.2. Introduction

The efficient and safe storage of hydrogen is a crucial component for the development of a hydrogen-based energy infrastructure.[1] Consequently, various hydrogen storage approaches are currently being investigated, including metal hydrides,[2] sorbent materials,[3] and chemical hydride systems.[4,5] Boron- and nitrogen-containing chemical hydrides have attracted much attention because of their high gravimetric hydrogen densities and fast kinetics of hydrogen release. Ammonia borane ($H_3N–BH_3$ or AB) is a

very promising candidate among the chemical hydride materials, exhibiting a gravimetric density of 19.6 wt % H_2.[6] While the release of H_2 from AB and its derivatives has been extensively investigated in the recent past,[7–15] the issue of spent fuel regeneration has received less attention.[16,17] This is arguably due to the complicated and ill-defined nature of the various spent fuel products from AB dehydrogenation. It has been reported that depending on dehydrogenation conditions, monomeric BN heterocycles (for example, cyclotriborazene, cyclopentaborazane, and borazine), polymeric amino- or iminoboranes, and/or polyborazylene materials can be generated.[4] In recent reports, Gordon, Dixon, and co-workers[18] elegantly demonstrated that polyborazylene spent fuel can be converted back to AB in a three-step protocol using benzenedithiol as the digestion reagent and nBu$_3$SnH and nBu$_2$SnH$_2$ as reductants.

Recyclability (that is, spent fuel regeneration) is critical to the success of any hydrogen storage system. The ideal reductant for regenerating any spent fuel would be molecular hydrogen itself. Our research group has been focusing on developing new chemical hydrogen storage materials that (a) are well-defined molecular species throughout the entire fuel lifecycle, (b) possess high H_2 storage capacities, (c) exhibit an appropriate enthalpy of H_2 desorption conducive to regeneration by H2, and (d) are liquids at operating temperatures.

Scheme 2.1 illustrates the proposed fuel cycle of our material. The charged fuel (highlighted in green) is a BN-heterocyclic analogue of cyclohexane, which upon release of 3 equiv of H_2 produces the spent fuel material, an aromatic BN heterocycle analogous to benzene (highlighted in red). As can be seen from Scheme 2.1, the charged and spent fuel and the potential intermediates are well-defined molecular compounds. Furthermore,

we have determined that the spent fuel and partially dehydrogenated intermediates are low-melting liquids (for R = *t*Bu, the melting points are below –30 °C). With regard to the thermodynamics of hydrogen release/uptake, we have predicted that the coupling of exothermic dehydrogenation from B–N bonds [e.g., dehydrogenation of AB is exergonic by –13.6 kcal mol^{-1} at 298 K (eq 1 in Scheme 2.1)][19] with endothermic dehydrogenation from C-C bonds [e.g., dehydrogenation of ethane is endergonic by +23.9 kcal mol^{-1} (eq 2 in Scheme 2.1)] in a cyclic six-membered framework (taking advantage of the aromatic stabilization energy) should lead to a reversible H_2 storage system (that is, $\Delta G \approx 0$ kcal mol^{-1}).[19] Indeed, electronic structure calculations at the CCSD(T) level indicate that the release of three H_2 molecules from BN heterocycle **1** exhibits overall thermodynamics conducive to reversible H_2 uptake/release (eq 3 in Scheme 2.1).[20] These features and the relatively high gravimetric density (up to 7.1 wt % H_2 for compound **1**) render BN heterocycle materials a potentially viable H_2 storage platform.

For our initial contribution in this area, we chose to focus on the issue of spent fuel regeneration. In this communication, we demonstrate that the BN spent fuel heterocycle can be converted to the fully charged material with molecular H_2 and H^+/H^- equivalents under mild temperatures and pressures. Furthermore, we provide the first crystallographic characterization of the reaction intermediates along the pathway from the spent fuel to the charged material, allowing direct observation of the structural changes associated with increasing hydrogen saturation.

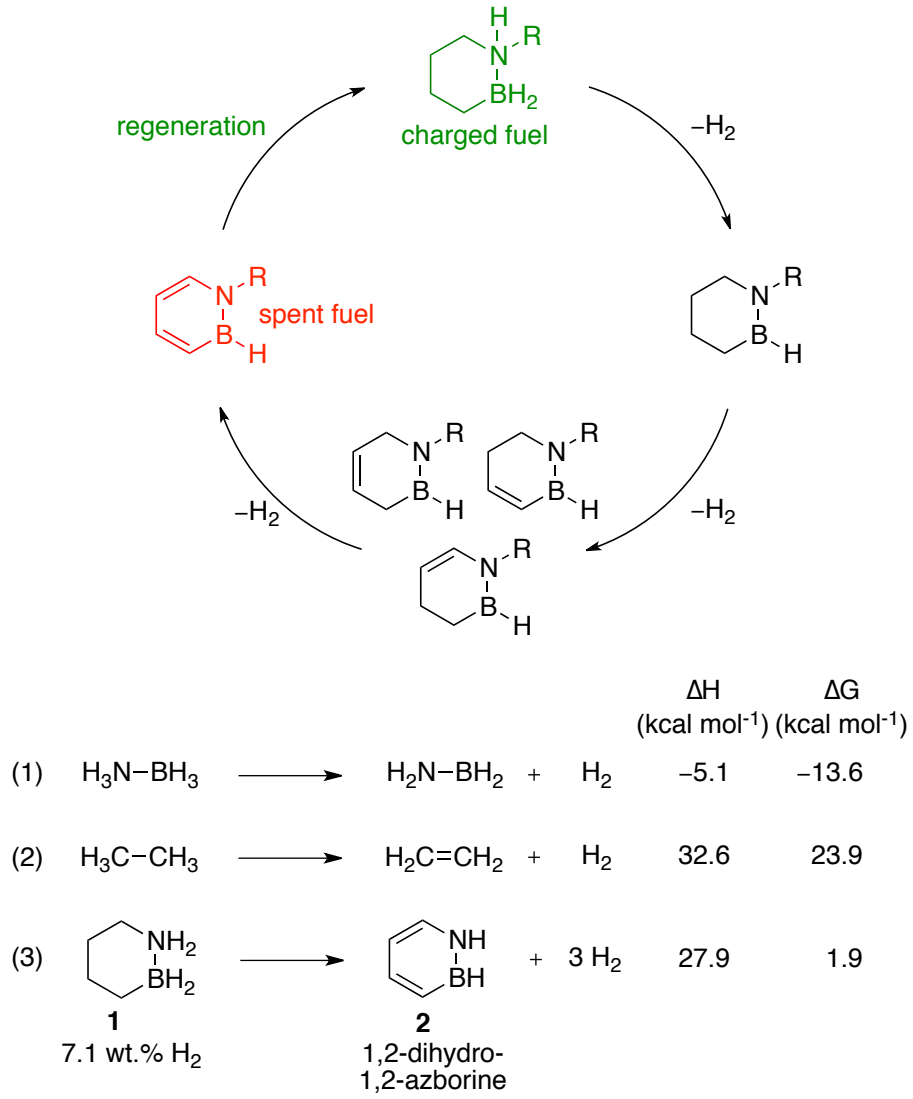

Scheme 2.1. Hydrogen storage by BN hetercycle materials. Electronic structure at the CCSD(T) level (298 K).

2.3. Material Synthesis and Regeneration

The spent fuel material illustrated in Scheme 2.1 belongs to the family of 1,2-dihydro-1,2-azaborines, a class of aromatic heterocycles that was initially explored by Dewar in the 1960s[21] and subsequently further developed by Ashe[22–24] and our group.[25–31] We recently reported the synthesis and characterization of the parent spent fuel material, 1,2-dihydro-1,2-azaborine **2** (see eq 3 in Scheme 2.1).[27] In this study, we chose to

investigate the regeneration of the N-substituted analog (Scheme 2.1, R = *t*Bu) because of its ready synthetic availability. Scheme 2.2 describes the preparation of N-*t*Bu-1,2-dihydro-1,2-azaborine (**5**). Treatment of the known precursor **3**[26] with $LiHBEt_3$ furnished partially spent fuel material **4** as a clear colorless liquid in 74% isolated yield. Subsequent dehydrogenation over catalytic amounts of Pd/C[25] produced the desired model spent fuel material **5**, also as a low-melting liquid.

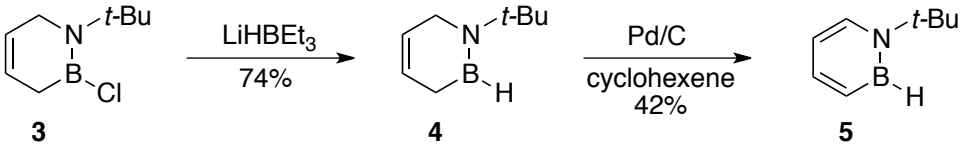

3 **4** **5**

Scheme 2.2. Synthesis of model spent fuel material **5**.

We determined that the **5** readily takes up 2 equiv of molecular H_2 to furnish **6** under mild conditions (eq 4 in Scheme 2.3). Full conversion was achieved in 4 h at a hydrogen pressure of 45 psi (~3 atm) at 80 °C in the presence of catalytic amounts of Pd/C. Heterocycle **6** was isolated as a clear low-melting liquid in 41% yield after distillation. In separate experiments, we determined by NMR and GC analysis that the actual hydrogenation reaction is a high-yield process. Thus, we believe that the moderate isolated yield of **6** is likely caused by the volatility of the product and loss through distillation. The NMR experiment (performed in C_6D_6) indicated no formation of cyclohexane derivatives (that is, benzene is not hydrogenated). To provide further support for this observation, we treated benzene and *tert*-butylbenzene under the same conditions as shown in eq 4 and observed only unreacted starting materials (eq 5 in Scheme 2.3).[32] Equations 4 and 5 in Scheme 3 suggest that the activation barrier for

hydrogen uptake is substantially lower for BN heterocycle material **5** than for the corresponding aromatic carbocycles.

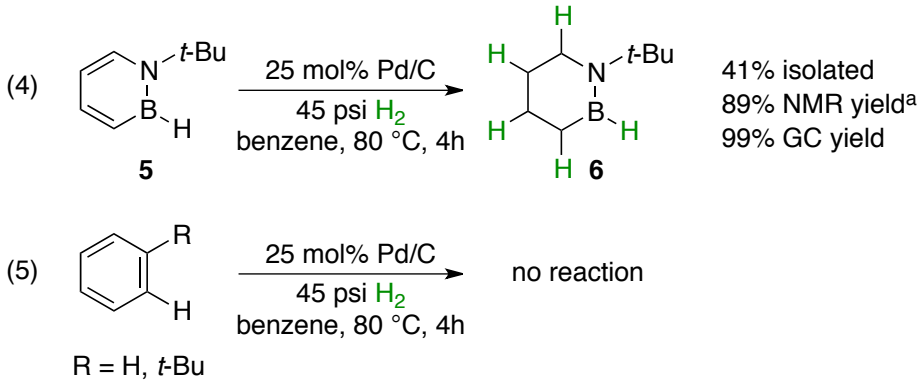

Scheme 2.3. Partial regeneration of spent fuel material **5** by molecular H_2. [a] Determined in C_6D_6 against a calibrated internal standard.

Scheme 2.3 also reveals that hydrogenation across the BN bond did not proceed with molecular H_2 to furnish the fully charged fuel. To the best of our knowledge, the isolation and characterization of monocyclic BN cyclohexane derivatives (e.g., **7** in Scheme 2.4) has remained elusive to date.[33] Inspired by Piers' work on Lewis amphoteric *o*-phenylene-bridged aminoboranes,[34] we envisioned that **7** could be prepared from **6** by sequential addition of hydride and proton equivalents (eq 6 in Scheme 2.4). Gratifyingly, we determined that treatment of **6** with KH in the presence of a crown ether furnished the desired adduct **8** in 90% isolated yield (eq 7 in Scheme 2.4). The isolated yield is in good agreement with the observed NMR yield. Subsequent protonation of **8** produced the fully charged material **7**, as observed by NMR spectroscopy. However the desired product **7** proved difficult to separate from the remaining crown ether byproduct. We were therefore delighted to discover that the use of 18-crown-6 is unnecessary. Addition of KH to **6** in THF followed by protonation with HCl in a single pot produced the charged fuel **7**

in 71% isolated yield over two steps (eq 8 in Scheme 2.4). Intermediate **9** was formed in high yield as measured by NMR analysis but was not isolated. The regeneration route described by eqs 4 and 8 represents a simple, atom-economical way to regenerate the spent BN heterocycle fuel. We also believe that the synthetic availability of BN cyclohexane derivatives (that is, the fully charged fuel) will now enable studies geared toward hydrogen desorption from these materials. BN cyclohexane **7** is a crystalline solid that has a melting point of 96-98 °C. It does not appear to decompose during melting and freezing cycles.

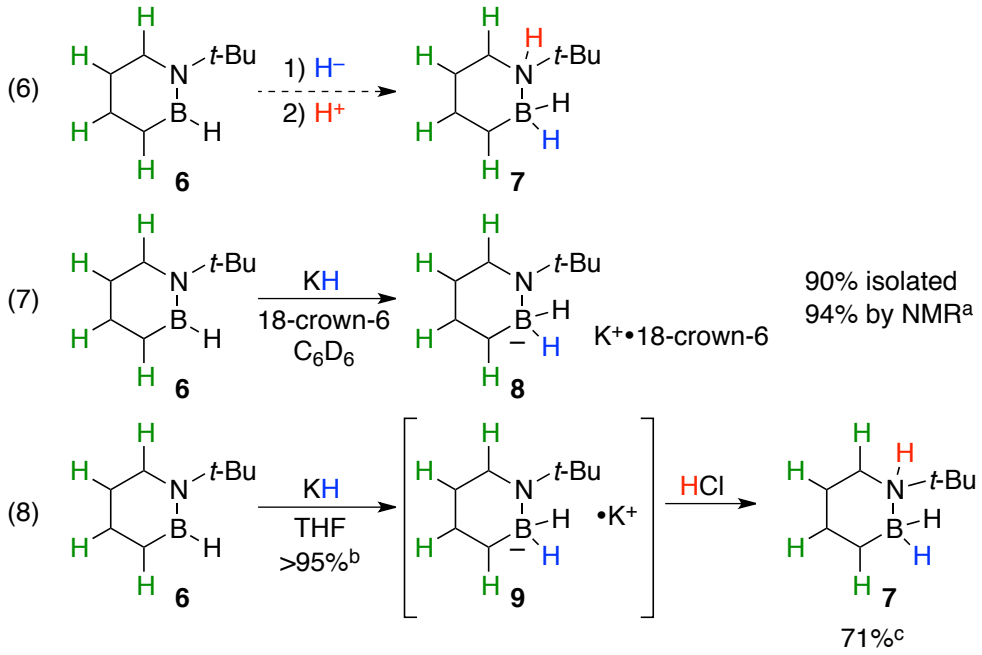

Scheme 2.4. Sequential addition of hydride and proton equivalents. [a] Determined in C_6D_6 against a calibrated internal standard. [b] Determined in THF-d_8 against a calibrated internal standard. [c] Isolated yield from **6** over two steps.

2.4. Discussion

We determined the X-ray structures of compounds **7** and **8** (Figure 2.1), thus unambiguously confirming our structural assignments. Changes in the bond lengths occur upon hydride addition and protonation. We used the previously determined crystal structure of compound **6′**[26] as a model for **6** because **6** is a low-melting liquid. The B–N bond length of 1.403(2) Å in **6′** has substantial double-bond character.[35] Upon addition of a hydride (see compound **8**), the B–N bond distance is significantly lengthened to 1.547(5) Å, which is more typical of a single B–N bond. Protonation on nitrogen leads to further lengthening of the B–N distance to 1.646(2) Å in compound **7**. This is consistent with the more dative rather than covalent bonding between the nitrogen and boron in **7** relative to **8**. The B–N bond distances in AB and $Me_2HN–BH_3$ in the solid state are 1.564(6) and 1.5965(13) Å, respectively.[36] The increased B–N distance in **7** versus AB and $Me_2HN–BH_3$ may be due to the steric bulk imposed by the N-*t*Bu group. Also interesting are the changes associated with the B–C distance. The B-C bond lengthens substantially upon hydride addition [1.584(3) Å in **6′** and 1.643(6) Å in **8**]. This is consistent with the change in hybridization of boron from sp^2 to sp^3 and a substantial increase in negative charge at boron. However, upon protonation at nitrogen, the B–C bond distance shortens to 1.615(2) Å in **7**. This contraction is consistent with the decrease in negative charge at boron in **7** relative to **8**. Also apparent from Figure 1 is the pyramidalization of boron and nitrogen upon hydride addition. The sums of the bond angles around boron and nitrogen in **6′** are 359.9(2) and 360.0(2)°, respectively. On the other hand, the corresponding values in **8** are 332.3(3)° for boron and 340.1(4)° for nitrogen, which are much closer to the 328.5° value for a perfect tetrahedron. Protonation

at nitrogen results only in minor changes in the pyramidalization of B and N. The sums of the equatorial bond angles around boron and nitrogen in **7** are 329.2(8) and 339.7(1)°, respectively.

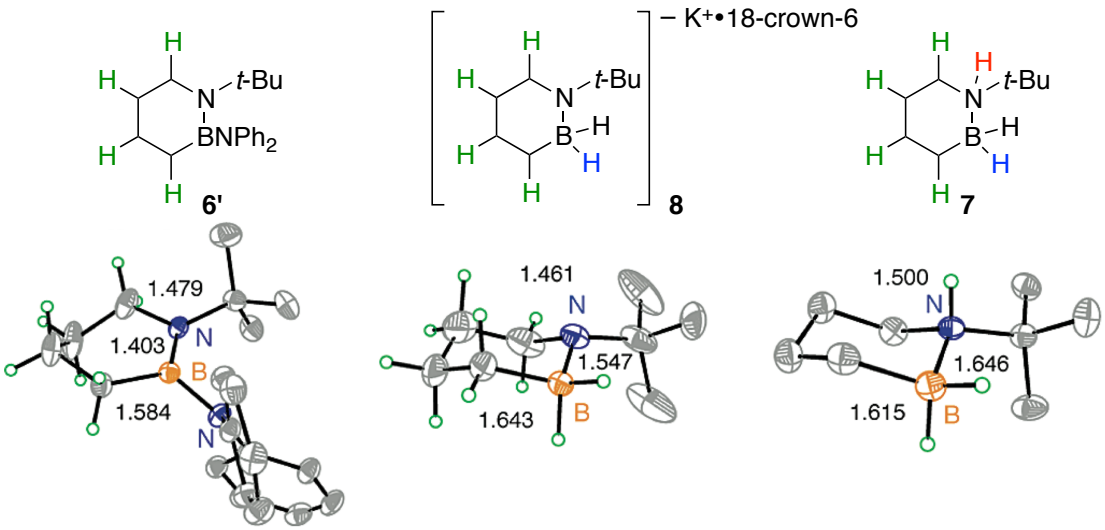

Figure 2.1. ORTEP illustrations, with thermal ellipsoids drawn at the 35% probability level, of BN heterocycles **6'**, **8** and **7**.

We performed a high-level [G3(MP2)] computational analysis of the overall dehydrogenation reaction for selected N-substituted BN cyclohexane fuels. Table 2.1 shows that hydrogen release from the charged fuel to produce the spent fuel is endothermic on the enthalpy scale but is essentially thermoneutral at 298 K on the free-energy scale for N-substituted BN cyclohexanes. The thermodynamic properties of these BN heterocycles are relatively independent of the nitrogen substituent, indicating that the results for our model system (R = *t*Bu) should be applicable to materials with higher storage capacities (for example, R = H, Me).

Table 2.1. Electronic structure calculations at the G3(MP2) Level (298 K).

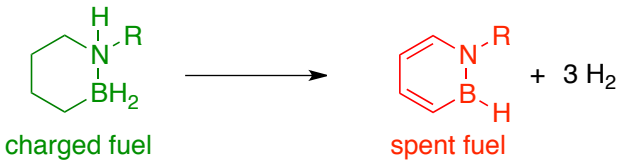

entry	R	ΔH (kcal mol^{-1})	ΔG (kcal mol^{-1})
1	H	23.5	–2.3
2	Me	26.0	–0.3
3	*t*-Bu	25.2	–0.4

2.5. Conclusion

In summary, we have described a potentially viable hydrogen storage platform based on well-defined BN heterocycle materials and demonstrated a simple route for the regeneration of model spent fuel material **5** to the charged fuel **7** using H_2 and H^-/H^+ sources. Crystallographic characterization of intermediates along the regeneration pathway established the correct structural assignments, revealing unique bonding changes associated with increasing hydrogen content on boron and nitrogen. While the described regeneration scheme is not yet optimal from an energetic point of view (that is, the use of highly energetic KH needs to be avoided),[38] the synthetic access to the fully charged BN cyclohexane fuels made possible by this work should enable investigations of these materials in hydrogen desorption studies.

2.6. Experimental

General

All oxygen- and moisture-sensitive manipulations were carried out under an inert atmosphere using either standard Schlenk techniques or a glove box. THF, Et_2O, CH_2Cl_2,

and pentane were purified by passing through a neutral alumina column under argon. Cyclohexene was dried over CaH_2 and distilled under N_2 prior to use. Potassium hydride (Strem) was washed with pentane three times and pumped dry under vacuum prior to use. All other chemicals and solvents were purchased (Aldrich or Strem) and used as received.

^{11}B NMR spectra were recorded on a Varian Unity/Inova 600 spectrometer or Varian Unity/Inova 500 spectrometer at ambient temperature. ^{1}H NMR spectra were recorded on a Varian Unity/Inova 300 or Varian Unity/Inova 600 spectrometer. ^{13}C NMR spectra were recorded on a Varian Unity/Inova 600 spectrometer. All chemical shifts are externally referenced: ^{11}B NMR to BF_3•Et_2O (δ 0). IR spectra were recorded on a Nicolet Magna 550 FT-IR instrument with OMNIC software.

Synthesis of Model Spent Fuel Material (Scheme 2.2)

Compound 4. A solution of $LiHBEt_3$ (1.0 M in THF, 13.7 mL, 13.7 mmol) was added dropwise via syringe to a stirring solution of **3**[26] (2.23 g, 13.0 mmol) in THF (40 mL) at −78 °C. The solution was allowed to warm to room temperature and solvent was removed under reduced pressure. Distillation under attenuated vacuum (bp: 55 °C at 3 Torr) furnished **4** as a colorless liquid (1.33 g, 75%). ^{1}H NMR (300 MHz, C_6D_6): δ 5.82(m br, 1H), 5.52 (m 1H), 3.39 (m, 2H), 1.70 (s br, 2H), 1.08 (s, 9H). ^{13}C NMR (150 MHz, C_6D_6): δ 124.9, 124.4, 54.5, 42.8, 29.8, 17.8 (br) ^{11}B NMR (160.5 MHz, CD_2Cl_2): δ 38.2 (d, $^{1}J_{BH}$ = 64 Hz). FTIR (thin film) 3023, 2974, 2910, 2861, 2531, 1494, 1479, 1441, 1395, 1364, 1331, 1295, 1242, 1210, 1185 cm^{-1}. This compound does not solidify when stored in a −30 °C freezer.

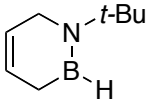

4

Compound 5. A 250 mL Schlenk flask equipped with a stirbar was charged with **4** (1.94 g, 14.2 mmol), 10 wt % Pd/C (0.1 equiv, 1.50 g, 1.42 mmol), and cyclohexene (75 mL). The flask was sealed and heated at 100 °C for 18 hours. The crude reaction mixture was filtered through a glass frit and solvent was removed under reduced pressure. Distillation under attenuated vacuum (bp: 50 °C at 3 Torr) furnished **5** as a colorless liquid (0.801 g, 42%). ^{1}H NMR (300 MHz, C_6D_6): δ 7.62 (dd, $^{3}J_{HH}$ = 10.3 Hz, $^{4}J_{HH}$ = 6.4 Hz, 1H), 7.28 (d, $^{3}J_{HH}$ = 11.7 Hz, 1H), 7.25 (d, $^{3}J_{HH}$ = 7.0 Hz, 1H), 6.29 (dt, $^{3}J_{HH}$ = 6.6 Hz, $^{3}J_{HH}$ = 1.8 Hz, 1H), 5.50 (q br, $^{1}J_{BH}$ = 118 Hz, 1H), 1.21 (s, 9H). ^{13}C NMR (125 MHz, C_6D_6): δ 142.0, 134.9, 131 (br), 111.7, 57.7, 31.7. ^{11}B NMR (96.27 MHz, C_6D_6): δ 31.0 (d, $^{1}J_{BH}$ = 125 Hz). FTIR (thin film) 2978, 2560, 1606, 1515, 1464, 1397, 1369, 1295, 1240, 1197, 1019, 954, 879, 797, 744, 714 cm^{-1}. This compound does not solidify when stored in a −30 °C freezer.

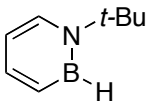

5

Partial Regeneration of Spent Fuel 5 by Molecular H_2 (Scheme 2.3)

Compound 6 (Preparatory Scale). A stirbar equipped pressure reaction vessel was charged with **5** (1.09 g, 7.63 mmol), 10 wt % Pd/C (0.25 equiv, 2.12 g, 2.00 mmol), and benzene (45 mL). The vessel was pressurized with H_2 (45 psi) and heated at 80 °C for 4 hours. Distillation under attenuated vacuum (bp: 50 °C, 3T) furnished **6** as a colorless liquid (0.460 g, 41%). ^{1}H NMR (300 MHz, CD_2Cl_2): δ 3.05 (t, $^{3}J_{HH}$ = 4.2 Hz, 2H), 1.69 (m, 2H), 1.44 (m, 2H), 1.27 (s, 9H), 0.96 (m, 2H). ^{13}C NMR (150 MHz, C_6D_6) δ 54.5, 43.6, 29.7, 28.8, 20.6, 17.0 (br). ^{11}B NMR (160 MHz, C_6D_6): δ 38.7 (d, $^{2}J_{BH}$ = 61 Hz). FTIR (thin film) 2974, 2930, 2858, 2507, 1481, 1459, 1440, 1403, 1363, 1347, 1326, 1244, 1211, 1172 cm^{-1}.

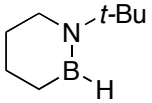

6

Compound 6 (NMR Experiment). A stirbar equipped pressure reaction vessel was charged with **5** (0.050 g, 0.37 mmol), 10 wt % Pd/C (0.25 equiv, 0.098 g, 0.0925 mmol), hexamethylbenzene (0.0103 g, 0.061 mmol) and C_6D_6 (5 mL). The vessel was pressurized with H_2 (45 psi) and heated at 80 °C for 4 hours. ^{1}H NMR analysis indicated the formation of **6** in 89% yield versus hexamethylbenzene.

Compound 6 (GC Experiment). A pressure reaction vessel equipped with a stirbar was charged with **5** (0.100 g, 0.741 mmol), 10 wt % Pd/C (0.25 equiv, 0.197 g, 0.185 mmol) and benzene (10 mL). The vessel was pressurized with H_2 (45 psi) and heated at 80 °C for 4 hours. GC analysis of the reaction mixture versus a calibrated internal standard (undecane) indicated the formation of **6** in 99% yield.

"Blank" Hydrogenation of Benzene and t-Bu Benzene

A pressure reaction vessel equipped with a stirbar was charged with 10 wt% Pd/C (0.100 g, 0.0940 mmol) and 5 mL of either benzene or *t*-Bu-benzene solvent. The vessel was pressurized with H_2 (45 psi) and heated to 80 °C for 4 hours. ^{1}H NMR analysis indicated no hydrogenation of solvent molecules.

Stepwise Addition of H^-/H^+ to Compound 6 (Scheme 2.4)

Compound 7 (eq 8). A solution of **6** (0.050 g, 0.36 mmol) in THF (5.0 mL) was added to a vial containing KH (0.057 g, 1.4 mmol) at room temperature. ^{11}B NMR indicated that the reaction was complete after

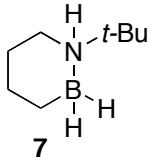

7

stirring the mixture for 12 hours at room temperature. The crude slurry was passed through an Acrodisc. An HCl solution (~2M in Et_2O, 0.135 mL) was added dropwise to the filtrate at −30 °C. The resulting mixture was passed through an Acrodisc and concentrated under vacuum. X-ray quality crystals were grown from a concentrated THF solution of this crude material by slow evaporation to yield the desired product **7** as clear, colorless crystals. (0.036 g, 71%). ^{1}H NMR (300 MHz, C_6D_6): δ 2.41 (d, $^3J_{HH}$ = 10.2 Hz, 2H), 2.23 (m, 2H), 2.01 (br, 2H), 1.58 (m br, 2H), 1.41 (d, $^3J_{HH}$ = 7.8 Hz, 2H), 0.85 (s, 9H). ^{13}C NMR (150 MHz, C_6D_6) δ 56.4, 47.3, 30.0, 26.9, 26.2, 18.4 (br). ^{11}B NMR (160.5 MHz, C_6D_6): δ -10.7 (t, $^3J_{BH}$ = 96 Hz). FTIR (thin film) 3194, 3000, 2960, 2910, 2892, 2353, 2299, 2234, 1707, 1447, 1398, 1372, 1311, 1283, 1250, 1231, 1194, 1180, 1140, 1070, 1041, 1013. Melting point: 96-98 °C.

Compound 8. KH (0.044 g, 1.1 mmol) was added to a stirring solution of **6** (0.050 g, 0.36 mmol) and 18-crown-6 ether (0.095 g, 0.36 mmol) in C_6D_6 (5 mL). After 12 hours at room temperature, solvent was removed under reduced pressure. A cold pentane rinse followed by 2 hours under high vacuum afforded **8** as a colorless solid in 90% isolated yield. ^{1}H NMR (300 MHz, C_6D_6): δ 3.29 (s, 24H), 2.3 (m br, 4H), 1.75 (s, 9H), 1.4 (m br, 2H) 1.0 (m br, 2H). ^{13}C NMR (125 MHz, C_6D_6): δ 70.1, 53.3, 50.5, 33.7, 30.7, 29.4, 20.5 (br). ^{11}B NMR (160.5 MHz, C_6D_6): δ -13.0 (t, $^1J_{BH}$ = 80 Hz).

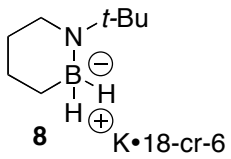

8

Compound 8 (NMR Experiment). KH (0.044 g, 1.1 mmol) was added to a stirring solution of **6** (0.050 g, 0.36 mmol) and 18-crown-6 ether (0.095 g, 0.36 mmol) and

hexamethylbenzene (approx. 0.010 g) in C_6D_6 (5 mL). After 12 hours at room temperature, ^{1}H NMR analysis indicated the formation of **8** in 94% yield versus hexamethylbenzene.

Compound 9 (NMR Experiment). A solution of **6** (0.050 g, 0.36 mmol) in THF-d8 (3.0 mL) was added to a vial containing KH (0.057 g, 1.4 mmol) and hexamethylbenzene (approx. 0.010 g) at room temperature. The mixture was stirred at room temperature for 12 hours. ^{1}H NMR analysis of the crude slurry indicated quantitative (>95%) formation of the potassium salt **9** versus hexamethylbenzene.

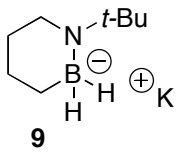

9

Melt/Freeze Cycling of 7

A single crystal of **7** (approx. 5 mg) was sealed in a J. Young tube. The solid was melted in a 120 °C oil bath and allowed to re-solidify at room temperature. The melt/freeze cycle was repeated three times at which point C_6D_6 was added to dissolve the sample. ^{1}H and ^{11}B NMR analysis indicated no degradation of **7**.

CHAPTER III

RESONANCE STABILIZAITON ENERGY OF 1,2-AZABORINES: A QUANTITATIVE EXPERIMENTAL STUDY BY REACTION CALORIMETRY

3.1. General Overview

This chapter describes the experimental determination of the resonance stabilization energy (RSE) of 1,2-azaborines by calorimetric measurement of enthalpy of hydrogenation of aromatic and non-aromatic model compounds. The RSE for 1,2-azaborines was determined to be 16.6 ± 1.3 kcal mol^{-1}, which is consistent with substantial aromatic character but significantly less than the RSE of benzene (32.4 kcal mol^{-1}). This chapter contains previously published material: Campbell, P. G.; Abbey, E. R.; Neiner, D.; Grant, D. J.; Dixon, D. A.; Liu, S.-Y. *J. Am. Chem. Soc.* **2010**, *132*, 18048–18050. I performed the lab work with technical assistance from Doinita Neiner, Daniel J. Grant and David A. Dixon provided computational data, and Shih-Yuan Liu provided editorial assistance and scientific guidance.

3.2. Introduction

Since the isolation and structural description of benzene in the 19th century,[1] the concept of aromaticity has become one of the cornerstones of chemistry.[2] However, despite its relatively long history and the profusion of aromatic compounds in nature, the concept of aromaticity still lacks a single exact definition and has been a source of controversy.[3] Several indices related to the energetic,[4,5] geometric,[6] and magnetic[7–9]

properties of aromatic compounds have been developed to quantitatively characterize aromaticity.[10] One classic experimental method to quantitatively evaluate aromaticity is to determine the resonance stabilization energy (RSE) of a given aromatic compound.[11] This can be accomplished by comparing the heats of hydrogenation of the aromatic molecule in question against those of suitable nonaromatic reference compounds. The first reported use of this technique to measure the RSE of benzene was the work by Kistiakowsky and co-workers in 1936, who determined the RSE to be 36 kcal mol^{-1}.[12]

1,2-Azaborines are benzene mimics in which one CC bond unit has been replaced with an isoelectronic BN unit.[13] These compounds are the focus of research in our group.[14-20] Due to the ubiquity of the phenyl ring as a chemical building block, 1,2-azaborines show promise in potential biological[21] and materials science[22,23] applications. Because of the electronic and structural similarities between 1,2-azaborines and benzene, the characterization of aromaticity in 1,2-azaborines has received considerable attention.[24,25] However, the extent of resonance stabilization in 1,2-azaborines has remained elusive from an experimental point of view. In this work, we provide the first experimental quantitative assessment of the RSE of a 1,2-azaborine using isothermal reaction calorimetry.

We undertook an approach similar to that of Kistiakowsky's classic work and compared the heat of hydrogenation of the aromatic species **1** to the sum of the heats of hydrogenation of the "N-vinyl" (**2**) and "B-vinyl" (**3**) reference BN heterocycles (Scheme 3.1, right diagram). Consequently, the RSE of a 1,2-azaborine can be determined using the equation RSE = $\Delta H_1 - (\Delta H_2 + \Delta H_3)$. The left diagram in Scheme 3.1 shows the hydrogenation enthalpies of the corresponding all-carbon system for direct comparison.

On the basis of this model, in which the enthalpy of hydrogenation of the aromatic benzene to cyclohexene is compared with the hydrogenation of the nonaromatic cyclohexadiene to cyclohexene, an RSE of 32.4 kcal mol^{-1} for benzene can be derived;[i] this value is very similar to the one obtained by Kistiakowsky for conversion to cyclohexane.

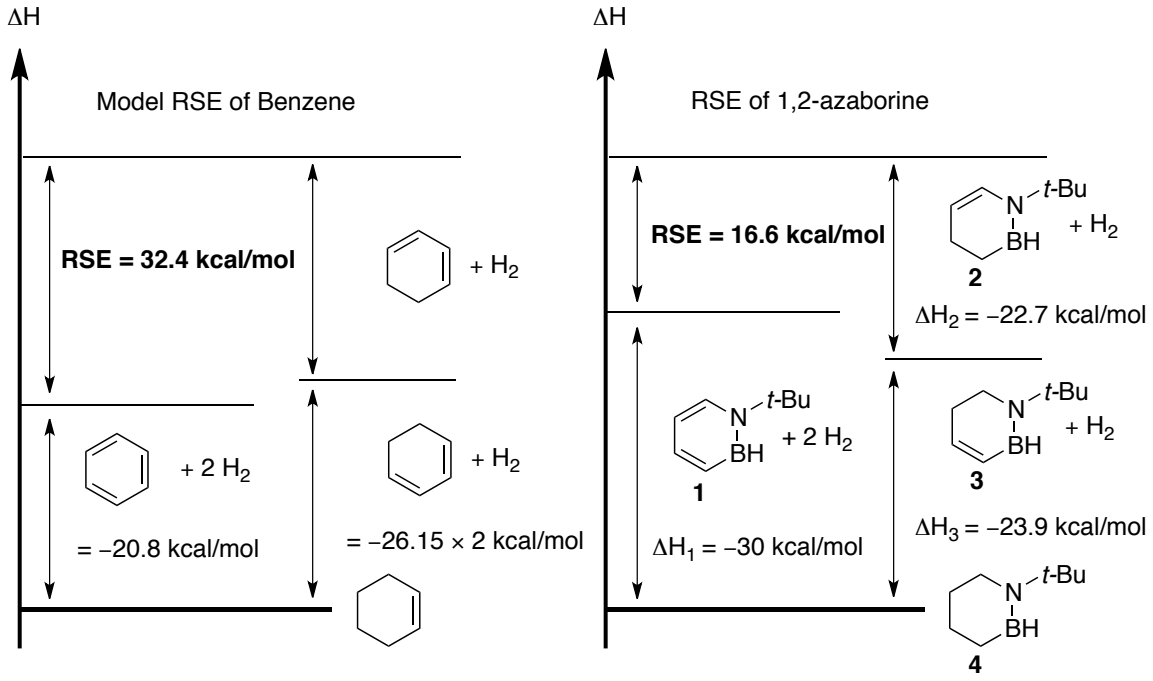

Scheme 3.1. RSE derived from hydrogenation enthalpies.

3.3. Materials Synthesis and Calorimetric Experiments

The synthesis of **1** has been recently published.[23] The preparation of N-vinyl heterocycle **2** was accomplished upon treatment of the previously reported precursor **5**[24a]

[i] The hydrogenation enthalpy values in the left diagram in Scheme 3.1 were derived from experimentally determined standard heats of formation ($\Delta H°_f$) of benzene (+11.67 kcal/mol), cyclohexadiene (+17.45 kcal/mol), and cyclohexene (-9.17 kcal/mol). See reference 26.

with $LiAlH_4$ (eq 1 in Scheme 3.2). We devised a new synthetic route for heterocycle **3** based on a modified version of our standard 1,2-azaborine synthesis. Condensation of the in situ-generated vinylboron dichloride with homoallyl-*tert*-butylamine in the presence of triethylamine generated bisolefin precursor **6** (eq 2 in Scheme 3.2). This material was carried through the subsequent ring-closing metathesis step with Grubbs first-generation catalyst to afford **7** in 69% isolated yield. Lastly, the addition of superhydride ($LiHBEt_3$) to **7** gave the desired B-vinyl product **3** in 54% yield.

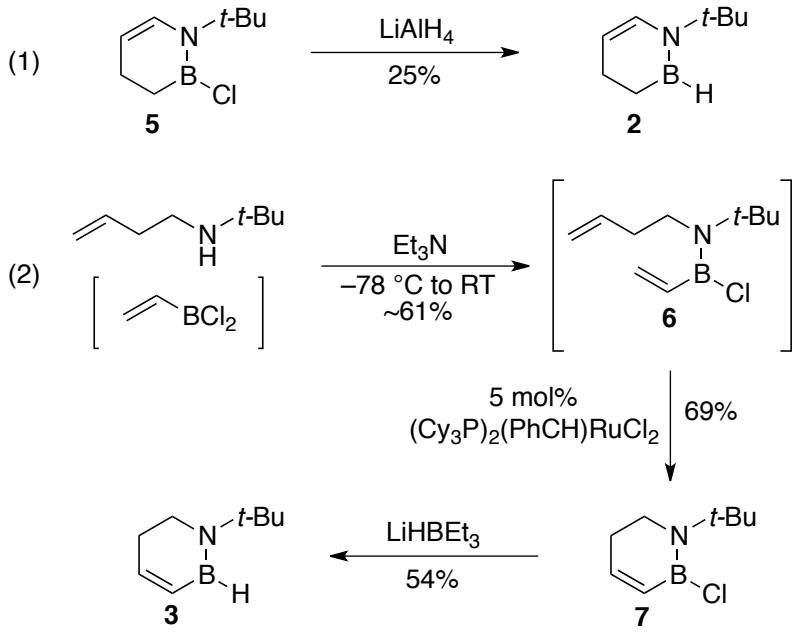

Scheme 3.2. Synthesis of N-vinyl and B-vinyl BN heterocycles **2** and **3**.

With the required compounds in hand, we endeavored to find a hydrogenation catalyst amenable to the limitations imposed by our calorimeter cell (chiefly that mechanical stirring was not an option). Attempts using heterogeneous Pd/C gave erratic results for the hydrogenation of 1,2-azaborine **1**, which we attributed to the lack of

effective mixing (Table 3.1, entry 1). We thus concluded that a homogeneous catalyst was required. After screening a series of homogeneous catalysts, we determined that Muetterties' allylcobalt catalyst (η^3-$C_3H_5Co[P(OMe)_3]_3$)[27] was uniquely suited for our purpose (Table 3.1, entry 2). As can be seen from Table 3.1, catalysts that have been reported to be active for olefin hydrogenations [for example, Wilkinson's catalyst,[28] Crabtree's catalyst,[29] $RuCl_2(PPh_3)_3$,[30] $Ru(H)(Cl)(CO)(PPh_3)_3$[31]] did not hydrogenate 1,2-azaborine **1** under our screening conditions (Table 3.1, entries 3–6). In contrast, the optimized conditions of 10 mol% Muetterties catalyst and 3.45 bar H_2 pressure at 60 °C in hexanes completely hydrogenated each of the compounds of interest (**1**–**3**) in less than 3 h as determined by GC methods.[32]

Table 3.1. Optimization survey for hydrogenation of **1**.

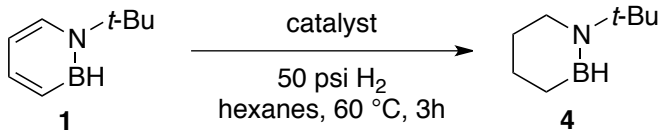

1 **4**

entry	catalyst	yield **4** (%) run 1[a]	run 2[a]
1	Pd/C	40 (49)	3 (84)
2	η^3-allylCo$(P(OMe)_3)_3$	98.5 (0)	95 (0)
3	$ClRh(PPh_3)_3$	0 (82)	0 (97)
4	$[Ir(cod)(py)PCy_3]^+ \ ^- PF_6$	0 (95)	0 (99)
5	$Cl_2Ru(PPh_3)_3$	1 (80)	1 (80)
6	$Ru(H)(Cl)(CO)(PPh_3)_3$	0 (99)	0 (99)

[a] Determined by GC analysis versus a calibrated internal standard. Numbers in parenthesis indicate % of remaining starting material.

The calorimetric experiments were performed in a Setaram C-80 Calvet calorimeter. The sample cell was loaded with the catalyst and substrate solutions in a glovebox, and the reference cell was left empty under N_2. The two cells were then inserted into the calorimeter and allowed to equilibrate at 60 °C for ~30 min. Data collection was started, and hydrogen gas was introduced to both cells, initiating the reaction. Data collection continued until the reaction was complete (3 h). Postrun data processing was limited to subtraction of the baseline run (to eliminate the thermal effects of introducing cold H_2 gas) and integration of the resulting curve to give the corresponding internal energy of hydrogenation, ΔE. The corresponding enthalpy value could then be determined via the equation $\Delta H = \Delta E + \Delta n_g RT$, where Δn_g is the number of moles of gas consumed or generated by the reaction. Figure 3.1 illustrates representative heat flow traces for the hydrogenation reactions. Under identical reaction conditions, the hydrogenation of compound **1** (Figure 3.1a) was slower than the hydrogenations of **2** and **3** (Figure 3.1b and c, respectively). The distinctive shape of Figure 3.1a may be indicative of two sequential hydrogenation steps for compound **1**. The heat flow traces for **1**–**3** are also consistent with non-zeroth-order reaction kinetics with respect to the substrate, suggesting that mass transfer is not rate-limiting under the reaction conditions.[33]

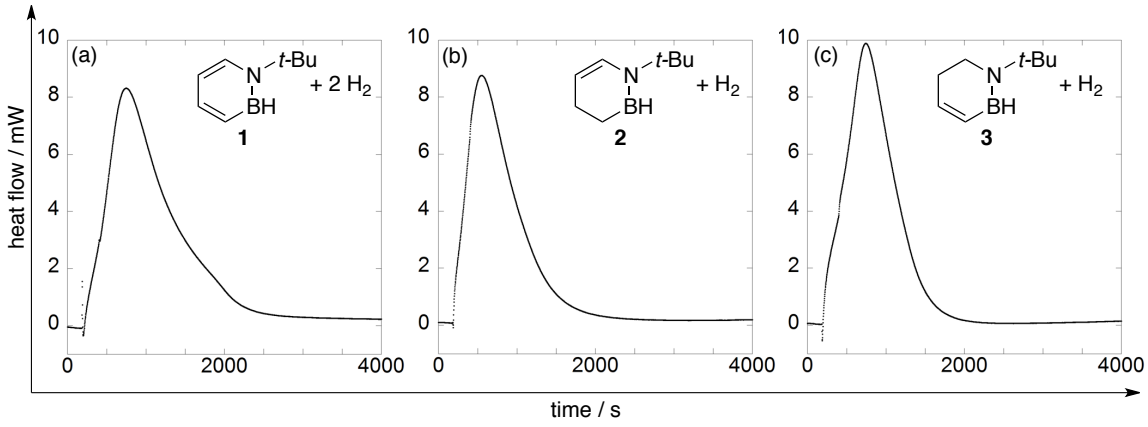

Figure 3.1. Heat flow traces for the hydrogenation reactions of **1**, **2**, and **3**.

3.4. Results and Discussion

A summary of the experimentally determined hydrogenation enthalpies (averages of three runs) is shown in Table 3.2 together with computational predictions at the G3(MP2) level[34] obtained by using the Gaussian 09 program.[35] The experimental heats of hydrogenation are –30 ± 1, –22.7 ± 0.5, and –23.9 ± 0.7 kcal mol^{-1} for **1**, **2**, and **3**, respectively. These values are within 1.1 kcal mol^{-1} of the computationally derived (gas-phase) results and follow the same general energetic trend (that is, the hydrogenation of **3** is slightly more exothermic than that of **2**). The experimentally derived RSE for 1,2-azaborine **1** is 16.6 ± 1.3 kcal mol^{-1}, as calculated from the equation RSE = $\Delta H_1 - (\Delta H_2 + \Delta H_3)$. The G3MP2 value for the RSE is 18.4 kcal mol^{-1}, in good agreement with the experimental value. The effect of the *tert*-butyl substituent on the RSE is small (1.2 kcal mol^{-1}), as use of our previously reported G3MP2 results[18] for the RSE of the parent 1,2-dihydro-1,2-azaborine gives 19.6 kcal mol^{-1}. This is significantly less than the RSE of benzene (32.4 kcal mol^{-1} according to the model in Scheme 3.1) and is consistent with

nucleus-independent chemical shift (NICS) calculations indicating that 1,2-azaborines are less aromatic than benzene.[15,25b]

3.5. Conclusion

In summary, we have provided the first experimental determination of the resonance stabilization energy of 1,2-azaborines through hydrogenation enthalpy measurements. Muetterties' allyl- cobalt catalyst served as a uniquely capable "homogeneous" catalyst for hydrogenation of 1,2-azaborine **1**. We found the RSE of 1,2-azaborine **1** to be 16.6 kcal mol^{-1}, indicating that significant additional stability is imparted by six-π-electron delocalization in six-membered BN heterocyclic ring systems. This result is consistent with previous findings that 1,2-azaborines are less aromatic than their all-carbon counterparts and aids in completing the "aromatic picture" of 1,2-azaborines by making available a quantitative experimental assessment.

Table 3.2. Experimental versus calculated heats of hydrogenation

	reaction	ΔH experimental (kcal mol^{-1})	ΔH(298 K) calculated G3(MP2) (kcal mol^{-1})
1	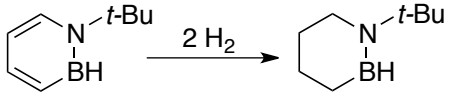	$\Delta H_1 = -30 \pm 1$	–30.1
2	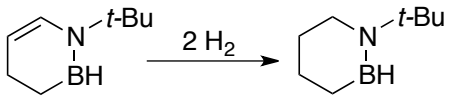	$\Delta H_2 = -22.7 \pm 0.5$	–23.8
3	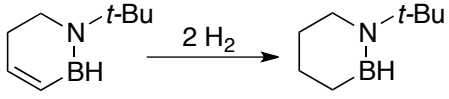	$\Delta H_3 = -23.9 \pm 0.7$	–24.7

3.6. Experimental

General

All oxygen- and moisture-sensitive manipulations were carried out under an inert atmosphere using either standard Schlenk techniques or a glove box. THF, Et_2O, CH_2Cl_2, and pentane were purified by passing through a neutral alumina column under argon. Potassium hydride (Aldrich) was washed with pentane three times and pumped dry under vacuum prior to use. All other chemicals and solvents were purchased (TCI, Aldrich or Strem) and used as received.

^{11}B NMR spectra were recorded on a Varian Unity/Inova 600 spectrometer or Varian Unity/Inova 500 spectrometer at ambient temperature. ^{1}H NMR spectra were recorded on a Varian Unity/Inova 300 or Varian Unity/Inova 600 spectrometer. ^{13}C NMR spectra were recorded on a Varian Unity/Inova 600 spectrometer. All chemical shifts are externally referenced: ^{11}B NMR to $BF_3 \bullet Et_2O$ (δ 0). IR spectra were recorded on a Nicolet Magna 550 FT-IR instrument with OMNIC software.

Synthesis of N-vinyl and B-vinyl compounds (Scheme 2)

Compound 2. A stirbar equipped 100 mL r.b.f. was charged with **5** (2.69 g, 8.84 mmol) and Et_2O (25 mL) and cooled to −20 °C. $LiAlH_4$ (0.352 g, 9.28 mmol) was dissolved in Et_2O (10 mL) in a scintillation vial and also cooled to −20 °C. The $LiAlH_4$ soln. was added to the soln. of **5** via pipette and the mixture was allowed to warm to room temperature and react for 2 hours. The mixture was filtered through an acrodisc and the solvent was removed under reduced pressure.

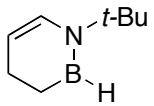

2

Distillation under attenuated vacuum (bp: 50 °C at 2 Torr) furnished **2** as a colorless liquid (0.300 g, 25%).

^{1}H NMR (300 MHz, C_6D_6): δ 6.17 (dd, $^{3}J_{HH}$ = 8.4 Hz, 1H), 5.30 (br q, $^{1}J_{BH}$ = 120 Hz, 1H), 5.16 (m, 1H), 2.09 (m, 2H), 1.33 (t, $^{3}J_{HH}$ = 8.7 Hz, 2H), 1.20 (s, 9H). ^{13}C NMR (125 MHz, C_6D_6): δ 129.2, 110.3, 30.12, 30.04, 17.6, 15.2 (br). ^{11}B NMR (96.3 MHz, C_6D_6): δ 42.5 (d, $^{1}J_{BH}$ = 122 Hz). FTIR (thin film) 3234, 2974, 2925, 2858, 2388, 1618, 1453, 1392, 1162, 868, 698, 544 cm^{-1}.

Compound 7. In a glove box, a 100 mL r.b.f. was charged with CH_2=$CHSnBu_3$ (15.0 g, 47.3 mmol), and pentane (15 mL). A 250 mL r.b.f. was charged with BCl_3 soln. (4.83 mL, 1 M in hexanes) and cooled to −78 °C under N_2. The solution containing CH_2=$CHSnBu_3$ was added dropwise via cannula to the flask containing BCl_3 and the reaction mixture was stirred at −78 °C for 1 h, warmed to room temperature for 30 min, then cooled to −10 °C. Then a degassed soln. of homoallyl-*tert*-butylamine (6.32 g, 49.7 mmol) in pentane (15 mL) was added dropwise via cannula and the mixture stirred for 15 h. At the conclusion of the reaction, solvent was removed under reduced pressure. Vacuum distillation of the resulting crude material (bp: ~50 °C at 700 mT) afforded intermediate **6** as liquid product (approx. 5.77 g, 61%), which was carried on to prepare compound **7**. A 500 mL flask equipped with a stirbar was charged with **6** (4.71 g, 23.6 mmol) in CH_2Cl_2 (100 mL). Grubbs' first generation catalyst ($(Cy_3P)_2$)PhCH)$RuCl_2$) (0.971 g, 1.18 mmol) was dissolved in 10 mL CH_2Cl_2 in a scintillation vial and added quickly to the mixture containing **6**. The flask was sealed with a rubber septum vented by a needle and the mixture stirred in a glove box for 15 h at

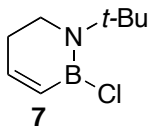

7

room temperature. At the conclusion of the reaction, solvent was removed under reduced pressure. The resulting crude material was purified by distillation (bp: 35 °C at 550 mTorr) to furnish **7** as a colorless liquid (2.76 g, 69%).

^{1}H NMR (600 MHz, CD_2Cl_2): δ 6.60 (d, $^{3}J_{HH}$ = 9.0 Hz, 1H), 5.69 (d, $^{3}J_{HH}$ = 11.5 Hz, 1H), 3.21 (t, $^{3}J_{HH}$ = 7.1 Hz, 2H), 2.22 (m, 2H), 1.42 (s, 9H). ^{13}C NMR (125 MHz, CD_2Cl_2): δ 144.6, 131.1(br), 44.0, 30.6, 30.1, 29.9. ^{11}B NMR (192.5 MHz, CD_2Cl_2): δ 32.3 (s). FTIR (thin film) 2965, 2354, 2315, 1700, 1652, 1261, 1203, 1093, 1019, 999, 798, 744, 667 cm^{-1}.

Compound 3. A stirbar equipped 250 mL round bottom flask was charged with **7** (3.28 g, 19.1 mmol) and Et_2O (60 mL) and cooled to −78 °C. A solution of $LiHBEt_3$ (20 mL, 1.0 M in THF) was added dropwise via syringe. The stirring mixture was allowed to warm to room temperature, and the solvent was removed under reduced pressure. The resulting crude material was purified by distillation under attenuated vacuum (bp: 30 °C at 2 Torr) furnished **3** as a colorless liquid (1.42 g, 54 %).

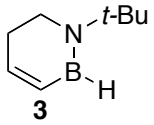

3

^{1}H NMR (300 MHz, C_6D_6): δ 6.61 (d, $^{3}J_{HH}$ = 11.4 Hz, 1H), 6.37 (d, $^{3}J_{HH}$ = 11.4 Hz, 1H), 4.99 (br q, $^{1}J_{BH}$ = 118 Hz, 1H), 2.87 (t, $^{3}J_{HH}$ = 7.2 Hz, 2H), 2.04 (m, 2H), 1.19 (s, 9H). ^{13}C NMR (125 MHz, C_6D_6): δ 141.6, 131.2(br), 54.5, 40.8, 29.8, 29.6. ^{11}B NMR (96.3 MHz, C_6D_6): δ 32.5 (d, $^{1}J_{BH}$ = 125 Hz). FTIR (thin film): 2956, 2799, 2523, 1260, 1019, 799, 741, 667, 457 cm^{-1}. HRMS (CI+) calcd. for $C_8H_{17}BN$ ($M+H^+$) 138.14541, found 138.14566.

Optimizaiton Survey for Hydrogenation of 1 (Table 1)

A general procedure is as follows: A pressure reaction vessel was charged with **1** (0.020 g, 0.148 mmol), catalyst (10 mol%, 0.015 mmol) and hexanes (2 mL). The vessel was sealed, pressurized with H_2 (50 psi), and heated at 60 °C for 3 hours without stirring. GC analysis of the reaction mixture versus a calibrated internal standard (undecane) gave yields of product formation **4** and recovered starting material shown in Table 3.1.

Calorimetric Hydrogenation Experiment (Figure 1 and Table 2)

Sock solutions of **1**, **2** and **3** were made in hexanes (~0.100 g of **1**, **2** or **3** in 5.0 mL hexanes, ~0.15 mM; exact concentrations for each experiment were recorded and used to determine ΔH). A stock solution of Muetterties' catalyst was also made in hexanes (η^3-$C_3H_5Co[P(OMe)_3]_3$, 0.035 g in 5.0 mL, 0.015 mM) In a glovebox, 0.5 mL of both the BN-heterocycle soln. and catalyst soln. were added to the sample cell (Hastelloy, approx. vol. 5 mL) via syringe. The reference cell was left empty under N_2. Both cells were loaded into the Setaram C-80 calorimeter, allowed to equilibrate at 60 °C until zero heat flow was achieved (which took approximately 30 min). Data collection was initiated and both the sample and reference cells were pressurized with 50 psi H_2. The valves were left open for <1 min, then closed again and kept closed for the remainder of the experiment. Data collection continued until heat flow returned to zero and the reaction was complete. A baseline run (sample cell filled with 0.5 mL cat. soln. and 0.5 mL hexanes, charged with H_2 in the calorimeter in the same manner as an experimental run) was subtracted from the heat-flow trace and the resulting curve was integrated using the Setaram

software SetSoft 2000 to give the corresponding internal energy of hydrogenation, ΔE. For reactions involving gaseous compounds, internal energy is related to enthalpy through the equation $\Delta H = \Delta E + \Delta n_g RT$, where Δn_g is the moles of gas consumed or generated by the reaction. Solving the equation gives enthalpy values more exothermic than the measured heat by −0.662 kcal/mol (for reactions 2 and 3, 1 mol H_2 consumed) and −1.32 kcal/mol (for reaction 1, 2 moles H_2 consumed). The calorimetric measurements were repeated three times for each compound and the average value of ΔH with standard deviation is reported. The products of each run were characterized using ^{11}B NMR and were found to be exclusively **4**.

CHAPTER IV

BORON-SUBSTITUTED AMMONIA BORANE DERIATIVES: HYDROGEN RELEASE AND SPENT MATERIAL REGENERATION

4.1. General Overview

This chapter describes the synthesis of novel ammonia borane (AB, $H_3N–BH_3$) derivatives with a methyl substituent on the boron atom. We compare the rate and extent of H_2 loss under catalytic dehydrogenation conditions to the known compounds AB, $MeH_2N–BH_3$ (**3**, *N*-Me-AB), and the cyclic AB derivative **2**. Methyl substitution on boron significantly accelerates the rate of dehydrogenation and facilitates the recovery of a single dehydrogenated product. We also demonstrate that the spent material can be regenerated using formic acid and $LiAlH_4$. This chapter contains unpublished material. I performed the lab work. Lev N. Zakharov provided single crystal X-ray analysis and Shih-Yuan Liu provided editorial assistance and scientific guidance.

4.2. Introduction

Hydrogen has the potential to replace petroleum as the primary fuel for transportation and remote power applications.[1-3] One significant hurdle that must be overcome is the development of safe (for example, ambient pressure and temperature, non-toxic), efficient (high gravimetric hydrogen density), and convenient (mild H_2 release conditions) storage methods for hydrogen. Boron-nitrogen containing chemical hydride compounds have received considerable recent attention as possible hydrogen

storage materials due to their high gravimetric density and favorable kinetics of hydrogen release.[4,5] Ammonia borane (AB, H_3N-BH_3, 19.6 wt.% H_2) and *N*-substituted derivatives of AB have been the focus of numerous literature reports detailing hydrogen release conditions,[6,7] and characterization and regeneration of spent-fuel material.[8,9] Additionally, solution-phase mechanistic studies have been published, for both thermal[10] and catalytic[11,12] dehydrogenation of AB, providing insights that have led to catalyst and product optimization in subsequent work.

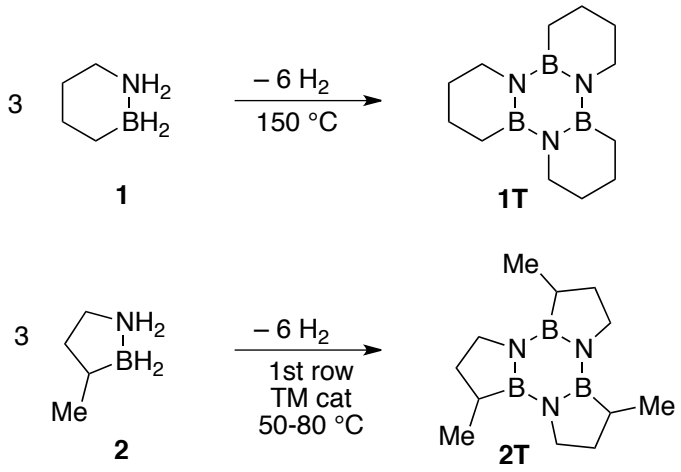

Scheme 4.1. Hydrogen storage by boron-nitrogen heterocycles.

Research in our group centers on developing the fundamental chemistry and applications of boron-nitrogen heterocycles.[13-21] We recently reported the synthesis of 1,2-BN-cyclohexane **1**,[22] a cyclic amine-borane, and noted that it cleanly releases hydrogen to form a trimer when thermally activated (Scheme 4.1). Invigorated by this discovery, we developed the BN-methylcyclopentane material **2**,[3] which is liquid at room temperature. Compound **2** also cleanly releases hydrogen (two equiv. H_2 per molecule **2**) both thermally and catalytically using cheap, first-row transition metal halide catalysts such as $CoCl_2$, $NiCl_2$ and $FeCl_2$ at moderate temperature (50-80 °C). Under both thermal

and catalytic conditions the exclusive product is trimer **2T**, which is also a liquid at room temperature.

There are only limited reports of the use of first-row metal-halide catalysts for the dehydrogenation of AB. Ramachandran and coworkers reported the use of $NiCl_2$ and $CoCl_2$ as catalysts for the methanolysis of AB,[23] and Jagirdar and coworkers used $CoCl_2$, $NiCl_2$, and $CuCl_2$ as reactants to assist in the hydrolysis of AB.[24] The use of iron halide salts for the AB dehydrogenation in the solid state was recently reported by Chen and coworkers.[25] Motivated by the successful use of the cheap cobalt and iron halide catalysts to promote dehydrogenation from **2** at mild reaction temperatures, we were curious to see if these catalysts are effective for AB dehydrogenation under similar conditions. We treated samples of AB with 5 mol% $CoCl_2$, $FeCl_2$ and $FeCl_3$ in THF at 80 °C and monitored reaction progress via ^{11}B NMR (see experimental section for details). $FeCl_3$ promoted the quickest and cleanest dehydrogenation from AB. The starting material was completely consumed within 120 minutes, and by 240 min >90% borazine/polyborazylene (PB)[10] formation was observed; however, unidentified intermediate species remained and gradually diminished over 20 hours. $FeCl_2$ and $CoCl_2$ also promoted dehydrogenation from AB but both were slower and messier. Complete consumption of the starting material occurred after 240 minutes, along with >85% borazine/PB formation, but again unidentified intermediates remained after 20 hours. For all three catalysts, the rate of AB dehydrogenation was considerably slower than for dehydrogenation reactions of **2** under the same conditions.

We were struck by the stark contrast in rate and extent of hydrogen release between AB and our cyclic compounds **1** and **2**. We speculated that the carbon

substituent on the boron atom in **1** and **2**, as well as the cyclic structure of these compounds could play a role in their enhanced hydrogen release kinetics and clean single-product formation. Therefore, we wished to compare the rate and extent of dehydrogenation of compounds **2,** AB, and *N*-Me-AB **3** to linear *B*-alkyl (methyl) substituted compounds such as **4** and **5**, under identical conditions (Figure 4.1). Surprisingly, the seemingly simple boron-substituted AB derivatives **4** and **5** are unknown in the literature, so before we could study their dehydrogenation properties we needed to synthesize these novel compounds.

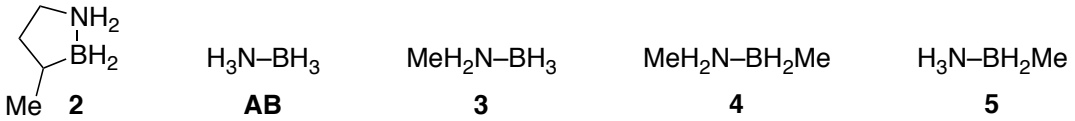

Figure 4.1. Compounds of interest for comparing rates and extent of dehydrogenation.

4.3. Synthesis of Compounds 4 and 5

The syntheses of **4** and **5** are illustrated in Scheme 4.2. Salt metathesis of $NaBH_4$ and NH_4Cl has been used to synthesize ammonia borane in very high yield.[26] Using an analogous synthetic strategy, we were pleased to find that treating the known compound $Li[MeBH_3]$[27] with the appropriate commercially available amine-hydrochloride salt led to the loss of one equivalent of H_2 and generated compounds **4** and **5** in 88% and 75% isolated yield, respectively.

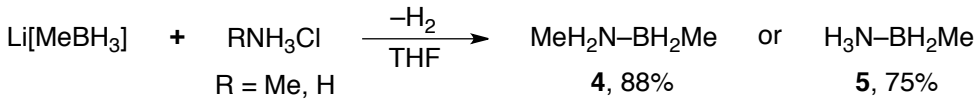

Scheme 4.2. Synthesis of novel B-substituted AB derivatives **4** and **5**.

4.4. Comparison of Rates and Extent of Dehydrogenation

We performed our dehydrogenation experiments using an automated gas burette apparatus,[28] which enabled us to determine both the rate and amount of hydrogen released. We chose to use $CoCl_2$ as the catalyst for these studies, as it was found in our prior work to be the most active catalyst screened for the dehydrogenation of compound **2**. The results of our burette experiment are depicted in Figure 4.2. Under the identical dehydrogenation conditions previously established for compound **2** (5 mol% catalyst loading, 80 °C, diglyme solvent), the *B*-methyl substituted linear AB derivatives **4** and **5** displayed a rapid rate of hydrogen release; in the case of **5,** releasing ca. 1.75 equivalents of H_2 even more quickly than the release of the equivalent amount of H_2 from **2**.[i] Notably, both of the non-*B*-alkyl substituted compounds, **3** and AB, displayed markedly slower rates of hydrogen release under these conditions. Ammonia borane released ca. 2 equiv. H_2 in 150 minutes and **3** released only ca. 1.25 equiv. H_2 in 240 minutes. These results indicate that the novel *B*-substituted AB derivatives **4** and **5** could potentially be useful as hydrogen storage materials, storing 6.8 wt.% and 9.0 wt.% hydrogen, respectively.

[i] We noticed bubbling immediately upon addition of $CoCl_2$ to THF solutions of **4** and **5**, at room temperature, before we could begin data collection. We attribute the release of less than 2 equiv. H_2 from compounds **4** and **5** to the loss of hydrogen before we could begin our experiment.

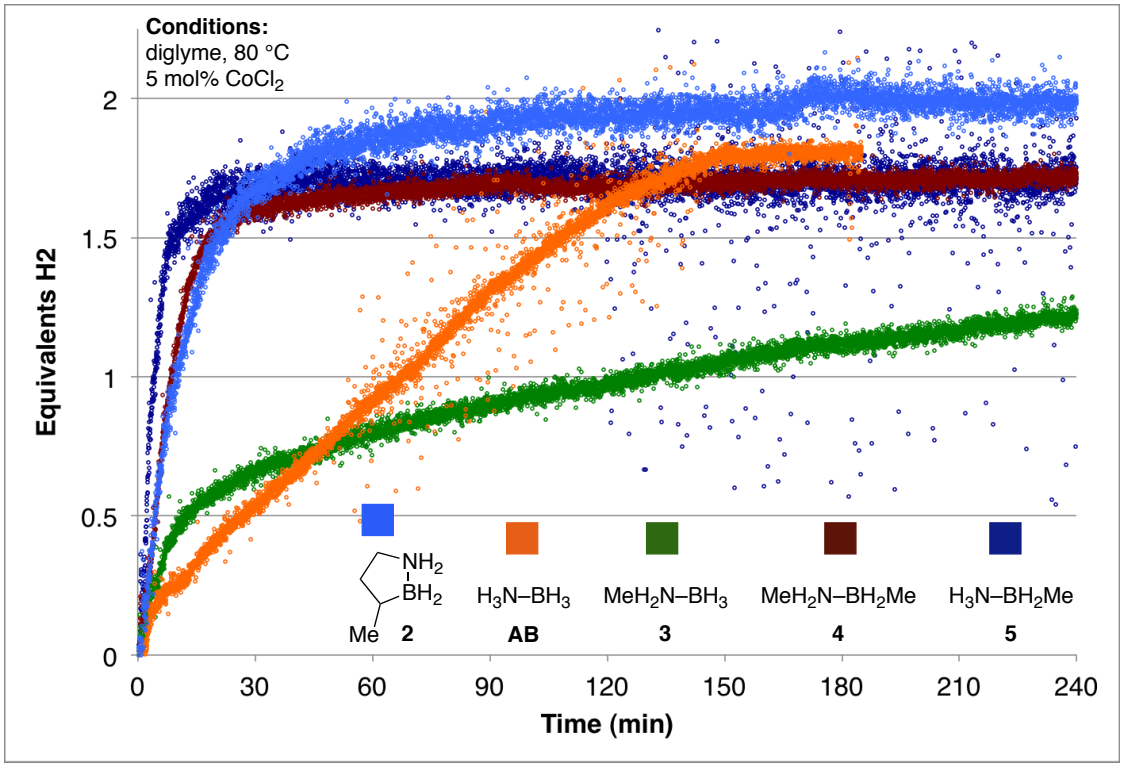

Figure 4.2. Automated burette measurement of dehydrogenation catalyzed by 5 mol% $CoCl_2$ at 80 °C.

4.5. Regeneration

Facile recharging of spent material with fresh hydrogen equivalents is critical for the widespread adoption of any chemical platform for hydrogen storage. In the case of ammonia borane, researchers have recently developed methods for the regeneration of a model AB spent fuel material, polyborazylene (PB), using digestion strategies based on benzenedidthol/Sn–H[9] or hydrazine/NH_3.[8] However, PB is just one of several potential products that can result from AB dehydrogenation. In contrast, the cyclic AB derivatives **1** and **2** each cleanly form one trimeric product upon hydrogen release (**1T** and **2T**, Scheme 4.1).[28] We found that under both thermal and catalytic conditions, **4** and **5** initially form a mixture of dehydrogenated compounds. Extended heating of the mixture (36 hours) causes the intermediate species to converge to a single product, which we have

identified as the trimeric species hexamethylborazine **6** in the case of **4**, and 2,4,6-trimethylborazine **7** in the case of **5**, on the basis of their ^{11}B NMR chemical shifts (Scheme 4.3). After catalytic dehydrogenation of **4** in refluxing THF using our standard catalyst and loading (5 mol% $CoCl_2$), we were able to isolated **6** in 71 % yield (see experimental section for details).

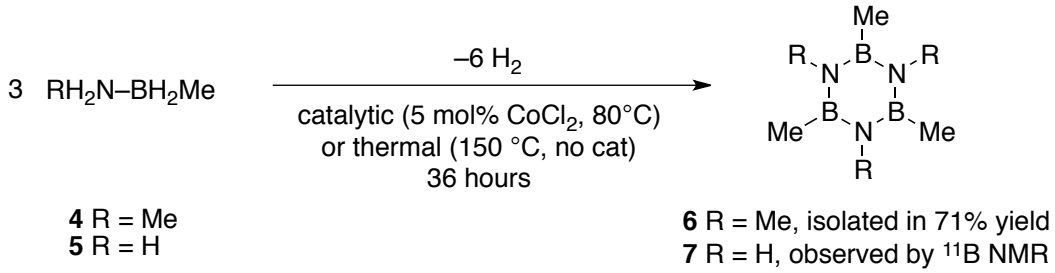

Scheme 4.3. Single product formation in the dehydrogenation of **4** and **5**.

We have developed a route to regenerate the fully charged compound **4** from the spent material **6**, which is illustrated in Scheme 4.4. Activation of **6** with 3 equiv. formic acid generates the BN-cyclohexane analog **8**. We have isolated a crystal of **8** suitable for single X-ray diffraction, which unambiguously confirms our structural assignment. Interestingly, additional equivalents of formic acid do not add to boron or break the central BN ring, even in 10-fold excess. However, addition of $LiAlH_4$ to **8** does break apart the trimer and cleaves the B–O bonds to install the $B(H)_2$ moieties. (Treatment of **6** directly with $LiAlH_4$ without pre-treatment with formic acid was not sufficient to break the ring; only unreacted starting material was recovered.) Workup using wet THF as a proton source gives **4**, which was isolated in 46% yield. While we acknowledge that the use of energetic reagents such as $LiAlH_4$ and the modest yield afforded by this proposed regeneration pathway are not ideal for use on a large scale, further optimization may

enable us to take advantage of the well-defined nature of the spent-fuel products to devise a lower energy, higher yielding regeneration protocol.

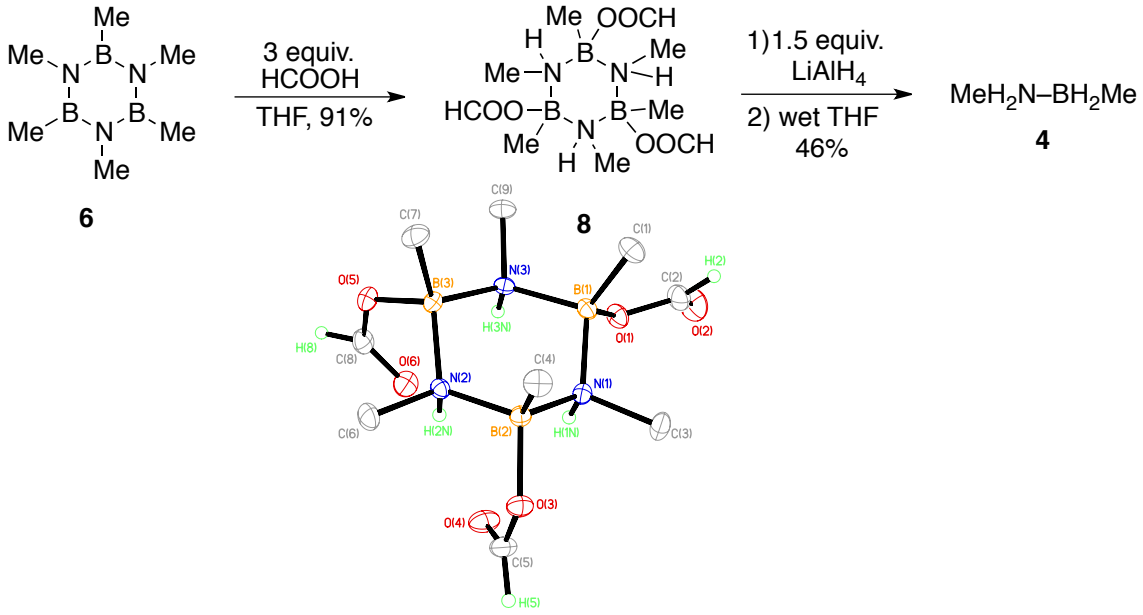

Scheme 4.4. Regeneration of spent fuel trimer **6** to fully charged compound **4**.

4.6. Conclusion

In summary, we have synthesized two novel *B*-Me substituted AB derivatives **4** and **5**, and have investigated their hydrogen release properties. We have shown that the addition of a *B*-alkyl substituent can dramatically increase the rate of $CoCl_2$ catalyzed hydrogen release compared with parent AB and also facilitates the recovery of a single spent fuel product. The spent fuel material of **4**, hexamethylborazine **6**, can be regenerated to **4**, which makes possible a potential hydrogen storage fuel cycle based on this material.

4.7. Experimental

General

All oxygen- and moisture-sensitive manipulations were carried out under an inert atmosphere using either standard Schlenk techniques or a glove box. THF, Et_2O, CH_2Cl_2, and pentane were purified by passing through a neutral alumina column under argon. Ammonia borane was purchased from GFS Chemicals and used as received, *N*-Me-AB **3**,[29] BN heterocycle **2**,[28] and Li[$MeBH_3$][27] were prepared according to literature methods. All other chemicals and solvents were purchased (Aldrich or Strem) and used as received.

^{11}B NMR spectra were recorded on a Varian Unity/Inova 600 spectrometer or Varian Unity/Inova 300 spectrometer at ambient temperature. ^{1}H NMR spectra were recorded on a Varian Unity/Inova 300 or Varian Unity/Inova 600 spectrometer. ^{13}C NMR spectra were recorded on a Varian Unity/Inova 600 spectrometer. All chemical shifts are externally referenced: ^{11}B NMR to BF_3•Et_2O (δ 0). IR spectra were recorded on a Nicolet Magna 550 FT-IR instrument with OMNIC software.

NMR Evaluation of First-Row Transition Metals for the Dehydrogenation of Ammonia Borane

General Procedure. A J.Young Tube was charged with AB (0.020 g) and metal catalyst (0.05 mol%) in THF (0.5 mL). The tube was submerged in a preheated oil bath and taken for ^{11}B NMR evaluation at regular intervals. The time-lapse NMR spectra are presented in Scheme 4.5. Peaks are assigned according to reference 10.

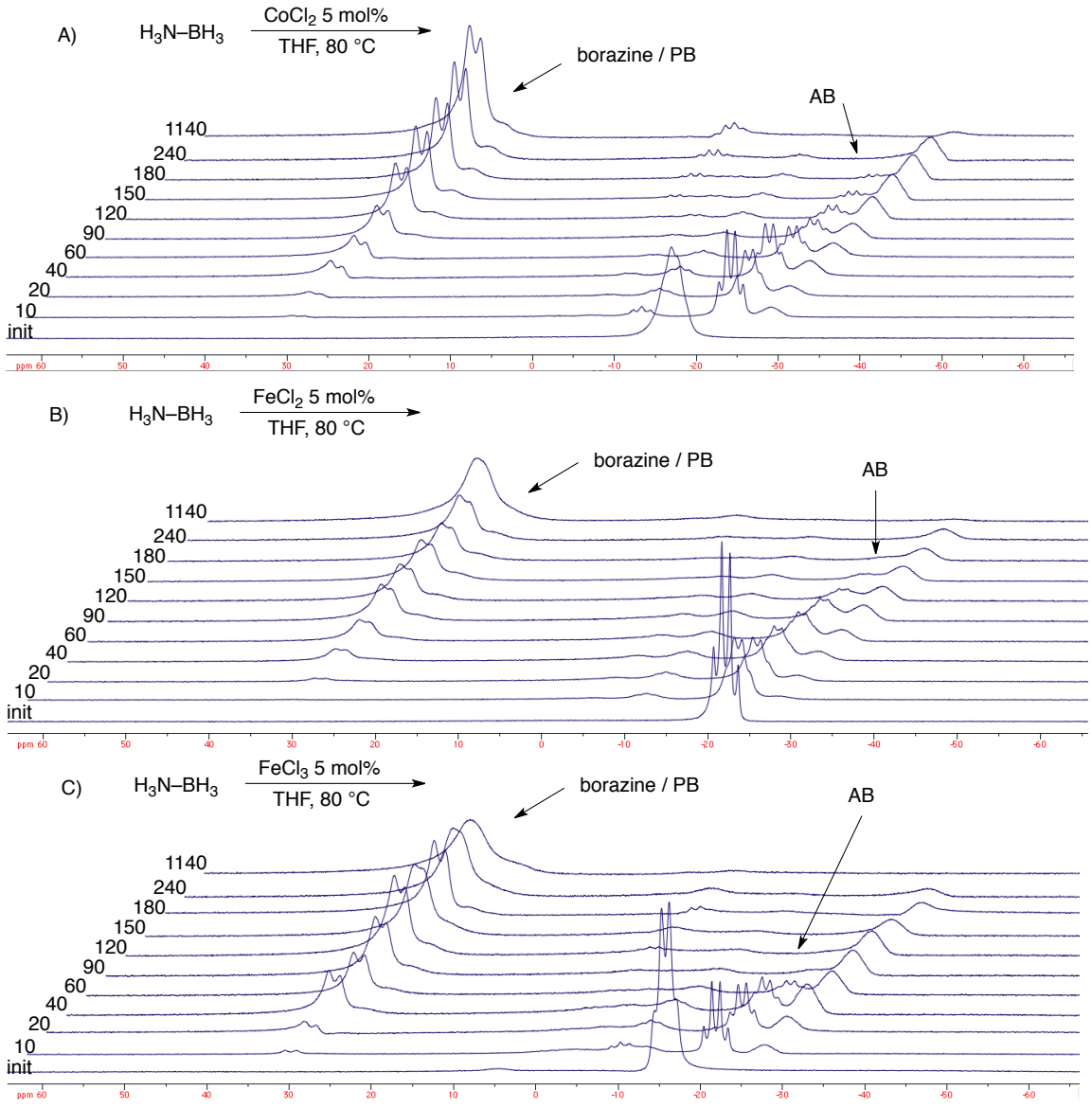

Scheme 4.5. ^{11}B NMR evaluation of the dehydrogenation of AB catalyzed by A) $CoCl_2$, B) $FeCl_2$ and C) $FeCl_3$.

Synthesis of Novel AB Derivatives

Compound 4. To a stirring solution of $Li[MeBH_3]$ (0.135 g, 3.77 mmol) in Et_2O (10 mL) was added $MeNH_3Cl$ (0.255 g, 3.77 mmol). The slurry was allowed to stir for 1 hour, and then filtered through an Acrodisc. The majority of the solvent (75%) was removed under reduced pressure and pentane was

$MeH_2N–BH_2Me$

4

added to cause precipitation of the product. The solvent layer was removed by pipet and the solid residue was washed two times with pentane to give **4** as a white crystalline solid (0.191 g, 88% yield).

^{1}H NMR (300 MHz, CD_2Cl_2): δ 3.35 (t br, 2H, N–H), 2.54 (t, $^{3}J_{HH}$ = 4.0 Hz, 3H, N–Me), 1.82 (q br, $^{4}J_{BH}$ = 90 Hz, 2H, B–H), 0.20 (s br, 3H, B–Me). ^{13}C NMR (125 MHz, THF-d8): δ 30.64, 0.49 (br). ^{11}B NMR (96.27 MHz, CD_2Cl_2): δ –11.17 (t, $^{3}J_{BH}$ = 95 Hz). HRMS (EI+) calcd. for C_2H_8NB (–H_2) 57.074980 found 57.074987.

Compound 5. To a stirring solution of Li[$MeBH_3$] (0.075 g, 2.10 mmol) in Et_2O (10 mL) was added NH_4Cl (0.112 g, 2.10 mmol). The slurry was allowed to stir for 1 hour, and then filtered through an Acrodisc. The majority of the solvent (75%) was removed under reduced pressure and pentane was added to cause precipitation of the product. The solvent layer was removed by pipet and the solid residue was washed two times with pentane to give **5** as a white crystalline solid (0.072 g, 75% yield).

$H_3N–BH_2Me$

5

^{1}H NMR (300 MHz, CD_2Cl_2): δ 3.37 (t br, 3H, N–H), 2.93 (q br, $^{4}J_{BH}$ = 90 Hz, 2H, B–H), –0.17 (s br, 3H, B–Me). ^{11}B NMR (96.27 MHz, CD_2Cl_2): δ –14.56 (t, $^{3}J_{BH}$ = 93 Hz).

Dehydrogenation Experiments on the Automated Burette Apparatus

General Procedure. The automated gas burette used was based on the design reported by Sneddon.[30,31] The burette system was purged of air by repeated evacuation/nitrogen cycles (3x). In a glovevox, a 100 mL two-neck flask was charged with ca. 0.075 g BN material, 0.05 mol% $CoCl_2$ catalyst and diglyme solvent (3 mL). The flask was attached

to the burette apparatus under flowing N_2. Once the system pressure equalized, the data collection program was started and the flask was immersed into a preheated oil bath (80 °C). Agitation was provided for each run using the same type of Teflon coated magnetic stir bar, and care was taken to insure that the rate of agitation was comparable in each experiment.

Isolation of Dehydrogenation Product of 4, Hexamethylborazine

Compound 6. A round-bottom flask equipped with a reflux condenser was charged with **4** (0.035 g, 0.61 mmol), $CoCl_2$ (0.004 g, 0.03 mmol) and THF (5 mL). The reaction was stirred at reflux for 24 hours. The crude mixture was filtered through an Acrodisc and the solvent was removed under reduced pressure. The residue was washed with pentane and hexamethylborazine was recovered (0.024, 71% yield). ^{1}H and ^{11}B spectra are consistent with spectra collected from authentic hexamethylborazine, prepared by literature method.[32]

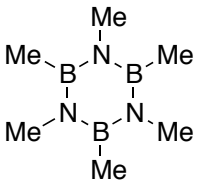

6

Regeneration of Spent Material

Compound 8. A round bottom flask was charged with hexamethylborazine **6** (prepared as in reference 32, 0.085 g, 0.52 mmol), formic acid (0.071 g, 1.55 mmol) and CH_2Cl_2 (10 mL). The reaction mixture was stirred for 1 hour and the solvent

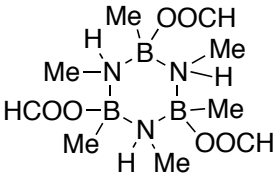

8

was removed under reduced pressure. The residue was washed with cold Et_2O and compound **8** was recovered (0.142 g, 91% yield). X-ray quality crystals were grown from slow evaporation of Et_2O (see below).

^1H NMR (300 MHz, CD_2Cl_2): δ 8.23 (s, 3H, OOC–H), 5.41 (s br, 3H, N–H), 2.17 (m, 9H, N–Me), –0.05 (s, 9H B–Me). ^{11}B NMR (96.27 MHz, CD_2Cl_2): δ 4.717 (s). HRMS (ES+) calcd. for $C_9H_{24}B_3N_3O_6Na$ 326.1842 found 326.1839.

Compound 4 from 8. A round bottom flask was charged with **8** (0.071 g, 0.24 mmol) and Et_2O (10 mL). $LiAlH_4$ (0.013 g, 0.35 mmol) was added and the mixture was stirred for 20 minutes, at which time the reaction flask was opened to the air and wet THF (5 mL, 5 drops H_2O) was added. The crude mixture was filtered through an Acrodisc, the solvent was removed under reduced pressure, and the residue was washed with cold pentane to give compound **4** (0.020g, 46% yield). ^1H and ^{11}B NMR spectra are consistent with authentic **4** prepared as above.

CHAPTER V

SYNTHESIS AND ELECTRONIC PARAMETER DETERMINATION OF AN AZABORINE-CONTAINING PHOSPHINE LIGAND

5.1. General Overview

This chapter describes the synthesis of an azaborine-containing triarylphosphine ligand analog and the determination of its electronic parameter using an Ir-carbonyl complex. It was found that azaborine-containing analog of tri(*o*-tolyl)phosphine is a stronger net electron donor than all-carbon tri-(*o*-tolyl)phosphine**.** This chapter contains unpublished material. The lab work was performed by me and by an undergraduate researcher in the group, Carey R. Fristoe, under my direction. Lev N. Zakharov provided single crystal X-ray analysis and Shih-Yuan Liu provided editorial assistance and scientific guidance.

5.2. Introduction

Tertiary aryl-phosphines are omnipresent ligands in transition metal chemistry.[1,2] Phosphine ligands are typically spectators in transition metal catalyzed reactions and do not react with substrates undergoing catalysis.[3] Instead, they coordinate strongly with metals, stabilizing lower oxidization states as well as imparting selectivity through both steric and electronic effects.[4] In the 1970s, Tolman pioneered the methods, still used today, to characterize the steric (cone angle) and electronic (net donating ability) parameters of phosphine ligands. His seminal 1977 review on the subject has received

nearly 3500 citations to date.[5] The Tolman Electronic Parameter (TEP) of a ligand is the frequency of the A^1 carbonyl vibrational mode of $Ni(CO)_3L$ and has been measured for scores of tertiary phosphine ligands.[6,7] More recently, the TEP has been experimentally determined for N-heterocyclic carbenes (NHCs)[8,9] and computationally determined for other ligands, such as NH_3, NMe_3, and CH_3CN.[10] Due to the toxicity of nickel-carbonyl complexes, an alternative system based on $Ir(CO)_2ClL$ has been developed for measuring the electronic parameter.[11] The net electron donor ability trend is the same whether $Ni(CO)_3L$ or $Ir(CO)_2ClL$ is used and correlations have been established relating one scale to the other.[8]

Research in our group explores the fundamental properties and applications of 1,2-dihydro-1,2-azaborines (henceforth referred to as azaborines), which are arene isosteres that have a C=C unit replaced with an isoelectronic B–N unit.[12-15] The resulting aromatic molecules have similar structures to their all-carbon analogs, but different electronic properties due to the polarized B–N bond.[16-18] The inherent differences between C=C and B–N bonds make the substitution of an azaborine moiety into traditionally all-carbon arene systems interesting from a synthetic and fundamental point-of-view, and may have practical implications as well (for example, favorable optoelectronic properties).[19-23] The utility of phosphine ligands is due in part to the ease with which they can be synthesized with a broad scope of substituents, allowing for tunability with regard to their steric and electronic parameters. Both can have significant impact on the reactivity of a metal complex; however, it is not usually possible to modify one parameter without affecting the other. Incorporation of one or more azaborine units into a tertiary aryl phosphine could provide the unique opportunity to alter the electronic

parameter without significantly changing the steric parameter. Herein, we report the first synthesis of an azaborine-containing phosphine ligand[24] and its incorporation into an iridium-carbonyl complex, which enabled the experimental determination of its electronic parameter using IR spectroscopy.

5.3. Results and Discussion

Initially, we chose to target an analog of the parent tertiary aryl-phosphine, triphenylphosphine, in which one of phenyl rings has been replaced with an N–H containing azaborine ring (**1**, Scheme 5.1). Our plan was to form the boron-phosphorous bond using a nitrogen-protected B–Cl precursor, then use late-stage deprotection to generate **1**, which is a synthetic strategy analogous to the one that led to the successful isolation of the parent 1,2-dihydro-1,2-azaborine.[14] We were delighted to find that diphenylphosphide cleanly added to the known versatile B–Cl species **2** to afford N–TBS [TBS = *tert*-butyl(dimethyl)silyl] protected species **3** in 67 % yield after purification by recrystallization. We were able to obtain crystals of **3** suitable for single crystal X-ray diffraction, which unambiguously confirmed our structural assignment.

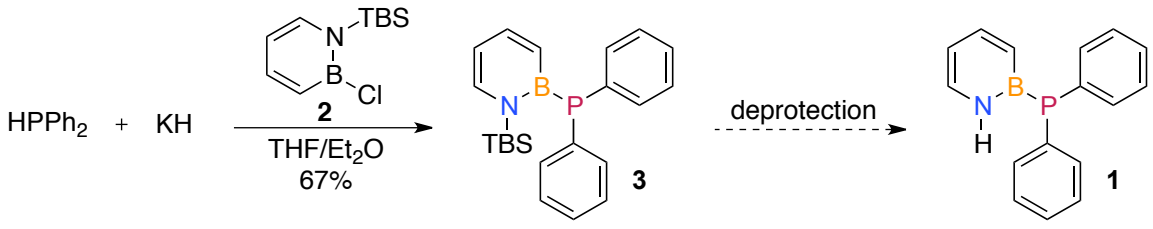

Scheme 5.1. Attempted synthesis of triphenylphosphine analog **1**.

Unfortunately, our attempts to remove the silyl protecting group to generate the parent N–H compound **1** were met with frustration. We investigated traditional fluoride mediated deprotection methods using reagents such as TBAF, HF-pyridine, and TAS-F, as well as Lewis and Brønsted acid mediated routes. None of the conditions screened provided any evidence for the formation of **1**, presumably due to the lability of the boron-phosphorous bond. We also synthesized the η^6–chromium complex of **3** in an attempt to activate the N–Si bond toward cleavage;[14] however this, too, proved futile.

Instead, we chose to target a different aryl-phosphine analog, tri(*o*-tolyl)phosphine, in which one tolyl group has been replaced with an N-methyl substituted azaborine (**4**, Scheme 5.2). In this case, we were able to avoid the use of nitrogen protecting-groups entirely and still investigate the electronic and steric effects of azaborine incorporation into a known ligand motif. Tri(*o*-tolyl)phosphine is a widely used ligand and has been shown to impart favorable reactivity to catalytic transformations such as palladium-catalyzed cross-coupling reactions[25] and aminocarbonylation of anilines.[26]

The synthesis of **4** is illustrated in Scheme 5.2. Condensation of *in situ* generated allyldichloroborane and allylmethylamine in the presence of triethylamine afforded the bisallyl ring-closing precursor **5** in 43% yield. Grubbs' first generation catalyst was used to facilitate the ring-closing metathesis of **5** to furnish heterocycle **6**. Without purification, **6** was treated with 5 mol% Pd/C to generate the aromatic species **7** in 34% yield over two steps. A solution of **7** in THF was added to potassium di(*o*-tolyl)phosphide generated *in situ* from potassium hydride and di(*o*-tolyl)phosphine to give the desired product **4** in 45% yield.

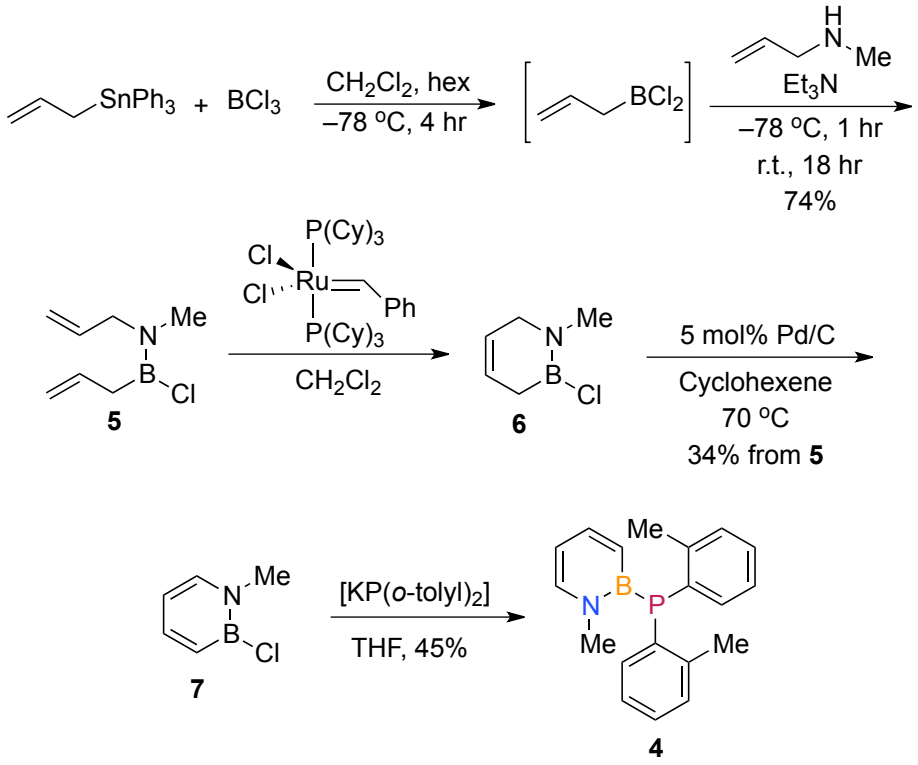

Scheme 5.2. Synthesis of N-methyl substituted tri(*o*-tolyl)phosphine analog **4**.

We were able to obtain single crystals of **4** suitable for X-ray diffraction and thus unambiguously confirm the assigned structure (see ORTEP illustration, Figure 5.1). A comparison of relevant bond lengths between **1** and the known structure of tri(*o*-tolyl)phosphine[27] **8** is reveals only minor differences (bond length values for tri(*o*-tolyl)phosphine presented here are the average of the three chemically identical tolyl groups). For instance, the bond lengths for the P–B in **4** and P–C(1) in **8** are 1.929(2) Å and 1.835 Å, respectively; the distance between B–N in **4** and C(1)–C(2) in **8** are 1.435(2) Å and 1.406 Å, respectively; and the bond lengths for N–Me in **4** and the equivalent C(2)–Me in **8** are 1.480(2) Å and 1.500 Å, respectively

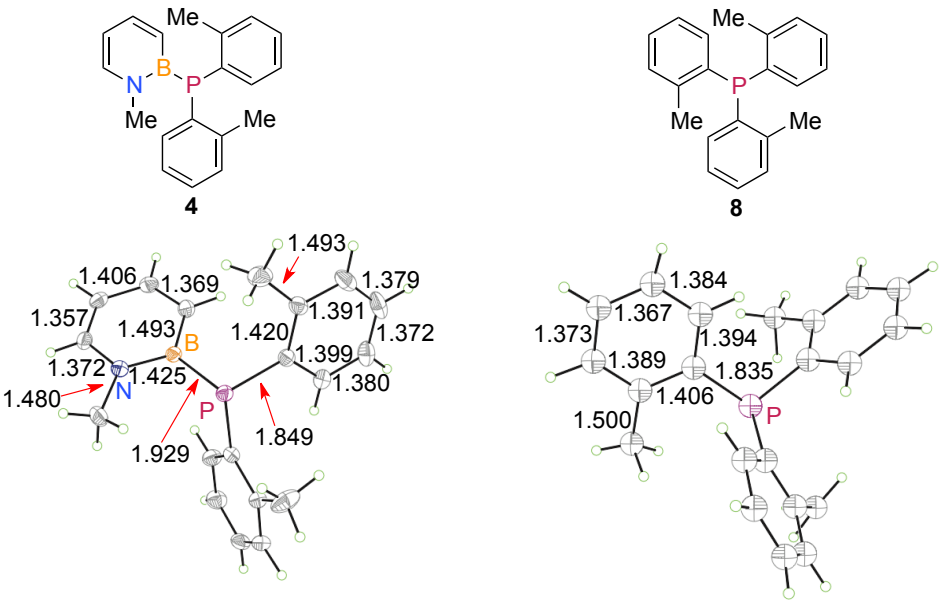

Figure 5.1. Structure and selected bond lengths (Å) for compounds **4** and **8**.

The iridium-carbonyl complex **10** was synthesized in two steps (Scheme 5.3). First, addition of **4** to a solution of $[Ir(cod)Cl]_2$ afforded complex **9** in 93% yield. Then, a dichloromethane solution of **9** was stirred under an atmosphere of carbon monoxide for 10 minutes and the desired product **10** was isolated by removing the solvent under reduced pressure.

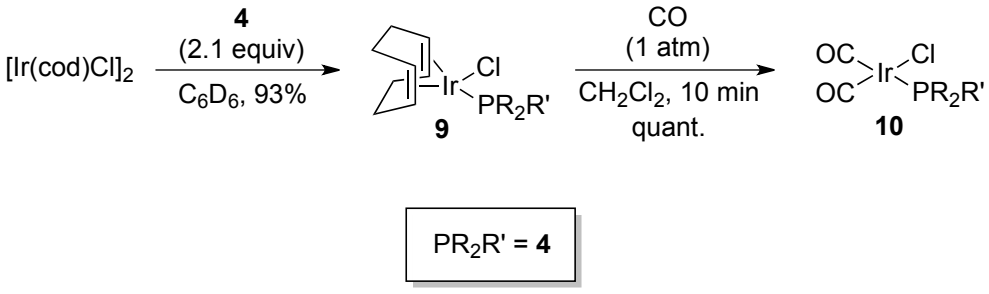

Scheme 5.3. The synthesis of iridium metal complex for determination of electronic parameter.

Complex **10** is a powdery solid and, despite valiant efforts, we were unable to grow single crystals suitable for X-ray diffraction. However, we were able to obtain crystal structures for the precursor **9** as well as its all-carbon analog **11** (Figure 5.2) and they were used to evaluate the ligand geometry when bound to an Ir metal center. While resolving the structure of **9**, we found that we could not differentiate between the two *o*-tolyl groups and the azaborine group (that is, the azaborine is disordered over the three possible positions) and therefore the reported bond lengths can only be interpreted as the average of three possible orientations. The bond lengths in **9** compare well with the equivalent bonds in **11**. Moreover, the average angles for Ir–P–R in complexes **9** and **11** are 114.18° and 114.15°, respectively – effectively identical within the error associated with this measurement. Though this crystallographic data cannot be used to confirm the presence of an azaborine moiety in complex **9**, clean starting materials and careful ^{1}H and ^{11}B NMR characterization, combined with the unambiguous structural assignment of the free ligand, make us confident of our assigned structure.

With the desired complex **10** in hand, acquiring the infrared spectrum was the next step in determining the electronic parameter. The convention for finding the electronic parameter using *cis*-carbonyl $Ir(CO)_2ClL$ complexes is to report the average of the symmetric and asymmetric A^1 carbonyl vibrational mode. The FTIR data for **10** and the all-carbon analog **12** are presented in Table 5.1. Under our measurement conditions (KCl plate) we found that for complex **10**, $\upsilon(CO)_{avg}$ = 2006 cm^{-1} and for complex **12**, $\upsilon(CO)_{avg}$ = 2029 cm^{-1}. The smaller $\upsilon(CO)_{avg}$ indicates a greater net electron donating ability for the azaborine-substituted phosphine ligand **4** compared with all-carbon tri(*o*-

tolyl)phosphine **8**. This can be rationalized intuitively by the incorporation of the less electronegative boron atom (P–B vs. P–C), which leaves more electron density with the phosphorous. The electronic parameter determined using $Ir(CO)_2ClL$ is related to the Tolman Electronic Parameter (defined using $Ni(CO)_3L$ systems) by the equation: TEP = $0.722[\upsilon(CO)_{avg}] + 539$ cm^{-1}.[8] Therefore, the TEP for our azaborine-substituted tri(*o*-tolyl)phosphine analog is 2041 cm^{-1}.

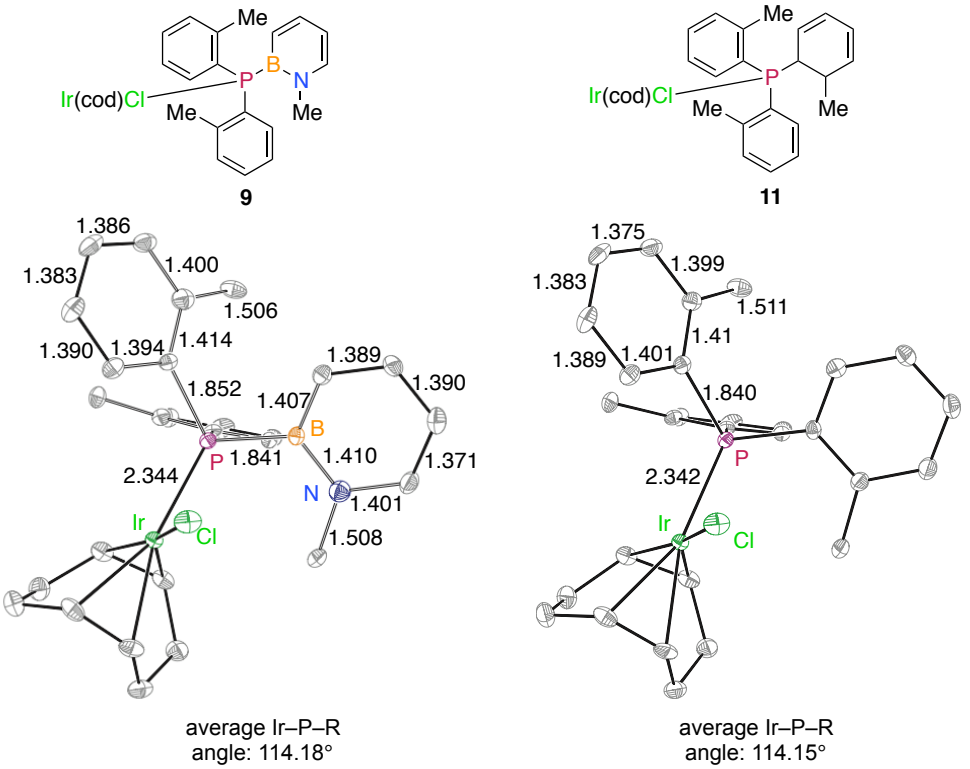

Figure 5.2. Comparison of the average bond lengths (Å) and angles in the crystal structures of **9** and **11.** Note that the tolyl groups in **9** are disordered in the crystal lattice.

Table 5.1. Experimentally determined υ(CO) for the symmetric and asymmetric vibrational mode and the average υ(CO) for $Ir(CO)_2ClL$ with ligands **4** and **8**, as well as calculated TEP.

$Ir(CO)_2Cl$**L**	υ(CO) (cm^{-1})	$υ(CO)_{avg}$ (cm^{-1})	TEP (cm^{-1})
L = 4	2048, 1963	2006	2041[a]
L = 8	2070, 1988	2029	2058[a], 2067[b]

a. Calculated using the equation $TEP=0.722[υ(CO)_{avg}] + 539\ cm^{-1}$
b. From reference 7

5.4. Conclusion

In summary, we have successfully synthesized the first azaborine-containing phosphine ligand, the tri(*o*-toly)phosphine analog **4**, as well as the iridium complexes **9** and **10**. We obtained crystal structures for the free ligand **4** as well as the iridium complex **9** and found that incorporation of azaborine did not appreciably alter the steric parameter compared with the carbonaceous analogs. We measured the electronic parameter in an $Ir(CO)_2ClL$ system using FT-IR and found the $υ(CO)_{avg} = 2006\ cm^{-1}$ using ligand **4** compared with $υ(CO)_{avg} = 2029\ cm^{-1}$ for the all-carbon ligand **8**. This remarkable difference indicates that **4** is a stronger net electron donor ligand than tri-(*o*-tolyl)phosphine**.** This study opens the door for the creation of a family of ligands with independently tunable steric and electronic parameters. Future plans include synthesizing tertiary phosphorous ligands substituted with two or three azaborines, as well as studies probing ligand performance in transition metal catalyzed reactions.

5.5. Experimental

General

All oxygen- and moisture-sensitive manipulations were carried out under an inert atmosphere using either standard Schlenk techniques or a glove box. THF, Et_2O, CH_2Cl_2 and pentane were purified by passing through a neutral alumina column under argon. Potassium hydride (Aldrich) was washed with pentane three times and pumped dry under vacuum prior to use. All other chemicals and solvents were purchased (TCI, Aldrich or Strem) and used as received. ^{11}B NMR spectra were recorded on a Varian Unity/Inova 600 spectrometer or Varian Unity/Inova 300 spectrometer at ambient temperature. ^{1}H NMR spectra were recorded on a Varian Unity/Inova 300 or Varian Unity/Inova 600 spectrometer. ^{13}C NMR spectra were recorded on a Varian Unity/Inova 600 spectrometer. All chemical shifts are externally referenced: ^{11}B NMR to $BF_3 \bullet Et_2O$ (δ 0) and ^{31}P NMR to 1% H_3PO_4 (δ 0). IR spectra were recorded on a Nicolet Magna 550 FT-IR instrument with OMNIC software.

Compound 3: In a glove box, a solution of diphenylphosphine (0.41 g, 2.2 mmol) in THF (15 mL) was added to KH (0.097 g, 2.42 mmol) in a stirbar equipped 20 mL scintillation vial and stired until there was no visible release of gas, about 1 hour. The solution was filtered through an Acrodisc and the filtrate cooled to –20 °C. The filtrate was added dropwise to a cold solution of **2** (0.500 g, 2.20 mmol) in Et_2O (7 mL) and stired at RT for 16 hours. Solvent was removed under reduced pressure and the crude mixture was redissolved in pentane. The pentane solution was passed through an Acrodisc and pentane was removed under

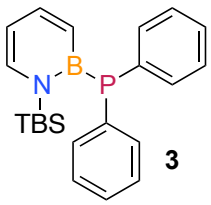

3

reduced pressure. The remaining solid was dissolved in a minimal amount of pentane and placed in the freezer. Recrystallization afforded **3** (0.500 g, 67% yield).

^{1}H NMR (300 MHz, C_6D_6): δ 7.58 (t, 4H), 7.41 (m, 1H), 7.32 (d, 1H), 7.1 (m, 6H), 6.92 (d, 1H), 6.24 (t, 1H), 0.94 (s, 9H), 0.38 (s, 6H). ^{11}B NMR (192.5 MHz, C_6D_6): δ 42.1. ^{31}P NMR (121.4 MHz, C_6D_6): δ -50.

Compound 5. Allyldichloroborane was generated *in-situ* through transmetallation of allyltriphenyltin (24.99 g, 63.91 mmol) with boron trichloride (1 M in hex, 63.91 mL, 63.91 mmol) added dropwise and allowed to stir at –78 °C for 4 hours. A solution of allylmethylamine (5.00 g, 70.30 mmol) and triethylamine (6.84 g, 67.11 mmol) in pentane was added dropwise to the allyldichloroborane solution at –78 °C and allowed to stir cold for 1 hour. The temperature was slowly raised to room temperature and the solution was allowed to stir over night to form the bis-allyl ring-closed precursor, **2**, which was isolated via vacuum distillation (4.36 g, 43% yield).

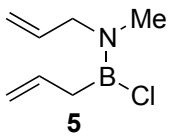

5

^{1}H NMR (300 MHz, C_6D_6) δ 5.9 (m, 4H), 5.4 (m, 1H), 5.0 (m, 1H), 3.5 (d, 2H), 3.2 (d, 2H), 2.6 (s, 3H); ^{13}C NMR (150 MHz, CD_2Cl_2) δ 135.8, 135.6, 135.2, 135.1, 116.6, 116.5, 114.8 (2x), 54.9, 54.6, 37.5, 36.9, 27.2 (br, 2x); ^{11}B NMR (96 MHz, C_6D_6) δ 37.8. IR (thin film) 3072, 2933, 1625, 1500, 1410, 1251, 1168, 1078, 981, 898, 635 cm^{-1}. HRMS (CI+) calcd. for $C_7H_{14}BNCl$ ($M+H^+$) 158.0908, found 158.0909.

Compound 7. Grubbs' 1st generation catalyst (0.99 g, 1.21 mmol) was added to a solution of **5** (3.80 g, 24.14 mmol) in DCM to give the

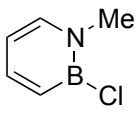

7

heterocycle **6**. After removal of the DCM under reduced pressure, the crude material was redissolved in cyclohexene and Pd/C (10%) (0.383 g, 0.36 mmol) was added. The mixture was allowed to react overnight in a pressure vessel at 70 °C. The desired product, **7**, was isolated by vacuum distillation (1.04 g, 34% yield).

^{1}H NMR (300 MHz, C_6D_6)-δ 7.3 (s, 1H), 6.8 (d, 1H), 6.3 (s, 1H), 5.9 (m, 1H), 2.8 (s, 3H). ^{11}B NMR (96 MHz, C_6D_6)-δ 32.1. ^{13}C NMR (125 MHz, C_6D_6)-δ 145.3, 140.3, 111.2, 98.8. IR (thin film) 2940, 1610, 1514, 1396, 1403, 1028, 801, 732, 656 cm^{-1}. HRMS (CI+) calcd. for C_5H_8ClBN ($M+H^+$) 128.0438, found 128.0443.

Compound 4. A solution of di(*o*-tolyl)phosphine (0.839 g, 3.92 mmol) in THF was treated with potassium hydride (0.188 g, 4.71 mmol) to generate di(*o*-tolyl)phosphide *in situ*. A solution of **7** (0.50 g, 3.92 mmol) in THF was added to the filtered phosphide solution at –20 °C and allowed to warm to room temperature. The desired product was isolated by extraction with pentane (0.54 g, 45% yield).

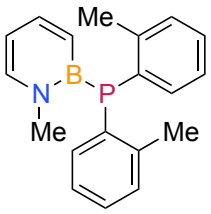

4

^{1}H NMR (300 MHz, C_6D_6): δ 7.2(s, 1H), 7.1(s, 1H), 6.9(m, 5H), 6.7(m, 4H), 6.5(s, 1H), 3.1(s, 6H), 2.4(s, 3H). ^{11}B NMR (96 MHz, C_6D_6): δ 38.8. ^{13}C NMR (125 MHz, C_6D_6): δ 145.3, 144.4, 143.1, 138.3, 137.2, 135.5, 114.8, 45.3, 36.5, 24.3, 16.5. ^{31}P NMR (300 MHz, C_6D_6): δ -68.2.

Compound 9. A solution of **4** (0.050 g, 0.163 mmol) in benzene was added to a solution of $[Ir(cod)Cl]_2$ dimer (0.051 g, 0.077 mmol) in benzene and was stirred for 18 hours. The benzene was removed under

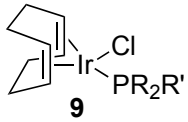

9

PR_2R' = **4**

reduced pressure and the desired product was isolated by recrystallization by slow evaporation from a 1:2 solution of DCM/pentane (0.094 g, 93% yield). The crystals isolated were suitable for analysis by single crystal X-ray diffraction, which confirmed the assigned structure.

^{1}H NMR (300 MHz, CD_2Cl_2): δ 8.14 (s br, 1H), 7.60 (m, 1H), 7.4–7.2 (m, 8H) 6.84 (m, 1H) 6.53 (m, 1H), 4.83 (s, 2H) 3.63, (s, 4H), 2.72 (s br, 3H), 2.45 (s, 2H) 2.23 (s br, 6H) 1.73 (m, 4H), 1.53 (m, 4H). ^{11}B NMR (96 MHz, C_6D_6): δ 32.7. ^{13}C NMR (125 MHz, CD_2Cl_2): δ 142.8, 141.9, 134.4, 131.3, 129.8, 127.5, 125.2, 112.7, 86.9, 33.0, 29.5, 23.4 ^{31}P NMR (300 MHz, C_6D_6): δ –18.3. FT-IR (KCl salt plate) 2962, 1962, 1614, 1409, 1125, 1074, 1031, 802, 748.

Compound 10. A Solution of **9** (0.050 g, 0.078 mmol) in DCM (10 mL) was stirred under an atmosphere of CO for 10 minutes. The desired product was isolated by removing the solvent at reduced pressure and washing with cold pentane (0.045 g, 99% yield).

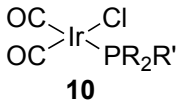

10

PR_2R' = **4**

^{1}H NMR (300 MHz, CD_2Cl_2): δ 7.5–7.25 (m, 8H), 7.12 (m, 1H), 6.97 (s, 1H), 6.87 (s, 1H), 6.33 (m, 1H) 2.49 (s br, 3H), 2.30 (s br, 6H). ^{11}B NMR (96 MHz, C_6D_6): δ 28.1. ^{13}C NMR (125 MHz, CD_2Cl_2): δ 144.9, 139.7, 136.9 131.46, 128.5, 126.2, 125.1, 120.2, 106.05, 37.1, 27.9. 22.3. ^{31}P NMR (300 MHz, C_6D_6): δ –25.0. FT-IR (KCl salt plate) 3053, 2962, 2919, 2850, 2054, 2007, 1964, 1614, 1465, 1410, 1261, 1094, 1020, 802, 749.

Compound 11. Tri(*o*-tolyl)phosphine (0.049 g, 0.164 mmol) was dissolved in benzene and added to a solution of $[Ir(cod)Cl]_2$ (0.051 g, 0.078 mmol) in benzene. The mixture was allowed to react for 18 hours. Benzene was removed under reduced pressure and the desired product **8** was recrystallized by slow evaporation of a 1:2 solution of DCM:pentane (0.090 g, 90% yield).

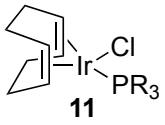

11

R = *o*-tol

^{1}H NMR (300 MHz, C_6D_6): δ 7.5 (m, 2H), 7.2–7.4 (m, 3H), 5.5 (m, 4H), 2.5 (s, 4H), 2.3 (m, 9H), 2.2 (s, 4H). ^{13}C NMR (125 MHz, C_6D_6): δ 142.7, 142.6, 134.7, 133.3, 132.8, 130.4, 129.9, 128.9, 128.3, 128.1, 126.5, 126.1, 20.9, 15.1, 13.8. ^{31}P NMR (300 MHz, C_6D_6): δ 19.0. FT-IR (KCl salt plate) 2962, 2917, 2849, 1965, 1578, 1473, 1448, 1384, 1261, 1092, 1020, 800.

Compound 12. A Solution of **11** (0.050 g, 0.074 mmol) in DCM was stirred under an atmosphere of CO for 10 minutes. The desired compound was isolated as a powdery solid by removing the solvent and washing with cold pentane (0.044 g, 99% yield).

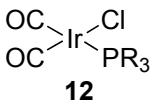

12

R = *o*-tol

^{1}H NMR (300 MHz, CD_2Cl_2): δ 7.3 (m, 2H), 7.0 (m, 6H), 6.8 (m, 4H), 3.3 (s, 9H). ^{13}C NMR (125 MHz, CD_2Cl_2): δ 142.8, 132.1, 131.5, 130.4, 129.9, 128.5, 125.8, 125.0, 23.3. ^{31}P NMR (300 MHz, CD_2Cl_2): δ 20.6. FT-IR (KCl salt plate) 3053, 2920, 2071, 1988, 1957, 1565, 1384, 1263, 1067, 1031, 803.

APPENDIX

COMPLETE CRYSTALLOGRAPHIC DATA

Chapter II

Crystallographic Data for 7 (liu62)

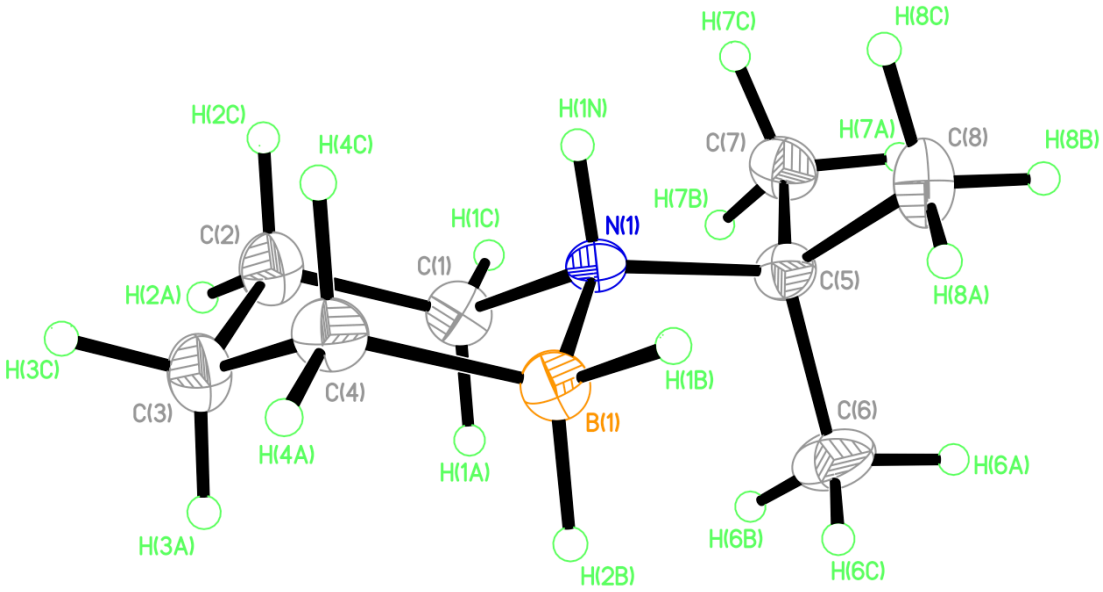

Table 1. Crystal data and structure refinement for liu62.

Identification code	liu62	
Empirical formula	C8 H20 B N	
Formula weight	141.06	
Temperature	173(2) K	
Wavelength	0.71073 Å	
Crystal system	Monoclinic	
Space group	P2(1)/n	
Unit cell dimensions	a = 6.265(2) Å	a= 90°.
	b = 9.606(3) Å	b= 93.660(6)°.
	c = 15.868(5) Å	g = 90°.
Volume	953.0(5) Å^3	
Z	4	

Density (calculated)	0.983 Mg/m^3
Absorption coefficient	0.055 mm^{-1}
F(000)	320
Crystal size	0.40 x 0.38 x 0.04 mm^3
Theta range for data collection	2.48 to 25.00°.
Index ranges	-7<=h<=7, -10<=k<=11, -18<=l<=18
Reflections collected	5830
Independent reflections	1684 [R(int) = 0.0205]
Completeness to theta = 25.00°	99.9 %
Absorption correction	Semi-empirical from equivalents
Max. and min. transmission	0.9978 and 0.9784
Refinement method	Full-matrix least-squares on F^2
Data / restraints / parameters	1684 / 0 / 171
Goodness-of-fit on F^2	1.038
Final R indices [I>2sigma(I)]	R1 = 0.0447, wR2 = 0.1118
R indices (all data)	R1 = 0.0561, wR2 = 0.1224
Largest diff. peak and hole	0.163 and -0.112 $e.Å^{-3}$

Table 2. Atomic coordinates (x 10^4) and equivalent isotropic displacement parameters ($Å^2$x 10^3) for liu62. U(eq) is defined as one third of the trace of the orthogonalized U^{ij} tensor.

	x	y	z	U(eq)
N(1)	765(2)	1669(1)	2574(1)	29(1)
B(1)	2556(3)	2737(2)	2219(1)	37(1)
C(1)	-1161(2)	1655(2)	1962(1)	38(1)
C(2)	-606(3)	1175(2)	1093(1)	43(1)
C(3)	1004(3)	2119(2)	701(1)	45(1)
C(4)	3034(2)	2217(2)	1281(1)	40(1)
C(5)	205(2)	1832(2)	3497(1)	34(1)
C(6)	-655(4)	3285(2)	3635(1)	58(1)
C(7)	-1463(3)	756(2)	3713(1)	45(1)
C(8)	2236(3)	1563(2)	4052(1)	51(1)

Table 3. Bond lengths [Å] and angles [°] for liu62.

N(1)-C(1)	1.5002(18)
N(1)-C(5)	1.5359(18)
N(1)-B(1)	1.646(2)
N(1)-H(1N)	0.901(17)
B(1)-C(4)	1.615(2)
B(1)-H(1B)	1.137(15)
B(1)-H(2B)	1.161(16)
C(1)-C(2)	1.515(2)
C(1)-H(1A)	0.992(17)
C(1)-H(1C)	0.973(17)
C(2)-C(3)	1.518(2)
C(2)-H(2A)	1.002(16)
C(2)-H(2C)	0.984(17)
C(3)-C(4)	1.525(2)
C(3)-H(3A)	1.021(18)
C(3)-H(3C)	0.999(18)
C(4)-H(4A)	1.009(19)
C(4)-H(4C)	1.035(19)
C(5)-C(6)	1.516(2)
C(5)-C(8)	1.523(2)
C(5)-C(7)	1.524(2)
C(6)-H(6A)	1.01(2)
C(6)-H(6B)	1.01(2)
C(6)-H(6C)	0.96(3)
C(7)-H(7A)	0.983(18)
C(7)-H(7B)	0.999(18)
C(7)-H(7C)	0.973(19)
C(8)-H(8A)	0.99(2)
C(8)-H(8B)	0.989(18)
C(8)-H(8C)	1.02(2)
C(1)-N(1)-C(5)	113.29(11)
C(1)-N(1)-B(1)	108.74(11)
C(5)-N(1)-B(1)	117.71(10)

C(1)-N(1)-H(1N)	105.1(9)
C(5)-N(1)-H(1N)	104.0(9)
B(1)-N(1)-H(1N)	106.9(10)
C(4)-B(1)-N(1)	107.05(12)
C(4)-B(1)-H(1B)	113.3(8)
N(1)-B(1)-H(1B)	108.8(8)
C(4)-B(1)-H(2B)	111.8(7)
N(1)-B(1)-H(2B)	103.9(8)
H(1B)-B(1)-H(2B)	111.4(10)
N(1)-C(1)-C(2)	111.73(12)
N(1)-C(1)-H(1A)	106.6(9)
C(2)-C(1)-H(1A)	110.1(9)
N(1)-C(1)-H(1C)	108.2(8)
C(2)-C(1)-H(1C)	111.5(9)
H(1A)-C(1)-H(1C)	108.6(13)
C(1)-C(2)-C(3)	112.80(14)
C(1)-C(2)-H(2A)	105.6(9)
C(3)-C(2)-H(2A)	111.9(9)
C(1)-C(2)-H(2C)	108.4(9)
C(3)-C(2)-H(2C)	110.3(10)
H(2A)-C(2)-H(2C)	107.7(12)
C(2)-C(3)-C(4)	109.89(13)
C(2)-C(3)-H(3A)	108.0(10)
C(4)-C(3)-H(3A)	109.3(10)
C(2)-C(3)-H(3C)	109.0(10)
C(4)-C(3)-H(3C)	112.9(10)
H(3A)-C(3)-H(3C)	107.6(14)
C(3)-C(4)-B(1)	112.25(13)
C(3)-C(4)-H(4A)	110.5(9)
B(1)-C(4)-H(4A)	109.3(10)
C(3)-C(4)-H(4C)	108.3(9)
B(1)-C(4)-H(4C)	109.4(9)
H(4A)-C(4)-H(4C)	107.0(14)
C(6)-C(5)-C(8)	111.34(15)
C(6)-C(5)-C(7)	109.67(14)
C(8)-C(5)-C(7)	108.35(13)

C(6)-C(5)-N(1)	109.69(12)
C(8)-C(5)-N(1)	107.51(12)
C(7)-C(5)-N(1)	110.25(12)
C(5)-C(6)-H(6A)	108.8(11)
C(5)-C(6)-H(6B)	111.4(13)
H(6A)-C(6)-H(6B)	109.6(17)
C(5)-C(6)-H(6C)	110.5(14)
H(6A)-C(6)-H(6C)	107.2(17)
H(6B)-C(6)-H(6C)	109.2(19)
C(5)-C(7)-H(7A)	108.0(10)
C(5)-C(7)-H(7B)	112.5(10)
H(7A)-C(7)-H(7B)	108.0(14)
C(5)-C(7)-H(7C)	111.0(11)
H(7A)-C(7)-H(7C)	109.7(15)
H(7B)-C(7)-H(7C)	107.6(14)
C(5)-C(8)-H(8A)	110.4(11)
C(5)-C(8)-H(8B)	109.0(10)
H(8A)-C(8)-H(8B)	107.0(14)
C(5)-C(8)-H(8C)	110.7(11)
H(8A)-C(8)-H(8C)	110.4(15)
H(8B)-C(8)-H(8C)	109.3(14)

Symmetry transformations used to generate equivalent atoms:

Table 4. Anisotropic displacement parameters ($Å^2 x\ 10^3$)for liu62. The anisotropic displacement factor exponent takes the form: $-2p^2[\ h^2a^{*2}U^{11} + ... + 2\ h\ k\ a^*\ b^*\ U^{12}\ ]$

	U^{11}	U^{22}	U^{33}	U^{23}	U^{13}	U^{12}
N(1)	26(1)	26(1)	35(1)	0(1)	3(1)	1(1)
B(1)	32(1)	39(1)	40(1)	2(1)	2(1)	-9(1)
C(1)	26(1)	43(1)	45(1)	2(1)	1(1)	-4(1)
C(2)	38(1)	49(1)	41(1)	-3(1)	-2(1)	-11(1)
C(3)	47(1)	52(1)	36(1)	0(1)	4(1)	-8(1)
C(4)	34(1)	41(1)	46(1)	3(1)	9(1)	-6(1)
C(5)	34(1)	33(1)	36(1)	-1(1)	10(1)	2(1)
C(6)	80(2)	36(1)	63(1)	-4(1)	35(1)	6(1)
C(7)	45(1)	45(1)	46(1)	9(1)	12(1)	-2(1)
C(8)	47(1)	71(1)	34(1)	-4(1)	2(1)	-5(1)

Table 5. Hydrogen coordinates (x 10^4) and isotropic displacement parameters ($Å^2$x 10^3) for liu62.

	x	y	z	U(eq)
H(1N)	1310(20)	803(18)	2552(9)	37(4)
H(1B)	4030(20)	2732(16)	2676(9)	44(4)
H(2B)	1710(20)	3812(17)	2206(9)	45(4)
H(1A)	-1710(30)	2622(19)	1933(10)	46(4)
H(1C)	-2240(20)	1059(17)	2190(9)	41(4)
H(2A)	-2000(30)	1140(17)	745(10)	48(4)
H(2C)	-50(20)	219(18)	1141(10)	43(4)
H(3A)	340(30)	3085(19)	630(11)	52(5)
H(3C)	1280(30)	1764(17)	126(11)	56(5)
H(4A)	4100(30)	2867(19)	1036(11)	58(5)
H(4C)	3740(30)	1240(20)	1317(10)	54(5)
H(6A)	-930(30)	3395(19)	4250(12)	67(6)
H(6B)	-2010(40)	3460(20)	3279(15)	92(8)
H(6C)	390(40)	3980(30)	3506(14)	93(7)
H(7A)	-1580(30)	771(19)	4327(12)	60(5)
H(7B)	-2910(30)	960(19)	3436(11)	58(5)
H(7C)	-1050(30)	-170(20)	3536(11)	59(5)
H(8A)	3300(30)	2300(20)	3971(11)	63(6)
H(8B)	1890(30)	1595(17)	4652(11)	55(5)
H(8C)	2860(30)	610(20)	3924(12)	75(6)

Table 6. Torsion angles [°] for liu62.

C(1)-N(1)-B(1)-C(4)	-56.11(15)
C(5)-N(1)-B(1)-C(4)	173.36(11)
C(5)-N(1)-C(1)-C(2)	-167.26(12)
B(1)-N(1)-C(1)-C(2)	59.84(16)
N(1)-C(1)-C(2)-C(3)	-61.29(19)
C(1)-C(2)-C(3)-C(4)	57.27(19)
C(2)-C(3)-C(4)-B(1)	-55.91(19)
N(1)-B(1)-C(4)-C(3)	55.33(17)
C(1)-N(1)-C(5)-C(6)	-69.01(17)
B(1)-N(1)-C(5)-C(6)	59.40(18)
C(1)-N(1)-C(5)-C(8)	169.78(13)
B(1)-N(1)-C(5)-C(8)	-61.81(16)
C(1)-N(1)-C(5)-C(7)	51.86(16)
B(1)-N(1)-C(5)-C(7)	-179.73(12)

Symmetry transformations used to generate equivalent atoms:

Crystallographic Data for 8 (liur55)

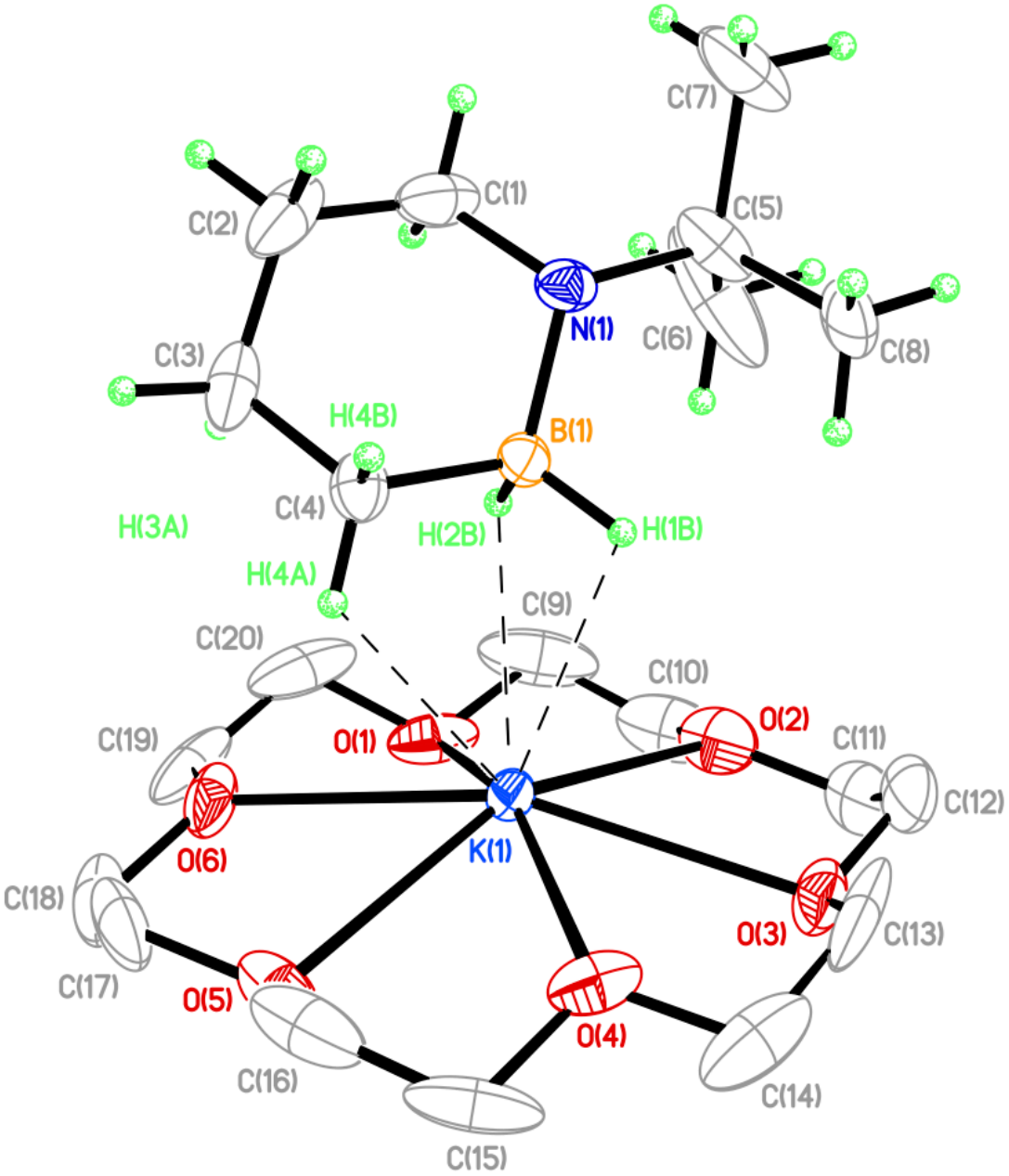

Table 1. Crystal data and structure refinement for liur55.

Identification code	liur55
Empirical formula	C20 H43 B K N O6

Formula weight	443.46	
Temperature	173(2) K	
Wavelength	0.71073 Å	
Crystal system	Monoclinic	
Space group	P2(1)/c	
Unit cell dimensions	a = 9.883(5) Å	a= 90°.
	b = 11.830(6) Å	b= 92.087(8)°.
	c = 22.453(10) Å	g = 90°.
Volume	2623(2) $Å^3$	
Z	4	
Density (calculated)	1.123 Mg/m^3	
Absorption coefficient	0.233 mm^{-1}	
F(000)	968	
Crystal size	0.36 x 0.12 x 0.04 mm^3	
Theta range for data collection	1.82 to 25.00°.	
Index ranges	-11<=h<=11, -11<=k<=14, -26<=l<=22	
Reflections collected	12183	
Independent reflections	4615 [R(int) = 0.0664]	
Completeness to theta = 25.00°	99.8 %	
Absorption correction	Semi-empirical from equivalents	
Max. and min. transmission	0.9907 and 0.9208	
Refinement method	Full-matrix least-squares on F^2	
Data / restraints / parameters	4615 / 0 / 398	
Goodness-of-fit on F^2	1.022	
Final R indices [I>2sigma(I)]	R1 = 0.0687, wR2 = 0.1669	
R indices (all data)	R1 = 0.1170, wR2 = 0.1993	
Largest diff. peak and hole	0.461 and -0.400 $e.Å^{-3}$	

Table 2. Atomic coordinates (x 10^4) and equivalent isotropic displacement parameters ($Å^2$x 10^3) for liur55. U(eq) is defined as one third of the trace of the orthogonalized U^{ij} tensor.

	x	y	z	U(eq)
K(1)	8029(1)	9871(1)	8007(1)	39(1)
O(1)	9665(4)	10963(3)	8929(1)	75(1)
O(2)	10669(3)	9151(3)	8273(2)	77(1)
O(3)	9523(3)	8644(3)	7151(2)	73(1)
O(4)	6903(3)	9488(3)	6854(1)	70(1)
O(5)	6041(3)	11397(3)	7487(2)	77(1)
O(6)	7003(4)	11728(2)	8634(2)	78(1)
N(1)	6807(3)	6990(2)	9204(1)	43(1)
B(1)	6931(4)	8016(3)	8782(2)	39(1)
C(1)	6362(6)	7375(5)	9783(2)	72(2)
C(2)	5013(6)	7999(5)	9742(3)	83(2)
C(3)	5058(5)	9038(4)	9351(2)	69(1)
C(4)	5479(4)	8690(4)	8733(2)	49(1)
C(5)	7980(5)	6188(3)	9247(2)	64(1)
C(6)	9283(7)	6776(5)	9479(4)	164(4)
C(7)	7637(9)	5179(4)	9654(3)	120(3)
C(8)	8212(5)	5688(4)	8642(2)	73(1)
C(9)	10637(10)	10178(7)	9165(4)	114(3)
C(10)	11473(7)	9768(7)	8689(5)	112(3)
C(11)	11415(7)	8601(7)	7818(4)	104(2)
C(12)	10439(8)	7921(6)	7462(4)	108(3)
C(13)	8544(8)	8089(7)	6761(4)	106(3)
C(14)	7694(9)	8936(9)	6442(3)	110(3)
C(15)	6075(9)	10385(6)	6592(3)	105(3)
C(16)	5215(7)	10863(6)	7053(4)	103(3)
C(17)	5220(6)	11922(6)	7931(4)	108(3)
C(18)	6106(8)	12515(5)	8359(5)	116(3)
C(19)	7861(9)	12208(6)	9103(3)	110(3)
C(20)	8732(9)	11318(7)	9358(3)	108(3)

Table 3. Bond lengths [Å] and angles [°] for liur55.

K(1)-O(2)	2.788(3)
K(1)-O(4)	2.817(3)
K(1)-O(6)	2.817(3)
K(1)-O(3)	2.861(3)
K(1)-O(5)	2.884(3)
K(1)-O(1)	2.886(3)
K(1)-B(1)	3.027(4)
K(1)-C(4)	3.355(5)
K(1)-C(20)	3.530(6)
K(1)-H(1B)	2.73(3)
K(1)-H(2B)	2.62(3)
K(1)-H(4A)	2.81(4)
O(1)-C(20)	1.420(8)
O(1)-C(9)	1.424(9)
O(2)-C(10)	1.407(9)
O(2)-C(11)	1.437(7)
O(3)-C(12)	1.412(8)
O(3)-C(13)	1.440(8)
O(4)-C(14)	1.396(8)
O(4)-C(15)	1.451(8)
O(5)-C(16)	1.399(8)
O(5)-C(17)	1.448(7)
O(6)-C(18)	1.412(8)
O(6)-C(19)	1.445(8)
N(1)-C(1)	1.461(6)
N(1)-C(5)	1.498(5)
N(1)-B(1)	1.547(5)
B(1)-C(4)	1.643(6)
B(1)-H(1B)	1.12(4)
B(1)-H(2B)	1.19(4)
C(1)-C(2)	1.523(8)
C(1)-H(1A)	0.93(5)
C(1)-H(1C)	1.06(4)
C(2)-C(3)	1.512(8)

C(2)-H(2A)	1.11(5)
C(2)-H(2C)	1.01(6)
C(3)-C(4)	1.520(6)
C(3)-H(3A)	1.12(4)
C(3)-H(3B)	0.99(6)
C(4)-H(4A)	1.00(4)
C(4)-H(4B)	1.03(4)
C(5)-C(8)	1.506(7)
C(5)-C(6)	1.538(7)
C(5)-C(7)	1.548(7)
C(6)-H(6A)	0.9800
C(6)-H(6B)	0.9800
C(6)-H(6C)	0.9800
C(7)-H(7A)	0.9800
C(7)-H(7B)	0.9800
C(7)-H(7C)	0.9800
C(8)-H(8A)	0.9800
C(8)-H(8B)	0.9800
C(8)-H(8C)	0.9800
C(9)-C(10)	1.458(12)
C(9)-H(9A)	1.01(10)
C(9)-H(9B)	0.95(6)
C(10)-H(10A)	1.03(8)
C(10)-H(10B)	1.01(5)
C(11)-C(12)	1.470(10)
C(11)-H(11A)	1.07(7)
C(11)-H(11B)	1.03(6)
C(12)-H(12A)	0.92(5)
C(12)-H(12B)	0.96(6)
C(13)-C(14)	1.476(11)
C(13)-H(13A)	1.01(6)
C(13)-H(13B)	0.87(6)
C(14)-H(14A)	1.07(6)
C(14)-H(14B)	1.00(6)
C(15)-C(16)	1.477(10)
C(15)-H(15A)	0.96(7)

C(15)-H(15B)	0.96(6)
C(16)-H(16A)	1.03(5)
C(16)-H(16B)	1.08(7)
C(17)-C(18)	1.456(11)
C(17)-H(17A)	0.94(6)
C(17)-H(17B)	1.00(5)
C(18)-H(18A)	1.00(5)
C(18)-H(18B)	0.96(9)
C(19)-C(20)	1.464(11)
C(19)-H(19A)	0.97(5)
C(19)-H(19B)	0.85(9)
C(20)-H(20A)	1.05(6)
C(20)-H(20B)	0.96(6)

O(2)-K(1)-O(4)	118.90(11)
O(2)-K(1)-O(6)	118.82(12)
O(4)-K(1)-O(6)	116.53(12)
O(2)-K(1)-O(3)	59.17(12)
O(4)-K(1)-O(3)	59.84(11)
O(6)-K(1)-O(3)	159.20(9)
O(2)-K(1)-O(5)	153.68(9)
O(4)-K(1)-O(5)	59.19(11)
O(6)-K(1)-O(5)	57.44(12)
O(3)-K(1)-O(5)	113.96(12)
O(2)-K(1)-O(1)	59.17(12)
O(4)-K(1)-O(1)	157.47(9)
O(6)-K(1)-O(1)	59.67(12)
O(3)-K(1)-O(1)	114.83(12)
O(5)-K(1)-O(1)	111.47(12)
O(2)-K(1)-B(1)	90.43(11)
O(4)-K(1)-B(1)	105.90(11)
O(6)-K(1)-B(1)	97.78(11)
O(3)-K(1)-B(1)	102.89(11)
O(5)-K(1)-B(1)	115.70(11)
O(1)-K(1)-B(1)	96.62(11)
O(2)-K(1)-C(4)	118.84(11)

O(4)-K(1)-C(4)	95.78(10)
O(6)-K(1)-C(4)	77.98(10)
O(3)-K(1)-C(4)	122.02(10)
O(5)-K(1)-C(4)	86.82(10)
O(1)-K(1)-C(4)	104.42(10)
B(1)-K(1)-C(4)	29.25(11)
O(2)-K(1)-C(20)	79.1(2)
O(4)-K(1)-C(20)	157.88(19)
O(6)-K(1)-C(20)	41.9(2)
O(3)-K(1)-C(20)	137.14(19)
O(5)-K(1)-C(20)	98.9(2)
O(1)-K(1)-C(20)	22.88(15)
B(1)-K(1)-C(20)	85.47(14)
C(4)-K(1)-C(20)	84.97(12)
O(2)-K(1)-H(1B)	85.7(7)
O(4)-K(1)-H(1B)	89.8(7)
O(6)-K(1)-H(1B)	118.4(8)
O(3)-K(1)-H(1B)	82.4(8)
O(5)-K(1)-H(1B)	119.7(7)
O(1)-K(1)-H(1B)	111.7(7)
B(1)-K(1)-H(1B)	21.6(8)
C(4)-K(1)-H(1B)	43.0(8)
C(20)-K(1)-H(1B)	105.2(8)
O(2)-K(1)-H(2B)	77.7(8)
O(4)-K(1)-H(2B)	128.7(8)
O(6)-K(1)-H(2B)	87.3(8)
O(3)-K(1)-H(2B)	111.1(8)
O(5)-K(1)-H(2B)	125.5(8)
O(1)-K(1)-H(2B)	73.8(8)
B(1)-K(1)-H(2B)	22.8(8)
C(4)-K(1)-H(2B)	42.7(8)
C(20)-K(1)-H(2B)	64.7(8)
H(1B)-K(1)-H(2B)	40.5(11)
O(2)-K(1)-H(4A)	134.6(9)
O(4)-K(1)-H(4A)	86.7(8)
O(6)-K(1)-H(4A)	70.8(8)

O(3)-K(1)-H(4A)	126.9(8)
O(5)-K(1)-H(4A)	71.1(9)
O(1)-K(1)-H(4A)	110.5(8)
B(1)-K(1)-H(4A)	44.7(9)
C(4)-K(1)-H(4A)	15.7(9)
C(20)-K(1)-H(4A)	88.6(8)
H(1B)-K(1)-H(4A)	55.5(12)
H(2B)-K(1)-H(4A)	57.7(11)
C(20)-O(1)-C(9)	112.8(6)
C(20)-O(1)-K(1)	104.9(3)
C(9)-O(1)-K(1)	109.1(3)
C(10)-O(2)-C(11)	114.5(6)
C(10)-O(2)-K(1)	119.0(4)
C(11)-O(2)-K(1)	119.1(4)
C(12)-O(3)-C(13)	115.4(6)
C(12)-O(3)-K(1)	108.2(3)
C(13)-O(3)-K(1)	106.8(3)
C(14)-O(4)-C(15)	113.2(6)
C(14)-O(4)-K(1)	118.2(4)
C(15)-O(4)-K(1)	117.0(4)
C(16)-O(5)-C(17)	110.2(6)
C(16)-O(5)-K(1)	111.8(3)
C(17)-O(5)-K(1)	112.4(4)
C(18)-O(6)-C(19)	113.7(6)
C(18)-O(6)-K(1)	121.8(4)
C(19)-O(6)-K(1)	117.3(4)
C(1)-N(1)-C(5)	113.4(4)
C(1)-N(1)-B(1)	109.4(3)
C(5)-N(1)-B(1)	117.3(3)
N(1)-B(1)-C(4)	109.5(3)
N(1)-B(1)-K(1)	163.5(3)
C(4)-B(1)-K(1)	86.5(2)
N(1)-B(1)-H(1B)	111.1(18)
C(4)-B(1)-H(1B)	111.7(17)
K(1)-B(1)-H(1B)	64.1(18)
N(1)-B(1)-H(2B)	111.2(17)

C(4)-B(1)-H(2B)	106.1(17)
K(1)-B(1)-H(2B)	58.7(17)
H(1B)-B(1)-H(2B)	107(2)
N(1)-C(1)-C(2)	112.9(4)
N(1)-C(1)-H(1A)	111(3)
C(2)-C(1)-H(1A)	111(3)
N(1)-C(1)-H(1C)	113(2)
C(2)-C(1)-H(1C)	105(2)
H(1A)-C(1)-H(1C)	102(4)
C(3)-C(2)-C(1)	112.6(4)
C(3)-C(2)-H(2A)	115(3)
C(1)-C(2)-H(2A)	102(3)
C(3)-C(2)-H(2C)	108(3)
C(1)-C(2)-H(2C)	112(3)
H(2A)-C(2)-H(2C)	108(4)
C(2)-C(3)-C(4)	108.9(4)
C(2)-C(3)-H(3A)	109(2)
C(4)-C(3)-H(3A)	109(2)
C(2)-C(3)-H(3B)	109(3)
C(4)-C(3)-H(3B)	118(3)
H(3A)-C(3)-H(3B)	103(4)
C(3)-C(4)-B(1)	109.7(4)
C(3)-C(4)-K(1)	124.5(3)
B(1)-C(4)-K(1)	64.2(2)
C(3)-C(4)-H(4A)	115(2)
B(1)-C(4)-H(4A)	113(2)
K(1)-C(4)-H(4A)	49(2)
C(3)-C(4)-H(4B)	108(2)
B(1)-C(4)-H(4B)	112(2)
K(1)-C(4)-H(4B)	126(2)
H(4A)-C(4)-H(4B)	99(3)
N(1)-C(5)-C(8)	109.4(3)
N(1)-C(5)-C(6)	111.8(4)
C(8)-C(5)-C(6)	109.3(6)
N(1)-C(5)-C(7)	110.0(5)
C(8)-C(5)-C(7)	105.9(4)

C(6)-C(5)-C(7)	110.3(5)
C(5)-C(6)-H(6A)	109.5
C(5)-C(6)-H(6B)	109.5
H(6A)-C(6)-H(6B)	109.5
C(5)-C(6)-H(6C)	109.5
H(6A)-C(6)-H(6C)	109.5
H(6B)-C(6)-H(6C)	109.5
C(5)-C(7)-H(7A)	109.5
C(5)-C(7)-H(7B)	109.5
H(7A)-C(7)-H(7B)	109.5
C(5)-C(7)-H(7C)	109.5
H(7A)-C(7)-H(7C)	109.5
H(7B)-C(7)-H(7C)	109.5
C(5)-C(8)-H(8A)	109.5
C(5)-C(8)-H(8B)	109.5
H(8A)-C(8)-H(8B)	109.5
C(5)-C(8)-H(8C)	109.5
H(8A)-C(8)-H(8C)	109.5
H(8B)-C(8)-H(8C)	109.5
O(1)-C(9)-C(10)	109.7(5)
O(1)-C(9)-H(9A)	114(5)
C(10)-C(9)-H(9A)	109(5)
O(1)-C(9)-H(9B)	107(3)
C(10)-C(9)-H(9B)	106(3)
H(9A)-C(9)-H(9B)	111(6)
O(2)-C(10)-C(9)	109.7(5)
O(2)-C(10)-H(10A)	96(4)
C(9)-C(10)-H(10A)	120(4)
O(2)-C(10)-H(10B)	98(3)
C(9)-C(10)-H(10B)	119(3)
H(10A)-C(10)-H(10B)	109(5)
O(2)-C(11)-C(12)	106.9(5)
O(2)-C(11)-H(11A)	100(4)
C(12)-C(11)-H(11A)	115(3)
O(2)-C(11)-H(11B)	108(3)
C(12)-C(11)-H(11B)	108(3)

H(11A)-C(11)-H(11B)	118(5)
O(3)-C(12)-C(11)	109.5(5)
O(3)-C(12)-H(12A)	108(3)
C(11)-C(12)-H(12A)	112(3)
O(3)-C(12)-H(12B)	113(3)
C(11)-C(12)-H(12B)	108(3)
H(12A)-C(12)-H(12B)	107(4)
O(3)-C(13)-C(14)	110.1(6)
O(3)-C(13)-H(13A)	98(3)
C(14)-C(13)-H(13A)	119(3)
O(3)-C(13)-H(13B)	107(3)
C(14)-C(13)-H(13B)	111(3)
H(13A)-C(13)-H(13B)	112(5)
O(4)-C(14)-C(13)	108.6(5)
O(4)-C(14)-H(14A)	109(3)
C(13)-C(14)-H(14A)	105(3)
O(4)-C(14)-H(14B)	110(3)
C(13)-C(14)-H(14B)	110(4)
H(14A)-C(14)-H(14B)	113(4)
O(4)-C(15)-C(16)	109.0(5)
O(4)-C(15)-H(15A)	112(3)
C(16)-C(15)-H(15A)	109(4)
O(4)-C(15)-H(15B)	110(3)
C(16)-C(15)-H(15B)	105(3)
H(15A)-C(15)-H(15B)	112(5)
O(5)-C(16)-C(15)	109.0(5)
O(5)-C(16)-H(16A)	108(3)
C(15)-C(16)-H(16A)	113(3)
O(5)-C(16)-H(16B)	106(3)
C(15)-C(16)-H(16B)	110(3)
H(16A)-C(16)-H(16B)	111(4)
O(5)-C(17)-C(18)	108.8(5)
O(5)-C(17)-H(17A)	106(3)
C(18)-C(17)-H(17A)	112(3)
O(5)-C(17)-H(17B)	101(3)
C(18)-C(17)-H(17B)	117(3)

H(17A)-C(17)-H(17B)	111(4)
O(6)-C(18)-C(17)	108.9(5)
O(6)-C(18)-H(18A)	113(3)
C(17)-C(18)-H(18A)	109(3)
O(6)-C(18)-H(18B)	108(5)
C(17)-C(18)-H(18B)	115(4)
H(18A)-C(18)-H(18B)	102(5)
O(6)-C(19)-C(20)	108.8(5)
O(6)-C(19)-H(19A)	108(3)
C(20)-C(19)-H(19A)	116(3)
O(6)-C(19)-H(19B)	113(5)
C(20)-C(19)-H(19B)	110(5)
H(19A)-C(19)-H(19B)	101(6)
O(1)-C(20)-C(19)	109.6(5)
O(1)-C(20)-K(1)	52.2(2)
C(19)-C(20)-K(1)	85.4(4)
O(1)-C(20)-H(20A)	102(3)
C(19)-C(20)-H(20A)	114(3)
K(1)-C(20)-H(20A)	153(3)
O(1)-C(20)-H(20B)	114(3)
C(19)-C(20)-H(20B)	107(3)
K(1)-C(20)-H(20B)	79(3)
H(20A)-C(20)-H(20B)	110(4)

Symmetry transformations used to generate equivalent atoms:

Table 4. Anisotropic displacement parameters ($Å^2 x\ 10^3$) for liur55. The anisotropic displacement factor exponent takes the form: $-2p^2[\ h^2\ a^{*2}U^{11} + ...\ + 2\ h\ k\ a^*\ b^*\ U^{12}\ ]$

	U^{11}	U^{22}	U^{33}	U^{23}	U^{13}	U^{12}
K(1)	39(1)	37(1)	40(1)	0(1)	11(1)	1(1)
O(1)	96(2)	81(2)	47(2)	12(2)	-1(2)	-48(2)
O(2)	40(2)	89(2)	103(3)	30(2)	3(2)	1(2)
O(3)	74(2)	57(2)	93(3)	-11(2)	51(2)	-1(2)
O(4)	80(2)	87(2)	43(2)	5(2)	2(2)	-29(2)
O(5)	39(2)	58(2)	134(3)	35(2)	-3(2)	-2(2)
O(6)	91(2)	34(2)	113(3)	-17(2)	65(2)	-9(2)
N(1)	56(2)	35(2)	39(2)	0(1)	2(2)	-8(1)
B(1)	40(2)	33(2)	43(3)	-2(2)	6(2)	-2(2)
C(1)	114(5)	59(3)	42(3)	4(3)	12(3)	-23(3)
C(2)	83(4)	98(4)	70(4)	-30(3)	40(3)	-25(3)
C(3)	48(3)	72(3)	86(4)	-31(3)	19(3)	4(2)
C(4)	40(2)	49(2)	59(3)	-6(2)	1(2)	2(2)
C(5)	77(3)	37(2)	76(3)	2(2)	-35(3)	0(2)
C(6)	110(5)	62(4)	309(12)	-46(5)	-135(7)	28(4)
C(7)	243(9)	45(3)	70(4)	8(3)	-29(5)	24(4)
C(8)	59(3)	57(3)	104(4)	4(3)	15(3)	27(2)
C(9)	142(7)	112(6)	83(5)	50(5)	-66(5)	-68(6)
C(10)	63(4)	124(6)	147(8)	69(6)	-37(5)	-24(4)
C(11)	58(3)	103(5)	155(7)	47(5)	50(4)	36(4)
C(12)	108(5)	66(4)	157(7)	17(4)	98(6)	23(4)
C(13)	99(5)	104(5)	119(6)	-72(5)	81(5)	-36(4)
C(14)	111(6)	162(8)	58(4)	-34(5)	27(4)	-64(6)
C(15)	119(6)	110(5)	82(4)	63(4)	-61(5)	-58(5)
C(16)	61(3)	84(4)	161(7)	67(5)	-30(5)	-18(3)
C(17)	54(3)	56(4)	216(9)	43(5)	57(5)	26(3)
C(18)	106(5)	39(3)	211(8)	5(4)	109(6)	5(4)
C(19)	168(7)	62(4)	108(5)	-48(4)	106(6)	-67(5)
C(20)	179(7)	96(5)	51(3)	-23(3)	36(4)	-101(6)

Table 5. Hydrogen coordinates (x 10^4) and isotropic displacement parameters ($Å^2$x 10^{-3}) for liur55.

	x	y	z	U(eq)
H(6A)	9492	7409	9216	246
H(6B)	10033	6234	9486	246
H(6C)	9154	7059	9883	246
H(7A)	6807	4810	9500	180
H(7B)	7502	5453	10059	180
H(7C)	8385	4634	9659	180
H(8A)	8441	6292	8365	109
H(8B)	7387	5304	8495	109
H(8C)	8958	5144	8673	109
H(1A)	6340(50)	6780(40)	10050(20)	77(15)
H(1B)	7270(30)	7750(30)	8335(16)	43(10)
H(1C)	7050(40)	7940(30)	10001(17)	52(11)
H(2A)	4310(50)	7320(50)	9570(20)	96(16)
H(2B)	7740(30)	8680(30)	8975(15)	46(10)
H(2C)	4700(50)	8240(40)	10150(20)	92(16)
H(3A)	5820(40)	9640(30)	9547(18)	58(12)
H(3B)	4200(60)	9460(50)	9380(20)	101(17)
H(4A)	5480(40)	9310(40)	8429(18)	54(12)
H(4B)	4730(40)	8190(30)	8544(17)	48(10)
H(9A)	11250(90)	10490(70)	9490(40)	190(30)
H(9B)	10150(50)	9540(50)	9300(20)	93(17)
H(10A)	12180(70)	9140(60)	8770(30)	140(30)
H(10B)	11860(50)	10340(40)	8400(20)	82(15)
H(11A)	12120(70)	8130(60)	8090(30)	130(20)
H(11B)	11790(50)	9220(50)	7550(20)	96(17)
H(12A)	10860(50)	7480(40)	7190(20)	84(16)
H(12B)	10000(50)	7420(40)	7730(20)	89(16)
H(13A)	8110(60)	7590(50)	7070(30)	101(18)
H(13B)	9000(50)	7690(40)	6510(20)	87(16)
H(14A)	8390(60)	9520(50)	6260(20)	99(17)

H(14B)	7100(60)	8560(50)	6130(30)	110(20)
H(15A)	5510(60)	10110(50)	6270(30)	110(20)
H(15B)	6650(60)	11000(50)	6470(20)	102(18)
H(16A)	4660(40)	10260(40)	7260(20)	70(13)
H(16B)	4570(60)	11510(60)	6860(30)	120(20)
H(17A)	4740(50)	11340(50)	8110(20)	95(18)
H(17B)	4600(50)	12400(40)	7680(20)	76(14)
H(18A)	6580(50)	13140(40)	8150(20)	82(15)
H(18B)	5650(80)	12910(60)	8670(40)	160(30)
H(19A)	8330(50)	12850(40)	8940(20)	81(14)
H(19B)	7420(80)	12520(60)	9380(40)	160(30)
H(20A)	9380(50)	11600(50)	9710(30)	97(17)
H(20B)	8150(50)	10720(50)	9490(20)	89(15)

Table 6. Torsion angles [°] for liur55.

O(2)-K(1)-O(1)-C(20)	-147.9(4)
O(4)-K(1)-O(1)-C(20)	120.4(5)
O(6)-K(1)-O(1)-C(20)	33.8(4)
O(3)-K(1)-O(1)-C(20)	-168.9(4)
O(5)-K(1)-O(1)-C(20)	59.6(4)
B(1)-K(1)-O(1)-C(20)	-61.3(4)
C(4)-K(1)-O(1)-C(20)	-32.6(4)
O(2)-K(1)-O(1)-C(9)	-26.8(4)
O(4)-K(1)-O(1)-C(9)	-118.5(5)
O(6)-K(1)-O(1)-C(9)	154.9(5)
O(3)-K(1)-O(1)-C(9)	-47.8(5)
O(5)-K(1)-O(1)-C(9)	-179.3(4)
B(1)-K(1)-O(1)-C(9)	59.7(5)
C(4)-K(1)-O(1)-C(9)	88.4(5)
C(20)-K(1)-O(1)-C(9)	121.1(6)
O(4)-K(1)-O(2)-C(10)	148.5(4)
O(6)-K(1)-O(2)-C(10)	-3.9(5)
O(3)-K(1)-O(2)-C(10)	152.2(5)
O(5)-K(1)-O(2)-C(10)	70.3(5)
O(1)-K(1)-O(2)-C(10)	-5.6(4)
B(1)-K(1)-O(2)-C(10)	-103.0(4)
C(4)-K(1)-O(2)-C(10)	-95.7(4)
C(20)-K(1)-O(2)-C(10)	-17.7(4)
O(4)-K(1)-O(2)-C(11)	0.2(4)
O(6)-K(1)-O(2)-C(11)	-152.1(4)
O(3)-K(1)-O(2)-C(11)	3.9(4)
O(5)-K(1)-O(2)-C(11)	-78.0(5)
O(1)-K(1)-O(2)-C(11)	-153.8(4)
B(1)-K(1)-O(2)-C(11)	108.7(4)
C(4)-K(1)-O(2)-C(11)	116.0(4)
C(20)-K(1)-O(2)-C(11)	-166.0(4)
O(2)-K(1)-O(3)-C(12)	29.6(4)
O(4)-K(1)-O(3)-C(12)	-154.1(4)
O(6)-K(1)-O(3)-C(12)	120.2(5)

O(5)-K(1)-O(3)-C(12)	-179.1(4)
O(1)-K(1)-O(3)-C(12)	50.6(4)
B(1)-K(1)-O(3)-C(12)	-53.0(4)
C(4)-K(1)-O(3)-C(12)	-77.2(4)
C(20)-K(1)-O(3)-C(12)	44.3(5)
O(2)-K(1)-O(3)-C(13)	154.5(5)
O(4)-K(1)-O(3)-C(13)	-29.3(5)
O(6)-K(1)-O(3)-C(13)	-115.0(6)
O(5)-K(1)-O(3)-C(13)	-54.3(5)
O(1)-K(1)-O(3)-C(13)	175.4(5)
B(1)-K(1)-O(3)-C(13)	71.8(5)
C(4)-K(1)-O(3)-C(13)	47.6(5)
C(20)-K(1)-O(3)-C(13)	169.1(5)
O(2)-K(1)-O(4)-C(14)	0.5(5)
O(6)-K(1)-O(4)-C(14)	153.5(5)
O(3)-K(1)-O(4)-C(14)	-3.2(5)
O(5)-K(1)-O(4)-C(14)	150.1(5)
O(1)-K(1)-O(4)-C(14)	79.1(6)
B(1)-K(1)-O(4)-C(14)	-99.1(5)
C(4)-K(1)-O(4)-C(14)	-127.1(5)
C(20)-K(1)-O(4)-C(14)	142.0(5)
O(2)-K(1)-O(4)-C(15)	-140.2(4)
O(6)-K(1)-O(4)-C(15)	12.8(4)
O(3)-K(1)-O(4)-C(15)	-143.9(4)
O(5)-K(1)-O(4)-C(15)	9.4(4)
O(1)-K(1)-O(4)-C(15)	-61.6(5)
B(1)-K(1)-O(4)-C(15)	120.2(4)
C(4)-K(1)-O(4)-C(15)	92.2(4)
C(20)-K(1)-O(4)-C(15)	1.3(5)
O(2)-K(1)-O(5)-C(16)	118.5(5)
O(4)-K(1)-O(5)-C(16)	24.9(4)
O(6)-K(1)-O(5)-C(16)	-151.6(5)
O(3)-K(1)-O(5)-C(16)	50.0(4)
O(1)-K(1)-O(5)-C(16)	-178.0(4)
B(1)-K(1)-O(5)-C(16)	-69.0(5)
C(4)-K(1)-O(5)-C(16)	-73.8(4)

C(20)-K(1)-O(5)-C(16)	-158.2(4)
O(2)-K(1)-O(5)-C(17)	-117.0(4)
O(4)-K(1)-O(5)-C(17)	149.4(4)
O(6)-K(1)-O(5)-C(17)	-27.0(4)
O(3)-K(1)-O(5)-C(17)	174.5(4)
O(1)-K(1)-O(5)-C(17)	-53.5(4)
B(1)-K(1)-O(5)-C(17)	55.6(4)
C(4)-K(1)-O(5)-C(17)	50.7(4)
C(20)-K(1)-O(5)-C(17)	-33.7(4)
O(2)-K(1)-O(6)-C(18)	144.8(4)
O(4)-K(1)-O(6)-C(18)	-8.2(4)
O(3)-K(1)-O(6)-C(18)	66.3(5)
O(5)-K(1)-O(6)-C(18)	-4.8(3)
O(1)-K(1)-O(6)-C(18)	146.5(4)
B(1)-K(1)-O(6)-C(18)	-120.3(4)
C(4)-K(1)-O(6)-C(18)	-98.7(4)
C(20)-K(1)-O(6)-C(18)	165.4(4)
O(2)-K(1)-O(6)-C(19)	-3.8(4)
O(4)-K(1)-O(6)-C(19)	-156.8(3)
O(3)-K(1)-O(6)-C(19)	-82.3(5)
O(5)-K(1)-O(6)-C(19)	-153.4(4)
O(1)-K(1)-O(6)-C(19)	-2.1(3)
B(1)-K(1)-O(6)-C(19)	91.0(3)
C(4)-K(1)-O(6)-C(19)	112.7(4)
C(20)-K(1)-O(6)-C(19)	16.8(3)
C(1)-N(1)-B(1)-C(4)	-56.3(5)
C(5)-N(1)-B(1)-C(4)	172.7(3)
C(1)-N(1)-B(1)-K(1)	110.2(10)
C(5)-N(1)-B(1)-K(1)	-20.8(11)
O(2)-K(1)-B(1)-N(1)	-0.4(10)
O(4)-K(1)-B(1)-N(1)	119.9(10)
O(6)-K(1)-B(1)-N(1)	-119.6(10)
O(3)-K(1)-B(1)-N(1)	58.0(10)
O(5)-K(1)-B(1)-N(1)	-177.1(9)
O(1)-K(1)-B(1)-N(1)	-59.4(10)
C(4)-K(1)-B(1)-N(1)	-167.2(11)

C(20)-K(1)-B(1)-N(1)	-79.4(10)
O(2)-K(1)-B(1)-C(4)	166.8(2)
O(4)-K(1)-B(1)-C(4)	-72.9(2)
O(6)-K(1)-B(1)-C(4)	47.6(2)
O(3)-K(1)-B(1)-C(4)	-134.8(2)
O(5)-K(1)-B(1)-C(4)	-9.9(3)
O(1)-K(1)-B(1)-C(4)	107.8(2)
C(20)-K(1)-B(1)-C(4)	87.8(3)
C(5)-N(1)-C(1)-C(2)	-168.8(4)
B(1)-N(1)-C(1)-C(2)	58.2(5)
N(1)-C(1)-C(2)-C(3)	-59.7(6)
C(1)-C(2)-C(3)-C(4)	57.5(6)
C(2)-C(3)-C(4)-B(1)	-55.8(5)
C(2)-C(3)-C(4)-K(1)	-127.5(4)
N(1)-B(1)-C(4)-C(3)	56.5(5)
K(1)-B(1)-C(4)-C(3)	-119.7(3)
N(1)-B(1)-C(4)-K(1)	176.2(3)
O(2)-K(1)-C(4)-C(3)	82.0(4)
O(4)-K(1)-C(4)-C(3)	-150.4(4)
O(6)-K(1)-C(4)-C(3)	-34.5(4)
O(3)-K(1)-C(4)-C(3)	151.7(3)
O(5)-K(1)-C(4)-C(3)	-91.8(4)
O(1)-K(1)-C(4)-C(3)	19.5(4)
B(1)-K(1)-C(4)-C(3)	97.1(4)
C(20)-K(1)-C(4)-C(3)	7.4(4)
O(2)-K(1)-C(4)-B(1)	-15.1(3)
O(4)-K(1)-C(4)-B(1)	112.5(2)
O(6)-K(1)-C(4)-B(1)	-131.6(3)
O(3)-K(1)-C(4)-B(1)	54.7(3)
O(5)-K(1)-C(4)-B(1)	171.1(2)
O(1)-K(1)-C(4)-B(1)	-77.6(2)
C(20)-K(1)-C(4)-B(1)	-89.7(3)
C(1)-N(1)-C(5)-C(8)	170.5(4)
B(1)-N(1)-C(5)-C(8)	-60.4(5)
C(1)-N(1)-C(5)-C(6)	-68.3(6)
B(1)-N(1)-C(5)-C(6)	60.9(6)

C(1)-N(1)-C(5)-C(7)	54.6(5)
B(1)-N(1)-C(5)-C(7)	-176.3(4)
C(20)-O(1)-C(9)-C(10)	174.4(5)
K(1)-O(1)-C(9)-C(10)	58.2(6)
C(11)-O(2)-C(10)-C(9)	-173.5(5)
K(1)-O(2)-C(10)-C(9)	36.8(7)
O(1)-C(9)-C(10)-O(2)	-64.7(7)
C(10)-O(2)-C(11)-C(12)	174.9(5)
K(1)-O(2)-C(11)-C(12)	-35.4(7)
C(13)-O(3)-C(12)-C(11)	177.2(5)
K(1)-O(3)-C(12)-C(11)	-63.3(5)
O(2)-C(11)-C(12)-O(3)	66.7(6)
C(12)-O(3)-C(13)-C(14)	-177.3(5)
K(1)-O(3)-C(13)-C(14)	62.4(5)
C(15)-O(4)-C(14)-C(13)	176.9(5)
K(1)-O(4)-C(14)-C(13)	34.8(7)
O(3)-C(13)-C(14)-O(4)	-67.1(6)
C(14)-O(4)-C(15)-C(16)	176.3(5)
K(1)-O(4)-C(15)-C(16)	-41.1(6)
C(17)-O(5)-C(16)-C(15)	177.2(5)
K(1)-O(5)-C(16)-C(15)	-57.1(5)
O(4)-C(15)-C(16)-O(5)	66.0(6)
C(16)-O(5)-C(17)-C(18)	-177.3(5)
K(1)-O(5)-C(17)-C(18)	57.3(6)
C(19)-O(6)-C(18)-C(17)	-175.2(5)
K(1)-O(6)-C(18)-C(17)	35.2(6)
O(5)-C(17)-C(18)-O(6)	-60.2(6)
C(18)-O(6)-C(19)-C(20)	179.4(5)
K(1)-O(6)-C(19)-C(20)	-29.5(5)
C(9)-O(1)-C(20)-C(19)	174.0(5)
K(1)-O(1)-C(20)-C(19)	-67.3(5)
C(9)-O(1)-C(20)-K(1)	-118.7(4)
O(6)-C(19)-C(20)-O(1)	67.5(5)
O(6)-C(19)-C(20)-K(1)	20.5(4)
O(2)-K(1)-C(20)-O(1)	27.7(4)
O(4)-K(1)-C(20)-O(1)	-118.6(5)

O(6)-K(1)-C(20)-O(1)	-134.0(4)
O(3)-K(1)-C(20)-O(1)	14.9(5)
O(5)-K(1)-C(20)-O(1)	-125.6(4)
B(1)-K(1)-C(20)-O(1)	119.0(4)
C(4)-K(1)-C(20)-O(1)	148.4(4)
O(2)-K(1)-C(20)-C(19)	147.0(3)
O(4)-K(1)-C(20)-C(19)	0.7(6)
O(6)-K(1)-C(20)-C(19)	-14.7(3)
O(3)-K(1)-C(20)-C(19)	134.2(3)
O(5)-K(1)-C(20)-C(19)	-6.3(3)
O(1)-K(1)-C(20)-C(19)	119.3(5)
B(1)-K(1)-C(20)-C(19)	-121.7(3)
C(4)-K(1)-C(20)-C(19)	-92.3(3)

Symmetry transformations used to generate equivalent atoms:

Chapter IV

Crystallographic data for 8 (liu153)

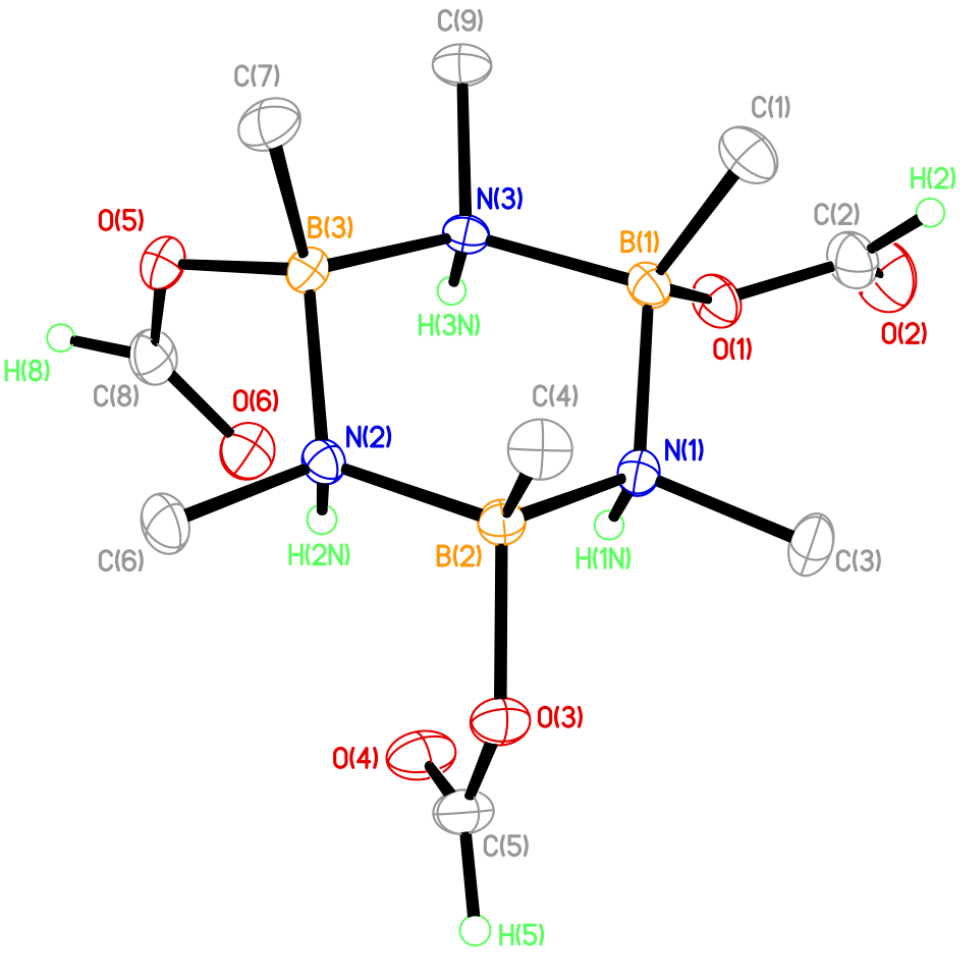

Table 1. Crystal data and structure refinement for liu153.

Identification code	liu153	
Empirical formula	C9 H24 B3 N3 O6	
Formula weight	302.74	
Temperature	173(2) K	
Wavelength	0.71073 Å	
Crystal system	Monoclinic	
Space group	P2(1)/n	
Unit cell dimensions	a = 7.5759(14) Å	a= 90°.
	b = 24.347(4) Å	b= 96.923(3)°.

	c = 8.4374(15) Å g = 90°.
Volume	1544.9(5) $Å^3$
Z	4
Density (calculated)	1.302 Mg/m^3
Absorption coefficient	0.102 mm^{-1}
F(000)	648
Crystal size	0.32 x 0.26 x 0.14 mm^3
Theta range for data collection	1.67 to 27.00°.
Index ranges	-9<=h<=9, -31<=k<=31, -10<=l<=10
Reflections collected	17175
Independent reflections	3378 [R(int) = 0.0385]
Completeness to theta = 27.00°	100.0 %
Absorption correction	Semi-empirical from equivalents
Max. and min. transmission	0.9859 and 0.9682
Refinement method	Full-matrix least-squares on F^2
Data / restraints / parameters	3378 / 0 / 286
Goodness-of-fit on F^2	1.062
Final R indices [I>2sigma(I)]	R1 = 0.0394, wR2 = 0.1065
R indices (all data)	R1 = 0.0437, wR2 = 0.1103
Largest diff. peak and hole	0.356 and -0.187 $e.Å^{-3}$

Table 2. Atomic coordinates (x 10^4) and equivalent isotropic displacement parameters ($Å^2$x 10^3) for liu153. U(eq) is defined as one third of the trace of the orthogonalized U^{ij} tensor.

	x	y	z	U(eq)
O(1)	1410(1)	1424(1)	718(1)	32(1)
O(2)	3450(2)	1540(1)	2785(1)	57(1)
O(3)	-3786(1)	303(1)	-1139(1)	29(1)
O(4)	-1301(1)	-174(1)	-1356(1)	39(1)
O(5)	59(1)	1150(1)	-4859(1)	30(1)
O(6)	1457(1)	451(1)	-3494(1)	38(1)
N(1)	-1498(1)	999(1)	-122(1)	22(1)
N(2)	-2152(1)	824(1)	-3094(1)	21(1)
N(3)	294(1)	1500(1)	-2050(1)	21(1)
B(1)	-329(2)	1535(1)	-303(2)	24(1)
B(2)	-3063(2)	865(1)	-1495(2)	22(1)
B(3)	-1057(2)	1341(1)	-3578(2)	22(1)
C(1)	-1288(2)	2094(1)	71(2)	34(1)
C(2)	2028(2)	1652(1)	2067(2)	39(1)
C(3)	-2135(2)	968(1)	1489(2)	35(1)
C(4)	-4723(2)	1271(1)	-1614(2)	30(1)
C(5)	-2822(2)	-143(1)	-1069(2)	33(1)
C(6)	-3424(2)	619(1)	-4461(2)	33(1)
C(7)	-2210(2)	1846(1)	-4335(2)	33(1)
C(8)	1138(2)	728(1)	-4681(2)	33(1)
C(9)	1354(2)	1998(1)	-2387(2)	31(1)

Table 3. Bond lengths [Å] and angles [°] for liu153.

O(1)-C(2)	1.3023(16)
O(1)-B(1)	1.5096(15)
O(2)-C(2)	1.2018(19)
O(3)-C(5)	1.3065(15)
O(3)-B(2)	1.5169(14)
O(4)-C(5)	1.2081(17)
O(5)-C(8)	1.3096(16)
O(5)-B(3)	1.5228(15)
O(6)-C(8)	1.2078(17)
N(1)-C(3)	1.4980(15)
N(1)-B(2)	1.5884(15)
N(1)-B(1)	1.5939(16)
N(1)-H(1N)	0.845(16)
N(2)-C(6)	1.4972(15)
N(2)-B(3)	1.5870(15)
N(2)-B(2)	1.5908(15)
N(2)-H(2N)	0.879(15)
N(3)-C(9)	1.4987(15)
N(3)-B(3)	1.5944(16)
N(3)-B(1)	1.6037(16)
N(3)-H(3N)	0.849(15)
B(1)-C(1)	1.5921(17)
B(2)-C(4)	1.5927(17)
B(3)-C(7)	1.5974(17)
C(1)-H(1A)	0.97(2)
C(1)-H(1B)	0.939(18)
C(1)-H(1C)	1.01(2)
C(2)-H(2)	1.004(18)
C(3)-H(3A)	0.948(18)
C(3)-H(3B)	0.937(18)
C(3)-H(3C)	0.931(18)
C(4)-H(4A)	0.943(19)
C(4)-H(4B)	0.94(2)
C(4)-H(4C)	0.97(2)

C(5)-H(5)	0.939(17)
C(6)-H(6A)	0.939(18)
C(6)-H(6B)	0.945(18)
C(6)-H(6C)	0.942(17)
C(7)-H(7A)	0.964(18)
C(7)-H(7B)	0.995(19)
C(7)-H(7C)	0.97(2)
C(8)-H(8)	0.950(19)
C(9)-H(9A)	0.954(17)
C(9)-H(9B)	0.972(17)
C(9)-H(9C)	0.938(16)

C(2)-O(1)-B(1)	128.26(11)
C(5)-O(3)-B(2)	123.07(9)
C(8)-O(5)-B(3)	123.36(10)
C(3)-N(1)-B(2)	110.97(9)
C(3)-N(1)-B(1)	111.83(10)
B(2)-N(1)-B(1)	118.20(9)
C(3)-N(1)-H(1N)	103.5(10)
B(2)-N(1)-H(1N)	105.8(10)
B(1)-N(1)-H(1N)	105.1(10)
C(6)-N(2)-B(3)	111.98(9)
C(6)-N(2)-B(2)	111.72(9)
B(3)-N(2)-B(2)	117.51(8)
C(6)-N(2)-H(2N)	104.9(9)
B(3)-N(2)-H(2N)	106.3(9)
B(2)-N(2)-H(2N)	103.1(9)
C(9)-N(3)-B(3)	110.50(9)
C(9)-N(3)-B(1)	110.83(9)
B(3)-N(3)-B(1)	121.61(9)
C(9)-N(3)-H(3N)	104.4(10)
B(3)-N(3)-H(3N)	105.3(10)
B(1)-N(3)-H(3N)	102.3(10)
O(1)-B(1)-C(1)	115.36(10)
O(1)-B(1)-N(1)	104.79(9)
C(1)-B(1)-N(1)	114.10(10)

O(1)-B(1)-N(3)	100.45(9)
C(1)-B(1)-N(3)	114.77(10)
N(1)-B(1)-N(3)	105.91(8)
O(3)-B(2)-N(1)	107.26(9)
O(3)-B(2)-N(2)	108.36(9)
N(1)-B(2)-N(2)	105.65(9)
O(3)-B(2)-C(4)	105.71(9)
N(1)-B(2)-C(4)	115.63(10)
N(2)-B(2)-C(4)	113.90(10)
O(5)-B(3)-N(2)	107.06(9)
O(5)-B(3)-N(3)	106.89(9)
N(2)-B(3)-N(3)	106.85(9)
O(5)-B(3)-C(7)	105.92(10)
N(2)-B(3)-C(7)	115.86(10)
N(3)-B(3)-C(7)	113.73(10)
B(1)-C(1)-H(1A)	115.9(12)
B(1)-C(1)-H(1B)	112.9(10)
H(1A)-C(1)-H(1B)	103.7(15)
B(1)-C(1)-H(1C)	115.3(11)
H(1A)-C(1)-H(1C)	100.6(16)
H(1B)-C(1)-H(1C)	107.1(15)
O(2)-C(2)-O(1)	123.37(15)
O(2)-C(2)-H(2)	121.5(10)
O(1)-C(2)-H(2)	115.1(10)
N(1)-C(3)-H(3A)	108.3(10)
N(1)-C(3)-H(3B)	110.4(10)
H(3A)-C(3)-H(3B)	110.4(14)
N(1)-C(3)-H(3C)	109.6(10)
H(3A)-C(3)-H(3C)	110.9(15)
H(3B)-C(3)-H(3C)	107.3(14)
B(2)-C(4)-H(4A)	115.1(12)
B(2)-C(4)-H(4B)	109.9(12)
H(4A)-C(4)-H(4B)	108.3(17)
B(2)-C(4)-H(4C)	112.9(11)
H(4A)-C(4)-H(4C)	110.6(16)
H(4B)-C(4)-H(4C)	98.7(16)

O(4)-C(5)-O(3)	125.77(12)
O(4)-C(5)-H(5)	122.7(10)
O(3)-C(5)-H(5)	111.5(10)
N(2)-C(6)-H(6A)	108.5(11)
N(2)-C(6)-H(6B)	108.6(10)
H(6A)-C(6)-H(6B)	110.3(15)
N(2)-C(6)-H(6C)	107.8(10)
H(6A)-C(6)-H(6C)	110.9(14)
H(6B)-C(6)-H(6C)	110.7(14)
B(3)-C(7)-H(7A)	110.6(10)
B(3)-C(7)-H(7B)	115.3(10)
H(7A)-C(7)-H(7B)	105.0(15)
B(3)-C(7)-H(7C)	112.1(11)
H(7A)-C(7)-H(7C)	106.4(15)
H(7B)-C(7)-H(7C)	106.8(15)
O(6)-C(8)-O(5)	126.33(12)
O(6)-C(8)-H(8)	122.0(11)
O(5)-C(8)-H(8)	111.6(11)
N(3)-C(9)-H(9A)	109.0(9)
N(3)-C(9)-H(9B)	109.4(10)
H(9A)-C(9)-H(9B)	110.6(13)
N(3)-C(9)-H(9C)	107.8(10)
H(9A)-C(9)-H(9C)	109.3(13)
H(9B)-C(9)-H(9C)	110.7(14)

Symmetry transformations used to generate equivalent atoms:

Table 4. Anisotropic displacement parameters ($Å^2 x\ 10^3$)for liu153. The anisotropic displacement factor exponent takes the form: $-2p^2[\ h^2a^{*2}U^{11} + ... + 2\ h\ k\ a^*\ b^*\ U^{12}\ ]$

	U^{11}	U^{22}	U^{33}	U^{23}	U^{13}	U^{12}
O(1)	30(1)	32(1)	30(1)	-5(1)	-6(1)	2(1)
O(2)	48(1)	71(1)	47(1)	-8(1)	-20(1)	-2(1)
O(3)	26(1)	27(1)	36(1)	2(1)	7(1)	-4(1)
O(4)	38(1)	27(1)	56(1)	9(1)	15(1)	6(1)
O(5)	33(1)	36(1)	22(1)	1(1)	7(1)	1(1)
O(6)	37(1)	37(1)	39(1)	0(1)	9(1)	10(1)
N(1)	23(1)	23(1)	20(1)	0(1)	3(1)	3(1)
N(2)	21(1)	21(1)	20(1)	-1(1)	0(1)	0(1)
N(3)	20(1)	17(1)	26(1)	1(1)	2(1)	1(1)
B(1)	24(1)	22(1)	23(1)	-3(1)	-1(1)	1(1)
B(2)	20(1)	22(1)	23(1)	1(1)	3(1)	-1(1)
B(3)	24(1)	24(1)	20(1)	2(1)	2(1)	1(1)
C(1)	35(1)	27(1)	41(1)	-7(1)	3(1)	5(1)
C(2)	42(1)	40(1)	33(1)	-6(1)	-5(1)	-4(1)
C(3)	39(1)	46(1)	21(1)	0(1)	7(1)	-2(1)
C(4)	21(1)	32(1)	37(1)	1(1)	4(1)	3(1)
C(5)	35(1)	24(1)	40(1)	4(1)	10(1)	-3(1)
C(6)	33(1)	39(1)	25(1)	-6(1)	-3(1)	-7(1)
C(7)	33(1)	30(1)	34(1)	10(1)	-2(1)	4(1)
C(8)	32(1)	38(1)	32(1)	-7(1)	11(1)	1(1)
C(9)	28(1)	24(1)	41(1)	4(1)	4(1)	-6(1)

Table 5. Hydrogen coordinates (x 10^4) and isotropic displacement parameters ($Å^2$x 10^3) for liu153.

	x	y	z	U(eq)
H(1A)	-560(30)	2423(8)	90(20)	63(6)
H(1B)	-2270(20)	2176(7)	-680(20)	44(4)
H(1C)	-1710(30)	2116(8)	1150(30)	63(5)
H(1N)	-780(20)	734(6)	-114(17)	28(4)
H(2)	1220(20)	1931(7)	2480(20)	48(5)
H(2N)	-1380(20)	557(6)	-2888(17)	28(4)
H(3A)	-2500(20)	603(7)	1660(20)	44(4)
H(3B)	-1230(20)	1071(7)	2290(20)	41(4)
H(3C)	-3070(20)	1213(7)	1530(20)	42(4)
H(3N)	1050(20)	1242(6)	-1945(17)	26(3)
H(4A)	-4490(30)	1633(8)	-1930(20)	55(5)
H(4B)	-5650(30)	1130(8)	-2330(30)	63(6)
H(4C)	-5320(20)	1272(7)	-650(20)	51(5)
H(5)	-3460(20)	-449(7)	-773(19)	38(4)
H(6A)	-4030(20)	314(7)	-4110(20)	44(4)
H(6B)	-2770(20)	517(7)	-5300(20)	43(4)
H(6C)	-4220(20)	906(7)	-4784(19)	40(4)
H(7A)	-1470(20)	2100(7)	-4840(20)	48(5)
H(7B)	-2790(20)	2072(8)	-3560(20)	52(5)
H(7C)	-3140(30)	1730(8)	-5160(20)	55(5)
H(8)	1690(20)	662(7)	-5620(20)	49(5)
H(9A)	2270(20)	2053(6)	-1520(20)	36(4)
H(9B)	1860(20)	1945(7)	-3380(20)	40(4)
H(9C)	580(20)	2301(7)	-2462(19)	36(4)

Table 6. Torsion angles [°] for liu153.

C(2)-O(1)-B(1)-C(1)	16.87(19)
C(2)-O(1)-B(1)-N(1)	-109.47(14)
C(2)-O(1)-B(1)-N(3)	140.84(13)
C(3)-N(1)-B(1)-O(1)	72.68(12)
B(2)-N(1)-B(1)-O(1)	-156.61(9)
C(3)-N(1)-B(1)-C(1)	-54.44(14)
B(2)-N(1)-B(1)-C(1)	76.28(13)
C(3)-N(1)-B(1)-N(3)	178.36(10)
B(2)-N(1)-B(1)-N(3)	-50.93(12)
C(9)-N(3)-B(1)-O(1)	-73.44(11)
B(3)-N(3)-B(1)-O(1)	154.16(9)
C(9)-N(3)-B(1)-C(1)	50.94(13)
B(3)-N(3)-B(1)-C(1)	-81.45(13)
C(9)-N(3)-B(1)-N(1)	177.75(9)
B(3)-N(3)-B(1)-N(1)	45.35(12)
C(5)-O(3)-B(2)-N(1)	-61.00(14)
C(5)-O(3)-B(2)-N(2)	52.63(14)
C(5)-O(3)-B(2)-C(4)	175.09(11)
C(3)-N(1)-B(2)-O(3)	-56.30(12)
B(1)-N(1)-B(2)-O(3)	172.59(9)
C(3)-N(1)-B(2)-N(2)	-171.74(10)
B(1)-N(1)-B(2)-N(2)	57.16(12)
C(3)-N(1)-B(2)-C(4)	61.31(13)
B(1)-N(1)-B(2)-C(4)	-69.79(13)
C(6)-N(2)-B(2)-O(3)	57.04(12)
B(3)-N(2)-B(2)-O(3)	-171.52(9)
C(6)-N(2)-B(2)-N(1)	171.73(9)
B(3)-N(2)-B(2)-N(1)	-56.84(12)
C(6)-N(2)-B(2)-C(4)	-60.28(13)
B(3)-N(2)-B(2)-C(4)	71.15(12)
C(8)-O(5)-B(3)-N(2)	-53.58(14)
C(8)-O(5)-B(3)-N(3)	60.64(14)
C(8)-O(5)-B(3)-C(7)	-177.77(11)
C(6)-N(2)-B(3)-O(5)	-63.33(12)

B(2)-N(2)-B(3)-O(5)	165.36(9)
C(6)-N(2)-B(3)-N(3)	-177.57(9)
B(2)-N(2)-B(3)-N(3)	51.12(12)
C(6)-N(2)-B(3)-C(7)	54.55(14)
B(2)-N(2)-B(3)-C(7)	-76.76(13)
C(9)-N(3)-B(3)-O(5)	67.29(11)
B(1)-N(3)-B(3)-O(5)	-160.18(9)
C(9)-N(3)-B(3)-N(2)	-178.36(9)
B(1)-N(3)-B(3)-N(2)	-45.82(12)
C(9)-N(3)-B(3)-C(7)	-49.24(13)
B(1)-N(3)-B(3)-C(7)	83.29(13)
B(1)-O(1)-C(2)-O(2)	-178.92(14)
B(2)-O(3)-C(5)-O(4)	-4.3(2)
B(3)-O(5)-C(8)-O(6)	-3.3(2)

Symmetry transformations used to generate equivalent atoms:

Table 7. Hydrogen bonds for liu153 [Å and °].

D-H...A	d(D-H)	d(H...A)	d(D...A)	<(DHA)
N(1)-H(1N)...O(4)#1	0.845(16)	2.326(15)	3.0747(14)	147.9(13)
N(1)-H(1N)...O(4)	0.845(16)	2.458(15)	3.0505(15)	127.9(12)
N(2)-H(2N)...O(4)	0.879(15)	2.196(15)	2.8709(14)	133.3(12)
N(2)-H(2N)...O(6)	0.879(15)	2.282(15)	2.9385(14)	131.5(12)
N(3)-H(3N)...O(6)	0.849(15)	2.367(15)	3.0066(14)	132.5(12)

Symmetry transformations used to generate equivalent atoms:

#1 -x,-y,-z

Chapter V

Crystallographic Data for Compound 3 (Liu82)

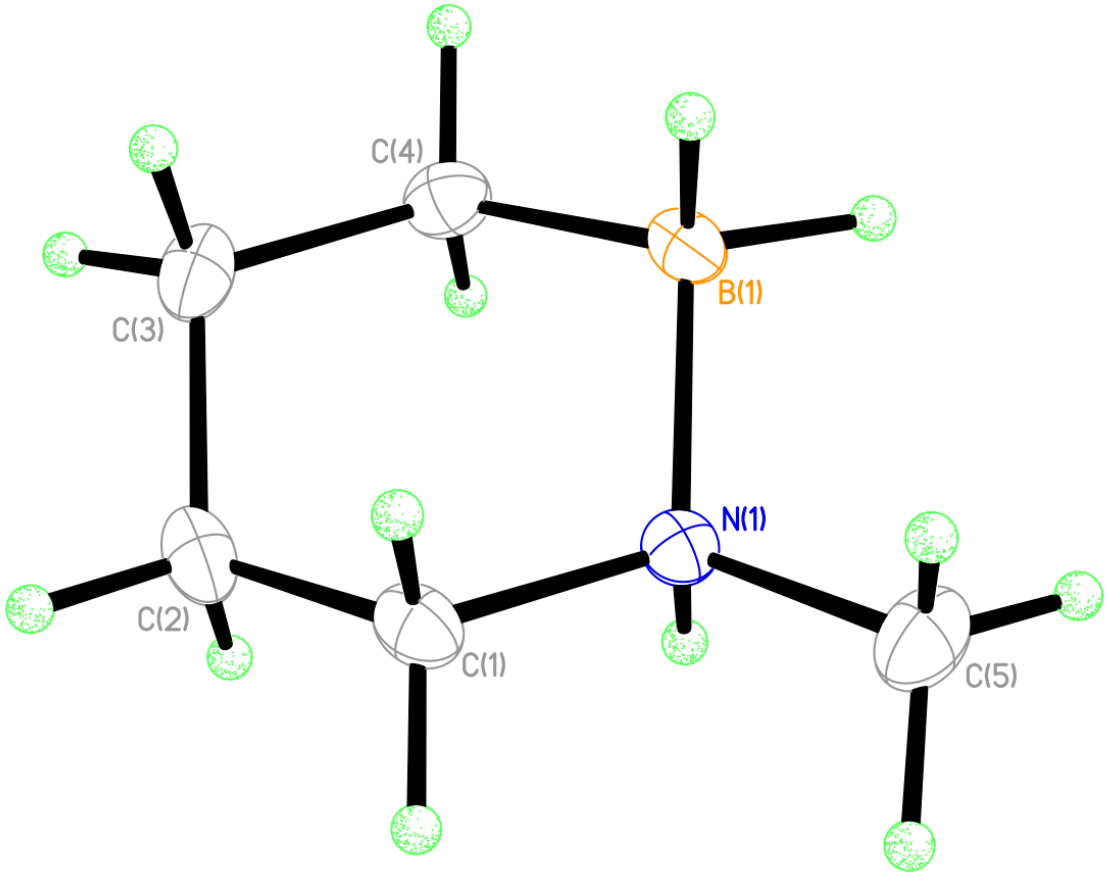

Table 1. Crystal data and structure refinement for liu82.

Identification code	liu82	
Empirical formula	C5 H14 B N	
Formula weight	98.98	
Temperature	173(2) K	
Wavelength	0.71073 Å	
Crystal system	Monoclinic	
Space group	P2(1)/n	
Unit cell dimensions	a = 7.812(3) Å	a= 90°.
	b = 8.139(3) Å	b= 102.399(6)°.
	c = 11.020(4) Å	g = 90°.
Volume	684.3(4) Å^3	
Z	4	

Density (calculated)	0.961 Mg/m^3
Absorption coefficient	0.054 mm^{-1}
F(000)	224
Crystal size	0.37 x 0.24 x 0.03 mm^3
Theta range for data collection	2.92 to 26.98°.
Index ranges	-9<=h<=9, -10<=k<=10, -14<=l<=13
Reflections collected	7100
Independent reflections	1489 [R(int) = 0.0485]
Completeness to theta = 26.98°	99.9 %
Absorption correction	Semi-empirical from equivalents
Max. and min. transmission	0.9984 and 0.9803
Refinement method	Full-matrix least-squares on F^2
Data / restraints / parameters	1489 / 0 / 120
Goodness-of-fit on F^2	1.030
Final R indices [I>2sigma(I)]	R1 = 0.0470, wR2 = 0.1226
R indices (all data)	R1 = 0.0681, wR2 = 0.1362
Largest diff. peak and hole	0.218 and -0.149 $e.Å^{-3}$

Table 2. Atomic coordinates (x 10^4) and equivalent isotropic displacement parameters ($Å^2$x 10^3) for liu82. U(eq) is defined as one third of the trace of the orthogonalized U^{ij} tensor.

	x	y	z	U(eq)
N(1)	1696(1)	7247(1)	1546(1)	27(1)
B(1)	1385(2)	5925(2)	2558(1)	30(1)
C(1)	34(2)	7652(2)	649(1)	33(1)
C(2)	-1344(2)	8281(2)	1302(1)	39(1)
C(3)	-1777(2)	7058(2)	2238(1)	41(1)
C(4)	-126(2)	6600(2)	3196(1)	36(1)
C(5)	3079(2)	6763(2)	890(2)	43(1)

Table 3. Bond lengths [Å] and angles [°] for liu82.

N(1)-C(5)	1.4767(16)
N(1)-C(1)	1.4896(16)
N(1)-B(1)	1.6055(17)
N(1)-H(1N)	0.881(14)
B(1)-C(4)	1.5961(19)
B(1)-H(1B)	1.174(13)
B(1)-H(2B)	1.149(13)
C(1)-C(2)	1.5076(19)
C(1)-H(1A)	0.972(14)
C(1)-H(1C)	0.982(13)
C(2)-C(3)	1.523(2)
C(2)-H(2A)	1.003(15)
C(2)-H(2C)	0.968(15)
C(3)-C(4)	1.5271(19)
C(3)-H(3A)	0.989(17)
C(3)-H(3C)	1.010(15)
C(4)-H(4A)	0.981(14)
C(4)-H(4C)	1.031(14)
C(5)-H(5A)	0.975(16)
C(5)-H(5B)	0.980(17)
C(5)-H(5C)	0.970(17)

C(5)-N(1)-C(1)	111.06(10)
C(5)-N(1)-B(1)	113.37(11)
C(1)-N(1)-B(1)	111.64(10)
C(5)-N(1)-H(1N)	106.3(9)
C(1)-N(1)-H(1N)	104.8(9)
B(1)-N(1)-H(1N)	109.2(9)
C(4)-B(1)-N(1)	108.17(10)
C(4)-B(1)-H(1B)	112.9(6)
N(1)-B(1)-H(1B)	104.0(6)
C(4)-B(1)-H(2B)	114.4(6)
N(1)-B(1)-H(2B)	106.5(6)
H(1B)-B(1)-H(2B)	110.1(8)

N(1)-C(1)-C(2)	111.61(10)
N(1)-C(1)-H(1A)	107.3(8)
C(2)-C(1)-H(1A)	111.4(8)
N(1)-C(1)-H(1C)	106.8(8)
C(2)-C(1)-H(1C)	110.5(8)
H(1A)-C(1)-H(1C)	109.0(11)
C(1)-C(2)-C(3)	112.77(11)
C(1)-C(2)-H(2A)	108.8(8)
C(3)-C(2)-H(2A)	110.0(8)
C(1)-C(2)-H(2C)	108.7(8)
C(3)-C(2)-H(2C)	109.1(8)
H(2A)-C(2)-H(2C)	107.3(11)
C(4)-C(3)-C(2)	110.48(11)
C(4)-C(3)-H(3A)	112.4(9)
C(2)-C(3)-H(3A)	110.0(8)
C(4)-C(3)-H(3C)	108.0(8)
C(2)-C(3)-H(3C)	109.2(8)
H(3A)-C(3)-H(3C)	106.4(12)
C(3)-C(4)-B(1)	111.99(11)
C(3)-C(4)-H(4A)	110.1(8)
B(1)-C(4)-H(4A)	109.3(8)
C(3)-C(4)-H(4C)	110.0(8)
B(1)-C(4)-H(4C)	110.3(7)
H(4A)-C(4)-H(4C)	105.0(11)
N(1)-C(5)-H(5A)	108.9(9)
N(1)-C(5)-H(5B)	109.6(9)
H(5A)-C(5)-H(5B)	108.0(13)
N(1)-C(5)-H(5C)	108.3(9)
H(5A)-C(5)-H(5C)	113.5(13)
H(5B)-C(5)-H(5C)	108.4(13)

Symmetry transformations used to generate equivalent atoms:

Table 4. Anisotropic displacement parameters ($Å^2 x\ 10^3$)for liu82. The anisotropic displacement factor exponent takes the form: $-2p^2[\ h^2 a^{*2} U^{11} + ... + 2\ h\ k\ a^*\ b^*\ U^{12}\ ]$

	U^{11}	U^{22}	U^{33}	U^{23}	U^{13}	U^{12}
N(1)	28(1)	28(1)	24(1)	-3(1)	2(1)	-2(1)
B(1)	33(1)	30(1)	25(1)	2(1)	-1(1)	1(1)
C(1)	37(1)	34(1)	25(1)	3(1)	-2(1)	1(1)
C(2)	32(1)	43(1)	36(1)	0(1)	-5(1)	7(1)
C(3)	28(1)	50(1)	44(1)	-6(1)	7(1)	-1(1)
C(4)	39(1)	41(1)	28(1)	2(1)	8(1)	-4(1)
C(5)	39(1)	50(1)	43(1)	-1(1)	16(1)	0(1)

Table 5. Hydrogen coordinates (x 10^4) and isotropic displacement parameters ($Å^2$x 10^3) for liu82.

	x	y	z	U(eq)
H(1N)	2039(18)	8183(17)	1922(13)	34(4)
H(1B)	981(15)	4725(16)	1976(11)	37(3)
H(2B)	2716(17)	5741(15)	3230(12)	38(3)
H(1A)	313(18)	8462(16)	73(13)	37(4)
H(1C)	-363(17)	6637(16)	192(13)	35(3)
H(2A)	-927(18)	9342(19)	1728(13)	48(4)
H(2C)	-2398(19)	8519(16)	686(14)	47(4)
H(3A)	-2710(20)	7507(17)	2627(14)	48(4)
H(3C)	-2267(18)	6022(18)	1790(13)	46(4)
H(4A)	-402(18)	5767(17)	3768(13)	52(4)
H(4C)	316(18)	7601(16)	3749(13)	40(4)
H(5A)	3270(20)	7661(18)	349(16)	51(4)
H(5B)	4180(20)	6569(18)	1495(15)	54(4)
H(5C)	2730(20)	5740(20)	449(15)	61(5)

Table 6. Torsion angles [°] for liu82.

C(5)-N(1)-B(1)-C(4)	179.76(11)
C(1)-N(1)-B(1)-C(4)	-53.90(13)
C(5)-N(1)-C(1)-C(2)	-175.36(11)
B(1)-N(1)-C(1)-C(2)	57.05(14)
N(1)-C(1)-C(2)-C(3)	-58.53(15)
C(1)-C(2)-C(3)-C(4)	56.86(16)
C(2)-C(3)-C(4)-B(1)	-55.05(16)
N(1)-B(1)-C(4)-C(3)	53.09(14)

Symmetry transformations used to generate equivalent atoms:

Crystallographic Data for Compound 9 (Liu143)

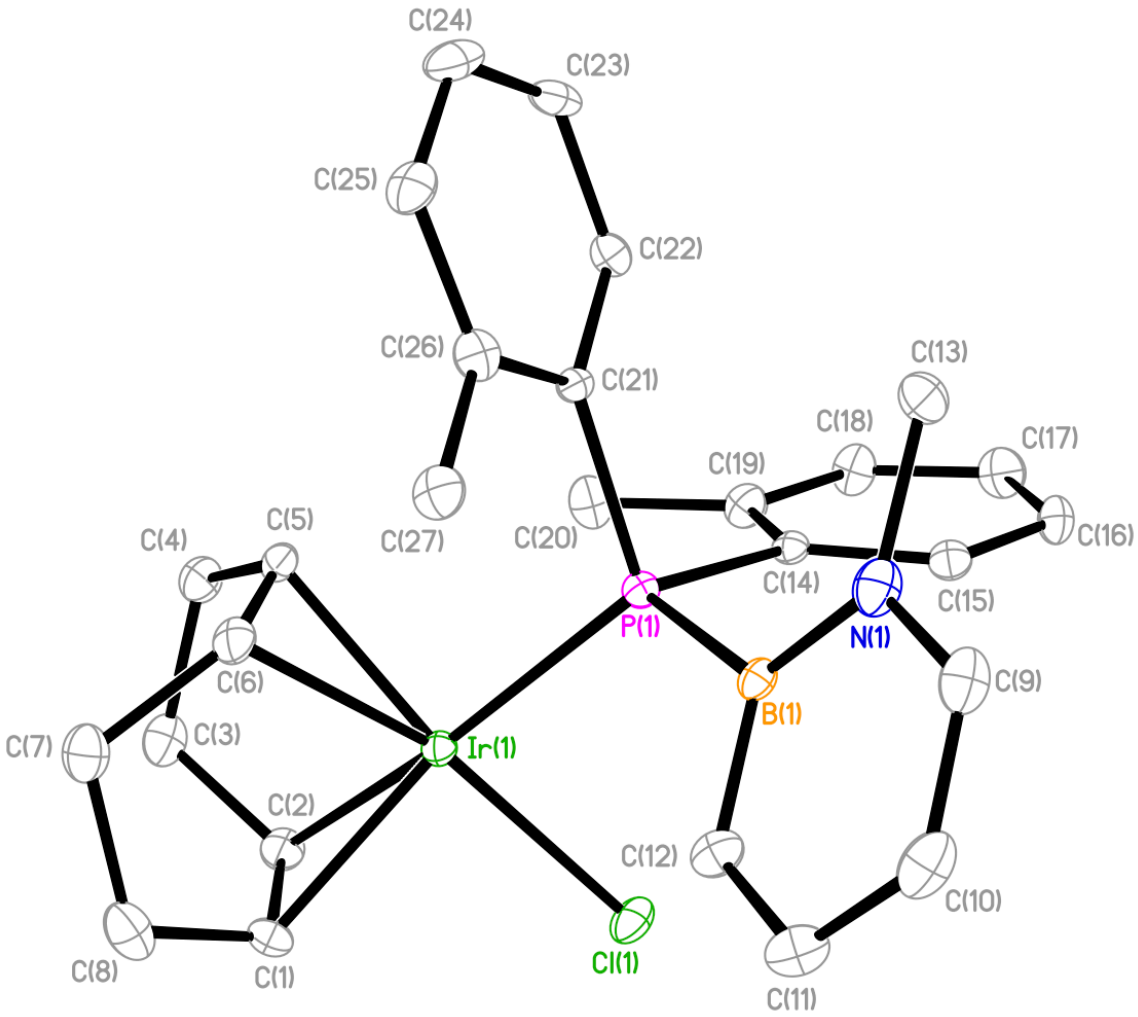

Table 1. Crystal data and structure refinement for liu143.

Identification code	liu143	
Empirical formula	C27 H32 B Cl Ir N P	
Formula weight	639.97	
Temperature	173(2) K	
Wavelength	0.71073 Å	
Crystal system	Monoclinic	
Space group	P2(1)/n	
Unit cell dimensions	a = 8.205(4) Å	a= 90°.
	b = 17.482(8) Å	b= 90.773(7)°.
	c = 16.955(7) Å	g = 90°.
Volume	2431.9(18) Å^3	

Z	4
Density (calculated)	1.748 Mg/m^3
Absorption coefficient	5.682 mm^{-1}
F(000)	1260
Crystal size	0.17 x 0.14 x 0.11 mm^3
Theta range for data collection	1.67 to 26.99°.
Index ranges	-10<=h<=10, -22<=k<=22, -21<=l<=21
Reflections collected	26578
Independent reflections	5316 [R(int) = 0.0611]
Completeness to theta = 26.99°	100.0 %
Absorption correction	Semi-empirical from equivalents
Max. and min. transmission	0.5738 and 0.4451
Refinement method	Full-matrix least-squares on F^2
Data / restraints / parameters	5316 / 0 / 289
Goodness-of-fit on F^2	1.062
Final R indices [I>2sigma(I)]	R1 = 0.0267, wR2 = 0.0676
R indices (all data)	R1 = 0.0298, wR2 = 0.0694
Largest diff. peak and hole	1.067 and -0.802 $e.Å^{-3}$

Table 2. Atomic coordinates (x 10^4) and equivalent isotropic displacement parameters ($Å^2$x 10^3) for liu143. U(eq) is defined as one third of the trace of the orthogonalized U^{ij} tensor.

	x	y	z	U(eq)
Ir(1)	7028(1)	1509(1)	8358(1)	16(1)
Cl(1)	4457(1)	925(1)	8119(1)	27(1)
P(1)	5724(1)	2433(1)	9128(1)	16(1)
N(1)	3740(4)	3784(2)	8876(2)	28(1)
B(1)	4391(4)	3097(2)	8577(2)	17(1)
CB1	4391(4)	3097(2)	8577(2)	17(1)
CN1	3740(4)	3784(2)	8876(2)	28(1)
C(1)	7913(5)	933(2)	7312(2)	28(1)
C(2)	8231(5)	463(2)	7952(2)	26(1)
C(3)	9921(5)	356(2)	8320(3)	30(1)
C(4)	10191(5)	875(2)	9027(2)	30(1)
C(5)	9327(4)	1637(2)	8928(2)	24(1)
C(6)	9309(4)	2086(2)	8237(2)	25(1)
C(7)	10218(5)	1892(2)	7491(2)	32(1)
C(8)	9180(6)	1424(3)	6906(3)	37(1)
C(9)	2816(5)	4242(2)	8359(2)	28(1)
C(10)	2555(4)	4047(2)	7584(2)	31(1)
C(11)	3222(5)	3379(2)	7282(3)	29(1)
C(12)	4139(5)	2904(2)	7777(2)	24(1)
C(13)	3991(5)	4067(2)	9709(2)	31(1)
C(14)	4416(4)	2000(2)	9890(2)	16(1)
C(19)	4971(5)	1385(2)	10365(2)	27(1)
B(14A)	4416(4)	2000(2)	9890(2)	16(1)
N(19A)	4971(5)	1385(2)	10365(2)	27(1)
C(15)	2851(4)	2287(2)	10000(2)	21(1)
C(16)	1866(4)	2024(2)	10603(2)	25(1)
C(17)	2442(6)	1453(2)	11097(3)	33(1)
C(18)	3957(5)	1128(2)	10968(2)	29(1)
C(20)	6577(5)	983(2)	10259(2)	29(1)
C(21)	7103(4)	3074(2)	9686(2)	15(1)
C(26)	8022(4)	3642(2)	9310(2)	24(1)

B(21A)	7103(4)	3074(2)	9686(2)	15(1)
N(26A)	8022(4)	3642(2)	9310(2)	24(1)
C(22)	7295(4)	2971(2)	10503(2)	20(1)
C(23)	8399(5)	3398(2)	10943(2)	26(1)
C(24)	9352(5)	3926(2)	10566(3)	31(1)
C(25)	9164(5)	4048(2)	9759(2)	26(1)
C(27)	7794(5)	3890(2)	8454(2)	25(1)

Table 3. Bond lengths [Å] and angles [°] for liu143.

Ir(1)-C(5)	2.120(4)
Ir(1)-C(6)	2.138(4)
Ir(1)-C(1)	2.173(4)
Ir(1)-C(2)	2.193(4)
Ir(1)-P(1)	2.3442(11)
Ir(1)-Cl(1)	2.3739(12)
P(1)-B(1)	1.841(4)
P(1)-C(21)	1.844(3)
P(1)-C(14)	1.853(4)
N(1)-C(9)	1.402(5)
N(1)-B(1)	1.411(5)
N(1)-C(13)	1.508(5)
B(1)-C(12)	1.411(5)
C(1)-C(2)	1.382(6)
C(1)-C(8)	1.520(6)
C(1)-H(1A)	1.0000
C(2)-C(3)	1.525(5)
C(2)-H(2A)	1.0000
C(3)-C(4)	1.517(6)
C(3)-H(3A)	0.9900
C(3)-H(3B)	0.9900
C(4)-C(5)	1.517(5)
C(4)-H(4A)	0.9900
C(4)-H(4B)	0.9900
C(5)-C(6)	1.411(6)
C(5)-H(5A)	1.0000
C(6)-C(7)	1.515(5)
C(6)-H(6A)	1.0000
C(7)-C(8)	1.536(6)
C(7)-H(7A)	0.9900
C(7)-H(7B)	0.9900
C(8)-H(8A)	0.9900
C(8)-H(8B)	0.9900
C(9)-C(10)	1.372(6)

C(9)-H(9A)	0.9500
C(10)-C(11)	1.391(6)
C(10)-H(10A)	0.9500
C(11)-C(12)	1.393(5)
C(11)-H(11A)	0.9500
C(13)-H(13A)	0.9800
C(13)-H(13B)	0.9800
C(13)-H(13C)	0.9800
C(14)-C(15)	1.394(5)
C(14)-C(19)	1.414(5)
C(19)-C(18)	1.401(5)
C(19)-C(20)	1.506(5)
C(15)-C(16)	1.391(5)
C(15)-H(15A)	0.9500
C(16)-C(17)	1.383(6)
C(16)-H(16A)	0.9500
C(17)-C(18)	1.386(6)
C(17)-H(17A)	0.9500
C(18)-H(18A)	0.9500
C(20)-H(20A)	0.9800
C(20)-H(20B)	0.9800
C(20)-H(20C)	0.9800
C(21)-C(22)	1.403(5)
C(21)-C(26)	1.405(5)
C(26)-C(25)	1.393(5)
C(26)-C(27)	1.523(5)
C(22)-C(23)	1.385(5)
C(22)-H(22A)	0.9500
C(23)-C(24)	1.373(6)
C(23)-H(23A)	0.9500
C(24)-C(25)	1.392(6)
C(24)-H(24A)	0.9500
C(25)-H(25A)	0.9500
C(27)-H(27A)	0.9800
C(27)-H(27B)	0.9800
C(27)-H(27C)	0.9800

C(5)-Ir(1)-C(6)	38.70(15)
C(5)-Ir(1)-C(1)	96.64(15)
C(6)-Ir(1)-C(1)	80.67(15)
C(5)-Ir(1)-C(2)	80.16(14)
C(6)-Ir(1)-C(2)	87.98(14)
C(1)-Ir(1)-C(2)	36.89(15)
C(5)-Ir(1)-P(1)	94.81(11)
C(6)-Ir(1)-P(1)	97.78(10)
C(1)-Ir(1)-P(1)	159.10(11)
C(2)-Ir(1)-P(1)	163.73(11)
C(5)-Ir(1)-Cl(1)	154.98(11)
C(6)-Ir(1)-Cl(1)	164.49(11)
C(1)-Ir(1)-Cl(1)	88.11(11)
C(2)-Ir(1)-Cl(1)	89.43(10)
P(1)-Ir(1)-Cl(1)	88.88(4)
B(1)-P(1)-C(21)	103.49(15)
B(1)-P(1)-C(14)	105.40(16)
C(21)-P(1)-C(14)	104.33(16)
B(1)-P(1)-Ir(1)	115.12(12)
C(21)-P(1)-Ir(1)	115.03(11)
C(14)-P(1)-Ir(1)	112.33(12)
C(9)-N(1)-B(1)	117.7(4)
C(9)-N(1)-C(13)	117.6(4)
B(1)-N(1)-C(13)	124.6(3)
N(1)-B(1)-C(12)	119.8(3)
N(1)-B(1)-P(1)	125.4(3)
C(12)-B(1)-P(1)	114.5(3)
C(2)-C(1)-C(8)	124.6(4)
C(2)-C(1)-Ir(1)	72.3(2)
C(8)-C(1)-Ir(1)	110.2(3)
C(2)-C(1)-H(1A)	114.0
C(8)-C(1)-H(1A)	114.0
Ir(1)-C(1)-H(1A)	114.0
C(1)-C(2)-C(3)	123.7(4)
C(1)-C(2)-Ir(1)	70.8(2)

C(3)-C(2)-Ir(1)	112.6(2)
C(1)-C(2)-H(2A)	114.1
C(3)-C(2)-H(2A)	114.1
Ir(1)-C(2)-H(2A)	114.1
C(4)-C(3)-C(2)	111.8(3)
C(4)-C(3)-H(3A)	109.3
C(2)-C(3)-H(3A)	109.3
C(4)-C(3)-H(3B)	109.3
C(2)-C(3)-H(3B)	109.3
H(3A)-C(3)-H(3B)	107.9
C(3)-C(4)-C(5)	112.0(3)
C(3)-C(4)-H(4A)	109.2
C(5)-C(4)-H(4A)	109.2
C(3)-C(4)-H(4B)	109.2
C(5)-C(4)-H(4B)	109.2
H(4A)-C(4)-H(4B)	107.9
C(6)-C(5)-C(4)	125.5(3)
C(6)-C(5)-Ir(1)	71.4(2)
C(4)-C(5)-Ir(1)	111.7(3)
C(6)-C(5)-H(5A)	113.6
C(4)-C(5)-H(5A)	113.6
Ir(1)-C(5)-H(5A)	113.6
C(5)-C(6)-C(7)	124.6(4)
C(5)-C(6)-Ir(1)	69.9(2)
C(7)-C(6)-Ir(1)	114.6(3)
C(5)-C(6)-H(6A)	113.4
C(7)-C(6)-H(6A)	113.4
Ir(1)-C(6)-H(6A)	113.4
C(6)-C(7)-C(8)	112.6(3)
C(6)-C(7)-H(7A)	109.1
C(8)-C(7)-H(7A)	109.1
C(6)-C(7)-H(7B)	109.1
C(8)-C(7)-H(7B)	109.1
H(7A)-C(7)-H(7B)	107.8
C(1)-C(8)-C(7)	112.6(3)
C(1)-C(8)-H(8A)	109.1

C(7)-C(8)-H(8A)	109.1
C(1)-C(8)-H(8B)	109.1
C(7)-C(8)-H(8B)	109.1
H(8A)-C(8)-H(8B)	107.8
C(10)-C(9)-N(1)	122.2(4)
C(10)-C(9)-H(9A)	118.9
N(1)-C(9)-H(9A)	118.9
C(9)-C(10)-C(11)	120.3(4)
C(9)-C(10)-H(10A)	119.9
C(11)-C(10)-H(10A)	119.9
C(10)-C(11)-C(12)	119.4(4)
C(10)-C(11)-H(11A)	120.3
C(12)-C(11)-H(11A)	120.3
C(11)-C(12)-B(1)	120.5(4)
N(1)-C(13)-H(13A)	109.5
N(1)-C(13)-H(13B)	109.5
H(13A)-C(13)-H(13B)	109.5
N(1)-C(13)-H(13C)	109.5
H(13A)-C(13)-H(13C)	109.5
H(13B)-C(13)-H(13C)	109.5
C(15)-C(14)-C(19)	119.2(3)
C(15)-C(14)-P(1)	119.3(3)
C(19)-C(14)-P(1)	121.5(3)
C(18)-C(19)-C(14)	118.0(3)
C(18)-C(19)-C(20)	117.8(3)
C(14)-C(19)-C(20)	124.2(3)
C(16)-C(15)-C(14)	121.6(3)
C(16)-C(15)-H(15A)	119.2
C(14)-C(15)-H(15A)	119.2
C(17)-C(16)-C(15)	119.2(4)
C(17)-C(16)-H(16A)	120.4
C(15)-C(16)-H(16A)	120.4
C(16)-C(17)-C(18)	120.0(4)
C(16)-C(17)-H(17A)	120.0
C(18)-C(17)-H(17A)	120.0
C(17)-C(18)-C(19)	121.8(4)

C(17)-C(18)-H(18A)	119.1
C(19)-C(18)-H(18A)	119.1
C(19)-C(20)-H(20A)	109.5
C(19)-C(20)-H(20B)	109.5
H(20A)-C(20)-H(20B)	109.5
C(19)-C(20)-H(20C)	109.5
H(20A)-C(20)-H(20C)	109.5
H(20B)-C(20)-H(20C)	109.5
C(22)-C(21)-C(26)	119.0(3)
C(22)-C(21)-P(1)	119.2(3)
C(26)-C(21)-P(1)	121.7(3)
C(25)-C(26)-C(21)	118.2(3)
C(25)-C(26)-C(27)	116.7(3)
C(21)-C(26)-C(27)	125.0(3)
C(23)-C(22)-C(21)	121.8(3)
C(23)-C(22)-H(22A)	119.1
C(21)-C(22)-H(22A)	119.1
C(24)-C(23)-C(22)	118.9(4)
C(24)-C(23)-H(23A)	120.5
C(22)-C(23)-H(23A)	120.5
C(23)-C(24)-C(25)	120.3(4)
C(23)-C(24)-H(24A)	119.9
C(25)-C(24)-H(24A)	119.9
C(24)-C(25)-C(26)	121.6(4)
C(24)-C(25)-H(25A)	119.2
C(26)-C(25)-H(25A)	119.2
C(26)-C(27)-H(27A)	109.5
C(26)-C(27)-H(27B)	109.5
H(27A)-C(27)-H(27B)	109.5
C(26)-C(27)-H(27C)	109.5
H(27A)-C(27)-H(27C)	109.5
H(27B)-C(27)-H(27C)	109.5

Symmetry transformations used to generate equivalent atoms:

Table 4. Anisotropic displacement parameters ($Å^2 x\ 10^3$)for liu143. The anisotropic displacement factor exponent takes the form: $-2p^2[\ h^2a^{*2}U^{11} + ... + 2\ h\ k\ a^*\ b^*\ U^{12}\ ]$

	U^{11}	U^{22}	U^{33}	U^{23}	U^{13}	U^{12}
Ir(1)	16(1)	15(1)	18(1)	-2(1)	0(1)	-1(1)
Cl(1)	19(1)	22(1)	38(1)	-3(1)	-5(1)	-4(1)
P(1)	16(1)	15(1)	17(1)	0(1)	0(1)	0(1)
N(1)	22(2)	27(2)	36(2)	2(2)	2(2)	-2(2)
B(1)	14(2)	14(2)	22(2)	2(1)	-1(1)	-2(1)
CB1	14(2)	14(2)	22(2)	2(1)	-1(1)	-2(1)
CN1	22(2)	27(2)	36(2)	2(2)	2(2)	-2(2)
C(1)	29(2)	32(2)	24(2)	-14(2)	2(2)	0(2)
C(2)	26(2)	18(2)	33(2)	-9(2)	0(2)	0(2)
C(3)	26(2)	21(2)	43(2)	2(2)	1(2)	3(2)
C(4)	23(2)	35(2)	30(2)	1(2)	-3(2)	6(2)
C(5)	15(2)	28(2)	28(2)	-8(2)	-1(2)	-2(1)
C(6)	22(2)	19(2)	35(2)	-6(2)	4(2)	-7(1)
C(7)	29(2)	33(2)	35(2)	5(2)	7(2)	-4(2)
C(8)	40(3)	42(3)	29(2)	2(2)	10(2)	3(2)
C(9)	24(2)	21(2)	40(2)	6(2)	3(2)	2(2)
C(10)	25(2)	28(2)	39(2)	16(2)	-5(2)	0(2)
C(11)	34(2)	24(2)	27(2)	5(2)	-7(2)	-5(2)
C(12)	25(2)	22(2)	26(2)	4(2)	-4(2)	-5(2)
C(13)	29(2)	24(2)	40(2)	-12(2)	0(2)	6(2)
C(14)	17(2)	15(2)	16(2)	0(1)	0(1)	-4(1)
C(19)	25(2)	28(2)	28(2)	2(2)	-1(2)	0(2)
B(14A)	17(2)	15(2)	16(2)	0(1)	0(1)	-4(1)
N(19A)	25(2)	28(2)	28(2)	2(2)	-1(2)	0(2)
C(15)	23(2)	19(2)	22(2)	0(1)	-1(1)	-2(1)
C(16)	19(2)	28(2)	29(2)	1(2)	6(2)	0(2)
C(17)	33(2)	35(2)	30(2)	6(2)	7(2)	-7(2)
C(18)	27(2)	27(2)	32(2)	12(2)	3(2)	-1(2)
C(20)	32(2)	27(2)	28(2)	11(2)	4(2)	9(2)
C(21)	15(2)	11(2)	18(2)	-2(1)	-2(1)	2(1)
C(26)	26(2)	21(2)	26(2)	2(1)	2(2)	2(1)

B(21A)	15(2)	11(2)	18(2)	-2(1)	-2(1)	2(1)
N(26A)	26(2)	21(2)	26(2)	2(1)	2(2)	2(1)
C(22)	23(2)	19(2)	19(2)	2(1)	3(1)	2(1)
C(23)	34(2)	25(2)	18(2)	-7(2)	-7(2)	6(2)
C(24)	32(2)	24(2)	38(2)	-7(2)	-12(2)	-3(2)
C(25)	24(2)	19(2)	35(2)	2(2)	1(2)	-6(1)
C(27)	26(2)	24(2)	26(2)	6(2)	3(2)	-7(2)

Table 5. Hydrogen coordinates (x 10^4) and isotropic displacement parameters ($Å^2$x 10^3) for liu143.

	x	y	z	U(eq)
H(1A)	7030	740	6952	34
H(2A)	7528	-3	7971	31
H(3A)	10053	-183	8487	36
H(3B)	10757	467	7920	36
H(4A)	11374	966	9101	36
H(4B)	9786	617	9506	36
H(5A)	9285	1944	9424	28
H(6A)	9245	2648	8343	30
H(7A)	11210	1597	7633	39
H(7B)	10566	2371	7233	39
H(8A)	8620	1777	6534	44
H(8B)	9903	1090	6595	44
H(9A)	2355	4702	8552	34
H(10A)	1917	4370	7252	37
H(11A)	3055	3247	6744	34
H(13A)	3421	4555	9775	47
H(13B)	5158	4140	9814	47
H(13C)	3556	3691	10079	47
H(15A)	2447	2673	9654	25
H(16A)	810	2234	10675	30
H(17A)	1801	1283	11526	39
H(18A)	4317	721	11297	35
H(20A)	6693	578	10655	44
H(20B)	7469	1352	10323	44
H(20C)	6613	759	9730	44
H(22A)	6651	2598	10761	24
H(23A)	8495	3327	11497	31
H(24A)	10143	4210	10858	38
H(25A)	9831	4417	9508	31
H(27A)	8579	4294	8332	38

H(27B)	6683	4084	8374	38
H(27C)	7972	3451	8106	38

Table 6. Torsion angles [°] for liu143.

C(5)-Ir(1)-P(1)-B(1)	135.98(16)
C(6)-Ir(1)-P(1)-B(1)	97.14(16)
C(1)-Ir(1)-P(1)-B(1)	12.9(3)
C(2)-Ir(1)-P(1)-B(1)	-152.9(4)
Cl(1)-Ir(1)-P(1)-B(1)	-68.80(13)
C(5)-Ir(1)-P(1)-C(21)	15.76(16)
C(6)-Ir(1)-P(1)-C(21)	-23.08(17)
C(1)-Ir(1)-P(1)-C(21)	-107.3(3)
C(2)-Ir(1)-P(1)-C(21)	86.9(4)
Cl(1)-Ir(1)-P(1)-C(21)	170.98(13)
C(5)-Ir(1)-P(1)-C(14)	-103.38(16)
C(6)-Ir(1)-P(1)-C(14)	-142.22(16)
C(1)-Ir(1)-P(1)-C(14)	133.6(3)
C(2)-Ir(1)-P(1)-C(14)	-32.3(4)
Cl(1)-Ir(1)-P(1)-C(14)	51.84(12)
C(9)-N(1)-B(1)-C(12)	1.8(5)
C(13)-N(1)-B(1)-C(12)	-177.2(3)
C(9)-N(1)-B(1)-P(1)	176.6(3)
C(13)-N(1)-B(1)-P(1)	-2.3(6)
C(21)-P(1)-B(1)-N(1)	-40.3(4)
C(14)-P(1)-B(1)-N(1)	68.9(3)
Ir(1)-P(1)-B(1)-N(1)	-166.7(3)
C(21)-P(1)-B(1)-C(12)	134.8(3)
C(14)-P(1)-B(1)-C(12)	-116.0(3)
Ir(1)-P(1)-B(1)-C(12)	8.4(3)
C(5)-Ir(1)-C(1)-C(2)	63.8(2)
C(6)-Ir(1)-C(1)-C(2)	99.2(2)
P(1)-Ir(1)-C(1)-C(2)	-173.4(2)
Cl(1)-Ir(1)-C(1)-C(2)	-91.6(2)
C(5)-Ir(1)-C(1)-C(8)	-57.4(3)
C(6)-Ir(1)-C(1)-C(8)	-22.0(3)
C(2)-Ir(1)-C(1)-C(8)	-121.2(4)
P(1)-Ir(1)-C(1)-C(8)	65.3(5)
Cl(1)-Ir(1)-C(1)-C(8)	147.2(3)

C(8)-C(1)-C(2)-C(3)	-2.1(6)
Ir(1)-C(1)-C(2)-C(3)	-104.9(3)
C(8)-C(1)-C(2)-Ir(1)	102.8(4)
C(5)-Ir(1)-C(2)-C(1)	-115.2(3)
C(6)-Ir(1)-C(2)-C(1)	-77.1(2)
P(1)-Ir(1)-C(2)-C(1)	171.6(3)
Cl(1)-Ir(1)-C(2)-C(1)	87.6(2)
C(5)-Ir(1)-C(2)-C(3)	4.2(3)
C(6)-Ir(1)-C(2)-C(3)	42.4(3)
C(1)-Ir(1)-C(2)-C(3)	119.5(4)
P(1)-Ir(1)-C(2)-C(3)	-68.9(5)
Cl(1)-Ir(1)-C(2)-C(3)	-152.9(3)
C(1)-C(2)-C(3)-C(4)	96.1(5)
Ir(1)-C(2)-C(3)-C(4)	14.8(4)
C(2)-C(3)-C(4)-C(5)	-34.0(5)
C(3)-C(4)-C(5)-C(6)	-44.3(5)
C(3)-C(4)-C(5)-Ir(1)	37.8(4)
C(1)-Ir(1)-C(5)-C(6)	66.0(2)
C(2)-Ir(1)-C(5)-C(6)	99.2(2)
P(1)-Ir(1)-C(5)-C(6)	-96.4(2)
Cl(1)-Ir(1)-C(5)-C(6)	165.9(2)
C(6)-Ir(1)-C(5)-C(4)	-121.7(4)
C(1)-Ir(1)-C(5)-C(4)	-55.7(3)
C(2)-Ir(1)-C(5)-C(4)	-22.5(3)
P(1)-Ir(1)-C(5)-C(4)	141.9(3)
Cl(1)-Ir(1)-C(5)-C(4)	44.2(4)
C(4)-C(5)-C(6)-C(7)	-2.8(6)
Ir(1)-C(5)-C(6)-C(7)	-106.6(4)
C(4)-C(5)-C(6)-Ir(1)	103.8(4)
C(1)-Ir(1)-C(6)-C(5)	-113.1(2)
C(2)-Ir(1)-C(6)-C(5)	-76.7(2)
P(1)-Ir(1)-C(6)-C(5)	88.0(2)
Cl(1)-Ir(1)-C(6)-C(5)	-157.3(3)
C(5)-Ir(1)-C(6)-C(7)	119.9(4)
C(1)-Ir(1)-C(6)-C(7)	6.8(3)
C(2)-Ir(1)-C(6)-C(7)	43.1(3)

P(1)-Ir(1)-C(6)-C(7)	-152.1(3)
Cl(1)-Ir(1)-C(6)-C(7)	-37.4(6)
C(5)-C(6)-C(7)-C(8)	91.6(5)
Ir(1)-C(6)-C(7)-C(8)	9.8(4)
C(2)-C(1)-C(8)-C(7)	-48.2(5)
Ir(1)-C(1)-C(8)-C(7)	33.9(4)
C(6)-C(7)-C(8)-C(1)	-28.9(5)
B(1)-N(1)-C(9)-C(10)	-0.9(6)
C(13)-N(1)-C(9)-C(10)	178.1(4)
N(1)-C(9)-C(10)-C(11)	-0.4(6)
C(9)-C(10)-C(11)-C(12)	0.9(6)
C(10)-C(11)-C(12)-B(1)	0.0(6)
N(1)-B(1)-C(12)-C(11)	-1.3(5)
P(1)-B(1)-C(12)-C(11)	-176.7(3)
B(1)-P(1)-C(14)-C(15)	-8.4(3)
C(21)-P(1)-C(14)-C(15)	100.3(3)
Ir(1)-P(1)-C(14)-C(15)	-134.5(3)
B(1)-P(1)-C(14)-C(19)	171.8(3)
C(21)-P(1)-C(14)-C(19)	-79.5(3)
Ir(1)-P(1)-C(14)-C(19)	45.7(3)
C(15)-C(14)-C(19)-C(18)	-4.6(5)
P(1)-C(14)-C(19)-C(18)	175.2(3)
C(15)-C(14)-C(19)-C(20)	174.7(4)
P(1)-C(14)-C(19)-C(20)	-5.4(5)
C(19)-C(14)-C(15)-C(16)	4.9(5)
P(1)-C(14)-C(15)-C(16)	-174.9(3)
C(14)-C(15)-C(16)-C(17)	-1.2(6)
C(15)-C(16)-C(17)-C(18)	-2.7(6)
C(16)-C(17)-C(18)-C(19)	2.8(6)
C(14)-C(19)-C(18)-C(17)	0.9(6)
C(20)-C(19)-C(18)-C(17)	-178.5(4)
B(1)-P(1)-C(21)-C(22)	128.3(3)
C(14)-P(1)-C(21)-C(22)	18.2(3)
Ir(1)-P(1)-C(21)-C(22)	-105.3(3)
B(1)-P(1)-C(21)-C(26)	-54.6(3)
C(14)-P(1)-C(21)-C(26)	-164.7(3)

Ir(1)-P(1)-C(21)-C(26)	71.8(3)
C(22)-C(21)-C(26)-C(25)	3.9(5)
P(1)-C(21)-C(26)-C(25)	-173.2(3)
C(22)-C(21)-C(26)-C(27)	-171.8(3)
P(1)-C(21)-C(26)-C(27)	11.1(5)
C(26)-C(21)-C(22)-C(23)	-1.9(5)
P(1)-C(21)-C(22)-C(23)	175.3(3)
C(21)-C(22)-C(23)-C(24)	-1.3(6)
C(22)-C(23)-C(24)-C(25)	2.3(6)
C(23)-C(24)-C(25)-C(26)	-0.2(6)
C(21)-C(26)-C(25)-C(24)	-3.0(6)
C(27)-C(26)-C(25)-C(24)	173.1(4)

Symmetry transformations used to generate equivalent atoms:

Crystallographic Data for Compound 4 (Liu97)

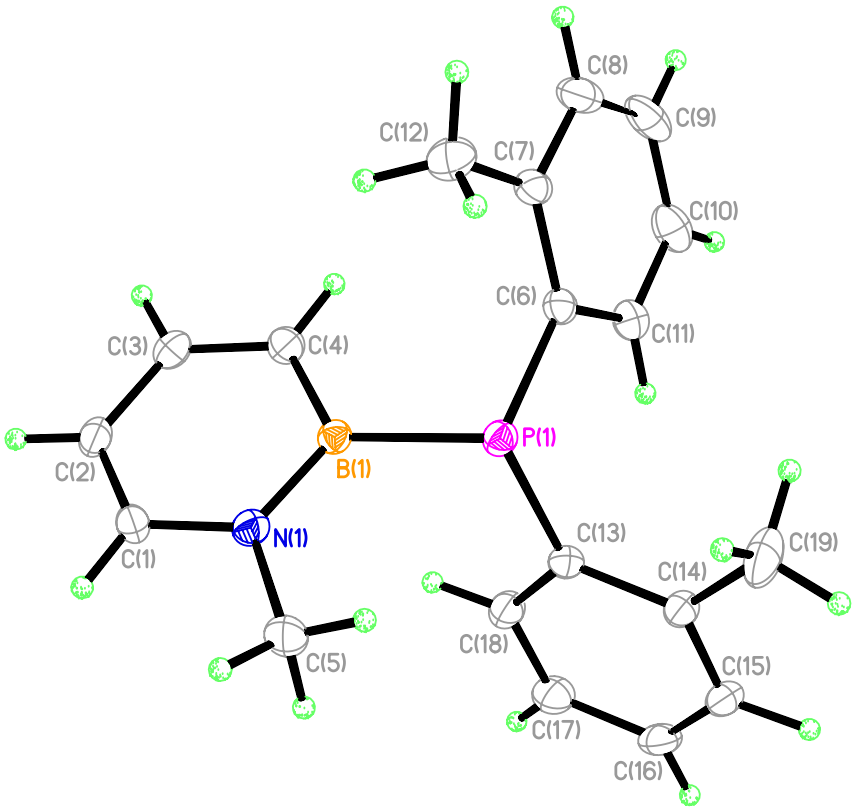

Table 1. Crystal data and structure refinement for liu97.

Identification code	liu97	
Empirical formula	C19 H21 B N P	
Formula weight	305.15	
Temperature	173(2) K	
Wavelength	0.71073 Å	
Crystal system	Monoclinic	
Space group	P2(1)/n	
Unit cell dimensions	a = 7.6132(9) Å	a= 90°.
	b = 7.9016(9) Å	b= 90.407(2)°.
	c = 28.864(3) Å	g = 90°.
Volume	1736.3(4) Å^3	
Z	4	

Density (calculated)	1.167 Mg/m^3
Absorption coefficient	0.154 mm^{-1}
F(000)	648
Crystal size	0.25 x 0.22 x 0.16 mm^3
Theta range for data collection	1.41 to 27.00°.
Index ranges	-9<=h<=9, -9<=k<=10, -36<=l<=36
Reflections collected	10512
Independent reflections	3763 [R(int) = 0.0233]
Completeness to theta = 27.00°	99.6 %
Absorption correction	Semi-empirical from equivalents
Max. and min. transmission	0.9758 and 0.9626
Refinement method	Full-matrix least-squares on F^2
Data / restraints / parameters	3763 / 0 / 283
Goodness-of-fit on F^2	1.039
Final R indices [I>2sigma(I)]	R1 = 0.0442, wR2 = 0.1101
R indices (all data)	R1 = 0.0562, wR2 = 0.1184
Largest diff. peak and hole	0.354 and -0.156 $e.Å^{-3}$

Table 2. Atomic coordinates (x 10^4) and equivalent isotropic displacement parameters ($Å^2$x 10^3) for liu97. U(eq) is defined as one third of the trace of the orthogonalized U^{ij} tensor.

	x	y	z	U(eq)
P(1)	8229(1)	-528(1)	1460(1)	26(1)
N(1)	10549(2)	-3206(2)	1151(1)	31(1)
B(1)	9526(2)	-1790(2)	1004(1)	25(1)
C(1)	11385(2)	-4216(2)	835(1)	32(1)
C(2)	11296(2)	-3914(2)	373(1)	33(1)
C(3)	10325(2)	-2534(2)	200(1)	34(1)
C(4)	9443(2)	-1479(2)	494(1)	32(1)
C(5)	10788(4)	-3662(3)	1645(1)	47(1)
C(6)	7117(2)	1078(2)	1096(1)	28(1)
C(7)	5641(2)	586(2)	824(1)	32(1)
C(8)	4797(3)	1816(3)	560(1)	44(1)
C(9)	5342(3)	3480(3)	560(1)	50(1)
C(10)	6755(3)	3962(3)	826(1)	45(1)
C(11)	7635(3)	2777(2)	1091(1)	35(1)
C(12)	4994(3)	-1198(3)	817(1)	47(1)
C(13)	9931(2)	730(2)	1760(1)	29(1)
C(14)	9534(2)	1540(2)	2182(1)	31(1)
C(15)	10842(3)	2465(2)	2407(1)	36(1)
C(16)	12512(3)	2609(3)	2232(1)	39(1)
C(17)	12914(3)	1819(3)	1819(1)	42(1)
C(18)	11640(2)	896(2)	1587(1)	36(1)
C(19)	7719(3)	1471(4)	2383(1)	55(1)

Table 3. Bond lengths [Å] and angles [°] for liu97.

P(1)-C(13)	1.8442(18)
P(1)-C(6)	1.8491(17)
P(1)-B(1)	1.9285(18)
N(1)-C(1)	1.372(2)
N(1)-B(1)	1.425(2)
N(1)-C(5)	1.480(2)
B(1)-C(4)	1.493(2)
C(1)-C(2)	1.357(3)
C(1)-H(1)	0.93(2)
C(2)-C(3)	1.406(3)
C(2)-H(2)	0.952(19)
C(3)-C(4)	1.369(2)
C(3)-H(3)	0.98(2)
C(4)-H(4)	0.97(2)
C(5)-H(5A)	1.03(4)
C(5)-H(5B)	0.97(3)
C(5)-H(5C)	0.90(3)
C(6)-C(11)	1.399(3)
C(6)-C(7)	1.420(2)
C(7)-C(8)	1.391(3)
C(7)-C(12)	1.493(3)
C(8)-C(9)	1.379(3)
C(8)-H(8)	0.93(2)
C(9)-C(10)	1.372(3)
C(9)-H(9)	0.93(3)
C(10)-C(11)	1.380(3)
C(10)-H(10)	0.95(3)
C(11)-H(11)	0.94(2)

C(12)-H(12A)	0.98(3)
C(12)-H(12B)	0.94(3)
C(12)-H(12C)	0.95(3)
C(13)-C(18)	1.403(2)
C(13)-C(14)	1.411(2)
C(14)-C(15)	1.392(3)
C(14)-C(19)	1.503(3)
C(15)-C(16)	1.375(3)
C(15)-H(15)	1.01(2)
C(16)-C(17)	1.383(3)
C(16)-H(16)	0.94(2)
C(17)-C(18)	1.382(3)
C(17)-H(17)	0.92(2)
C(18)-H(18)	0.96(2)
C(19)-H(19A)	1.02(4)
C(19)-H(19B)	0.93(3)
C(19)-H(19C)	0.93(3)

C(13)-P(1)-C(6)	102.36(8)
C(13)-P(1)-B(1)	103.73(8)
C(6)-P(1)-B(1)	101.65(7)
C(1)-N(1)-B(1)	121.01(14)
C(1)-N(1)-C(5)	116.32(16)
B(1)-N(1)-C(5)	122.67(15)
N(1)-B(1)-C(4)	116.13(15)
N(1)-B(1)-P(1)	119.03(12)
C(4)-B(1)-P(1)	124.68(13)
C(2)-C(1)-N(1)	122.06(17)
C(2)-C(1)-H(1)	122.5(12)
N(1)-C(1)-H(1)	115.5(12)

C(1)-C(2)-C(3)	120.45(16)
C(1)-C(2)-H(2)	117.8(12)
C(3)-C(2)-H(2)	121.7(12)
C(4)-C(3)-C(2)	120.77(16)
C(4)-C(3)-H(3)	121.8(12)
C(2)-C(3)-H(3)	117.4(12)
C(3)-C(4)-B(1)	119.58(17)
C(3)-C(4)-H(4)	119.5(11)
B(1)-C(4)-H(4)	120.8(11)
N(1)-C(5)-H(5A)	108.0(19)
N(1)-C(5)-H(5B)	111.2(19)
H(5A)-C(5)-H(5B)	107(3)
N(1)-C(5)-H(5C)	112.9(17)
H(5A)-C(5)-H(5C)	101(2)
H(5B)-C(5)-H(5C)	116(2)
C(11)-C(6)-C(7)	118.63(16)
C(11)-C(6)-P(1)	122.46(14)
C(7)-C(6)-P(1)	118.87(13)
C(8)-C(7)-C(6)	118.18(18)
C(8)-C(7)-C(12)	120.06(18)
C(6)-C(7)-C(12)	121.76(17)
C(9)-C(8)-C(7)	121.9(2)
C(9)-C(8)-H(8)	123.5(13)
C(7)-C(8)-H(8)	114.5(13)
C(10)-C(9)-C(8)	119.98(19)
C(10)-C(9)-H(9)	118.8(15)
C(8)-C(9)-H(9)	121.3(15)
C(9)-C(10)-C(11)	119.8(2)
C(9)-C(10)-H(10)	120.9(15)
C(11)-C(10)-H(10)	119.3(15)

C(10)-C(11)-C(6)	121.44(19)
C(10)-C(11)-H(11)	119.5(14)
C(6)-C(11)-H(11)	119.1(14)
C(7)-C(12)-H(12A)	112.2(15)
C(7)-C(12)-H(12B)	111.5(15)
H(12A)-C(12)-H(12B)	109(2)
C(7)-C(12)-H(12C)	111.7(17)
H(12A)-C(12)-H(12C)	106(2)
H(12B)-C(12)-H(12C)	105(2)
C(18)-C(13)-C(14)	118.01(16)
C(18)-C(13)-P(1)	122.27(13)
C(14)-C(13)-P(1)	119.71(13)
C(15)-C(14)-C(13)	118.93(16)
C(15)-C(14)-C(19)	119.72(16)
C(13)-C(14)-C(19)	121.32(17)
C(16)-C(15)-C(14)	122.17(17)
C(16)-C(15)-H(15)	120.4(11)
C(14)-C(15)-H(15)	117.4(11)
C(15)-C(16)-C(17)	119.34(18)
C(15)-C(16)-H(16)	120.9(12)
C(17)-C(16)-H(16)	119.8(12)
C(18)-C(17)-C(16)	119.79(18)
C(18)-C(17)-H(17)	121.7(14)
C(16)-C(17)-H(17)	118.6(14)
C(17)-C(18)-C(13)	121.77(17)
C(17)-C(18)-H(18)	118.5(12)
C(13)-C(18)-H(18)	119.7(12)
C(14)-C(19)-H(19A)	108.9(19)
C(14)-C(19)-H(19B)	112.5(17)
H(19A)-C(19)-H(19B)	107(3)

C(14)-C(19)-H(19C)	111.7(16)
H(19A)-C(19)-H(19C)	105(3)
H(19B)-C(19)-H(19C)	111(2)

Symmetry transformations used to generate equivalent atoms:

Table 4. Anisotropic displacement parameters ($Å^2 x\ 10^3$)for liu97. The anisotropic displacement factor exponent takes the form: $-2p^2[\ h^2 a^{*2} U^{11} + ... + 2\ h\ k\ a^*\ b^*\ U^{12}\ ]$

	U^{11}	U^{22}	U^{33}	U^{23}	U^{13}	U^{12}
P(1)	29(1)	26(1)	24(1)	-1(1)	0(1)	0(1)
N(1)	36(1)	30(1)	26(1)	0(1)	-3(1)	2(1)
B(1)	26(1)	23(1)	25(1)	-1(1)	-1(1)	-2(1)
C(1)	31(1)	27(1)	38(1)	-4(1)	-1(1)	5(1)
C(2)	32(1)	34(1)	34(1)	-11(1)	2(1)	-2(1)
C(3)	39(1)	37(1)	25(1)	-3(1)	0(1)	-3(1)
C(4)	36(1)	28(1)	31(1)	2(1)	-1(1)	0(1)
C(5)	66(2)	44(1)	30(1)	4(1)	-7(1)	20(1)
C(6)	26(1)	31(1)	26(1)	-1(1)	3(1)	3(1)
C(7)	26(1)	41(1)	29(1)	-2(1)	1(1)	4(1)
C(8)	30(1)	68(2)	35(1)	4(1)	-3(1)	11(1)
C(9)	46(1)	60(2)	45(1)	22(1)	9(1)	26(1)
C(10)	48(1)	35(1)	53(1)	10(1)	9(1)	10(1)
C(11)	36(1)	31(1)	38(1)	0(1)	2(1)	2(1)
C(12)	37(1)	51(1)	53(1)	-9(1)	-7(1)	-8(1)
C(13)	32(1)	29(1)	25(1)	1(1)	-4(1)	4(1)
C(14)	35(1)	30(1)	26(1)	-2(1)	-2(1)	2(1)
C(15)	45(1)	37(1)	27(1)	-4(1)	-8(1)	4(1)
C(16)	38(1)	39(1)	38(1)	-1(1)	-16(1)	-2(1)
C(17)	29(1)	54(1)	44(1)	-3(1)	-3(1)	-1(1)
C(18)	32(1)	43(1)	32(1)	-8(1)	0(1)	1(1)
C(19)	48(1)	69(2)	48(1)	-28(1)	17(1)	-10(1)

Table 5. Hydrogen coordinates (x 10^4) and isotropic displacement parameters ($Å^2$x 10^3) for liu97.

	x	y	z	U(eq)
H(1)	12020(30)	-5110(30)	959(7)	37(5)
H(2)	11880(20)	-4680(20)	172(7)	34(5)
H(3)	10320(30)	-2350(20)	-137(8)	43(6)
H(4)	8740(30)	-570(20)	369(7)	36(5)
H(5A)	11960(50)	-3160(40)	1757(12)	108(11)
H(5B)	9870(40)	-3170(40)	1835(11)	102(10)
H(5C)	10990(30)	-4770(40)	1687(9)	75(8)
H(8)	3810(30)	1430(30)	399(7)	40(5)
H(9)	4770(30)	4290(30)	381(8)	64(7)
H(10)	7150(30)	5100(30)	826(8)	63(7)
H(11)	8630(30)	3100(30)	1262(8)	51(6)
H(12A)	5790(30)	-1950(30)	652(9)	68(7)
H(12B)	3860(30)	-1270(30)	685(8)	56(7)
H(12C)	4880(30)	-1650(30)	1122(10)	78(8)
H(15)	10510(30)	3070(30)	2702(7)	41(5)
H(16)	13380(30)	3250(30)	2389(7)	42(5)
H(17)	14030(30)	1930(30)	1704(8)	52(6)
H(18)	11950(30)	330(30)	1305(7)	37(5)
H(19A)	6890(50)	2160(50)	2179(12)	111(12)
H(19B)	7270(40)	380(40)	2394(9)	75(8)
H(19C)	7680(30)	1980(40)	2673(10)	74(8)

Table 6. Torsion angles [°] for liu97.

C(1)-N(1)-B(1)-C(4)	-0.5(2)
C(5)-N(1)-B(1)-C(4)	178.81(18)
C(1)-N(1)-B(1)-P(1)	175.05(13)
C(5)-N(1)-B(1)-P(1)	-5.6(2)
C(13)-P(1)-B(1)-N(1)	75.57(15)
C(6)-P(1)-B(1)-N(1)	-178.45(13)
C(13)-P(1)-B(1)-C(4)	-109.26(15)
C(6)-P(1)-B(1)-C(4)	-3.28(17)
B(1)-N(1)-C(1)-C(2)	0.6(3)
C(5)-N(1)-C(1)-C(2)	-178.79(19)
N(1)-C(1)-C(2)-C(3)	-0.1(3)
C(1)-C(2)-C(3)-C(4)	-0.5(3)
C(2)-C(3)-C(4)-B(1)	0.5(3)
N(1)-B(1)-C(4)-C(3)	0.0(2)
P(1)-B(1)-C(4)-C(3)	-175.32(14)
C(13)-P(1)-C(6)-C(11)	0.54(15)
B(1)-P(1)-C(6)-C(11)	-106.51(14)
C(13)-P(1)-C(6)-C(7)	-177.04(12)
B(1)-P(1)-C(6)-C(7)	75.91(14)
C(11)-C(6)-C(7)-C(8)	1.0(2)
P(1)-C(6)-C(7)-C(8)	178.71(13)
C(11)-C(6)-C(7)-C(12)	-179.15(17)
P(1)-C(6)-C(7)-C(12)	-1.5(2)
C(6)-C(7)-C(8)-C(9)	-0.7(3)
C(12)-C(7)-C(8)-C(9)	179.45(19)
C(7)-C(8)-C(9)-C(10)	0.0(3)
C(8)-C(9)-C(10)-C(11)	0.5(3)
C(9)-C(10)-C(11)-C(6)	-0.2(3)

C(7)-C(6)-C(11)-C(10)	-0.6(3)
P(1)-C(6)-C(11)-C(10)	-178.19(14)
C(6)-P(1)-C(13)-C(18)	-92.87(15)
B(1)-P(1)-C(13)-C(18)	12.57(17)
C(6)-P(1)-C(13)-C(14)	88.20(14)
B(1)-P(1)-C(13)-C(14)	-166.35(13)
C(18)-C(13)-C(14)-C(15)	0.1(2)
P(1)-C(13)-C(14)-C(15)	179.11(13)
C(18)-C(13)-C(14)-C(19)	178.0(2)
P(1)-C(13)-C(14)-C(19)	-3.0(3)
C(13)-C(14)-C(15)-C(16)	-0.3(3)
C(19)-C(14)-C(15)-C(16)	-178.2(2)
C(14)-C(15)-C(16)-C(17)	0.3(3)
C(15)-C(16)-C(17)-C(18)	0.0(3)
C(16)-C(17)-C(18)-C(13)	-0.1(3)
C(14)-C(13)-C(18)-C(17)	0.1(3)
P(1)-C(13)-C(18)-C(17)	-178.87(15)

Symmetry transformations used to generate equivalent atoms:

Crystallographic Data for Compound 11 (Liu147)

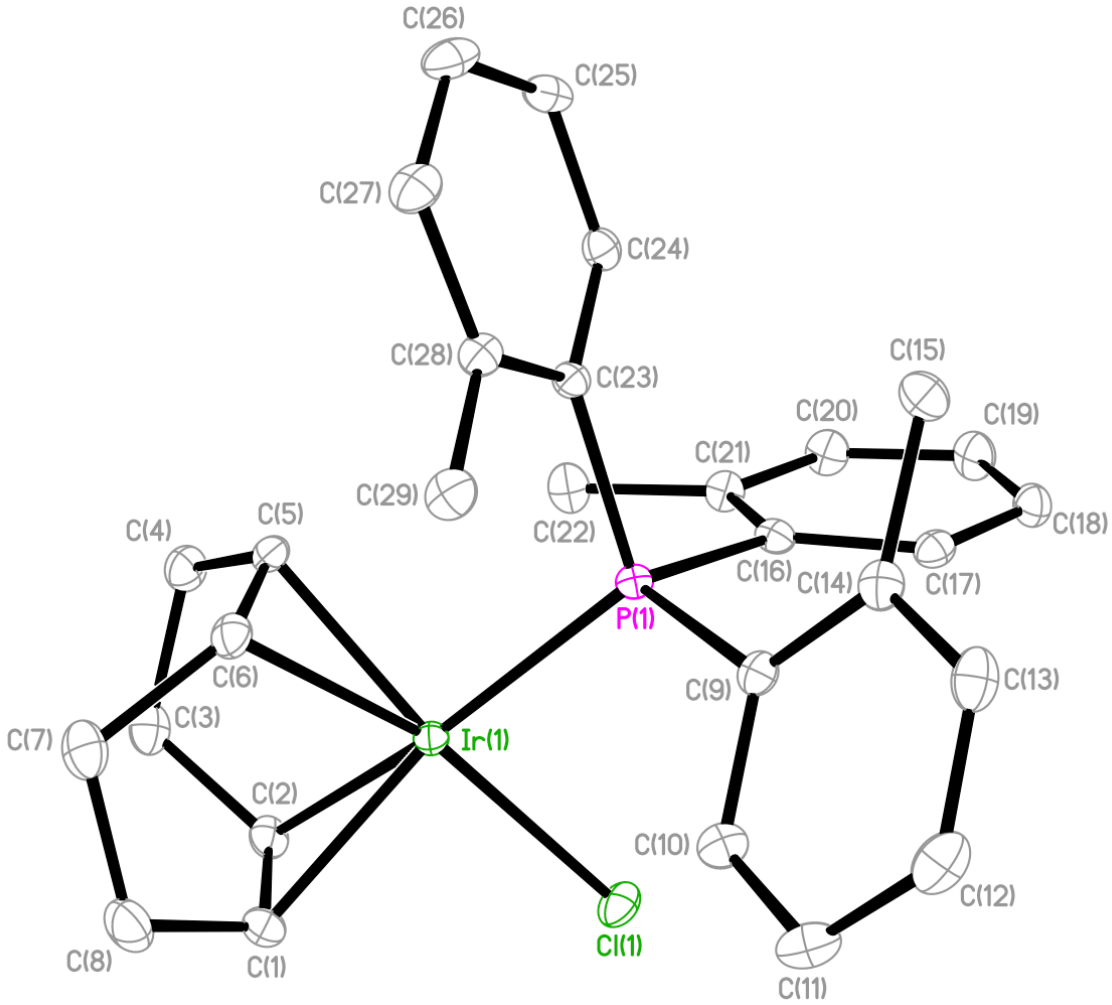

Table 1. Crystal data and structure refinement for liu147.

Identification code	liu147	
Empirical formula	C29 H33 Cl Ir P	
Formula weight	640.17	
Temperature	173(2) K	
Wavelength	0.71073 Å	
Crystal system	Monoclinic	
Space group	P2(1)/n	
Unit cell dimensions	a = 8.1953(19) Å	a= 90°.
	b = 17.467(4) Å	b= 90.693(4)°.
	c = 16.937(4) Å	g = 90°.
Volume	2424.4(10) Å^3	

Z	4
Density (calculated)	1.754 Mg/m^3
Absorption coefficient	5.699 mm^{-1}
F(000)	1264
Crystal size	0.17 x 0.12 x 0.07 mm^3
Theta range for data collection	1.67 to 27.00°.
Index ranges	-10<=h<=10, -22<=k<=22, -21<=l<=21
Reflections collected	26886
Independent reflections	5296 [R(int) = 0.0436]
Completeness to theta = 27.00°	99.9 %
Absorption correction	Semi-empirical from equivalents
Max. and min. transmission	0.6911 and 0.4442
Refinement method	Full-matrix least-squares on F^2
Data / restraints / parameters	5296 / 0 / 289
Goodness-of-fit on F^2	1.051
Final R indices [I>2sigma(I)]	R1 = 0.0220, wR2 = 0.0542
R indices (all data)	R1 = 0.0243, wR2 = 0.0555
Largest diff. peak and hole	1.226 and -0.499 $e.Å^{-3}$

Table 2. Atomic coordinates (x 10^4) and equivalent isotropic displacement parameters ($Å^2$x 10^3) for liu147. U(eq) is defined as one third of the trace of the orthogonalized U^{ij} tensor.

	x	y	z	U(eq)
Ir(1)	2971(1)	1510(1)	1641(1)	16(1)
Cl(1)	5541(1)	925(1)	1882(1)	26(1)
P(1)	4278(1)	2432(1)	869(1)	15(1)
C(1)	2082(4)	941(2)	2689(2)	27(1)
C(2)	1762(4)	465(2)	2054(2)	24(1)
C(3)	82(4)	354(2)	1681(2)	28(1)
C(4)	-186(4)	879(2)	969(2)	28(1)
C(5)	682(4)	1637(2)	1066(2)	23(1)
C(6)	693(4)	2086(2)	1761(2)	24(1)
C(7)	-223(4)	1892(2)	2507(2)	32(1)
C(8)	817(5)	1425(2)	3093(2)	34(1)
C(9)	5607(3)	3098(2)	1421(2)	19(1)
C(10)	5865(4)	2913(2)	2217(2)	23(1)
C(11)	6779(4)	3382(2)	2715(2)	27(1)
C(12)	7448(4)	4046(2)	2414(2)	29(1)
C(13)	7184(4)	4241(2)	1636(2)	27(1)
C(14)	6266(4)	3780(2)	1122(2)	23(1)
C(15)	6010(4)	4064(2)	287(2)	30(1)
C(16)	5587(3)	1999(2)	112(2)	18(1)
C(17)	7163(4)	2284(2)	1(2)	21(1)
C(18)	8132(4)	2021(2)	-606(2)	25(1)
C(19)	7563(4)	1454(2)	-1102(2)	29(1)
C(20)	6044(4)	1131(2)	-972(2)	28(1)
C(21)	5035(4)	1384(2)	-369(2)	22(1)
C(22)	3428(4)	981(2)	-260(2)	27(1)
C(23)	2902(3)	3074(2)	310(2)	16(1)
C(24)	2712(4)	2970(2)	-504(2)	20(1)
C(25)	1616(4)	3398(2)	-946(2)	24(1)
C(26)	640(4)	3929(2)	-566(2)	28(1)
C(27)	834(4)	4049(2)	237(2)	26(1)
C(28)	1982(4)	3643(2)	688(2)	19(1)

C(29)	2212(4)	3890(2)	1538(2)	24(1)

Table 3. Bond lengths [Å] and angles [°] for liu147.

Ir(1)-C(5)	2.114(3)
Ir(1)-C(6)	2.133(3)
Ir(1)-C(1)	2.169(3)
Ir(1)-C(2)	2.196(3)
Ir(1)-P(1)	2.3421(8)
Ir(1)-Cl(1)	2.3719(8)
P(1)-C(9)	1.840(3)
P(1)-C(23)	1.844(3)
P(1)-C(16)	1.845(3)
C(1)-C(2)	1.383(5)
C(1)-C(8)	1.508(5)
C(1)-H(1A)	1.0000
C(2)-C(3)	1.520(4)
C(2)-H(2A)	1.0000
C(3)-C(4)	1.529(5)
C(3)-H(3A)	0.9900
C(3)-H(3B)	0.9900
C(4)-C(5)	1.511(4)
C(4)-H(4A)	0.9900
C(4)-H(4B)	0.9900
C(5)-C(6)	1.415(5)
C(5)-H(5A)	1.0000
C(6)-C(7)	1.517(4)
C(6)-H(6A)	1.0000
C(7)-C(8)	1.535(5)
C(7)-H(7A)	0.9900
C(7)-H(7B)	0.9900
C(8)-H(8A)	0.9900
C(8)-H(8B)	0.9900
C(9)-C(10)	1.401(4)
C(9)-C(14)	1.405(4)
C(10)-C(11)	1.389(4)
C(10)-H(10A)	0.9500
C(11)-C(12)	1.383(5)

C(11)-H(11A)	0.9500
C(12)-C(13)	1.375(5)
C(12)-H(12A)	0.9500
C(13)-C(14)	1.399(4)
C(13)-H(13A)	0.9500
C(14)-C(15)	1.511(4)
C(15)-H(15A)	0.9800
C(15)-H(15B)	0.9800
C(15)-H(15C)	0.9800
C(16)-C(17)	1.399(4)
C(16)-C(21)	1.419(4)
C(17)-C(18)	1.384(4)
C(17)-H(17A)	0.9500
C(18)-C(19)	1.376(5)
C(18)-H(18A)	0.9500
C(19)-C(20)	1.387(5)
C(19)-H(19A)	0.9500
C(20)-C(21)	1.393(4)
C(20)-H(20A)	0.9500
C(21)-C(22)	1.507(4)
C(22)-H(22A)	0.9800
C(22)-H(22B)	0.9800
C(22)-H(22C)	0.9800
C(23)-C(24)	1.397(4)
C(23)-C(28)	1.406(4)
C(24)-C(25)	1.383(4)
C(24)-H(24A)	0.9500
C(25)-C(26)	1.388(5)
C(25)-H(25A)	0.9500
C(26)-C(27)	1.383(5)
C(26)-H(26A)	0.9500
C(27)-C(28)	1.398(4)
C(27)-H(27A)	0.9500
C(28)-C(29)	1.512(4)
C(29)-H(29A)	0.9800
C(29)-H(29B)	0.9800

C(29)-H(29C)	0.9800
C(5)-Ir(1)-C(6)	38.90(12)
C(5)-Ir(1)-C(1)	96.90(12)
C(6)-Ir(1)-C(1)	80.52(12)
C(5)-Ir(1)-C(2)	80.36(12)
C(6)-Ir(1)-C(2)	87.90(12)
C(1)-Ir(1)-C(2)	36.95(12)
C(5)-Ir(1)-P(1)	94.58(9)
C(6)-Ir(1)-P(1)	97.74(9)
C(1)-Ir(1)-P(1)	158.84(9)
C(2)-Ir(1)-P(1)	163.95(9)
C(5)-Ir(1)-Cl(1)	154.89(9)
C(6)-Ir(1)-Cl(1)	164.41(9)
C(1)-Ir(1)-Cl(1)	88.14(9)
C(2)-Ir(1)-Cl(1)	89.42(8)
P(1)-Ir(1)-Cl(1)	88.97(3)
C(9)-P(1)-C(23)	103.39(13)
C(9)-P(1)-C(16)	105.45(13)
C(23)-P(1)-C(16)	104.40(13)
C(9)-P(1)-Ir(1)	115.04(10)
C(23)-P(1)-Ir(1)	115.10(9)
C(16)-P(1)-Ir(1)	112.31(9)
C(2)-C(1)-C(8)	124.4(3)
C(2)-C(1)-Ir(1)	72.56(18)
C(8)-C(1)-Ir(1)	110.7(2)
C(2)-C(1)-H(1A)	113.9
C(8)-C(1)-H(1A)	113.9
Ir(1)-C(1)-H(1A)	113.9
C(1)-C(2)-C(3)	124.2(3)
C(1)-C(2)-Ir(1)	70.49(18)
C(3)-C(2)-Ir(1)	112.5(2)
C(1)-C(2)-H(2A)	114.0
C(3)-C(2)-H(2A)	114.0
Ir(1)-C(2)-H(2A)	114.0
C(2)-C(3)-C(4)	111.9(3)

C(2)-C(3)-H(3A)	109.2
C(4)-C(3)-H(3A)	109.2
C(2)-C(3)-H(3B)	109.2
C(4)-C(3)-H(3B)	109.2
H(3A)-C(3)-H(3B)	107.9
C(5)-C(4)-C(3)	112.1(3)
C(5)-C(4)-H(4A)	109.2
C(3)-C(4)-H(4A)	109.2
C(5)-C(4)-H(4B)	109.2
C(3)-C(4)-H(4B)	109.2
H(4A)-C(4)-H(4B)	107.9
C(6)-C(5)-C(4)	125.1(3)
C(6)-C(5)-Ir(1)	71.26(17)
C(4)-C(5)-Ir(1)	111.9(2)
C(6)-C(5)-H(5A)	113.7
C(4)-C(5)-H(5A)	113.7
Ir(1)-C(5)-H(5A)	113.7
C(5)-C(6)-C(7)	124.8(3)
C(5)-C(6)-Ir(1)	69.83(17)
C(7)-C(6)-Ir(1)	114.6(2)
C(5)-C(6)-H(6A)	113.4
C(7)-C(6)-H(6A)	113.4
Ir(1)-C(6)-H(6A)	113.4
C(6)-C(7)-C(8)	112.4(3)
C(6)-C(7)-H(7A)	109.1
C(8)-C(7)-H(7A)	109.1
C(6)-C(7)-H(7B)	109.1
C(8)-C(7)-H(7B)	109.1
H(7A)-C(7)-H(7B)	107.8
C(1)-C(8)-C(7)	112.6(3)
C(1)-C(8)-H(8A)	109.1
C(7)-C(8)-H(8A)	109.1
C(1)-C(8)-H(8B)	109.1
C(7)-C(8)-H(8B)	109.1
H(8A)-C(8)-H(8B)	107.8
C(10)-C(9)-C(14)	119.2(3)

C(10)-C(9)-P(1)	115.1(2)
C(14)-C(9)-P(1)	125.5(2)
C(11)-C(10)-C(9)	121.5(3)
C(11)-C(10)-H(10A)	119.2
C(9)-C(10)-H(10A)	119.2
C(12)-C(11)-C(10)	118.9(3)
C(12)-C(11)-H(11A)	120.5
C(10)-C(11)-H(11A)	120.5
C(13)-C(12)-C(11)	120.2(3)
C(13)-C(12)-H(12A)	119.9
C(11)-C(12)-H(12A)	119.9
C(12)-C(13)-C(14)	122.1(3)
C(12)-C(13)-H(13A)	119.0
C(14)-C(13)-H(13A)	119.0
C(13)-C(14)-C(9)	118.0(3)
C(13)-C(14)-C(15)	117.5(3)
C(9)-C(14)-C(15)	124.5(3)
C(14)-C(15)-H(15A)	109.5
C(14)-C(15)-H(15B)	109.5
H(15A)-C(15)-H(15B)	109.5
C(14)-C(15)-H(15C)	109.5
H(15A)-C(15)-H(15C)	109.5
H(15B)-C(15)-H(15C)	109.5
C(17)-C(16)-C(21)	118.7(3)
C(17)-C(16)-P(1)	119.6(2)
C(21)-C(16)-P(1)	121.7(2)
C(18)-C(17)-C(16)	121.3(3)
C(18)-C(17)-H(17A)	119.3
C(16)-C(17)-H(17A)	119.3
C(19)-C(18)-C(17)	119.9(3)
C(19)-C(18)-H(18A)	120.0
C(17)-C(18)-H(18A)	120.0
C(18)-C(19)-C(20)	119.6(3)
C(18)-C(19)-H(19A)	120.2
C(20)-C(19)-H(19A)	120.2
C(19)-C(20)-C(21)	122.0(3)

C(19)-C(20)-H(20A)	119.0
C(21)-C(20)-H(20A)	119.0
C(20)-C(21)-C(16)	118.2(3)
C(20)-C(21)-C(22)	118.0(3)
C(16)-C(21)-C(22)	123.8(3)
C(21)-C(22)-H(22A)	109.5
C(21)-C(22)-H(22B)	109.5
H(22A)-C(22)-H(22B)	109.5
C(21)-C(22)-H(22C)	109.5
H(22A)-C(22)-H(22C)	109.5
H(22B)-C(22)-H(22C)	109.5
C(24)-C(23)-C(28)	119.2(3)
C(24)-C(23)-P(1)	119.2(2)
C(28)-C(23)-P(1)	121.5(2)
C(25)-C(24)-C(23)	121.8(3)
C(25)-C(24)-H(24A)	119.1
C(23)-C(24)-H(24A)	119.1
C(24)-C(25)-C(26)	119.0(3)
C(24)-C(25)-H(25A)	120.5
C(26)-C(25)-H(25A)	120.5
C(27)-C(26)-C(25)	119.8(3)
C(27)-C(26)-H(26A)	120.1
C(25)-C(26)-H(26A)	120.1
C(26)-C(27)-C(28)	122.0(3)
C(26)-C(27)-H(27A)	119.0
C(28)-C(27)-H(27A)	119.0
C(27)-C(28)-C(23)	118.0(3)
C(27)-C(28)-C(29)	116.8(3)
C(23)-C(28)-C(29)	125.0(3)
C(28)-C(29)-H(29A)	109.5
C(28)-C(29)-H(29B)	109.5
H(29A)-C(29)-H(29B)	109.5
C(28)-C(29)-H(29C)	109.5
H(29A)-C(29)-H(29C)	109.5
H(29B)-C(29)-H(29C)	109.5

Symmetry transformations used to generate equivalent atoms:

Table 4. Anisotropic displacement parameters ($Å^2 x\ 10^3$)for liu147. The anisotropic displacement factor exponent takes the form: $-2p^2[\ h^2a^{*2}U^{11} + ... + 2\ h\ k\ a^*\ b^*\ U^{12}\ ]$

	U^{11}	U^{22}	U^{33}	U^{23}	U^{13}	U^{12}
Ir(1)	16(1)	15(1)	17(1)	2(1)	0(1)	1(1)
Cl(1)	19(1)	22(1)	36(1)	3(1)	-4(1)	4(1)
P(1)	16(1)	15(1)	15(1)	0(1)	-1(1)	1(1)
C(1)	26(2)	28(2)	26(2)	12(1)	1(1)	-1(1)
C(2)	24(2)	17(1)	32(2)	10(1)	4(1)	-1(1)
C(3)	26(2)	20(2)	39(2)	-2(1)	5(1)	-3(1)
C(4)	24(2)	32(2)	29(2)	-2(1)	-2(1)	-6(1)
C(5)	16(1)	28(2)	26(2)	8(1)	-4(1)	-1(1)
C(6)	19(1)	21(2)	31(2)	5(1)	2(1)	4(1)
C(7)	30(2)	31(2)	35(2)	-5(2)	10(2)	5(1)
C(8)	36(2)	42(2)	24(2)	-4(1)	7(2)	-3(2)
C(9)	17(1)	17(1)	22(2)	-2(1)	1(1)	3(1)
C(10)	26(2)	19(2)	24(2)	-1(1)	-3(1)	2(1)
C(11)	34(2)	23(2)	23(2)	-6(1)	-8(1)	9(1)
C(12)	27(2)	25(2)	34(2)	-14(1)	-6(1)	-1(1)
C(13)	23(2)	20(2)	38(2)	-6(1)	3(1)	-3(1)
C(14)	21(2)	18(2)	28(2)	-1(1)	2(1)	2(1)
C(15)	30(2)	24(2)	34(2)	10(1)	0(1)	-4(1)
C(16)	22(1)	16(1)	16(1)	1(1)	2(1)	5(1)
C(17)	21(1)	18(1)	23(2)	1(1)	-2(1)	2(1)
C(18)	20(2)	27(2)	27(2)	2(1)	4(1)	2(1)
C(19)	27(2)	33(2)	29(2)	-5(1)	8(1)	5(1)
C(20)	29(2)	27(2)	26(2)	-7(1)	2(1)	1(1)
C(21)	23(2)	20(2)	23(2)	-2(1)	1(1)	0(1)
C(22)	29(2)	27(2)	26(2)	-10(1)	4(1)	-5(1)
C(23)	17(1)	13(1)	18(1)	2(1)	0(1)	-1(1)
C(24)	20(1)	19(1)	21(2)	0(1)	2(1)	-3(1)
C(25)	31(2)	22(2)	19(2)	4(1)	-5(1)	-3(1)
C(26)	30(2)	20(2)	34(2)	4(1)	-11(1)	2(1)
C(27)	25(2)	18(2)	34(2)	-1(1)	-2(1)	4(1)
C(28)	20(1)	13(1)	24(2)	0(1)	-1(1)	0(1)

C(29)	24(2)	23(2)	24(2)	-6(1)	1(1)	5(1)

Table 5. Hydrogen coordinates (x 10^4) and isotropic displacement parameters ($Å^2$x 10^3) for liu147.

	x	y	z	U(eq)
H(1A)	2966	750	3051	32
H(2A)	2467	-2	2038	29
H(3A)	-762	461	2079	34
H(3B)	-41	-185	1512	34
H(4A)	214	620	488	34
H(4B)	-1370	973	896	34
H(5A)	728	1945	569	28
H(6A)	760	2649	1656	28
H(7A)	-1214	1596	2365	38
H(7B)	-575	2372	2765	38
H(8A)	1371	1779	3466	41
H(8B)	94	1088	3403	41
H(10A)	5405	2456	2421	28
H(11A)	6942	3249	3254	32
H(12A)	8092	4368	2745	34
H(13A)	7641	4703	1442	32
H(15A)	6586	4551	219	45
H(15B)	4841	4140	185	45
H(15C)	6436	3686	-84	45
H(17A)	7577	2666	349	25
H(18A)	9188	2232	-679	30
H(19A)	8208	1285	-1530	35
H(20A)	5680	726	-1304	33
H(22A)	3305	578	-658	41
H(22B)	2534	1350	-317	41
H(22C)	3399	752	269	41
H(24A)	3354	2594	-761	24
H(25A)	1532	3331	-1502	29
H(26A)	-160	4209	-856	34
H(27A)	168	4418	489	31

H(29A)	1428	4294	1661	36
H(29B)	3325	4083	1616	36
H(29C)	2034	3451	1887	36

Table 6. Torsion angles [°] for liu147.

C(5)-Ir(1)-P(1)-C(9)	136.03(13)
C(6)-Ir(1)-P(1)-C(9)	97.02(13)
C(1)-Ir(1)-P(1)-C(9)	13.3(3)
C(2)-Ir(1)-P(1)-C(9)	-153.2(3)
Cl(1)-Ir(1)-P(1)-C(9)	-68.86(10)
C(5)-Ir(1)-P(1)-C(23)	15.96(14)
C(6)-Ir(1)-P(1)-C(23)	-23.06(14)
C(1)-Ir(1)-P(1)-C(23)	-106.8(3)
C(2)-Ir(1)-P(1)-C(23)	86.7(3)
Cl(1)-Ir(1)-P(1)-C(23)	171.06(10)
C(5)-Ir(1)-P(1)-C(16)	-103.33(14)
C(6)-Ir(1)-P(1)-C(16)	-142.34(13)
C(1)-Ir(1)-P(1)-C(16)	133.9(3)
C(2)-Ir(1)-P(1)-C(16)	-32.5(3)
Cl(1)-Ir(1)-P(1)-C(16)	51.78(10)
C(5)-Ir(1)-C(1)-C(2)	63.8(2)
C(6)-Ir(1)-C(1)-C(2)	99.2(2)
P(1)-Ir(1)-C(1)-C(2)	-173.82(18)
Cl(1)-Ir(1)-C(1)-C(2)	-91.51(18)
C(5)-Ir(1)-C(1)-C(8)	-57.2(3)
C(6)-Ir(1)-C(1)-C(8)	-21.8(2)
C(2)-Ir(1)-C(1)-C(8)	-121.0(3)
P(1)-Ir(1)-C(1)-C(8)	65.2(4)
Cl(1)-Ir(1)-C(1)-C(8)	147.5(2)
C(8)-C(1)-C(2)-C(3)	-0.9(5)
Ir(1)-C(1)-C(2)-C(3)	-104.5(3)
C(8)-C(1)-C(2)-Ir(1)	103.6(3)
C(5)-Ir(1)-C(2)-C(1)	-115.4(2)
C(6)-Ir(1)-C(2)-C(1)	-77.0(2)
P(1)-Ir(1)-C(2)-C(1)	171.9(2)
Cl(1)-Ir(1)-C(2)-C(1)	87.67(18)
C(5)-Ir(1)-C(2)-C(3)	4.5(2)
C(6)-Ir(1)-C(2)-C(3)	42.9(2)
C(1)-Ir(1)-C(2)-C(3)	119.9(3)

P(1)-Ir(1)-C(2)-C(3)	-68.2(4)
Cl(1)-Ir(1)-C(2)-C(3)	-152.4(2)
C(1)-C(2)-C(3)-C(4)	95.1(4)
Ir(1)-C(2)-C(3)-C(4)	14.1(3)
C(2)-C(3)-C(4)-C(5)	-33.2(4)
C(3)-C(4)-C(5)-C(6)	-44.7(4)
C(3)-C(4)-C(5)-Ir(1)	37.2(3)
C(1)-Ir(1)-C(5)-C(6)	65.54(19)
C(2)-Ir(1)-C(5)-C(6)	98.70(19)
P(1)-Ir(1)-C(5)-C(6)	-96.65(17)
Cl(1)-Ir(1)-C(5)-C(6)	165.98(16)
C(6)-Ir(1)-C(5)-C(4)	-121.2(3)
C(1)-Ir(1)-C(5)-C(4)	-55.7(2)
C(2)-Ir(1)-C(5)-C(4)	-22.5(2)
P(1)-Ir(1)-C(5)-C(4)	142.1(2)
Cl(1)-Ir(1)-C(5)-C(4)	44.8(4)
C(4)-C(5)-C(6)-C(7)	-2.5(5)
Ir(1)-C(5)-C(6)-C(7)	-106.5(3)
C(4)-C(5)-C(6)-Ir(1)	104.0(3)
C(1)-Ir(1)-C(6)-C(5)	-113.6(2)
C(2)-Ir(1)-C(6)-C(5)	-77.21(19)
P(1)-Ir(1)-C(6)-C(5)	87.70(17)
Cl(1)-Ir(1)-C(6)-C(5)	-157.5(3)
C(5)-Ir(1)-C(6)-C(7)	120.0(3)
C(1)-Ir(1)-C(6)-C(7)	6.4(2)
C(2)-Ir(1)-C(6)-C(7)	42.8(2)
P(1)-Ir(1)-C(6)-C(7)	-152.3(2)
Cl(1)-Ir(1)-C(6)-C(7)	-37.5(5)
C(5)-C(6)-C(7)-C(8)	91.7(4)
Ir(1)-C(6)-C(7)-C(8)	10.0(4)
C(2)-C(1)-C(8)-C(7)	-49.0(4)
Ir(1)-C(1)-C(8)-C(7)	33.6(4)
C(6)-C(7)-C(8)-C(1)	-28.7(4)
C(23)-P(1)-C(9)-C(10)	134.9(2)
C(16)-P(1)-C(9)-C(10)	-115.8(2)
Ir(1)-P(1)-C(9)-C(10)	8.5(2)

C(23)-P(1)-C(9)-C(14)	-40.8(3)
C(16)-P(1)-C(9)-C(14)	68.6(3)
Ir(1)-P(1)-C(9)-C(14)	-167.1(2)
C(14)-C(9)-C(10)-C(11)	-1.0(4)
P(1)-C(9)-C(10)-C(11)	-177.0(2)
C(9)-C(10)-C(11)-C(12)	-0.1(5)
C(10)-C(11)-C(12)-C(13)	1.1(5)
C(11)-C(12)-C(13)-C(14)	-0.9(5)
C(12)-C(13)-C(14)-C(9)	-0.2(5)
C(12)-C(13)-C(14)-C(15)	178.1(3)
C(10)-C(9)-C(14)-C(13)	1.2(4)
P(1)-C(9)-C(14)-C(13)	176.6(2)
C(10)-C(9)-C(14)-C(15)	-177.0(3)
P(1)-C(9)-C(14)-C(15)	-1.5(4)
C(9)-P(1)-C(16)-C(17)	-8.2(3)
C(23)-P(1)-C(16)-C(17)	100.4(2)
Ir(1)-P(1)-C(16)-C(17)	-134.2(2)
C(9)-P(1)-C(16)-C(21)	172.2(2)
C(23)-P(1)-C(16)-C(21)	-79.2(3)
Ir(1)-P(1)-C(16)-C(21)	46.2(3)
C(21)-C(16)-C(17)-C(18)	5.3(4)
P(1)-C(16)-C(17)-C(18)	-174.3(2)
C(16)-C(17)-C(18)-C(19)	-1.7(5)
C(17)-C(18)-C(19)-C(20)	-2.3(5)
C(18)-C(19)-C(20)-C(21)	2.6(5)
C(19)-C(20)-C(21)-C(16)	1.1(5)
C(19)-C(20)-C(21)-C(22)	-178.1(3)
C(17)-C(16)-C(21)-C(20)	-4.9(4)
P(1)-C(16)-C(21)-C(20)	174.7(2)
C(17)-C(16)-C(21)-C(22)	174.2(3)
P(1)-C(16)-C(21)-C(22)	-6.1(4)
C(9)-P(1)-C(23)-C(24)	128.5(2)
C(16)-P(1)-C(23)-C(24)	18.4(3)
Ir(1)-P(1)-C(23)-C(24)	-105.2(2)
C(9)-P(1)-C(23)-C(28)	-54.5(3)
C(16)-P(1)-C(23)-C(28)	-164.6(2)

Ir(1)-P(1)-C(23)-C(28)	71.8(2)
C(28)-C(23)-C(24)-C(25)	-1.6(4)
P(1)-C(23)-C(24)-C(25)	175.5(2)
C(23)-C(24)-C(25)-C(26)	-2.2(4)
C(24)-C(25)-C(26)-C(27)	3.3(5)
C(25)-C(26)-C(27)-C(28)	-0.8(5)
C(26)-C(27)-C(28)-C(23)	-2.9(5)
C(26)-C(27)-C(28)-C(29)	173.1(3)
C(24)-C(23)-C(28)-C(27)	4.0(4)
P(1)-C(23)-C(28)-C(27)	-173.0(2)
C(24)-C(23)-C(28)-C(29)	-171.7(3)
P(1)-C(23)-C(28)-C(29)	11.3(4)

Symmetry transformations used to generate equivalent atoms:

REFERENCES CITED

Chapter I

(1) W. N. Lipscomb, *Angew. Chem.* **1977**, *89*, 685–696.

(2) H. C. Brown, *Angew. Chem.* **1980**, *92*, 675–683.

(3) A. Suzuki, *Angew. Chem. Int. Ed.* **2011**, *50*, 6722–6737.

(4) E. R. Burkhardt, K. Matos, *Chem. Rev.* **2006**, *106*, 2617–2650.

(5) N. Miyaura, A. Suzuki, *Chem. Rev.* **1995**, *95*, 2457–2483.

(6) M. Suginome, *J. Synth. Org. Chem., Jpn.* **2007**, *65*, 1048–1059.

(7) M. Yamashita, *Angew. Chem. Int. Ed.* **2010**, *49*, 2474–2475.

(8) S. J. Baker, J. W. Tomsho, S. J. Benkovic, *Chem. Soc. Rev.* **2011**, *40*, 4279–4285.

(9) Z. M. Hudson, S. Wang, *Dalton Trans.* **2011**, *40*, 7805–7816.

(10) R. H. Pritchard, C. W. Kern, *J. Am. Chem. Soc.* **1969**, *91*, 1631–1635.

(11) S. J. Blanksby, G. B. Ellison, *Acc. Chem. Res.* **2003**, *36*, 255–263.

(12) L. R. Thorne, R. D. Suenram, F. J. Lovas, *J. Chem. Phys.* **1983**, *78*, 167.

(13) D. J. Grant, D. A. Dixon, *J. Phys. Chem. A* **2006**, *110*, 12955–12962.

(14) I. Alkorta, J. Elguero, *Struct. Chem.* **1998**, *9*, 59–63.

(15) M. Sugie, H. Takeo, C. Matsumura, *Chem. Phys. Lett.* **1979**, *64*, 573–575.

(16) I. G. Green, K. M. Johnson, B. P. Roberts, *J. Chem. Soc., Perkin Trans. 2* **1989**, 1963–1972.

(17) A. Stock, E. Pohland, *Ber. Dtsch. Chem. Ges.* **1926**, *59*, 2210−2215.

(18) (a) E. Wiberg, A. Bolz, *Ber. Dtsch. Chem. Ges.* **1940**, *73*, 209-232. (b) E. Wiberg, K. Hertwig, A. Bolz, *Z. Anorg. Allg. Chem.* **1948**, *256*,177-252. (c) E. Wiberg, K. Hertwig, *Z. Anorg. Allg. Chem.* **1948**, *257*,138-144.

(19) J.-S. Li, C.-R. Zhang, Bin Li, F. Cao, S.-Q. Wang, *Inorg. Chim. Acta* **2011**, *366*, 173–176.

(20) A. S. Lisovenko, A. Y. Timoshkin, *Inorg. Chem.* **2010**, *49*, 10357–10369.

(21) H. Braunschweig, H. Green, K. Radacki, K. Uttinger, *Dalton Trans.* **2008**, 3531–3534.

(22) M. K. Kesharwani, M. Suresh, A. Das, B. Ganguly, *Tetrahderon. Lett.* **2011**, *52*, 3636–3639.

(23) Y. Yamamoto, K. Miyamoto, J. Umeda, Y. Nakatani, T. Yamamoto, N. Miyaura, *J. Organomet. Chem.* **2006**, *691*, 4909–4917.

(24) R. Islas, E. Chamorro, J. Robles, T. Heine, J. C. Santos, G. Merino, *Struct. Chem.* **2007**, *18*, 833–839.

(25) D. E. Bean, P. W. Fowler, *J. Phys. Chem. A* **2011**, *115*, 13649–13656.

(26) A. Soncini, C. Domene, J. J. Engelberts, P. W. Fowler, A. Rassat, J. H. van Lenthe, R. W. A. Havenith, L. W. Jenneskens, *Chem. –Eur. J.* **2005**, *11*, 1257–1266.

(27) A. K. Phukan, A. K. Guha, B. Silvi, *Dalton Trans.* **2010**, *39*, 4126–4137.

(28) M. J. D. Bosdet, W. E. Piers, *Can. J. Chem.* **2009**, *87*, 8–29.

(28) G. Ulrich, R. Ziessel, A. Harriman, *Angew. Chem. Int. Ed.* **2008**, *47*, 1184–1201.

(30) C. G. Claessens, D. González-Rodríguez, T. Torres, *Chem. Rev.* **2002**, *102*, 835–853.

(31) M. J. S. Dewar, V. P. Kubba, R. Pettit, *J. Chem. Soc.* **1958**, 3073–3076.

(32) M. J. S. Dewar, *Tetrahedron* **1959**, *7*, 213–222.

(33) M. J. S. Dewar, V. P. Kubba, *J. Org. Chem.* **1960**, *25*, 1722–1724.

(34) M. J. S. Dewar, V. P. Kubba, *J. Am. Chem. Soc.* **1961**, *83*, 1757–1760.

(35) M. J. S. Dewar, P. M. Maitlis, *J. Am. Chem. Soc.* **1961**, *83*, 187–193.

(36) M. J. S. Dewar, *Tetrahedron* **1961**, *15*, 35–45.

(37) M. J. S. Dewar, R. Dietz, *J. Chem. Soc.* **1959**, 2728.

(38) M. J. S. Dewar, R. Dietz, V. P. Kubba, A. R. Lepley, *J. Am. Chem. Soc.* **1961**, *83*, 1754–1756.

(39) M. J. S. Dewar, *Tetrahedron* **1961**, *15*, 26–34.

(40) M. J. S. Dewar, R. Dietz, *J. Org. Chem.* **1961**, *26*, 3253–3256.

(41) M. J. S. Dewar, J. Hashmall, V. P. Kubba, *J. Org. Chem.* **1964**, *29*, 1755–1757.

(42) M. J. S. Dewar, G. J. Gleicher, B. P. Robinson, *J. Am. Chem. Soc.* **1964**, *86*, 5698–5699.

(43) M. J. S. Dewar, R. Jones, *Tet. Lett.* **1968**, *22*, 2707−2708.

(44) M. J. S. Dewar, P. A. Marr, *J. Am. Chem. Soc.* **1962**, *84*, 3782.

(45) D. G. White, *J. Am. Chem. Soc.* **1963**, *85*, 3634–3636.

(46) K. M. Davies, M. J. S. Dewar, P. Rona, *J. Am. Chem. Soc.* **1967**, *89*, 6294–6297.

(47) M. Ferles, Z. Polivka, *Collect. Czech. Chem. Commun.* **1968**, *33*, 2121−2129.

(48) Z. Polivka, V. Kubelka, N. Holubova, M. Ferles, *Collect. Czech. Chem. Commun.* **1970**, *35*, 1131−1146.

(49) H. Wille, J. Goubeau, *Chem. Ber.* **1972**, *105*, 2156−2168.

(50) H. Wille, J. Goubeau, *Chem. Ber.* **1974**, *107*, 110−116.

(51) S. Gronowitz, I. Ander, *Chemica Scripta* **1980**, *15*, 23–26.

(52) S. Gronowitz, I. Ander, *Chemica Scripta* **1980**, *15*, 135–144.

(53) S. Gronowitz, I. Ander, *Chemica Scripta* **1980**, *15*, 145–151.

(54) A. J. Ashe, Fang, *Org. Lett.* **2000**, *2*, 2089–2091.

(55) A. J. Ashe, X. Fang, X. Fang, J. Kampf, *Organometallics* **2001**, *20*, 5413–5418.

(56) J. Pan, J. W. Kampf, A. J. Ashe, *Organometallics* **2004**, *23*, 5626–5629.

(57) J. Pan, J. W. Kampf, A. J. Ashe, *Organometallics* **2008**, *27*, 1345–1347.

(58) X. Fang, H. Yang, J. Kampf, M. Holl, A. J. Ashe, *Organometallics* **2006**, *25*, 513–518.

(59) J. Pan, J. W. Kampf, A. J. Ashe, *Org. Lett.* **2007**, *9*, 679–681.

(60) J. Pan, J. W. Kampf, A. J. Ashe, *Organometallics* **2009**, *28*, 506–511.

(61) J. Pan, J. W. Kampf, A. J. Ashe, *J. Organomet. Chem.* **2009**, *694*, 1036–1040.

(62) A. J. V. Marwitz, E. R. Abbey, J. T. Jenkins, L. N. Zakharov, S.-Y. Liu, *Org. Lett.* **2007**, *9*, 4905–4908.

(63) C. Zúñiga, L. Garduño, M. A. del Carmen Cruz, M. A. Salazar, R. Pérez-Pastén, G. N. Chamorro, F. Labarrios, J. N. Tamariz, *Drug Dev. Res.* **2005**, *64*, 28–40.

(64) A. N. Lamm, S.-Y. Liu, *Mol. Biosyst.* **2009**, *5*, 1303–1305.

(65) A. J. V. Marwitz, S. P. McClintock, L. N. Zakharov, S.-Y. Liu, *Chem. Commun.* **2010**, *46*, 779–781.

(66) A. J. V. Marwitz, J. T. Jenkins, L. N. Zakharov, S.-Y. Liu, *Angew. Chem. Int. Ed.* **2010**, *49*, 7444–7447.

(67) A. J. V. Marwitz, J. T. Jenkins, L. N. Zakharov, S.-Y. Liu, *Organometallics* **2011**, *30*, 52–54.

(68) A. J. V. Marwitz, M. H. Matus, L. N. Zakharov, D. A. Dixon, S.-Y. Liu, *Angew. Chem. Int. Ed.* **2009**, *48*, 973–977.

(69) C. Tanjaroon, A. Daly, A. J. V. Marwitz, S.-Y. Liu, S. Kukolich, *J. Chem. Phys.* **2009**, *131*, 224312.

(70) E. R. Abbey, L. N. Zakharov, S.-Y. Liu, *J. Am. Chem. Soc.* **2008**, *130*, 7250–7252.

(71) P. G. Campbell, E. R. Abbey, D. Neiner, D. J. Grant, D. A. Dixon, S.-Y. Liu, *J. Am. Chem. Soc.* **2010**, *132*, 18048–18050.

(72) A. N. Lamm, E. B. Garner, D. A. Dixon, S.-Y. Liu, *Angew. Chem. Int. Ed.* **2011**, *50*, 8157–8160.

(73) L. Liu, A. J. V. Marwitz, B. W. Matthews, S.-Y. Liu, *Angew. Chem. Int. Ed.* **2009**, *48*, 6817–6819.

(74) D. Ulmschneider, J. Goubeau, *Chem. Ber.* **1957**, *90*, 2733–2738.

(75) E. R. Abbey, L. N. Zakharov, S.-Y. Liu, *J. Am. Chem. Soc.* **2010**, *132*, 16340–16342.

(76) E. R. Abbey, L. N. Zakharov, S.-Y. Liu, *J. Am. Chem. Soc.* **2011**, *133*, 11508–11511.

(77) P. G. Campbell, L. N. Zakharov, D. J. Grant, D. A. Dixon, S.-Y. Liu, *J. Am. Chem. Soc.* **2010**, *132*, 3289–3291.

(78) W. Luo, L. N. Zakharov, S.-Y. Liu, *J. Am. Chem. Soc.* **2011**, *133*, 13006–13009.

(79) W. Luo, P. G. Campbell, L. N. Zakharov, S.-Y. Liu, *J. Am. Chem. Soc.* **2011**, *133*, 19326–19329.

(80) A. J. V. Marwitz, A. N. Lamm, L. N. Zakharov, M. Vasiliu, D. A. Dixon, S.-Y. Liu, *Chem. Sci.* **2012**, DOI 10.1039/c1sc00500f.

(81) S. Xu, L. N. Zakharov, S.-Y. Liu, *J. Am. Chem. Soc.* **2011**, *133*, 20152–20155.

(82) M. Lepeltier, O. Lukoyanova, A. Jacobson, S. Jeeva, D. F. Perepichka, *Chem. Commun.* **2010**, *46*, 7007–7009.

(83) A. Wakamiya, K. Mori, S. Yamaguchi, *Angew. Chem. Int. Ed.* **2007**, *46*, 4273–4276.

(84) O. Lukoyanova, M. Lepeltier, M. Laferrière, D. F. Perepichka, *Macromolecules* **2011**, *44*, 4729–4734.

(85) T. Taniguchi, S. Yamaguchi, *Organometallics* **2010**, *29*, 5732–5735.

(86) T. Agou, J. Kobayashi, T. Kawashima, *Org. Lett.* **2006**, *8*, 2241–2244.

(87) T. Agou, J. Kobayashi, T. Kawashima, *Chem. Commun.* **2007**, 3204–3206.

(88) T. Agou, M. Sekine, J. Kobayashi, T. Kawashima, *Chem. –Eur. J.* **2009**, *15*, 5056–5062.

(89) T. Agou, M. Sekine, J. Kobayashi, T. Kawashima, *Chem. Commun.* **2009**, 1894–1896.

(90) T. Agou, M. Sekine, J. Kobayashi, T. Kawashima, *J. Organomet. Chem.* **2009**, *694*, 3833–3836.

(91) T. Agou, T. Kojima, J. Kobayashi, T. Kawashima, *Org. Lett.* **2009**, *11*, 3534–3537.

(92) T. Agou, H. Arai, T. Kawashima, *Chem. Lett.* **2010**, *39*, 612–613.

(93) T. Hatakeyama, S. Hashimoto, S. Seki, M. Nakamura, *J. Am. Chem. Soc.* **2011**, *133*, 18614–18617.

Chapter II

(1) Eberle, U.; Felderhoff, M.; Schüth, F. *Angew. Chem., Int. Ed.* **2009**, *48*, 6608.

(2) Graetz, J. *Chem. Soc. Rev.* **2009**, *38*, 73.

(3) Zhao, D.; Yuan, D.; Zhou, H.-C. *Energy Environ. Sci.* **2008**, *1*, 222.

(4) Stephens, F. H.; Pons, V.; Baker, R. T. *Dalton Trans.* **2007**, 2613.

(5) Hamilton, C. W.; Baker, R. T.; Staubitz, A.; Manners, I. *Chem. Soc. Rev.* **2009**, *38*, 279.

(6) Marder, T. B. *Angew. Chem., Int. Ed.* **2007**, *46*, 8116.

(7) Jaska, C.; Temple, K.; Lough, A. J.; Manners, I. *Chem. Commun.* **2001**, 962.

(8) (a) Gutowska, A.; Li, L.; Shin, Y.; Wang, C. M.; Li, X. S.; Linehan, J. C.; Smith, R. S.; Kay, B. D.; Schmid, B.; Shaw, W.; Gutowski, M.; Autrey, T. *Angew. Chem., Int. Ed.* **2005**, *44*, 3578. (b) Stephens, F. H.; Baker, R. T.; Matus, M. H.; Grant, D. J.; Dixon, D. A. *Angew. Chem., Int. Ed.* **2006**, *46*, 746.

(9) Bluhm, M. E.; Bradley, M. G.; Butterick, R.; Kusari, U.; Sneddon, L. G. *J. Am. Chem. Soc.* **2006**, *128*, 7748.

(10) Denney, M. C.; Pons, V.; Hebden, T. J.; Heinekey, D. M.; Goldberg, K. I. *J. Am. Chem. Soc.* **2006**, *128*, 12048.

(11) Keaton, R. J.; Blacquiere, J. M.; Baker, R. T. *J. Am. Chem. Soc.* **2007**, *129*, 1844.

(12) Yan, J. M.; Zhang, X. B.; Han, S.; Shioyama, H.; Xu, Q. *Angew. Chem.,*

Int. Ed. **2008**, *47*, 2287.

(13) Blaquiere, N.; Diallo-Garcia, S.; Gorelsky, S. I.; Black, D. A.; Fagnou, K. *J. Am. Chem. Soc.* **2008**, *130*, 14034.

(14) Käss, M.; Friedrich, A.; Drees, M.; Schneider, S. *Angew. Chem., Int. Ed.* **2009**, *48*, 905.

(15) Himmelberger, D. W.; Yoon, C. W.; Bluhm, M. E.; Carroll, P. J.; Sneddon, L. G. *J. Am. Chem. Soc.* **2009**, *131*, 14101.

(16) Ramachandran, P. V.; Gagare, P. D. *Inorg. Chem.* **2007**, *46*, 7810.

(17) Hausdorf, S.; Baitalow, F.; Wolf, G.; Mertens, F. O. R. L. *Int. J. Hydrogen Energy* **2008**, *33*, 608.

(18) (a) Davis, B. L.; Dixon, D. A.; Garner, E. B.; Gordon, J. C.; Matus, M. H.; Scott, B.; Stephens, F. H. *Angew. Chem., Int. Ed.* **2009**, *48*, 6812. (b) Sutton, A. D.; Davis, B. L.; Bhattacharyya, K. X.; Ellis, B. D.; Gordon, J. C.; Power, P. P. *Chem. Commun.* **2010**, *46*, 148.

(19) (a) Dixon, D. A.; Gutowski, M. *J. Phys. Chem. A* **2005**, *109*, 5129. (b) Matus, M. H.; Grant, D. J.; Nguyen, M. T.; Dixon, D. A. *J. Phys. Chem. C* **2009**, *113*, 16553. (c) Wechsler, D.; Cui, Y.; Dean, D.; Davis, B.; Jessop, P. G. *J. Am. Chem. Soc.* **2008**, *130*, 17195.

(20) Matus, M. H.; Liu, S.-Y.; Dixon, D. A. *J. Phys. Chem. A* [Online early access]. DOI: 10.1021/jp9102838. Published Online: Jan 29, 2010.

(21) Bosdet, M. J. D.; Piers, W. E. *Can. J. Chem.* **2009**, *87*, 8.

(22) Ashe, A. J.; Fang, X. *Org. Lett.* **2000**, *2*, 2089.

(23) Ashe, A. J., III.; Fang, X.; Fang, X.; Kampf, J. W. *Organometallics* **2001**, *20*, 5413.

(24) Ashe, A. J., III. *Organometallics* **2009**, *28*, 4236.

(25) Marwitz, A. J.; Abbey, E. R.; Jenkins, J. T.; Zakharov, L. N.; Liu, S.-Y. *Org. Lett.* **2007**, *9*, 4905.

(26) Abbey, E. R.; Zakharov, L. N.; Liu, S.-Y. *J. Am. Chem. Soc.* **2008**, *130*, 7250.

(27) Marwitz, A. J.; Matus, M. H.; Zakharov, L. N.; Dixon, D. A.; Liu, S.-Y. *Angew. Chem., Int. Ed.* **2009**, *48*, 973.

(28) Liu, L.; Marwitz, A. J.; Matthews, B. W.; Liu, S.-Y. *Angew. Chem., Int. Ed.* **2009**, *48*, 6817.

(29) Lamm, A. N.; Liu, S.-Y. *Mol. Biosyst.* **2009**, *5*, 1303.

(30) Tanjaroon, C.; Daly, A.; Marwitz, A. J. V.; Liu, S.-Y.; Kukolich, S. *J. Chem. Phys.* **2009**, *131*, 224312.

(31) Marwitz, A. J. V.; McClintock, S. P.; Zakharov, L. N.; Liu, S.-Y. *Chem. Commun.* **2010**, *46*, 779.

(32) Deshmukh, R. R.; Lee, J. W.; Shin, U. S.; Lee, J. Y.; Song, C. E. *Angew. Chem., Int. Ed.* **2008**, *47*, 8615.

(33) Scheideman, M.; Wang, G.; Vedejs, E. *J. Am. Chem. Soc.* **2008**, *130*, 8669.

(34) Roessler, R.; Piers, W. E.; Parvez, M. *J. Organomet. Chem.* **2003**, *680*, 218.

(35) (a) Ostby, K.-A.; Gundersen, G.; Haaland, A.; Nöth, H. *Dalton Trans.* **2005**, 2284. (b) Ostby, K.-A.; Haaland, A.; Gundersen, G.; Nöth, H. *Organometallics* **2005**, *24*, 5318. (c) Grant, D. J.; Dixon, D. A. *J. Phys. Chem. A* **2006**, *110*, 12955.

(36) (a) Bu¨hl, M.; Steinke, T.; Schleyer, P. v. R.; Boese, R. *Angew. Chem., Int. Ed.* **1991**, *30*, 1160. (b) Aldrige, S.; Downs, A. J.; Tang, C. Y.; Parsons, S.; Clarke, M. C.; Johnstone, R. D. L.; Robertson, H. R.; Rankin, D. W. H.; Wann, D. A. *J. Am. Chem. Soc.* **2009**, *131*, 2231.

(37) Mock, M. T.; Potter, R. G.; Camaioni, D. M.; Li, J.; Dougherty, W. G.; Kassel, W. S.; Twamley, B.; DuBois, D. L. *J. Am. Chem. Soc.* **2009**, *131*, 14454.

Chapter III

(1) Faraday, M. *Philos. Trans. R. Soc. London* **1825**, *115*, 440–466.

(2) Schleyer, P. v. R. *Chem. Rev.* **2001**, *101*, 1115–1118.

(3) Stanger, A. *Chem. Commun.* **2009**, 1939–1947.

(4) Slayden, S. W.; Liebman, J. F. *Chem. Rev.* **2001**, *101*, 1541–1566.

(5) Cyranski, M. K. *Chem. Rev.* **2005**, *105*, 3773–3811.

(6) Krygowski, T. M.; Cyranski, M. K. *Chem. Rev.* **2001**, *101*, 1385–1419.

(7) Chen, Z.; Wannere, C. S.; Corminboeuf, C.; Puchta, R.; Schleyer, P. v. R. *Chem. Rev.* **2005**, *105*, 3842–3888.

(8) Mitchell, R. H. *Chem. Rev.* **2001**, *101*, 1301–1315.

(9) Gomes, J. A.; Mallion, R. B. *Chem. Rev.* **2001**, *101*, 1349–1383.

(10) Katritzky, A. R.; Jug, K.; Oniciu, D. C. *Chem. Rev.* **2001**, *101*, 1421–1449.

(11) For caveats regarding the use of using energetic criteria to assess aromaticity, see refs. 3 and 7.

(12) Kistiakowsky, G. B.; Ruhoff, J. R.; Smith, H. A.; Vaughan, W. E. *J. Am. Chem. Soc.* **1936**, *58*, 146–153.

(13) (a) Bosdet, M. J. D.; Piers, W. E. *Can. J. Chem.* **2009**, *87*, 8–29. (b) Liu, Z.; Marder, T. B. *Angew. Chem., Int. Ed.* **2008**, *47*, 242–244.

(14) Marwitz, A. J. V.; Abbey, E. R.; Jenkins, J. T.; Zakharov, L. N.; Liu, S.- Y. *Org. Lett.* **2007**, *9*, 4905–4908.

(15) Marwitz, A. J. V.; Matus, M. H.; Zakharov, L. N.; Dixon, D. A.; Liu, S.-Y. *Angew. Chem., Int. Ed.* **2009**, *48*, 973–977.

(16) Marwitz, A. J. V.; McClintock, S. P.; Zakharov, L. N.; Liu, S.-Y. *Chem. Commun.* **2010**, *46*, 779–781.

(17) Daly, A. M.; Tanjaroon, C.; Marwitz, A. J. V.; Liu, S.-Y.; Kukolich, S. G. *J. Am. Chem. Soc.* **2010**, *132*, 5501–5506.

(18) Matus, M.; Liu, S.-Y.; Dixon, D. A. *J. Phys. Chem. A* **2010**, *114*, 2644– 2654.

(19) Tanjaroon, C.; Daly, A. M.; Marwitz, A. J. V.; Liu, S.-Y.; Kukolich, S. G. *J. Chem. Phys.* **2009**, *131*, 224312.

(20) Lamm, A. N.; Liu, S.-Y. *Mol. Biosyst.* **2009**, *5*, 1303–1305.

(21) Liu, L.; Marwitz, A. J. V.; Mathews, B. W.; Liu, S.-Y. *Angew. Chem., Int. Ed.* **2009**, *48*, 6817–6819.

(22) (a) Marwitz, A. J. V.; Jenkins, J. T.; Zakharov, L. N.; Liu, S.-Y. *Angew. Chem., Int. Ed.* **2010**, *49*, 7444–7447. (b) Campbell, P. G.; Zakharov, L. N.; Grant, D. J.; Dixon, D. A.; Liu, S.-Y. *J. Am. Chem. Soc.* **2010**, *132*, 3289– 3291.

(23) Taniguchi, T.; Yamaguchi, S. *Organometallics* **2010**, *29*, 5732–5735.

(24) (a) Abbey, E. R.; Zakharov, L. N.; Liu, S.-Y. *J. Am. Chem. Soc.* **2008**, *130*, 7250–7252. (b) Pan, J.; Kampf, J. W.; Ashe, A. J., III. *Org. Lett.* **2007**, *9*, 679–681.

(25) (a) Kranz, M.; Clark, T. *J. Org. Chem.* **1992**, *57*, 5492–5500. (b) Del Bene, J. E.; Ya´n˜ez, M.; Alkorta, I.; Elguero, J. *J. Chem. Theory Comput.* **2009**, *5*, 2239–2247. (c) Silva, P. J.; Ramos, M. J. *J. Org. Chem.* **2009**, *74*, 6120–6129. (d) Reference 15.

(26) Pedley, J. B. *Thermochemical Data and Structures of Organic Compounds*, Vol. 1; TRC Data Series; Thermodynamics Research Center: College Station, TX, 1994.

(27) Muetterties, E. L.; Hirsekorn, F. J. *J. Am. Chem. Soc.* **1974**, *96*, 7920– 7926.

(28) (a) Young, J. F.; Osborn, J. A.; Jardine, F. H.; Wilkinson, G. *Chem. Commun.* **1965**, 131–132. (b) Osborn, J. A.; Jardine, F. H.; Young, J. F.; Wilkinson, G. *J. Chem. Soc. A* **1966**, 1711–1732.

(29) Crabtree, R. H. *Acc. Chem. Res.* **1979**, *12*, 331–338.

(30) Evans, D.; Osborn, J. A.; Jardine, F. H.; Wilkinson, G. *Nature* **1965**, *208*, 1203–1204.

(31) Joseph, T.; Deshpande, S. S.; Haligudi, S. B.; Vinu, A.; Ernst, S.; Hartmann, M. *J. Mol. Catal. A: Chem.* **2003**, *206*, 13–21.

(32) See the Experimental Section for details.

(33) (a) Ferretti, A. C.; Mathew, J. S.; Blackmond, D. G. *Ind. Eng. Chem. Res.* **2007**, *46*, 8584–8589. (b) Blackmond, D. G. *Angew. Chem., Int. Ed.* **2005**, *44*, 4302–4320.

(34) Curtiss, L. A.; Redfern, P. C.; Raghavachari, K.; Rassolov, V.; Pople, J. A. *J. Chem. Phys.* **1999**, *110*, 4703–4709.

(35) Frisch, M. J.; et al. *Gaussian 09*, revision B.01; Gaussian, Inc.

Chapter IV

(1) Sartbaeva, A.; Kuznetsov, V. L.; Wells, S. A.; Edwards, P. P. *Energy Environ. Sci.* **2008**, *1*, 79–85.

(2) Turner, J. A. *Science* **2004**, *305*, 972–974.

(3) US Department of Energy: Hydrogen Posture Plan, http://www.hydrogen.energy.gov/.

(4) Hamilton, C. W.; Baker, R. T.; Staubitz, A.; Manners, I. *Chem. Soc. Rev.* **2009**, *38*, 279.

(5) Marder, T. B. *Angew. Chem. Int. Ed.* **2007**, *46*, 8116–8118.

(6) Staubitz, A.; Robertson, A. P. M.; Manners, I. *Chem. Rev.* **2010**, *110*, 4079–4124.

(7) Bowden, M.; Autrey, T. *Curr. Opin. Solid State Mater Sci.* **2011**, *15*, 73–79.

(8) Sutton, A. D.; Burrell, A. K.; Dixon, D. A.; Garner, E. B.; Gordon, J. C.; Nakagawa, T.; Ott, K. C.; Robinson, J. P.; Vasiliu, M. *Science* **2011**, *331*, 1426–1429.

(9) Davis, B. L.; Dixon, D. A.; Garner, E. B.; Gordon, J. C.; Matus, M. H.; Scott, B.; Stephens, F. H. *Angew. Chem. Int. Ed.* **2009**, *48*, 6812–6816.

(10) Shaw, W. J.; Linehan, J. C.; Szymczak, N. K.; Heldebrant, D. J.; Yonker, C.; Camaioni, D. M.; Baker, R. T.; Autrey, T. *Angew. Chem. Int. Ed.* **2008**, *47*, 7493–7496.

(11) Jaska, C. A.; Temple, K.; Lough, A. J.; Manners, I. *J. Am. Chem. Soc.* **2003**, *125*, 9424–9434.

(12) Pons, V.; Baker, R. T.; Szymczak, N. K.; Heldebrant, D. J.; Linehan, J. C.; Matus, M. H.; Grant, D. J.; Dixon, D. A. *Chem. Commun.* **2008**, 6597–6599.

(13) Marwitz, A. J. V.; Abbey, E. R.; Jenkins, J. T.; Zakharov, L. N.; Liu, S.-Y. *Org. Lett.* **2007**, *9*, 4905–4908.

(14) Abbey, E. R.; Zakharov, L. N.; Liu, S.-Y. *J. Am. Chem. Soc.* **2008**, *130*, 7250–7252.

(15) Marwitz, A. J. V.; Matus, M. H.; Zakharov, L. N.; Dixon, D. A.; Liu, S.-Y. *Angew. Chem. Int. Ed.* **2009**, *48*, 973–977.

(16) Campbell, P. G.; Abbey, E. R.; Neiner, D.; Grant, D. J.; Dixon, D. A.; Liu, S.-Y. *J. Am. Chem. Soc.* **2010**, *132*, 18048–18050.

(17) Abbey, E. R.; Zakharov, L. N.; Liu, S.-Y. *J. Am. Chem. Soc.* **2010**, *132*, 16340–16342.

(18) Lamm, A. N.; Garner, E. B.; Dixon, D. A.; Liu, S.-Y. *Angew. Chem. Int. Ed.* **2011**, *50*, 8157–8160.

(19) Abbey, E. R.; Zakharov, L. N.; Liu, S.-Y. *J. Am. Chem. Soc.* **2011**, *133*, 11508–11511.

(20) Pritchard, R. H.; Kern, C. W. *J. Am. Chem. Soc.* **1969**, *91*, 1631–1635.

(21) Campbell, P. G.; Zakharov, L. N.; Grant, D. J.; Dixon, D. A.; Liu, S.-Y. *J. Am. Chem. Soc.* **2010**, *132*, 3289–3291.

(22) Luo, W.; Zakharov, L. N.; Liu, S.-Y. *J. Am. Chem. Soc.* **2011**, *133*, 13006–13009.

(23) Ramachandran, P. V.; Gagare, P. D. *Inorg. Chem.* **2007**, *46*, 7810–7817.

(24) Kalidindi, S. B.; Indirani, M.; Jagirdar, B. R. *Inorg. Chem.* **2008**, *47*, 7424–7429.

(25) He, T.; Wang, J.; Wu, G.; Kim, H.; Proffen, T.; Wu, A.; Li, W.; Liu, T.; Xiong, Z.; Wu, C.; Chu, H.; Guo, J.; Autrey, T.; Zhang, T.; Chen, P. *Chem. Eur. J.* **2010**, *16*, 12814–12817.

(26) Heldebrant, D. J.; Karkamkar, A.; Linehan, J. C.; Autrey, T. *Energy Environ. Sci.* **2008**, *1*, 156.

(27) Singaram, B.; Cole, T. E.; Brown, H. C. *Organometallics* **1984**, *3*, 774–777.

(28) Luo, W.; Campbell, P. G.; Zakharov, L. N.; Liu, S.-Y. *J. Am. Chem. Soc.* **2011**, *133*, 19326–19329.

(29) Staubitz, A.; Sloan, M. E.; Robertson, A. P. M.; Friedrich, A.; Schneider, S.; Gates, P. J.; Schmedt auf der Günne, J.; Manners, I. *J. Am. Chem. Soc.* **2010**, *132*, 13332–13345.

(30) Wright, W. R. H.; Berkeley, E. R.; Alden, L. R.; Baker, R. T.; Sneddon, L. G. *Chem. Commun.* **2011**, *47*, 3177–3179.

(31) Zheng, F.; Rassat, S. D.; Helderandt, D. J.; Caldwell, D. D.; Aardahl, C. L.; Autrey, T.; Linehan, J. C.; Rappé, K. G. *Rev. Sci. Instrum.* **2008**, *79*, 084103.

(32) Forgeron, M. A. M.; Bryce, D. L.; Wasylishen, R. E.; Rösler, R. *J. Phys. Chem. A* **2003**, *107*, 726–735.

Chapter V

(1) R. H. Crabtree, *The Organometallic Chemistry of the Transition Metals*, 5th ed., John Wiley and Sons, 2009.

(2) M. T. Honaker, J. M. Hovland, R. Nicholas Salvatore, *Curr. Org. Synth.* 2007, **4**, 31–45.

(3) K. C. K. Nicolaou, P. G. P. Bulger, D. D. Sarlah *Angew. Chem. Int. Ed.* **2005**, *44*, 4442–4489.

(4) N. Fey, A. G. Orpen, J. N. Harvey, *Coord. Chem. Rev.* **2009**, *253*, 704–722.

(5) C. A. Tolman, *Chem. Rev.* **1977**, *77*, 313–348.

(6) T. Bartik, T. Himmler, H. G. Schulte, K. Seevogel, *J. Organomet. Chem.* **1984**, *272*, 29–41.

(7) O. Kühl, *Coord. Chem. Rev.* **2005**, *249*, 693–704.

(8) A. R. Chianese, L. Xingwei, M. C. Janzen, J. W. Faller, R. H. Crabtree, *Organometallics* **2003**, *22*, 1663–1667.

(9) R. A. Kelly III, H. Clavier, S. Giudice, N. M. Scott, E. D. Stevens, J. Bordner, I. Samardjiev, C. D. Hoff, L. Cavallo, S. P. Nolan, *Organometallics* **2008**, *27*, 202–210.

(10) D. G. Gusev, *Organometallics* **2009**, *28*, 763–770.

(11) W. Chen, M. A. Esteruelas, M. Martin, M. Olivan, L. A. Oro, *J. Organomet. Chem.* **1997**, *534*, 95–103.

(12) A. J. V. Marwitz, E. R. Abbey, J. T. Jenkins, L. N. Zakharov, S.-Y. Liu, *Org. Lett.* **2007**, *9*, 4905–4908.

(13) E. R. Abbey, L. N. Zakharov, S.-Y. Liu, *J. Am. Chem. Soc.* **2008**, *130*, 7250–7252.

(14) A. J. V. Marwitz, M. H. Matus, L. N. Zakharov, D. A. Dixon, S.-Y. Liu, *Angew. Chem. Int. Ed.* **2009**, *48*, 973–977.

(15) A. N. Lamm, S.-Y. Liu, *Mol. Biosyst.* **2009**, *5*, 1303–1305.

(16) C. Tanjaroon, A. Daly, A. J. V. Marwitz, S.-Y. Liu, S. G. Kukolich, *J. Chem. Phys.* **2009**, *131*, 224312.

(17) A. M. Daly, C. Tanjaroon, A. J. V. Marwitz, S.-Y. Liu, S. G. Kukolich, *J. Am. Chem. Soc.* **2010**, *132*, 5501–5506.

(18) P. G. Campbell, E. R. Abbey, D. Neiner, D. J. Grant, D. A. Dixon, S.-Y. Liu, *J. Am. Chem. Soc.* **2010,** *132*, 18048–18050.

(19) L. Liu, A. J. V. Marwitz, B. W. Matthews, S.-Y. Liu, *Angew. Chem. Int. Ed.* **2009**, *48*, 6817–6819.

(20) P. G. Campbell, L. N. Zakharov, D. J. Grant, D. A. Dixon, S.-Y. Liu, *J. Am. Chem. Soc.* **2010**, *132*, 3289–3291.

(21) E. R. Abbey, L. N. Zakharov, S.-Y. Liu, *J. Am. Chem. Soc.* **2010**, *132*, 16340–16342.

(22) E. R. Abbey, L. N. Zakharov, S.-Y. Liu, *J. Am. Chem. Soc.* **2011**, *133*, 11508–11511.

(23) A. J. V. Marwitz, A. N. Lamm, L. N. Zakharov, M. Vasiliu, D. A. Dixon, S.-Y. Liu, *Chem. Sci.* **2012**, *3*, 825-829.

(24) A. J. V. Marwitz, J. T. Jenkins, L. N. Zakharov, S.-Y. Liu, *Organometallics* **2011**, *30*, 52–54.

(25) B. Zimmermann, W. I. Dzik, T. Himmler, L. J. Gooßen, *J. Org. Chem.* **2011**, *76*, 8107–8112.

(26) X.-F. Wu, J. Schranck, H. Neumann, M. Beller, *Tet. Lett.* **2011**, *52*, 3702–3704.

(27) T. S. Cameron, B. Dahlen, *J. Chem. Soc., Perkin Trans. 2* **1975**, *15*, 1737–1751.